UNDRAINED STRENGTH ANISOTROPY OF AN OVERCONSOLIDATED THIXOTROPIC CLAY

Vol. 1

BY

DEIRDRE A. O'NEILL

B.S.C.E., Massachusetts Institute of Technology (1981)

B.S., Earth & Planetary Sciences, Massachusetts Institute of Technology (1981)

SUBMITTED IN PARTIAL FULFILLMENT

OF THE REQUIREMENTS FOR THE

DEGREE OF

MASTER OF SCIENCE

at the

MASSACHUSETTS INSTITUTE OF TECHNOLOGY

July 1985

Signature of Author: _____
Dept. of Civil Engineering, July 23, 1985

Certified by: _____
C. Ladd, Thesis Supervisor

Accepted by: _____
Chairman, Department Committee

UNDRAINED STRENGTH ANISOTROPY OF AN OVERCONSOLIDATED THIXOTROPIC CLAY

BY

DEIRDRE A. O'NEILL

Submitted to the Department of Civil Engineering on July 23, 1985 in partial fulfillment of the requirements for the Master of Science in Civil Engineering.

ABSTRACT

The need for the measurement of anisotropic parameters of low permeability materials has been increasingly voiced to aid in the development of realistic generalized soil models. The Directional Shear Cell (DSC) is a plane strain, stress-controlled device with flexible stress application elements capable of applying both normal stresses and shear tractions to four faces of a cubic membrane-encased sample which was developed at University College London. The DSC is one of only two devices currently available capable of orienting the major principal stress at angles from the depositional axis equal to 0°, 90° and any angle in between while maintaining a constant value of b and without incurring undue moments due to device dictation of the direction of strain.

The DSC has been used at UCL to research the undrained and drained shear behavior of sands. The DSC at MIT, acquired in 1978, has been used to develop procedures for the testing of saturated clays. This thesis employs the DSC in the measurement of the undrained stress-strain-strength (inherent) anisotropy of resedimented Boston Blue Clay (BBC) at an overconsolidation ratio (OCR) equal to four.

As testing of resedimented BBC progressed, it became apparent that this material exhibits significant thixotropic effects such as increased measured preconsolidation pressures (an approximately 100% increase over a two year storage period) and increased shear strength. From the results of a series of consolidated undrained triaxial compression and extension tests, a quantitative correction is developed to apply to the Recompression DSC test results.

The DSC and the associated experimental techniques are

evaluated by the performance of five tests in the isotropic (horizontal) plane of the resedimented BBC. Procedures are improved through the use of new pressure bag restraining vanes, higher contrast film and dot targets. The latter two improvements reduce the minimum measurable normal strain to about 0.02% ± 0.12 SD. The undrained shear strength and average effective stress at failure from the four good isotropic DSC tests, performed at different values of Ψ, demonstrate remarkable consistency with COV=0.052 and 0.069, respectively. However, the DSC is not perfect, as indicated by the large strains caused by the shear sheets in the outer portion of the sample, the fact that the angle between the direction of σ_1 during shear and the direction of ε_1 is not equal to zero, and its inability to measure strain hardening behavior.

Variations in the undrained shear behavior of resedimented BBC at OCR=4 with the angle of shear, δ, are investigated by the performance of eleven DSC tests in the cross anisotropic plane of the material. The DSC test results indicate very pronounced inherent anisotropy. As δ increases from 0° to 90°: undrained shear strength decreases by approximatelv 44%; yield shear stress decreases by 53%; stress-strain behavior changes from brittle to ductile; the yielded modulus decreases by about 80%; the strain at failure increases significantly; and Skempton's pore pressure parameter, A_f, approximately doubles. Behavior of overconsolidated BBC as measured in conventional devices such as the triaxial cell, a plane strain apparatus capable only of normal stress application and the Direct Simple Shear (DSS) device are compared with the DSC tests performed at the relevant angle of shear. Evaluations take into account the method of consolidation and the effect of sample age when the preconsolidation pressure is not exceeded prior to shear.

ACKNOWLEDGEMENTS

The author wishes to acknowledge the National Science Foundation whose funding, through a three-year Research Assistantship, enabled completion of most of the experimental work upon which this thesis is based. The author also wishes to acknowledge the following people:

- Prof. C.C.Ladd, her thesis and academic advisor and friend, for his intensive review of and contributions to the technical and literary content of this document and for his patience in awaiting its arrival in final form;
- Dr. J.T.Germaine, developer of many of the experimental techniques utilized in the pursuit of the information contained herein, for providing a high standard relative to the acquisition and interpretation of quality data;
- Profs. A.S.Azzouz and M.M.Baligh for their willingness to confront and to discuss virtually any issue and for their support and friendship;
- Dr. D.W.Hight for his insight on behavior, his helpful suggestions and comments and his friendship;
- Ms. R.Schwartz, the author's friend, for the accurate and timely typing of this document;
- Dr. B.E.Novich for his friendship and for introducing the author to Dr. R.T.Martin and experimental mineralogy;
- the author's family, for forever looking forward to the light at the end of the tunnel; and
- all of the author's friends on the third floor for creating diversions and providing comic relief.

TABLE OF CONTENTS

	Page No.
TITLE PAGE	1
ABSTRACT	2
ACKNOWLEDGEMENTS	4
TABLE OF CONTENTS	5
LIST OF SYMBOLS	10
LIST OF TABLES	16
LIST OF FIGURES	18
CHAPTER 1: INTRODUCTION	26
1.1 NEED FOR ANISOTROPIC PARAMETERS FOR REALISTIC CONSTITUTIVE RELATIONSHIPS	26
1.2 HISTORY OF THE DIRECTIONAL SHEAR CELL	28
1.3 OBJECTIVE AND SCOPE OF THESIS	29
CHAPTER 2: BACKGROUND	33
2.1 OVERVIEW OF TEST DEVICES FOR MEASUREMENT OF ANISOTROPIC CLAY PROPERTIES	33
2.1.1 Anisotropy	33
2.1.2 Experimental Capabilities Currently Available	35
2.2 OVERVIEW OF DSC CAPABILITIES AND TEST PROCEDURES	43
2.2.1 Conceptual Basis for Isotropic "Proof" Tests and Anisotropic Tests	43
2.2.2 Resedimentation and Preparation of Overconsolidated Boston Blue Clay Samples	47
CHAPTER 3: THIXOTROPIC NATURE OF RESEDIMENTED BOSTON BLUE CLAY	61
3.1 BEHAVIORAL CHANGES CONFORMING TO THE DEFINITION OF THIXOTROPY	61
3.1.1 Introduction	61

TABLE OF CONTENTS

		Page No.
3.1.1.1	Effect of Storage Time on Water Content and Index Properties	62
3.1.1.2	Fall Cone Test Series on Remolded BBC	63
3.1.2	Effect of Storage Time on Initial Pore Pressure	68
3.1.3	Effect of Storage Time on Consolidation Test Results	70
3.1.3.1	Variation in Measured Preconsolidation Pressure with Time	70
3.1.3.2	Determination of Storage Time	73
3.1.3.3	Variation in Consolidation Parameters with Time	75
3.2	DEVELOPMENT OF METHODS TO CORRECT UNDRAINED SHEAR DATA AFFECTED BY THIXOTROPY	79
3.2.1	K_o-consolidated Triaxial and Extension Results for Resedimented BBC at OCR=4	79
3.2.1.1	Variation in Stress-Strain Relationships with Elapsed Storage Time	80
3.2.1.2	Variation in Shear-Induced Pore Pressure with Elapsed Storage Time	88
3.2.2	K_o-consolidated Direct Simple Shear Test Results for Resedimented BBC at OCR=1.0 and 4.0	92
3.2.3	Correction of Stress-Strain Curves to Remove Storage Effects	99
3.2.4	Correction of Effective Stress Paths to Remove Storage Effects	103
CHAPTER 4:	EVALUATION OF AND IMPROVEMENTS TO DSC TESTING TECHNIQUES	149
4.1	OVERVIEW OF DSC TEST EVALUATION PROCEDURE	149
4.1.1	Strain Distribution Standard	150
4.1.2	Stress Application Standard	152
4.1.3	Silicon-Grease Resistance Correction	156
4.1.4	Membrane Correction for the DSC	161
4.2	IMPROVED DSC TESTING TECHNIQUES	166
4.2.1	New Pressure Bag Retaining Vanes	166
4.2.2	New Corner Prisms	168
4.2.3	Photographic Improvements	168

TABLE OF CONTENTS

		Page No.
4.3	RESULTS OF PROOF TESTING	171
4.3.1	Pore Pressure Response	172
4.3.2	Evaluation of Quality of Isotropic DSC Tests Using Established Standards	178
4.3.2.1	Evaluation of Strain Distribution	178
4.3.2.2	Evaluation of Stress Application	184
4.3.3	Presentation of Time Corrected Results	186
4.4	EVALUATION OF THE DSC AS A TESTING DEVICE FOR MEASUREMENT OF ANISOTROPY	191
4.4.1	Variations in Strength Behavior with ψ	191
4.4.2	Variations in Strain Distribution with ψ	192
CHAPTER 5:	MEASUREMENT OF UNDRAINED STRESS-STRAIN-STRENGTH ANISOTROPY OF OVERCONSOLIDATED BBC IN THE DIRECTIONAL SHEAR CELL	227
5.1	INTRODUCTION	227
5.2	RESULTS OF ANISOTROPIC DSC TESTING	229
5.2.1	Evaluation of Test Quality	229
5.2.1.1	Evaluation of Strain Distribution	229
5.2.1.2	Evaluation of Stress Application	233
5.2.2	Presentation of Time-Corrected Anisotropic DSC Test Results	237
5.3	DISCUSSION OF EFFECT OF ROTATION OF MAJOR PRINCIPAL STRESS DIRECTION ON STRESS-STRAIN-STRENGTH PARAMETERS OF OVERCONSOLIDATED BOSTON BLUE CLAY	243
5.3.1	Variations in Strength Behavior with δ	243
5.3.2	Variations in Strain Behavior with δ	247
CHAPTER 6:	EFFECTS OF CONSOLIDATION STRESS HISTORY AND COMPARISON OF DSC DATA WITH RESULTS FROM OTHER TEST DEVICES	269
6.1	INTRODUCTION	269
6.2	CONSOLIDATION STRESS HISTORY: RECOMPRESSION VS. SHANSEP	270
6.3	COMPARISON OF DATA AT $\delta=0°$	286
6.4	COMPARISON OF DATA AT $\delta=90°$	293

TABLE OF CONTENTS

		Page No.
6.5	COMPARISON OF DATA AT INTERMEDIATE VALUES OF δ	297
CHAPTER 7:	SUMMARY, CONCLUSIONS AND RECOMMENDATIONS	327
7.1	INTRODUCTION	327
7.2	SUMMARY AND CONCLUSIONS	329
7.2.1	Effect of Thixotropy on Overconsolidated Resedimented BBC	329
7.2.2	Proof Testing the DSC	332
7.2.3	Effect of Principal Stress Direction on the Undrained Shear Behavior of Overconsolidated Resedimented BBC	337
7.2.4	Comparison of DSC Test Results with Data from Other Devices	339
7.2.4.1	Introduction	339
7.2.4.2	Effect of the Method of Consolidation	340
7.2.4.3	Comparison of Results at $\delta=0°$	342
7.2.4.4	Comparison of Results at $\delta=90°$	344
7.2.4.5	Comparison of Results at Intermediate Values of δ	346
7.3	RECOMMENDATIONS FOR FUTURE RESEARCH	348
REFERENCES		353
APPENDIX A:	Resedimented BBC Batch Data	MISSING
APPENDIX B:	Silicon-Teflon Grease Stress-Strain Behavior	MISSING
APPENDIX C:	DSC Membrane Correction	MISSING
APPENDIX D:	DSC Testing Techniques	MISSING
APPENDIX E:	Isotropic DSC Test Data	MISSING
APPENDIX F:	Anisotropic DSC Test Data	MISSING

TABLE OF CONTENTS

		Page No.
APPENDIX G:	Consolidation Test Data	MISSING
APPENDIX H:	Triaxial Compression and Extension Test Data	MISSING
APPENDIX I:	DSS Test Data	MISSING

LIST OF SYMBOLS

Notes: Prefix Δ indicates a change
A prime over a stress indicates an effective stress
A subscript f indicates a final or failure condition
A subscript o indicates initial or in situ condition
A subscript t indicates value corrected for thixotropic effects
A bar over a test type indicates measurement of pore pressure

Symbol	Definition
ASTM	American Society for Testing Materials
BBC	Boston Blue Clay
CD	Consolidated Drained Triaxial Test
CID	Isotropically Consolidated Drained Triaxial Test
CIU	Isotropically Consolidated Undrained Triaxial Test
CK_oU	K_o Consolidated Drained Triaxial Test
CK_oD	K_o Consolidated Undrained Triaxial Test
CK_oUC	K_o Consolidated Undrained Compression Test
CK_oUDSS	K_o Consolidated Undrained Direct Simple Shear Test
CK_oUE	K_o Consolidated Undrained Extension Test
DSC	Plane Strain Directional Shear Cell Test
DSS	Direct Simple Shear
ESP	Effective Stress Path
FC	Fall Cone Test
LCT	Lower Cromer Till
LVDT	Linear Voltage Displacement Transducer
MIT	Massachusetts Institute of Technology
NSF	National Science Foundation
OCR	Overconsolidation Ratio
PSC	Plane Strain Compression Test
PSE	Plane Strain Extension Test

LIST OF SYMBOLS

PVC	Polyvinyl Chloride
SHANSEP	Stress History and Normalized Soil Engineering Properties
TC	Triaxial Compression Test
TC-H	Triaxial Compression Test on Horizontal Sample
TE	Triaxial Extension Test
TE-H	Triaxial Extension Test on Horizontal Sample
TTA	True Triaxial Apparatus
UCL	University College London
UU	Unconsolidated Undrained Triaxial Test
$A, (A_f)$	Skempton's pore pressure parameter (at failure)
b	Relative intermediate principal stress (= $(\sigma_2-\sigma_3)/(\sigma_1-\sigma_3)$)
B	Skempton's pore pressure parameter
c'	Cohesion intercept of effective envelope
COV[x]	Coefficient of variation (= SD[x]/$\bar{x}$)
CR	Virgin compression ratio
c_u	Undrained shear strength
$c_u(H)$	Undrained shear strength for horizontal loading
$c_u(V)$	Undrained shear strength for vertical loading
c_v	Coefficient of consolidation
C_α	Coefficient of secondary compression
d	Sample diameter
e	Void ratio
E_v, E_h	Young's Modulus for vertical and horizontal loading
G_{vh}	Shear modulus in vertical plane
G_y	Shear modulus after yielding in DSC test
h	Height of sample

LIST OF SYMBOLS

I_L	Liquidity Index
I_p	Plasticity index
K_c	Ratio of horizontal to vertical consolidation stress
K_o	Coefficient of earth pressure at rest (stress ratio for condition of no lateral strain)
K_s	Anisotropic strength ratio
ksc	Kilograms per square centimeter
m	Intermediate principal stress parameter (= $\frac{\sigma 2'}{(\sigma 1'+\sigma 3')}$
p'	Mean effective stress (= $(\sigma 1'+ \sigma 3')/2$)
p'_t	Mean effective stress corrected for thixotropic effects
q	Shear stress (= $(\sigma 1 - \sigma 3)/2$)
q_f	Shear stress at failure
q_t	Shear stress corrected for thixotropic effects
q_y	Shear stress at yield point
RR	Recompression ratio
SD[x]	Standard deviation of parameter x
t	Time
t_p	Time for primary consolidation
t_s	Time for which resedimented sample was stored before testing
u_i	Excess pore pressure in sample exposed to atmospheric pressure conditions
u_s	Shear induced pore pressure (= $\Delta u - \Delta \sigma_{oct}$)
w_L	Liquid limit
w_N	Natural water content

LIST OF SYMBOLS

w_p	Plastic limit
$\bar{x}$	Arithmetic mean of parameter x
x,y	Coordinates in digitizer measuring system
x',y'	Coordinates used by computer to calculate strains within square area
X,Y	Coordinates in the horizontal plane of the sample
Z	Deposition direction of the sample
α	No extension direction
$\alpha_1,\alpha_2,$ α_3,α_4	Sample corner angles in DSC
β	No extension direction
γ	Maximum shear strain
$\dot{\gamma}$	Shear strain rate
γ_{oct}	Octahedral shear strain $(= \frac{1}{3}[(\varepsilon_1-\varepsilon_2)^2+(\varepsilon_2-\varepsilon_3)^2+(\varepsilon_3-\varepsilon_1)^2])^{0.5}$
γ_r	Average maximum shear strain of sample ring
δ	Principal stress direction measured from deposition axis
Δ	Deviation of axes of principal stress and strain
$\varepsilon_1,\varepsilon_2,\varepsilon_3$	Major intermediate and minor principal normal strain
ε_f	Normal strain at failure
ε_x	Normal strain in x direction
ε_{xy}	Shear strain
ε_y	Normal strain in y direction
ε_v	Planar strain=volumetric strain in plane strain DSC test
ζ	Angle of rotation of DSC sample to correct for rigid body rotation
ν	Poisson's ratio

LIST OF SYMBOLS

ν_{hh}	Poisson's ratio for effect of horizontal strain on complementary horizontal strain
ν_{vh}	Poisson's ratio for effect of vertical strain on horizontal strain
ξ	Angle between major principal strain axis to deposition axis
σ	Total normal stress
$\sigma_1, \sigma_2, \sigma_3$	Major, intermediate and minor total normal stress
σ_a, σ_b	Applied normal stresses in DSC
σ_{bag}	DSC bag pressure during calibration
σ_c	Cell pressure
σ_{hc}	Horizontal total normal consolidation stress
σ_{vc}	Vertical total normal consolidation stress
σ_x	Total normal stress in x direction
σ_y	Total normal stress in y direction
σ_z	Total normal stress in z direction
σ_o	Total normal stress in o direction
σ_{oct}	Octahedral stress (= $(\sigma_1+\sigma_2+\sigma_3)/3$)
$\sigma'_1, \sigma'_2, \sigma'_3$	Major, intermediate and minor effective normal stress
σ'_c	Cell pressure minus back stress
σ'_p	Preconsolidation pressure
$\sigma'_p(t)$	Preconsolidation pressure as affected by storage time
σ'_v	Vertical effective normal stress
σ'_{vc}	Vertical effective normal consolidation stress
σ'_{vm}	Maximum value of σ'_{vc} for destructured clay
τ	Shear stress
τ_a, τ_b	Applied shear stress in DSC

LIST OF SYMBOLS

τ_{ff}	Shear stress at failure plane at failure
τ_h	Shear stress on horizontal plane
τ_{oct}	Octahedral shear stress $(= \frac{1}{3}[(\sigma_1-\sigma_2)^2+(\sigma_2-\sigma_3)^2+(\sigma_3-\sigma_1)^2])^{0.5}$
ϕ'	Effective friction angle
Ψ	Major principal stress direction in the isotropic plane
ω	Orientation of sample grid on digitizer

LIST OF TABLES

Table No.	Title	Page
2.1	Requirements for Measuring the Combined Anisotropy of Soft Clays in Laboratory Shear Devices (after Germaine, 1982).	52
2.2	Assessment of Laboratory Shear Devices for Measuring Combined Anisotropy of Soft Clays (from Germaine, 1982).	53
2.3	Summary of DSC Tests Performed on Resedimented BBC (OCR=4)	54
3.1	Index Properties for Resedimented BBC	110
3.2	Comparison of Preconsolidation Pressures for Resedimented BBC Using Three Methods	111
3.3	Summary of Consolidation Test Data for Resedimented BBC	112
3.4	Summary of Triaxial Compression and Extension Test Data for Resedimented BBC (OCR=4)	113
3.5	Summary of CK_oUDSS Test Data for Resedimented BBC (OCR's 1 and 4)	114
3.6	Correction Method for Effect of Thixotropy on Undrained Shear Strength Tests	115
4.1	Measurements of Membrane Thicknesses from Recent DSC Tests	196
4.2	Membrane and Grease Corrections Applied to Isotropic DSC Tests and $\delta=90°$ Anisotropic DSC Test on Resedimented BBC (OCR=4)	197
4.3	Effect of Film Type and Target on Scatter Associated with Strain Measurement	198
4.4	Summary of Isotropic DSC Test Data for Resedimented BBC (OCR=4)	199
5.1	Summary of Anisotropic DSC Test Data for Resedimented BBC (OCR=4)	252
6.1	Effect of Method of Consolidation on Undrained Shear Behavior	307
6.2	Summary of Triaxial Test Results on Resedimented BBC (OCR=4)	308

LIST OF TABLES

Table No.	Title	Page
6.3	Summary of δ=0° Test Results on Resedimented BBC (OCR=4)	309
6.4	Summary of δ=90° Test Results on Resedimented BBC (OCR=4)	310

LIST OF FIGURES

Figure No.	Title	Page
1.1	Example of Embankment Construction on a Soft Clay Foundation.	32
2.1	Combinations of b and δ Which Can be Achieved by Various Soil Shear Strength Testing Devices (after Germaine, 1982).	55
2.2	Schematic of Imperial College Hollow Cylinder Apparatus (from Symes, 1983).	56
2.3	View of (a) Partially Assembled DSC Showing Sample with Shear Sheets and Two of the Four Pressure Bags (Arthur et al., 1981) and (b) Fully Assembled DSC Showing Measurement Grid and Plate Camera.	57
2.4	Diagram of Method used to Apply Normal and Shear Stresses in the UCL Directional Shear Cell (Arthur et al., 1981).	58
2.5	Directional Shear Cell: Principle and Definitions (from Germaine, 1982).	59
2.6	Variation of K_o with OCR for Resedimented BBC from Laboratory Tests.	60
3.1	Initial Water Content vs. Storage Time for Samples of Resedimented BBC from Several Different Batches.	116
3.2	Effect of Thixotropy on Fall Cone Penetration Depths for Remolded Resedimented BBC.	117
3.3	Effect of Water Content on Thixotropic Regain of Strength in Clay.	118
3.4	Initial Pore Pressure vs. Elapsed Storage Time for Resedimented BBC (Sampling OCR=4).	119
3.5	Effect of Thixotropy on Measured Preconsolidation Pressure for Resedimented BBC.	120
3.6	Consolidation Stress-Strain Results for Resedimented BBC.	121
3.7	Effect of Storage Time on Recompression Ratio upon Initial Recompression of Resedimented BBC.	122
3.8	Effect of Storage Time on Compression Ratio of Resedimented BBC.	123

LIST OF FIGURES

Figure No.	Title	Page
3.9	Coefficient of Consolidation for Resedimented BBC.	124
3.10	Coefficient of Secondary Compression for Resedimented BBC.	125
3.11	Stress-Strain Curves from $\overline{CK_oU}$ Triaxial Compression Tests on Resedimented BBC (OCR=4).	126
3.12	Stress-Strain Curves from $\overline{CK_oU}$ Triaxial Extension Tests on Resedimented BBC (OCR=4).	127
3.13	Changes in Strength of Resedimented BBC (OCR=4) in Compression and Extension between Samples with Different Storage Times.	128
3.14	Anisotropy Ratio from Triaxial and Plane Strain Tests on Resedimented BBC.	129
3.15	Effect of Storage Time on Undrained Shear Yield Stress for Resedimented BBC (OCR=4, σ'_p=1.0 ksc).	130
3.16	Effect of Storage Time on Initial Stiffness under Undrained (Triaxial) Shear for Resedimented BBC (OCR=4).	131
3.17	Normalized Stress Paths from $\overline{CK_oU}$ Triaxial Compression Tests on Resedimented BBC (OCR=4).	132
3.18	Normalized Pore Pressure, Stress Ratio and A Parameter from CK_oU Triaxial Compression Tests on Resedimented BBC (OCR=4).	133
3.19	Normalized Stress Paths from $\overline{CK_oU}$ Triaxial Extension Tests on Resedimented BBC (OCR=4).	134
3.20	Normalized Pore Pressure, Stress Ratio and A Parameter from CK_oU Triaxial Extension Tests on Resedimented BBC (OCR=4).	135
3.21	Normalized Shear-Induced Pore Pressure vs. Maximum Shear Strain from CK_oU Triaxial Compression Tests on Resedimented BBC (OCR=4).	136
3.22	Normalized Shear-Induced Pore Pressure vs. Maximum Shear Strain from CK_oU Triaxial Extension Tests on Resedimented BBC (OCR=4).	137

LIST OF FIGURES

Figure No.	Title	Page
3.23	Effect of Storage Time on Undrained Shear Induced Pore Pressure for Resedimented BBC (OCR=4).	138
3.24	Summary Plot of Effect of Storage Time on Undrained Shear Yield Stress and Shear Induced Pore Pressure for Resedimented BBC (OCR=4, σ'_p=1.0 ksc).	139
3.25	Normalized Stress-Strain Relationships from CK_oUDSS Tests on Resedimented BBC (OCR=4).	140
3.26	Normalized Horizontal Shear Stress vs. Vertical Normal Stress from CK_oUDSS Tests on Resedimented BBC (OCR=4).	141
3.27	Normalized Shear-Induced Pore Pressures from CK_oUDSS Tests and Anisotropic DSC Tests (δ=40° and 65°) on Resedimented BBC (OCR=4).	142
3.28	Normalized Stress-Strain Relationships and Stress Paths from CK_oUDSS Tests following Recompression and SHANSEP type Consolidation on Resedimented BBC (OCR=4).	143
3.29	Normalized Stress-Strain Relationships from CK_oUDSS Tests on Resedimented BBC (OCR=1).	144
3.30	Normalized Horizontal Shear Stress vs. Vertical Normal Stress from CK_oUDSS Tests on Resedimented BBC (OCR=1).	145
3.31	Normalized Pore Pressure vs. Maximum Shear Strain from CK_oUDSS Tests on Resedimented BBC (OCR=1).	146
3.32	Effect of Ratio of Vertical Consolidation Stress to Thixotropically Increased Maximum Past Pressure on Horizontal Shear Strength and Vertical Effective Stress on Resedimented BBC (OCR=1).	147
3.33	Effect of Storage Time on Post-Yield Moduli from Tests Performed on Resedimented BBC (OCR=1 and 4).	148
4.1	Definition of Sample Zones over which Average Strain Values are Computed (from Germaine, 1982).	200

LIST OF FIGURES

Figure No.	Title	Page
4.2	Variation of Normalized Ring Strain from DSC-4 (δ=45°) Performed Without Plexiglass Prisms on Resedimented BBC (OCR=4).	201
4.3	Possible Explanation for Anomalous Effective Stress Paths from DSC Tests on Resedimented BBC (OCR=4).	202
4.4	Illustration of the Effect of Confinement by Shear Sheets on Effective Stress Paths from Isotropic DSC Tests.	203
4.5	Silicon-Teflon Grease Stress-Strain Characteristics.	204
4.6	DSC Shear Sheet Corrections.	205
4.7	Effect of Unstressed Shear Sheets on Soil Behavior as measured by the DSC.	206
4.8	New Retaining Vanes for DSC Pressure Bags.	207
4.9	Plexiglass Prisms used to Protect DSC Samples from Stress Concentrations.	208
4.10	Effect of Prism Shape on the Protection of the DSC Sample Corners during Tests Performed at Intermediate Angles of Shear.	209
4.11	Stress-Strain Curves from Isotropic DSC Tests on Resedimented BBC (OCR=4); (not Corrected for Thixotropic Effects).	210
4.12	Effective Stress Paths from Isotropic DSC Tests on Resedimented BBC (OCR=4); (not Corrected for Thixotropic Effects).	211
4.13	Effect of Nonuniform Stress Application at Sample Corners on Pore Pressure Response.	212
4.14	Relationship Between Pore Pressure Parameter, B, and the Initial Negative Pore Pressure as Measured in the DSC on Resedimented BBC (OCR=4).	213
4.15	Variation of Maximum Shear Strain Distribution (NRS) with Maximum Shear Strain Level from Entire Sample from Isotropic DSC Tests on Resedimented BBC (OCR=4).	214

LIST OF FIGURES

Figure No.	Title	Page
4.16	Coefficient of Variation vs. Shear Strain from Isotropic DSC Tests on Resedimented BBC (OCR=4).	215
4.17	Illustration of Grid Deformations which led to Increases in Coefficients of Variation for Maximum Shear Strain.	216
4.18	Deviation of the Direction of Principal Strain from that of Principal Stress for Isotropic DSC Tests on Resedimented BBC (OCR=4).	217
4.19	Measured and Corrected Shear-Induced Pore Pressure vs. Strain from Isotropic DSC Tests on Resedimented BBC (OCR=4).	218
4.20	Variation of Shear-Induced Pore Pressure with Angle of Shear from Isotropic DSC Tests on Resedimented BBC (OCR=4).	219
4.21	Stress-Strain Relationships (Corrected for Thixotropic Effects) from Isotropic DSC Tests on Resedimented BBC (OCR=4).	220
4.22	Effective Stress Paths (Corrected for Thixotropic Effects) from Isotropic DSC Tests on Resedimented BBC (OCR=4).	221
4.23	Variation in Normalized Young's Modulus with Stress Level from Isotropic DSC Tests on Resedimented BBC (OCR=4).	222
4.24	Shear Strain Rates from Isotropic DSC Tests on Resedimented BBC (OCR=4).	223
4.25	Volumetric Strain vs. Maximum Shear Strain from Isotropic DSC Tests on Resedimented BBC (OCR=4).	224
4.26	Effect of Angle of Shear on Strength Parameters from Isotropic DSC Tests on Resedimented BBC (OCR=4).	225
4.27	Effect of Angle of Shear on Strain Behavior from Isotropic DSC Tests on Resedimented BBC (OCR=4).	226

LIST OF FIGURES

Figure No.	Title	Page
5.1	Variation of Maximum Shear Strain Distribution (NRS) with Maximum Shear Strain from Entire Sample from Anisotropic DSC Tests on Resedimented BBC (OCR=4).	252
5.2	Variation of Maximum Shear Strain Distribution (NRS) with Maximum Shear Strain from Entire Sample for Anisotropic DSC Tests on Resedimented BBC (OCR=4).	253
5.3	Variation of COV[γ] With Maximum Shear Strain from Anisotropic DSC Tests on Resedimented BBC (OCR=4).	254
5.4	Variation of Δ With Maximum Shear Strain from Anisotropic DSC Tests on Resedimented BBC (OCR=4).	255
5.5	Shear-Induced Pore Pressure (Corrected for Storage Time) vs. Maximum Shear Strain from Anisotropic DSC Tests on Resedimented BBC (OCR=4).	256
5.6	Effect of Angle of Shear on Corrected Shear-Induced Pore Pressure from Anisotropic DSC Tests on Resedimented BBC (OCR=4).	257
5.7	Stress-Strain Curves from Anisotropic DSC Tests on Resedimented BBC (OCR=4); (Corrected for Thixotropic Effects).	258
5.8	Normalized Effective Stress Paths from Anisotropic DSC Tests on Resedimented BBC (OCR=4); (Corrected for Thixotropic Effects).	259
5.9	Effect of Anisotropy on Effective Stress Envelope.	260
5.10	Variation of Normalized Young's Modulus with Shear Stress Level from Anisotropic DSC Tests on Resedimented BBC (OCR=4).	261
5.11	Obliquity and Pore Pressure Parameter vs. Maximum Shear Strain from Anisotropic DSC Tests on Resedimented BBC (OCR=4).	262
5.12	Rate of Maximum Shear Strain vs. Shear Stress Level for Anisotropic DSC Tests on Resedimented BBC (OCR=4).	263

LIST OF FIGURES

Figure No.	Title	Page
5.13	Variation in Undrained Shear Strength Parameters with δ from DSC Tests on Resedimented BBC (OCR=4).	264
5.14	Variation in Normalized Moduli and Shear Strain at Yield and Failure with δ from DSC Tests on Resedimented BBC (OCR=4).	265
5.15	Effect of Angle of Shear on Coefficient of Variation of γ and Normalized Ring Strain from Anisotropic DSC Tests on Resedimented BBC (OCR=4).	266
5.16	Deviation of the Direction of Principal Strain from that of Principal Stress vs. Angle of Shear from DSC Tests on Resedimented BBC (OCR=4).	267
6.1	Normalized Stress-Strain Curves and Effective Stress Data from $\overline{CK_oU}$(C) and $\overline{CK_oU}$(E) Triaxial Tests on East Windsor Varved Clay (OCR=4) (after Sambhandharaksa, 1977).	311
6.2	Normalized Stress Strain Curves and Effective Stress Paths from $\overline{CIU}$(C) Triaxial Tests on Lower Cromer Till (OCR=4) (after Gens, 1982).	312
6.3	Normalized Stress-Strain Curves from Recompression and SHANSEP Triaxial Compression Tests on Resedimented BBC (OCR=4).	313
6.4	Normalized Effective Stress Paths from Recompression and SHANSEP Triaxial Compression Tests on Resedimented BBC (OCR=4).	314
6.5	Obliquity and Skempton's Pore Pressure Parameter, A, vs. Axial Strain from Recompression and SHANSEP Triaxial Compression Tests on Resedimented BBC (OCR=4).	315
6.6	Normalized Stress-Strain Curves from δ=0° Tests on Resedimented BBC (OCR=4).	316
6.7	Normalized Effective Stress Paths from δ=0° Tests on Resedimented BBC (OCR=4).	317
6.8	Obliquity and Skempton's Pore Pressure Parameter, A, vs. Axial Strain from δ=0° Tests on Resedimented BBC (OCR=4).	318

LIST OF FIGURES

Figure No.	Title	Page
6.9	Normalized Octahedral Stress-Strain Curves from δ=0° and δ=90° Tests on Resedimented BBC (OCR=4).	319
6.10	Normalized Octahedral Effective Stress Paths from δ=0° and δ=90° Tests on Resedimented BBC (OCR=4).	320
6.11	Normalized Stress-Strain Curves from δ=90° Tests on Resedimented BBC (OCR=4).	321
6.12	Normalized Effective Stress Paths from δ=90° Tests on Resedimented BBC (OCR=4).	322
6.13	Obliquity and Skempton's Pore Pressure Parameter, A, vs. Axial Strain from δ=90° Tests on Resedimented BBC (OCR=4).	323
6.14	Normalized Stress-Strain Curves from DSC Tests at Intermediate δ Angles (δ=40°, 65° and 75°) and from DSS Tests on Resedimented BBC (OCR=4).	324
6.15	Normalized Effective Stress Paths from DSC Tests at Intermediate δ Angles (δ=40°, 65° and 75°) and Normalized Horizontal Shear Stress vs. Vertical Normal Stress from DSS Tests on Resedimented BBC (OCR=4).	325
6.16	Normalized Young's Modulus vs. Shear Stress Level from DSC Tests at Intermediate δ Angles (δ=40° and 65°) and from DSS Tests on Resedimented BBC (OCR=4).	326

CHAPTER 1

INTRODUCTION

1.1 NEED FOR ANISOTROPIC PARAMETERS FOR REALISTIC CONSTITUTIVE RELATIONSHIPS

The ability to predict the full response of cohesive soils in most soil-structure interaction problems of practical interest requires a computer code based on a generalized model of soil behavior. Such models must use effective stress constitutive relationships in order to predict undrained, drained and consolidation behavior. The Modified Cam-Clay (Roscoe and Burland, 1968) provided an elegant framework for describing the basic behavior observed in isotropically consolidated triaxial compression tests, but cannot predict the stress-strain-strength anisotropy exhibited by most natural clays. The Prevost Model (Prevost and Hoeg, 1977) considered anisotropy and strain softening, but is restricted to undrained shearing. The MIT-E1 model (Kavvadas, 1982) extends many of the features of the MCC to incorporate anisotropy, but is restricted to lightly overconsolidated clays and is not available in a computer code.

One reason for the slow progress in developing realistic generalized soil models is the lack of reliable data describing stress-strain-strength anisotropy during both drained and undrained shearing under a variety of stress conditions.

R.F. Scott's (1981) remark that "our ability to analyze

problems has ...outstripped our ability to describe the material ...to a comparable degree" was reiterated at the Blacksburg, Va. workshop on "Research Needs in Experimental Soil Engineering" (1983). The workshop identified the experimental determination of soil parameters as "of the greatest importance at the present time." Parameters associated with the anisotropic behavior of soils were specifically mentioned among those urgently requiring experimental attention.

An example of the need for anisotropic soil parameters in a common area of geotechnical analysis is provided in Fig. 1.1. In this case of stage construction of a long embankment over soft clay subsurface conditions, there are zones (e.g. element Y) which experience applied shear stresses that rotate the direction of the major principal stress, σ_1' (Germaine, 1982). Simulation of these conditions requires very sophisticated test devices and techniques. The Directional Shear Cell is uniquely suited for such a purpose since it has the ability to apply shear and normal forces to the four sides of a cubical sample.

MIT has been engaged in NSF supported research since 1978 for the purpose of creating a comprehensive data bank on stress-strain-strength anisotropy of soils. Specifically, MIT acquired the Directional Shear Cell and related equipment for first investigating the anisotropy of sands (NSF Grants ENG78-10435 and ENG78-10732) and then extending the capabilities to undrained shear of overconsolidated clay (NSF Grants CME80-14200 and CEE81-03695).

1.2 HISTORY OF THE DIRECTIONAL SHEAR CELL

The principal device chosen by MIT to investigate the stress-strain-strength anisotropy of resedimented Boston Blue Clay (BBC) is the Directional Shear Cell. The DSC was developed by Dr. J.R.F. Arthur and his colleagues in the mid-1970's at University College London (UCL) to measure the anisotropy of laboratory prepared sand samples. Descriptions of the device as it evolved are detailed by Arthur et al. (1977) and Rodriguez (1977).

In the late 1970's, a DSC system was installed at MIT as described by Arthur et al. (1981) and Bekenstein (1980). Tests were performed on the same sand used by UCL at MIT to gain confidence in the device and to check its reliability. Efforts were then focused on adapting the device for the testing of saturated clay. Development of a technique for resedimenting saturated batches of BBC, design and production of a pore pressure probe to measure effective stresses during consolidation and shear in the DSC, as well as sample preparation and actual DSC testing procedures were accomplished by Germaine (1982). This MIT doctoral thesis is frequently referred to for details and procedures by this (subsequent) research.

Although use of the DSC for testing on sands was aimed at examining strain induced anisotropy, the initial focus for fine grained materials is the inherent anisotropy acquired during deposition (Section 2.1.1 defines the various types of anisotropy). The DSC is considered an optimal device for

measurement of anisotropy since, unlike most other testing devices, the stress application conditions enable rotation of the principal stresses while maintaining a plane strain value of the relative intermediate stress ratio, $b = (\sigma_2-\sigma_3)/(\sigma_1-\sigma_3)$.

1.3 OBJECTIVE AND SCOPE OF THIS THESIS

The purpose of this research is, ultimately, to examine the initial anisotropy of Boston Blue Clay at various overconsolidation ratios (OCR's) under both undrained and drained conditions using the DSC. In the interest of alleviating several laboratory related problems (detailed by Germaine (1982)) during this development phase, the resedimented BBC is consolidated to an OCR equal to four and tested in undrained shear for anisotropic behavior having this stress history.

In order to ascertain anisotropic parameters it is of utmost importance to establish a high degree of confidence in both the quality of the material being tested and the reliability of the device employed. Therefore, these two tasks present themselves as preliminary objectives and are confronted in Chapters 3 and 4, respectively. Chapter 5 presents and discusses the undrained anisotropy of BBC as measured in the DSC, while Chapter 6 compares the DSC data with results of other devices.

For the most part, the objectives define the scope of this research. For example, during the initial phases of this research, it became apparent that the length of time that a

sample was stored prior to testing had a significant effect on the measured consolidation and strength parameters. In order to quantify the effect of elapsed time between resedimentation and strength testing on the behavior of the clay, i.e., thixotropic effects, a large number of triaxial compression and extension tests as well as oedometer tests were performed. Resedimented BBC samples were also tested in the Geonor Direct Simple Shear (DSS) device to further ascertain the possible anisotropy of the thixotropic effect. A series of fall cone tests were included to further understand the time-dependent nature of the "young" BBC.

The objective of "proving" the DSC device required several tests in the isotropic plane as well as some modifications in the DSC testing procedures put forward by Germaine (1982). And, in order to fully interpret the anisotropic DSC tests, the triaxial compression, DSS and triaxial extension test results on the same material were again necessary. Comparison of DSC data with the results of "standard" tests is made in Chapter 6.

The logical extension of establishing the anisotropy of overconsolidated BBC is to investigate the clay in the normally consolidated state. An immense amount of "groundwork" is necessary to achieve this intent, including establishing the stress-strain-strength parameters in the standard devices, determining the reloading value of K_o for reconsolidation, determining the minimum consolidation stress necessary to achieve a truly normally consolidated state and, finally, design of a technique for K_o consolidation and subsequent shear

in the DSC device. Some inroads have been made in preparation for normally consolidated testing in the DSC, as presented in Chapter 7.

(a) Field Situation for Strip Loading

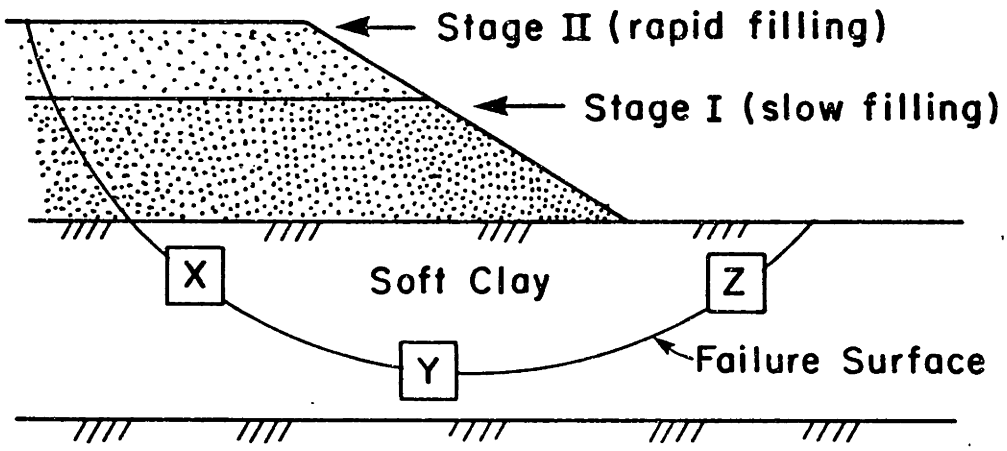

(b) States of Stress for Element Y (Plane Strain)

Condition	State of Stress
1. Prior to construction (K_o condition)	$\sigma'_{vo} = \sigma'_{1O}$; $\leftarrow \sigma'_{ho} = K_o\sigma'_{vo} = \sigma'_{3O}$; $\delta_1 = 0$
2. After consolidation under Stage I construction	σ'_{vc}; $\tau_{hc} = -\tau_{vc}$; $\leftarrow \sigma'_{hc}$ = σ'_{1c}; σ'_{3c}; δ_2
3. Undrained failure during Stage II construction	σ'_{vf}; $\tau_{hf} = -\tau_{vf}$; $\leftarrow \sigma'_{hf}$ = σ'_{1f}; σ'_{3f}; δ_3

Figure 1.1: Example of Embankment Construction on a Soft Clay Foundation.

CHAPTER 2

BACKGROUND

2.1 OVERVIEW OF TEST DEVICES FOR MEASUREMENT OF ANISOTROPIC CLAY PROPERTIES

2.1.1 Anisotropy

Anisotropy has a number of descriptive adjectives due to the variety of its causes. This research utilizes the definitions and connotations put forward by Ladd et al. (1977) as summarized by Germaine (1982). Specifically, the variation in the stress-strain-strength parameters of undisturbed natural soils as the direction of the major principal stress rotates with respect to the depositional direction is due primarily to the two following types of anisotropy:

(1) inherent anisotropy -that due to the depositional environment and subsequent K_o consolidation which characterized the material prior to the initiation of undrained shear; and

(2) stress system induced anisotropy - that due to the difference in the algebraic increment in shear stress necessary to cause failure as the major principal stress varies from parallel to the direction of deposition to perpendicular to the depositional axis. This type of anisotropy occurs only when $\frac{\sigma_{hc}'}{\sigma_{vc}'}$ is not equal to one.

Generally, most in situ cases involve both types of

anisotropy, particularly since normally consolidated, lightly overconsolidated and heavily overconsolidated clays have ratios of effective horizontal stress to vertical stress of either less than or greater than one. The anisotropy in such instances is termed "combined."

Previous tests in the DSC on sands refer to "strain-induced" anisotropy (Arthur et al., 1977) imparted to an initially isotropic sample by causing strain in a preferred direction. The effect of this anisotropy is then measured by orienting σ_1 at various angles with respect to the direction of prestraining. Strain induced anisotropy can be caused in either the originally isotropic plane of the sample or in a plane of the sample which already exhibits inherent anisotropy due to deposition and any subsequent K_o consolidation. The latter case, which is a combination of inherent and strain induced anisotropy is termed "initial" anisotropy (Ladd et al., 1977). The possible causes and effects for the aforementioned types of anisotropy are described by Germaine (1982).

The terminology adopted by this research with regards to anisotropy is as follows:

- inherent, combined or initial anisotropy - the angular variation of the direction of σ_1 from the direction of deposition and subsequent K_o consolidation (i.e. the vertical direction) is indicated by the Greek letter delta, δ. For example, for a compression test where σ_1 during shear is oriented parallel to the depositional axis, $\delta=0°$; for an extension test with σ_1 oriented

perpendicular to the depositional axis, $\delta=90°$.

- strain induced anisotropy or samples sheared in the isotropic plane without any preshear treatment -the angular variation of the direction of the major principal stress during shear is measured with respect to the direction of prestraining in the former case and with respect to an initially agreed upon direction (commonly associated with a specific feature of the test device) in the case of an isotropic plane. The angle is identified by the Greek letter psi, Ψ. $\Psi=0°$ when σ_1 is parallel to either the prestrained direction or the agreed upon direction in the isotropic case, and $\Psi=90°$ when σ_1 is perpendicular to either of these directions.

These symbols are in accord with those adopted by Arthur et al. (1981) and Germaine (1982).

2.1.2 Experimental Capabilities Currently Available

The elusive nature of anisotropic parameters coupled with the established need for these data have over the years inspired many to attempt their measurement. Germaine (1982) reviewed the variety of approaches currently taken and this research will briefly summarize his findings and incorporate subsequent advances.

Because the depositional environment for most natural clay deposits involves a unidirectional gravity field, the anisotropy most commonly encountered can be completely characterized in any plane parallel to the direction of deposition. The plane

perpendicular to the depositional axis exhibits isotropic behavior. Clays exhibiting such anisotropic characteristics are called cross anisotropic (or transversely isotropic).

Cross anisotropy commonly includes both an inherent component and a stress system induced component, together termed combined anisotropy as mentioned above. Although the anisotropy of BBC measured by this research is solely inherent (Chapter 5) since $K_o \approx 1.0$, the testing capabilities reviewed in this section are evaluated with respect to their ability to measure combined anisotropy.

Reference to Tables 2.1 and 2.2 (after Germaine, 1982) enables an organized approach to consideration of currently available soil testing devices for measuring combined anisotropy. The first table lists the capabilities necessary for accurate measurement of the change in stress-strain-strength behavior with rotation of σ_1. Table 2.2 considers six soil testing devices in light of each of the necessary capabilities. In general, in order to evaluate anisotropy one needs to apply a uniform, known stress state in which the direction of the principal stress can be chosen at will. The magnitude as well as the direction of the principal strains caused by the imposed stresses should also be uniform and measureable.

To accurately measure combined anisotropy, it is necessary first to reconsolidate the sample to the anisotropic in situ stresses. Therefore, previous studies involving UU, CIU and unconfined compression tests (e.g., experimental studies by Bishop, Hvorslev, Jacobson and Lo as cited by Duncan and Seed

(1966)) are an unreliable source of anisotropic strength data because of unrepresentative preshear (isotropic) stress states. Furthermore, even K_o-consolidated triaxial samples are suspect when the samples are "cut" such that the direction of deposition does not coincide with the long axis of the cylindrical sample since, again, in situ stresses cannot be duplicated.

In addition to the problems associated with consolidation, triaxial tests cannot accurately measure the behavior of clays at intermediate values of δ because the triaxial device transmits the axial force through rigid end platens. When the end caps are frictional, bending moments and shear stresses are induced in the inclined samples. When the end caps are lubricated, the rigid platens still induce bending moments but the sample is free to move laterally, causing the sample to deform in an "S" shape (Saada and Bianchini, 1977).

And, finally, although the triaxial cell can be used to measure the strength of clays at $\delta=0°$ and 90°, it incorporates the effect of very different values of b, the relative intermediate stress, with compression ($\delta=0°$) having b=0 and extension ($\delta=90°$) having b=1. It is concluded, therefore, that triaxial test results cannot be relied upon to generate anisotropic data.

Graham and Houlsby (1983) have developed an analytical technique which can approximate the prevield anisotropy of a material using the results generated by standard K_o-consolidated triaxial tests. The authors assume the material can be characterized using the theory of elasticity and further

simplify by assuming cross anisotropy which reduces the necessary elastic parameters from 21 to 5. The authors realize that the results are only approximations of the anisotropy of the material and are not of research quality. The same is true of anisotropic results generated experimentally by the triaxial device.

In order to mitigate confusion upon introduction of the variation in the relative value of σ_2, as quantified by $b \left(= \frac{(\sigma_2-\sigma_3)}{(\sigma_1-\sigma_3)}\right)$, with the various types of triaxial tests, Fig. 2.1 locates these tests relative to one another in a stress state space defined by b and δ. Germaine (1982) identifies which triaxial tests occupy the four corners of this plot as well as where the True Triaxial Apparatus (TTA), the Hollow Cylinder Apparatus (HCA) and the Directional Shear Cell (DSC) fall. Because $K_o \approx 1.0$ for the overconsolidated BBC tested in this research, the triaxial tests labelled TE-H and TC-H were possible since consolidation stresses are isotropic. The hatching on the samples illustrated in Fig. 2.1 is perpendicular to the direction of deposition.

The TTA is designed only to measure the effect of various relative magnitudes of the intermediate principal stress. Tests can be performed at the extreme values of δ (i.e., $\delta=0°$ and 90°) but not at intermediate values.

The Geonor Direct Simple Shear (DSS) device (not shown in Fig. 2.1) simulates plane strain behavior ($b \approx 0.4$) but the direction of σ_1 rotates continuously throughout the test. In addition, the state of stress in the DSS is not uniform and is,

to date, open to interpretation. Therefore, although the DSS may be used to determine an approximate intermediate δ strength - as originally suggested by Bjerrum (1973) and discussed by Ladd at the 1973 Moscow ICSMFE (Hansen and Clough, 1980) - the device cannot be used to detail the anisotropy of a material.

The Hollow Cylinder Apparatus allows controlled rotation of the principal stress direction by the application of axial normal and torsional forces as well as inner and outer cell pressures. By varying these stresses, theoretically any combination of b and δ should be possible. According to Germaine (1982), however, the HCA tests performed in the early 1960's (Wu et al., 1963 and Broms and Casbarian, 1965) involved different inner and outer cell pressures which caused a disturbingly high gradient of stress across the wall of the sample. The nonuniform stress state as well as the fact that failure did not occur simultaneously throughout the sample have caused researchers to question these data.

A.S. Saada has investigated the anisotropy of several clays using the HCA (e.g., Saada and Zamani, 1969; Saada, 1970 and Saada and Ou, 1973). Saada sidestepped the problem of stress nonuniformity by maintaining equal values of the inner and outer cell pressures. By so doing, the value of the relative intermediate stress is uniquely related to the angle of shear, δ, as indicated by the dashed line in Fig. 2.1. Therefore, results generated following these tactics do not separate the effect of the relative magnitude of σ_2 from that of anisotropy.

Rather than requiring equality of inner and outer pressures in the HCA, researchers at Imperial College, London investigated the minimization of the stress gradient across the wall thickness by varying the sample geometry (Hight et al., 1983). The result was a cylindrical sample ten inches in outside diameter with a one inch thick wall. Isotropic linear elastic finite element and elasto-plastic constitutive model (modified Cam clay) analyses reported by Hight et al. (1983) indicate that for samples of this geometry, the gradient across the wall is approximately 10%. Imperial College HCA accepts samples ten inches in height, designed to allow for stress and strain distributions at mid-height which are unaffected by end effects (Symes, 1983). Fig. 2.2 schematically illustrates the device.

Because of the above design considerations in addition to the careful attention given to other details of the experimental procedure, the Imperial College HCA is a device capable of generating quality data concerning the effect of inherent, stress system induced and strain induced anisotropy as well as the effect of the relative intermediate stress on soil behavior at various angles of shear. To date, however, it has been employed in the investigation of the effect of anisotropy on the stress-strain-strength parameters of cohesionless materials (e.g., Hight et al., 1983 and Symes et al., 1984).

Testing of saturated clays in the HCA requires either development of resedimentation and consolidation techniques within the device or design of procedures to reconstitute

relatively massive samples elsewhere and subsequently sample and install them in the device without causing disturbance. Measurement of pore pressure at mid-height in the sample would also be necessary but could be easily accomplished using the probe developed by Hight (1982). Should the Imperial College HCA be adapted for undrained clay testing it would be valuable to perform HCA tests similar to the DSC tests performed in this research on the same material for comparison. Although the HCA is a stress-controlled device (as is the DSC) the computer control and immediate calculation of strains enable reduction of stresses to maintain strain rates thereby enabling measurement of strain softening behavior.

Besides the HCA, the only other presently available device capable of measuring the effect of anisotropy on the behavior of cohesionless materials and, as yet, the only device suitably adapted to measure the anisotropic behavior of clay is the Directional Shear Cell. As seen in the last device entry of Table 2.2, the DSC fulfills all the necessary qualifications for accurate measurement of anisotropic behavior. Photographs of the DSC in partially and fully assembled states are provided in Fig. 2.3.

One can recreate the in situ K_o consolidation conditions by applying σ_1 and σ_3 and allowing the glass platens to restrict strain in the σ_2 direction. Fig. 2.3a illustrates the stress application capabilities of the DSC. In addition to the four accordian-like flexible pressure bags for the application of normal stress (only two are shown) there are two sets of

shear sheets to apply shear tractions to the non-plane strain faces of the cubical (4 in.) sample. Details of the shear sheets and the pressure bags can be found in Germaine (1982). Aspects of those receiving attention in this research are discussed in Chapter 4.

Fig. 2.4 depicts a cross section through a dense sand sample similar to those performed by Bekenstein (1980). To measure strains, tungsten carbide ball bearings were embedded mid-height in the sample and, rather than taking a photograph of a grid inked on the membrane encasing the sample as is the practice with clay samples, a radiograph is taken. Note that retaining vanes are attached to only one side of each pressure bag. This feature is altered in this research by the use of thin stainless steel vanes on both sides of the bags to improve the stress application (Chapter 4).

The shear and normal stress application systems are adjustable to enable "following" the sample as strain progresses. The bags and sheets must be parallel to each face of the sample in order to apply the correct stress. Stress corrections are made as the sample distorts, but it is very important that the sample be allowed to strain naturally. Monitoring the pore pressure during an increment of stress provides an indication of when strain is inhibited by either shear sheet or pressure bag misplacement. With careful operator attention, the DSC can successfully handle up to approximately 15% shear strain.

Although the MIT DSC is not so equipped, steps have been

taken to measure the intermediate principal stress, σ_2, both prior to and during shear (Arthur, 1983, pers. communication). The method involves flexible bags such as those used to apply σ_a and σ_b with a slightly different design. However, Arthur reports some normal strain in the plane strain direction using these bags.

An extensive testing program on dense and loose Leighton Buzzard Sand (Bekenstein, 1980 and Arthur et al., 1981) indicates that the DSC yields reliable data with regard to the anisotropy of cohesionless materials. The purpose of this research is to prove that the DSC is capable of generating research quality data on the anisotropy of saturated clay.

2.2 OVERVIEW OF DSC CAPABILITIES AND TEST PROCEDURES

2.2.1 Conceptual Basis for Isotropic "Proof" Tests and Anisotropic Tests

This sections describes the DSC in detail. The DSC is a plane strain device in which application of normal and shear stresses is achieved, respectively, through flexible pressure bags and shear sheets. Photographs and a schematic diagram of the device identifying the key components are shown in Figs. 2.3 and 2.4, respectively.

The uniqueness of the DSC lies in its capability to apply a shear traction to four faces of the prismatic (cubic) sample while simultaneously applying a normal stress to each face. This capability enables rotation of the major principal stress by up to 90 degrees during a test (shear tractions are capable

of acting in one direction only and hence the origin of planes on the Mohr circle cannot change from the positive shear stress side to the negative side or vice versa). Fig. 2.5 illustrates the stress application scheme in the DSC as well as the reference axes used to determine the angles of shear.

One of the most important features of the DSC adapted for testing saturated clay samples is the ability to measure pore pressures. This measurement is accomplished by a probe developed and completely described by Germaine (1982). Germaine also describes the design of the shear sheets and the pressure bags, as well as the construction of the latter element in detail.

Since the DSC creates a plane strain environment for the membrane encased cubical sample, one plane of the material can be investigated at a time. The cross anisotropic nature of the resedimented Boston Blue Clay (BBC) yields one plane - that perpendicular to the deposition direction - which is isotropic. The fact that the behavior of this isotropic plane can be investigated in the DSC by setting the "top" of the sample (i.e. the plane normal to the depositional axis) flush with the glass platen allows the researcher to study device induced errors. With no further treatment such as prestraining, all orientations of the major principal stress should yield identical stress-strain-strength characteristics as well as identical strain distributions. Thus, an extensive series of isotropic tests were performed to determine whether or not the DSC device could actually perform as intended. This effort is

considered to be a vital part of the research. The results of these "proof" tests are presented in Chapter 4.

The anisotropic test series in the DSC are performed by orienting the direction of deposition parallel to the plane strain platens. Such placement of the sample (wherein the sample is essentially tipped on its side) tests the planes exhibiting cross-anisotropic behavior. In this position one can measure compression behavior at $\delta=0°$ (a plane strain active test) and extension behavior at $\delta=90°$ (a plane strain passive test) as well as the behavior at any intermediate δ angle.

Due to the sample resedimentation and reconsolidation procedures followed (discussed in Section 2.2.2) the BBC samples tested in the DSC at MIT to date have been at an OCR=4.0. Such a preshear stress state, where $K_o \simeq 1.0$, means that the type of anisotropy measured in the BBC is inherent.

Actual measurement of K_o upon reconsolidation to a vertical stress equal to one quarter of the preconsolidation pressure of 1.0 ksc in both the triaxial cell and the MIT Lateral Stress Oedometer reveal that $K_o \simeq 0.74$ (see Fig. 2.6, reloading curve at OCR=4). In the DSC, linear consolidation strains upon reconsolidation were generally on the order of a quarter of a percent with $\varepsilon_h \simeq \varepsilon_v$ (see Tables 4.2 and 5.1). Because of the "perfect sampling" which all the resedimented BBC samples experienced one would expect very small reconsolidation strains. However, such low strains involve a large error due to both differential film shrinkage and the digitization technique (Section 4.2), rendering them useless

in assessing whether or not K_o conditions existed. Regardless of consolidation strains, since vertical and horizontal consolidation stresses were equal, the preshear stress state is isotropic, precluding any stress system induced anisotropy.

Table 2.3 lists some of the physical aspects of all the DSC tests (anisotropic and isotropic) performed for this research on resedimented BBC. DSC-1 through DSC-8 were originally reported by Germaine (1982) without consideration for the effect of extended storage time on the undrained shear behavior. Since DSC's 1 through 16 were performed in the developmental stage of the adaptation of the DSC for clay testing, items such as film type and use of prisms were different for selected tests. In addition, the direction of digitization, primarily a function of the quality of the zero point image, is recorded in order to appropriately align the strain axes, x and y, with the vertical and horizontal axes of the sample (as defined in Fig. 2.5), Z and X, for the anisotropic tests and with X and Y for the isotropic tests. This information allows determination of the orientation of the strains with the sample's position in the device.

The separation of the two plane strain platens is measured in four locations for each test. This measurement is necessary since the distance between the platens is dictated by the sample - i.e., when contact with the sample is made by the top platen, the platen is locked. The data presented are the average of four measurements and the standard deviation.

2.2.2 Resedimentation and Preparation of Overconsolidated Boston Blue Clay Samples

Development and proving of a new device requires samples which are uniform in and of themselves as well as between different batches. Research with the DSC falls into this category. In addition to uniformity, full saturation of the clay is also necessary due to the lack of backpressuring capabilities. Germaine (1982) developed a resedimentation technique which produces saturated, uniform samples of BBC with a salt concentration of 16 grams per liter. The technique minimizes disturbance of the resulting batch of samples by completing the consolidation cycle, which has a maximum vertical stress of 1.0 ksc, at σ'_v=0.25 ksc thus establishing the final presampling stress state at an OCR=4 and hence under almost isotropic conditions.

As mentioned in Section 2.2.1, K_o is approximately equal to 0.74 for reloading to an OCR=4 for resedimented BBC. However, in the resedimentation procedure, the stress state at OCR=4.0 is reached via unloading for which the MIT Lateral Stress Oedometer and triaxial tests give $K_o \simeq 0.92$ (see Fig. 2.6). Therefore in the resedimentation chamber immediately prior to shear the sample is in an almost isotropic state of stress and hence "disturbance" associated with the release of shear stresses is minimized.

One of the drawbacks with the resedimentation procedure is the time required to complete a batch of clay (approximately one month). About three weeks of this time is required for

consolidation of the slurry. In the interest of increasing the rate of sample production, this research built a "bottom" chamber similar to that described by Germaine (1982) into which the deaired slurry is rained and ultimately consolidated. This second stainless steel bottom chamber allowed for overlapping the production of two batches of clay by about two weeks.

The batch is "sampled" by excavating approximately 1/8 in. around the perimeter of the cylindrical cake to release adhesive forces between the clay and the chamber, thus preserving the undisturbed nature of the 11-3/4 in. in diameter cake (Martin and Ladd, 1970; and Germaine, 1982). One feature of the sampling procedure suggested by Germaine which contributes to reducing the initial negative pore pressure is that the approximately five hour excavation step takes place while the cake is situated atop the saturated bottom porous stone. The negative pore pressures within the sample need only surpass the capillary forces of the stone to have access to its water. (The ceramic porous stone used by the batches of BBC prepared for this research has a capacity of approximately 80 milliliters of fluid while the ridges in the base itself and the filter paper can hold an additional 20 milliliters). An improvement to the present technique is suggested in Chapter 7.

Storage of samples coarsely trimmed for DSC testing, as well as of those for triaxial, DSS and oedometer tests, is carried out in accordance with Germaine (1982). Each batch of clay is always supported on a plate and is coated with Saran Wrap, a thin coat of wax, aluminum foil and finally sealed with

an approximately 1/16 to 1/8 in. covering of wax (one half (by volume) paraffin for strength and one half beeswax for moisture retention, both with a melting point of approximately 150°F). The clay is then shelved in a room maintained at 95 to 100% relative humidity.

As discussed in Chapter 3, the amount of time which elapses between the application of the final consolidation stress and when a specific sample is finally trimmed for testing and reconsolidated to the "overburden stress" of 0.25 ksc has a significant effect on the stress-strain-strength behavior measured. Therefore, documentation of the entire resedimentation and testing processes is very important.

Trimming of the cubic DSC sample in preparation for testing is facilitated by the mitre device designed by Germaine (1982). The details of trimming are provided in Appendix C of Germaine's thesis. If the sample is to be sheared at an intermediate value of Ψ or δ necessitating use of the shear sheets, the two diametrically opposite corners which are to be situated where the shear sheets intersect are removed and replaced by plexiglass prisms attached to the membrane.

Prior to trimming, the latex membrane treated with rutile (TiO_2) for an opaque white color, is prepared for placement over the trimmed block of clay. Each membrane is fabricated by dipping a very clean grease-free aluminum mold into a methanol-based coagulant which is then allowed to crystallize in a 60°C oven for approximately one hour. The warm mold is then dipped into liquid white latex for approximately five

seconds. The entire process is detailed by Germaine (1982).

A box-shaped plexiglass membrane stretcher, illustrated in Germaine (1982), enables preparation of the cured latex. The aforementioned plexiglass prisms, used in all tests involving use of the shear sheets, are glued to the appropriate corners of the membrane with a waterproof rubber adhesive. (A new prism design is discussed in Chapter 4). A one-grain thick coating of fine sand is glued to both the plexiglass and latex surfaces which are expected to adhere to the clay. The sand is uniform, having been passed through a U.S. No. 40 sieve and retained on a No. 50 sieve.

Germaine (1982) demonstrated both the necessity and the sufficiency of both the sand layer and the reinforcing prisms by performing $\delta=45°$ tests with and without these features. The DSC $\delta=45°$ test without sand proved that the membrane alone was inadequate in transferring shear as it was simply drawn along the sample surface. The test (DSC-3) was unloaded and then resheared at $\delta=0°$. DSC-4, also sheared at $\delta=45°$, was prepared with the layer of sand but without the prisms. The strain distribution data for this test (Fig. 4.2) demonstrate the early and progressive yield of the two vulnerable corners where the shear sheets intersect.

Once the vacuum-expanded membrane has been carefully lowered over the sample and the mold subsequently removed, the sample is overturned to expose the unprotected surface which will ultimately be flush with the bottom platen of the DSC. A channel is excavated and the pore pressure probe is penetrated

1.5 in. into the center of the sample. Two drainage tubes (1/8 in. O.D.) with fabric filters are installed in the corners where prisms are located (or where 1/4 in. wide strips of filter paper are located in the case of δ, ψ=0° and 90°). The base is then sealed with waterproof rubber contact adhesive and dental dam.

Unlike Germaine's procedure, wherein the grid is inked on the membrane before placement on the sample, this research drew the grid when the sample had been sealed in the membrane. This technique enabled improved and consistent alignment between the grid and the sample. (Calculation of the deviation of the direction of principal strains from that of the principal stresses assumes that the lines on the grid are parallel to the faces of the cube).

An additional alteration of the original technique (Germaine, 1982) was to remove the bottom platen from the DSC testing platform (Fig. 2.3) to facilitate the positioning of the sample without disturbance. The platen, with the centered sample and the shear sheets, if appropriate, in place, is easily reattached via four knurled nuts to the DSC frame. The top platen is lowered gently and locked in place with top and bottom wing nuts. Finally, the pressure bags are locked in place. A seating load of approximately 0.03 ksc is applied using all four pressure bags. This stress is left on overnight and the following day the initial pore pressure is recorded.

GENERAL	• Ability to apply or respond to a kinematic constraint with a uniform state of stress with known magnitude and direction of the three principal stresses • Ability to handle responding state of strain or to apply kinematic constraint such that the state of strain is uniform with known magnitude and direction of the three principal strains.
SPECIFIC	• Ability to consolidate sample one-dimensionally prior to shear with known value of K_o • Ability to monitor pore pressures prior to and during shear • Ability to control the direction of the applied major principal stress, σ_1, during shear such that the angle of shear, δ, can be rotated anywhere between δ=0° (vertical) and δ=90° (horizontal) • During stress axis rotation, ability either: (1) to maintain constant relative intermediate stress, b, condition or (2) to maintain constant intermediate principal strain condition (e.g., ε_2=0 for plane strain)

Table 2.1: Requirements for Measuring the Combined Anisotropy of Soft Clays in Laboratory Shear Devices (after Germaine, 1982).

APPARATUS	Stress State		Strain State		1-D Consolidation with Known K_o	Controlled σ_1 Direction	Independently Controlled ϵ_2 or σ_2 Condition
	Uniform	Known	Uniform	Known			
1. Triaxial Cell	Yes	Yes	Yes	Yes	Yes	No (only δ = 0 & 90°)	No
2. Plane Strain	Yes	Yes	Yes	Yes	Yes	No (only δ = 0 & 90°)	Yes
3. True Triaxial	Yes	Yes	Yes	Yes	Yes	No (only δ = 0 & 90°)	Yes
4. Geonor Direct Simple Shear	No	No	Yes?	Yes?	Yes?(1)	No. Continuous Rotation	Yes?
5. Hollow Cylinder							
a. $P_o = P_i$	Yes	Yes	Yes	Yes	Yes	Yes	No
b. $P_o \neq P_i$	No	Yes	No	Yes?	Yes	Yes	Yes
6. Directional Shear Cell	Yes	Yes (Except σ_2)	Yes	Yes	Yes	Yes	Yes ($\epsilon_2 = 0$)

(1) Usually assumed since measurement of K_o quite difficult.

Table 2.2: Assessment of Laboratory Shear Devices for Measuring Combined Anisotropy of Soft Clays (from Germaine, 1982).

TEST	BATCH NO.	t_s (days)	δ (°)	ψ (°)	FILM TYPE	MAGNIFICATION (TARGET)	DIGITIZED ORIENTATION	SHEAR SHEETS/ PRISMS	w_i (%)	w_f (%)	u_i (ksc)	Plate Sep. (cm) $x/\overline{SD}$	REMARKS
DSC-1	101	29	0		ILFORD	x 20 (GRID INTERSECTIONS)		No/No	40.56	39.39	-0.141	10.548/ 0.070	
DSC-2	101	44	90					No/No	40.81	40.31	-0.077	10.317/ 0.066	
DSC-3	102	60	0					Yes/No	39.70	39.39	-0.111	10.324/ 0.039	• sheared at δ=45° w/no sand on membrane; • resheared at δ=0°
DSC-4	102	71	45					Yes/No	39.81	39.78	-0.093	10.330/ 0.064	• sand on membrane but no prisms
DSC-5	103	34	45					Yes/Yes	40.06	39.99	-0.070	10.292/ 0.025	
DSC-6	103	48		0				No/No	40.2	39.6	-0.147	10.321/ 0.031	
DSC-7	104	15		45				Yes/Yes	39.6	39.9	-0.074	10.311/ 0.056	
DSC-8	104	167	65					Yes/Yes	40.62	40.43	-0.145	10.329/ 0.069	
DSC-9	105	169		25				Yes/Yes	40.9	40.8	-0.122	10.595/ 0.118	• deleted prisms from strain calculations
DSC-10	105	207	20					Yes/Yes	41.10	40.90	-0.118	10.312/ 0.031	• deleted prisms from strain calculations
DSC-11	106	71	75					Yes/Yes	40.88	40.56	-0.103	10.314/ 0.043	• deleting prisms has no effect on strain calculations
DSC-12	106	91		0				Yes/Yes	40.6	40.8	-0.148	10.292/ 0.025	• deleting prisms has no effect on strain calculations
DSC-13	107	39	40					Yes/Yes	41.76	41.15	-0.094	10.327/ 0.065	• vanes on both sides of bags
DSC-14	109	79		40	KODAK ORTHO-LITH			Yes/Yes	42.07	42.08	-0.101	10.311/ 0.033	• deleted prisms from strain calculations
DSC-15	109	92	20					Yes/Yes	41.57	41.89	-0.130	10.318/ 0.070	• deleted prisms from strain calculations
DSC-16	110	105	75			x50 (DOTS)		Yes/Yes	40.31	39.99	-0.152	10.337/ 0.087	• new chevron-shaped prisms

Table 2.3: Summary of DSC Tests Performed on Resedimented BBC (OCR=4)

Pg. 55

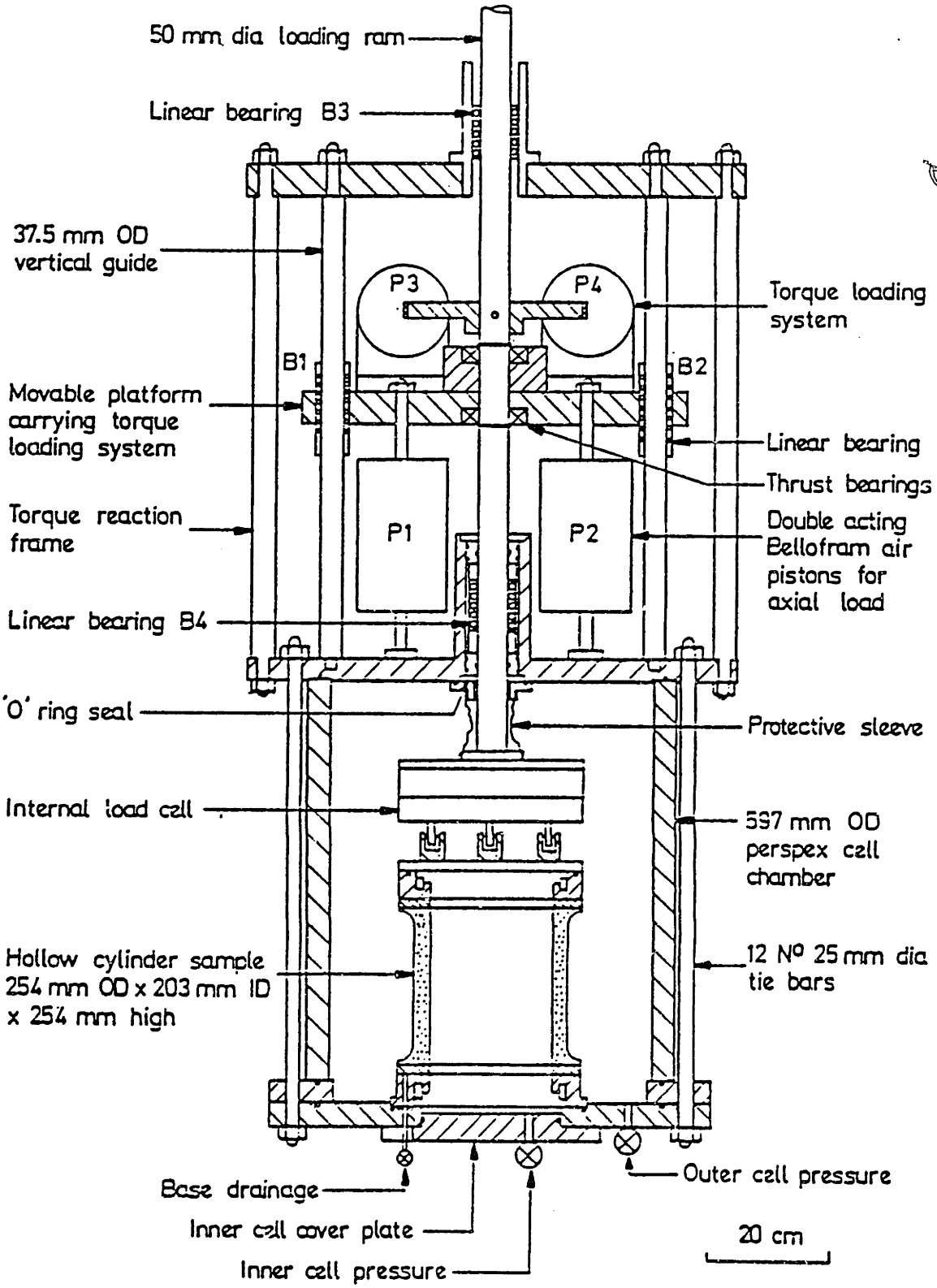

Figure 2.2: Schematic of Imperial College Hollow Cylinder Apparatus (from Symes, 1983).

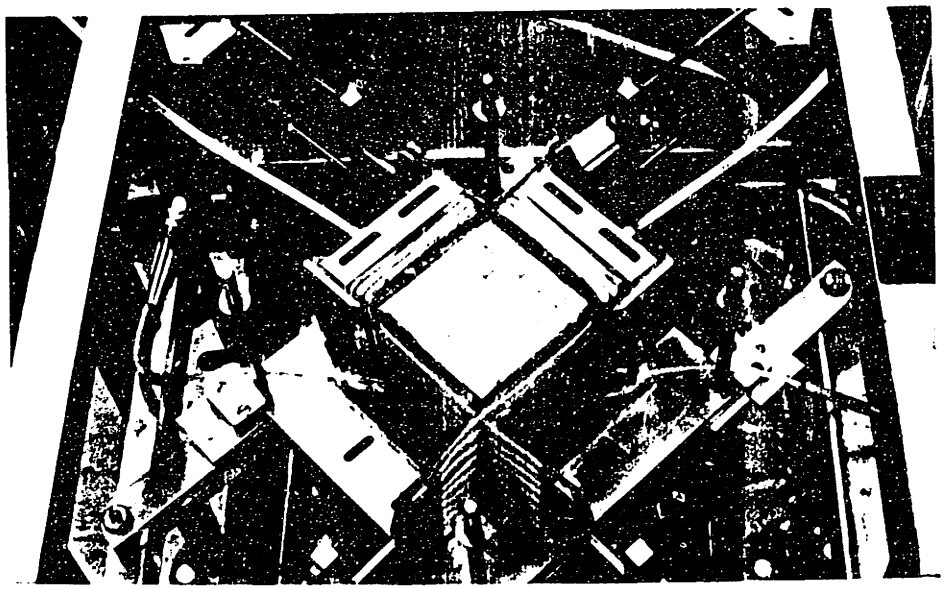

(a) View of Partially Assembled DSC Showing Sample with Shear Sheets and Two of the Four Pressure Bags (Arthur et al., 1981)

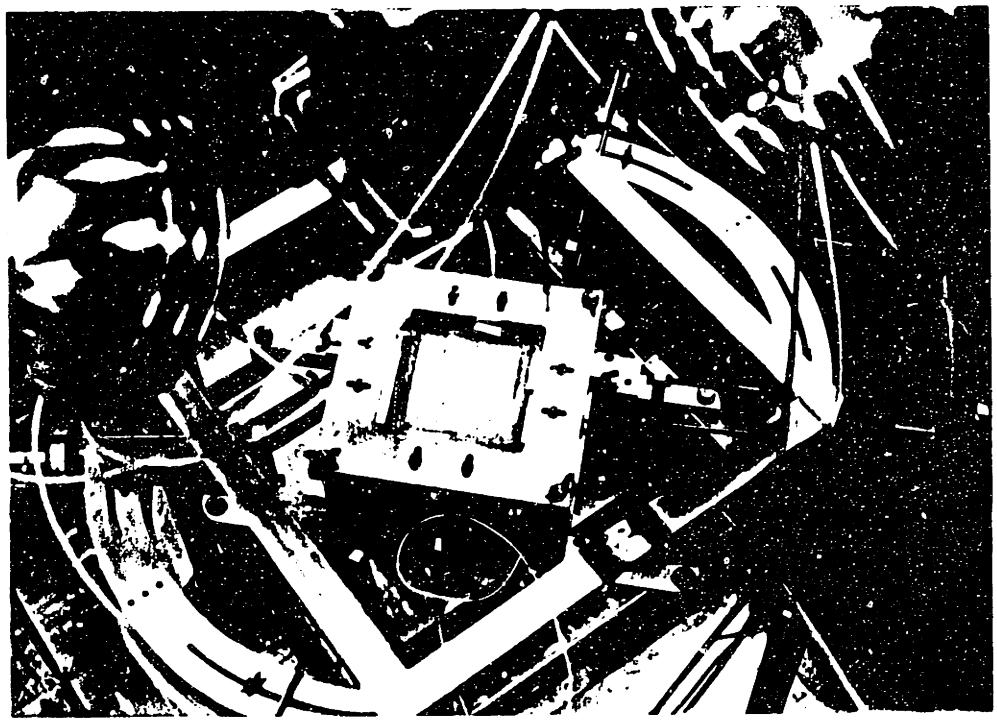

(b) View of Fully Assembled DSC Showing Measurement Grid and Plate Camera

Figure 2.3: View of (a) Partially Assembled DSC Showing Sample with Shear Sheets and Two of the Four Pressure Bags (Arthur et al., 1981) and (b) Fully Assembled DSC Showing Measurement Grid and Plate Camera.

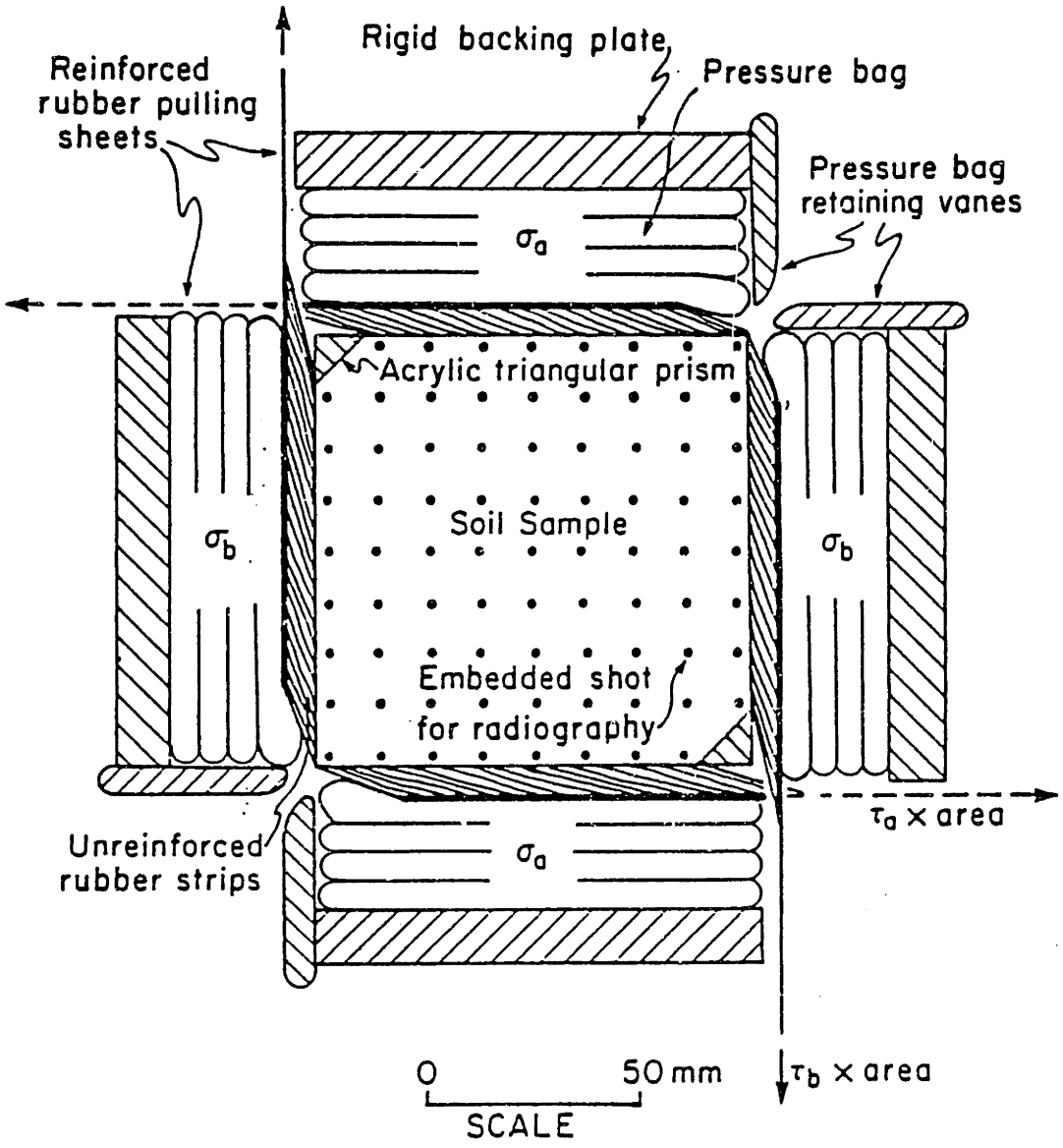

Figure 2.4: Diagram of Method used to Apply Normal and Shear Stresses in the UCL Directional Shear Cell (Arthur et al., 1981).

(a) Principle Underlying DSC (At small strains)

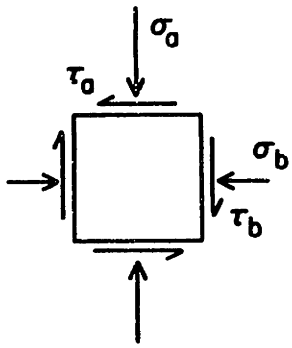

- σ_a & σ_b applied via "normal pressure bags"
- $\tau_a = -\tau_b$ applied via two sets of "shear sheets"
- Varying σ_a, σ_b and $\tau_a = -\tau_b$ controls σ_i direction

(b) Reference Axes and Angles for DSC Testing

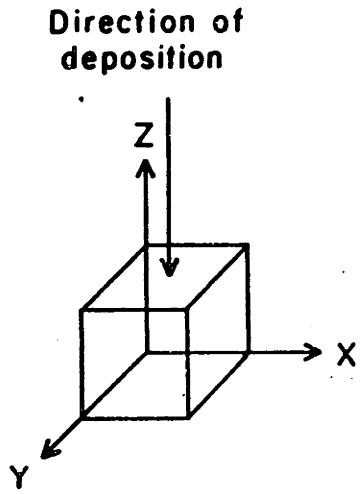

(1) Sample orientation

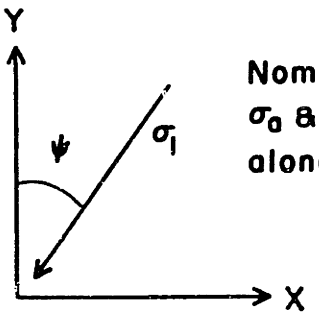

Nominally:
σ_a & σ_b act
along Y & X axes

(2) Tests in X-Y plane
(no anisotropy)

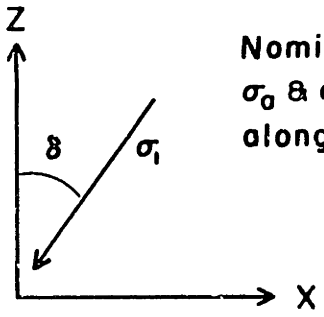

Nominally:
σ_a & σ_b act
along Z & X axes

(3) Tests in X-Z plane
(with anisotropy)

Figure 2.5: Directional Shear Cell: Principle and Definitions (from Germaine, 1982).

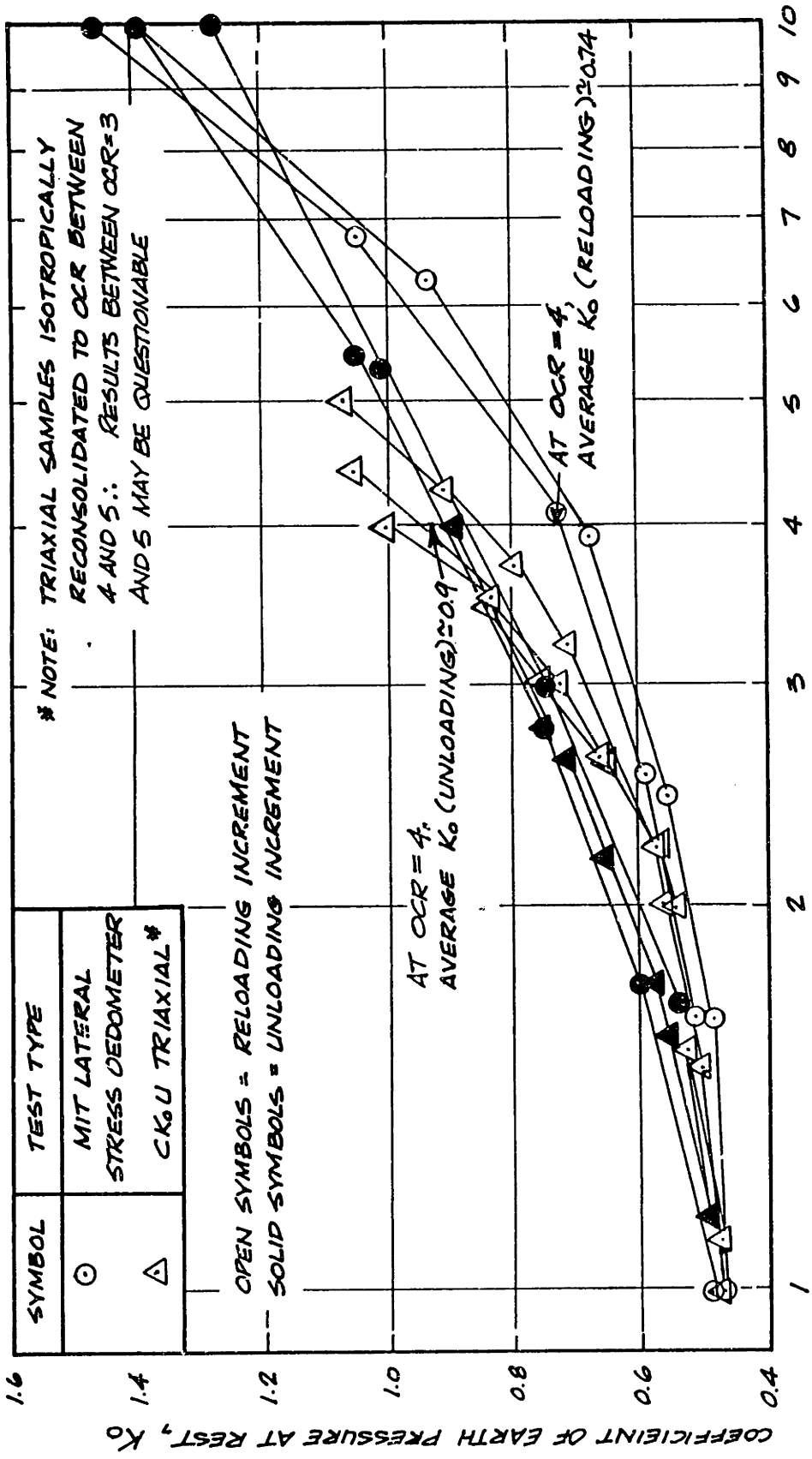

Figure 2.6: Variation of K_o with OCR for Resedimented BBC from Laboratory Tests.

CHAPTER 3

THIXOTROPIC NATURE OF RESEDIMENTED BOSTON BLUE CLAY

3.1 BEHAVIORAL CHANGES CONFORMING TO THE DEFINITION OF THIXOTROPY

An extensive laboratory testing program on undisturbed resedimented Boston Blue Clay (BBC) has revealed its propensity for changes in strength and compressibility as the time of storage between sampling and testing is varied. Specifically, the material exhibits an increasing preconsolidation pressure, decreasing recompression ratio and increasing undrained shear strength and initial stiffness (as measured via recompression-type triaxial compression and extension tests) as the elapsed storage time lengthens. As these phenomena are not accompanied by a measurable trend with respect to changes in water content the suspected cause is thixotropy.

3.1.1 Introduction

The term 'thixotropy', coined in 1927 by Arch. F. Peterfi and first defined in 1935 by H. Freundlich is presently "defined as an isothermal, reversible, time dependent process occurring under conditions of constant composition and volume whereby a material stiffens while at rest and softens or liquifies upon remolding" (Mitchell, 1976).

3.1.1.1 Effect of Storage Time on Water Content and Index Properties

The condition of constant composition requires that the water content of the sample remain unchanged with time. Fig. 3.1 illustrates the water content history for nine batches of resedimented BBC as determined for individual samples at the time of DSC, triaxial, DSS or consolidation testing. The rationale for the determination of the storage time parameter, t_s, is discussed in Section 3.1.3.2. There is no measurable trend of decreasing water content with increasing storage time within a given batch.

The constant composition condition further requires that neither the chemistry nor the mineralogy of the material change with time. Direct investigation of these aspects of composition is difficult as the changes may be small. X-ray diffraction of air-dried samples which have experienced varying storage times is a potential investigative method, although if the change is too small or if hardening is due to an amorphous precipitate (i.e., cement) diffraction would not be suitable. Adsorption studies may be necessary to conclusively document soil mineralogy and chemistry with time (Martin, 1958).

Indirectly, however, there are data substantiating the contention of constant composition. The Atterberg Limits, a measure of a particulate medium's remolded behavior in reaction to varying amounts of water, are presented in Table 3.1. These data vary slightly with the liquid limit, w_L, and the plasticity index, I_p, ranging from 40.2 to 42.4% and 16.2 to 20.8%,

respectively. Such variations in w_L are within both the expected accuracy of the test and the expected batch to batch consistency of the material. The variation in I_p is similar if one discounts the low value which has a questionable plastic limit determination.

The two cases in which one batch was tested at two different times (i.e., Batch Nos. 105 and 111) seem to indicate slight increases in w_L accompanied by even greater increases in I_p. In the case of Batch No. 111, the increase in w_L might be explained by use of a hard rubber base on the liquid limit device for the older sample and a micarta base for the younger. For Batch No. 105, however, although it is likely that a micarta base was used in the t_s=366 days test (it is not known for certain). In addition, error in the younger plastic limits may be due to operator inexperience which generally leads to overestimation of that parameter. It is concluded, therefore, that the Atterberg Limits do not demonstrate appreciable change with increasing storage time.

Furthermore, electrolyte concentration and organic content measurements presented in Table 3.1 do not show any appreciable change (in light of the expected precision of the various tests) with increasing storage time. In addition to these data, the following discussion of reversibility will imply constancy of composition.

3.1.1.2 Fall Cone Test Series on Remolded BBC

The definition of thixotropy put forth by Mitchell (1976)

is more readily applied to slurries and compacted or remolded materials where reversibility is concerned, as this feature is easier to evaluate for these cases than for consolidated samples. Seed and Chan (1957) performed a study in which samples of a lean silty clay (w_L=37%, w_P=23%) were compacted, stored, tested, broken up, recompacted, stored again for the same period of time and then tested again. The similarity of results indicate that the phenomenon is completely reversible. Since remolding a stored resedimented sample of BBC would remove the depositional structure accorded to the clay during consolidation, proof of reversibility would require complete reconstitution of the same material. Given the elaborate and time consuming nature of the resedimentation process (Germaine, 1982), the question of reversibility was addressed through investigation of remolded BBC material.

A test series was performed involving the fall cone penetrometer, an index strength device, and small containers of remolded, previously resedimented BBC. The thoroughly remolded clay was packed at a water content equal to its liquid limit (w_L≈40%) in cylindrical polyethylene containers (5.1 cm in height, 3.13 cm in diameter) taking care to avoid entrapment of air. The sample was then either tested immediately to determine t_s=0 penetration depths or waxed and stored in a humid environment for varying storage times. Water contents were carefully controlled during the testing program to eliminate the complicating factor of hardening due to loss of water content. The polished stainless steel cone with an apex of 30° was

outfitted to weigh approximately 75 grams and positioned at the surface of the clay before being allowed to fall freely for five seconds. Penetration was readable to 0.05 mm.

The results of the fall cone penetrometer tests on the remolded BBC are presented in Fig. 3.2. A definite trend of decreasing penetration depth with increasing storage time is indicated by the open circles. If one regards the fall cone results as measurements of strength (Wroth & Wood, 1978), the samples become stronger with time. However, since the sample containers violate the minimum diameter requirement (diameter $\geq$ 55 mm) suggested by, for example, the British Standard 1377 (1975), there is a possible problem of interaction of the wall with the region of deformation in the clay (Houlsby, 1982). Therefore, there is no attempt made in this study to relate penetration depth changes to actual strength changes.

A number of samples were remolded immediately after penetration of the cone and retested. The variation in the penetration depths indicated by the solid symbols is believed to be due to the entrapment of air upon remolding in the container. Accepting the scatter, the remolded material, when allowed no time to harden, returns to a penetration depth of approximately 11 mm. Reversibility is further established by the results of a sample tested at t_s=44 days which was subjected to the following testing sequence: (1) after 44 days storage, the penetration depth, d, was equal to 5.9 mm; (2) remolding within the container yielded d=11 mm; (3) repacking the clay (supplemented with additional prestored clay due to

material lost in measuring the water content) and restoring until t_s=1.2 days resulted in d=8.5 mm; and, finally, (4) once again remolding within the container yielding d=11.4 mm. These results prove that a sample of remolded BBC can repeatedly demonstrate a gain in strength upon remolding and subsequent storage.

The water content data at the top of Fig. 3.2 indicate that, although w is consistently lower for the sample at the time of testing, evaporation with storage time is not suggested. Slightly lower water contents at the time of the test are probably the result of the extended effort used to pack the samples in the polyethylene containers. (The water content for the sample was taken from the bowl of remolded clay before packing).

Hence, the fall cone results of decreasing penetration with storage time which can be interpreted as a completely reversible increase in strength or a stiffening of the material occurs under conditions of constant composition. The samples remained at room temperature and although slight shrinkage was exhibited by the sample no mass was added or lost so constant volume is assumed (thus implying 100% saturation when packed). In addition, upon remolding the sample softens. Therefore, the resedimented Boston Blue Clay used for this research at w=40% and a salt concentration of 16 grams/liter is susceptible to thixotropic effects.

As mentioned previously, the fall cone test series provides further evidence that the strengthening phenomenon is

not due to a chemical change such as cementation. Using the hypothesis of Mitchell (1960), mechanical remolding, although likely to destroy bonds strengthened by cementation, is unlikely to redissolve the precipitate. Fall cone tests were performed on material from a number of different batches. Since times of storage for these batches varied considerably, the rate at which cementation proceeds should vary due to the decreasing chemical gradient (i.e., the sample should be getting closer to attaining chemical equilibrium). Hence, the rate at which the strength increases should vary considerably; a feature not supported by the data in Fig. 3.2.

The thixotropic effect has been correlated to liquidity index ($I_L = \frac{w_N - w_P}{w_L - w_P}$) for several clays. Skempton and Northey (1952) performed a study wherein it was found that the thixotropic effect on remolded clay, packed in plexiglass containers and later tested with the lab vane, decreased for values of I_L less than one. The hardening effect was most pronounced at I_L=1.0, with the exception of the Beauharnois Clay, as presented in Fig. 3.3a.

Mitchell (1960) also referred to the maximizing of the thixotropic effect by varying the water content in his treatise on thixotropy (Fig. 3.3b), although he identified an $I_L \approx 0.3$ as that which resulted in the most significant stiffening effect. (The Thixotropic Strength Ratio in Fig. 3.3b is equal to the ratio of the strength at the time of testing with that at t=0). The difference between this study and Skempton and Northey's investigation is that Mitchell compacted his Vicksburg silty

clay samples thus imparting some structure and particle orientation compatible with a certain degree of applied stress.

The resedimented BBC studied in this research existed at an I_L = 1.0 after reconstitution as a batch. Reference to Skempton and Northey's work (1952) would indicate that in this state, the BBC should exhibit the maximum thixotropic effects possible for the material. On the other hand, Mitchell's (1960) work suggests that the BBC would demonstrate more significant thixotropic phenomena if it was at a water content in the vicinity of 26% ($I_L \approx 0.3$).

There are insufficient data available on the effect of water content, sample preparation and type of strength test performed on the ultimate thixotropic behavior on BBC to draw any conclusions. Information regarding thixotropy in this research, therefore, is specifically associated with resedimented BBC (and remolded BBC for the fall cone test series) at water contents approximately equal to 40%.

3.1.2 Effect of Storage Time on Initial Pore Pressure

Decreasing initial pore pressures with increasing storage time were reported by P.R. Day (1954) in his investigation into the effect of shear forces on the undrained strength of saturated remolded clays. In this study, Day remolded samples of clay at water contents approximately equal to the liquid limit and continuously monitored pore water tension with a tensiometer. When the pore pressure reached an essentially

constant value, the sample was again mechanically remolded and, when the stirring action had ceased, increasing pore water tension with time was again recorded (Mitchell, 1960).

Measurements of the initial pore pressures of individual resedimented BBC samples, as measured under conditions of zero total stress, are presented in Fig. 3.4. Although obscured by considerable scatter, there is a general trend toward increasing initial effective stress as measured with the DSC pore pressure probe with increasing storage time. Also included in Fig. 3.4 are data obtained from triaxial samples. These data exhibit even greater scatter than the DSC sample data for the following reasons: (1) triaxial samples are smaller in volume than DSC samples and hence pore pressures are inherently more susceptible to change due to disturbance; (2) triaxial pore pressures are measured at the surface of the samples and hence are dependent on the quality of contact made with the sample whereas the DSC probe is inserted into the center of the sample; and (3) the triaxial pore pressure measurement system has a greater reservoir volume to sample volume ratio than the DSC system even when the negative pore pressure base (Jordan, 1979) is used. (The volume between the transducer of the negative pore pressure base and the sample base is less than 0.1% of the sample volume but is still about eight times greater than the reservoir volume to sample volume relationship for the DSC system).

An attempt was made to monitor pore pressure changes with time for an unstressed "young" resedimented BBC sample.

Temperature control problems, however, precluded rational interpretation of the results. Such u_i vs t_s information, however, would be valuable as it would substantially reduce the variability inherent in Fig. 3.4 due to sample to sample differences.

Mitchell (1960) attributes lowering of the initial pore pressure to the samples' tendency to seek equilibrium by lowering its free energy. He does not rule out the possibility that some of the water may experience changing structure wherein the fluid proceeds from free water to a more ordered condition and that this phenomenon is reversible (Mitchell, 1976). The more negative pore pressure is not believed to be the cause of the increasing strength, altered shear-induced pore pressure behavior or the increasing preconsolidation pressure to be discussed in the following sections. Section 3.2 presents data substantiating and further explaining this contention.

3.1.3 Effect of Storage Time on Consolidation Test Results

3.1.3.1 Variation in Measured Preconsolidation Pressure with time

Perhaps the most remarkable consequence of extended storage times is the variation in measured maximum past pressure or preconsolidation pressure, $\sigma'_p(t)$. Perplexed by the seemingly disparate values obtained from the first few oedometer tests, an effort was launched to determine if there

was "batch to batch" variability in the resedimented BBC samples. Fig. 3.5 presents measurements of $\sigma'_p(t)$ versus elapsed storage time, t_s, for at least one sample from every batch produced to date. In addition, several samples from a given batch were tested following various periods of storage for five different batches (Batches 102, 104, 106, 107 & 109). These data provide virtually indisputable evidence substantiating a significant time-dependent, batch-independent stiffening of the resedimented BBC samples.

Using a method of temporal comparison loosely analogous to the Thixotropic Strength Ratio = $(\frac{\text{strength @ } t=t_s}{\text{strength @ } t=0})$ adopted by Seed and Chan (1957), BBC demonstrates a Thixotropic Yield Ratio (TYR= $\frac{\text{preconsolidation pressure @ } t=t_s}{\text{maximum consolidation stress}} = \frac{\sigma'_p(t)}{\sigma'_{p=1\ ksc}}$) equal to 1.35 after 100 days of storage. After approximately two years of storage, the TYR rises to 1.9, i.e., a 90% increase in the yield stress upon K_o-consolidation.

Most of the data presented in Fig. 3.5 were generated by oedometer tests performed with load increment ratios between 0.65 and 0.8 to enable better definition of the compression curve while avoiding generating Type III displacement vs. log time curves (Ladd, 1973). (Tabulated consolidation test data are contained in Appendix G). All the data in Fig. 3.5 were obtained via the Casagrande construction on compression curves (shown in Fig. 3.6) derived from end of primary consolidation strain values. Given the sometimes subjective nature of the construction method, a range of likely values for the

preconsolidation pressure is provided for each test.

Table 3.2 provides a comparison between the results of the Casagrande construction with the method for determination of the preconsolidation pressure suggested by Butterfield (1979) involving the natural logarithm of the specific volume (i.e., ℓn (1+e)) vs. the natural logarithm of the vertical stress. The results of the Strain Energy Method (Tavenas et al., 1979) are also provided for the same tests. These data, as well as visual inspection of the compression curves in Fig. 3.6, show a consistent and very dramatic increase in preconsolidation pressure with time.

Two $\sigma'_p(t)$ values were obtained from compression curves generated by K_o-consolidation in a triaxial cell. The essentially continuous loading of these samples ($\frac{\Delta\sigma_v}{\sigma_v}$ = 0.1 to 0.2) resulted in very well defined compression curves in the vicinity of the yield stress (Fig. 3.6). These data, plotted as solid symbols at t_s=115 and 195 days in Fig. 3.5, follow the same trend as the oedometer test results.

Pertinent consolidation test data are provided in Table 3.3. Particularly noteworthy is that the increase in $\sigma'_p(t)$ with time was not accompanied by a change in the slope of the virgin compression line (i.e., CR is essentially constant regardless of storage time). The significance of the fact that the virgin compression curves remain parallel to one another is that the "thixotropic" bonds which cause the increase in $\sigma'_p(t)$ are <u>not</u> being broken with large strains beyond the yield stress. This feature is discussed further in Section 3.1.3.3.

3.1.3.2 Determination of Storage Time

The method by which the elapsed storage time, t_s, is quantified is important, particularly for the younger samples (t_s<70 days). Without delving into causes of thixotropy at this time, a rather empirical technique was adopted simply to standardize determination of relative elapsed times of storage.

Onset of thixotropic hardening is believed to occur when changes in consolidation stress have ceased for sufficient time to allow soil particles to attain positions compatible with the mechanically applied stresses. More specifically, the effects of thixotropy probably become apparent at some time greater than the time to primary plus one to two cycles of secondary compression. Therefore, it was decided to count the days of storage starting five days after the final stress decrement of σ'_{vc}=0.25 ksc was applied to the batch (the time to primary for this increment is on the order of 100 minutes and hence five days since application includes approximately 1.9 cycles of secondary). In most cases the time increment of five days coincided with the time the batch of clay was extruded. It is hypothesized that once significant deformations in reaction to the applied stresses have ceased, the clay particles can begin to seek equilibrium with respect to internal "electro-chemical" forces, i.e., thixotropy can commence.

The following equation is used to determine t_s:

$$t_s(\text{days}) = t_r - t_c - 5$$

where: t_s = elapsed time of storage (days)

t_r = date on which the sample was reconsolidated to σ'_{vc}=0.25 ksc in some geotechnical laboratory testing device

t_c = date on which the final batch consolidation stress of σ'_{vc}=0.25 ksc was applied.

As mentioned previously, the five days allows for completion of primary in response to the stress decrement (t_p=100 min) as well as approximately 1.9 cycles of secondary compression. The batch preparation technique precluded any effects of thixotropic hardening during consolidation to 1.0 ksc and subsequent unloading to 0.25 ksc.

The above definition is supported by data from Batch 110 in Fig. 3.5. This batch was subjected to an extended period (25 extra days) under the final vertical load of 0.25 ksc (detailed data for Batch 110 can be found in Bensari, 1984). Fifteen days following sampling, an oedometer test was performed on a sample from the batch yielding $\sigma'_p(t)$=1.30 ksc. Incorporating the extra 25 days in the storage time causes the test to be plotted at t_s=40 days at which point the measured $\sigma'_p(t)$ fits well with the rest of the data in Fig. 3.5. These data also indicate that thixotropy does not depend upon development of negative pore pressures (i.e., increased sampling effective stress, σ'_s, with time) because the Batch 110 sample had to have a constant effective stress (and zero excess pore pressure) during the extra 25 days that it remained in the large consolidometer under the applied stress of 0.25

ksc.

3.1.3.3 Variation in Consolidation Parameters with Time

In order to further understand the extent of the hardening phenomena on the behavior of "stored" samples, it is advisable to determine the effect of t_s on consolidation characteristics other than σ'_p. As a method of studying the effect of time on initial compressibility, the recompression ratio ($RR = \Delta\varepsilon/\Delta\log\sigma'_{vc}$) is employed, considering the strain incurred over the same stress range for each test (0.15 ksc $\leq \sigma'_{vc} \leq$ 1.00 ksc). However, because the initial recompression curve is susceptible to changes due to disturbance, it is first necessary to assess test quality by considering the RR over a range of stress which takes into account the measured $\sigma'_p(t)$ of the sample. By using the range 0.15 ksc $\leq \sigma'_{vc} \leq 0.75\ \sigma'_p(t)$, samples which exhibit less strain at σ'_{vc}=1.00 ksc simply because they are at a higher OCR will be more fairly evaluated by considering strain at stress levels closer to the thixotropically attained preconsolidation pressure.

Measurements of RR between 0.15 ksc and 0.75 $\sigma'_p(t)$, presented as crosses (x and +) in Fig. 3.7, indicate no change with time. A value of RR=0.024 was chosen to evaluate test quality, above which tests are considered "fair" and below which the quality is "very good." This value was based primarily on the type of test performed and the operator's level of skill. Tests of questionable quality were as follows:

1) Lateral Stress Oedometer (LSO) tests where the entire device is submerged in water prior to loading;
2) a DSS test which has a wire reinforced membrane rather than solid lateral restraints;
3) an oedometer test performed in conjunction with falling head permeability tests; and
4) a conventional oedometer test performed by students.

It must be emphasized at this point that the "fair" tests are <u>not</u> seriously disturbed as can be verified by consulting Figs. 3.9 and 3.10 for variations of coefficient of consolidation, c_v, and coefficient of secondary compression, C_α, respectively, versus effective stress level. It is because the increase in stiffness due to thixotropy, as demonstrated by the decreasing RR values measured over the same stress range for each test (solid symbols in Fig. 3.7), is so small that the slightest deviation from a "good" test seems to be sufficient to destroy or mask the effect.

Considering only the "very good" tests in Fig. 3.7, it can be seen that there is a definite trend toward increasing initial stiffness (lower RR) with time. Over a period of storage from t_s=10 days to t_s≈600 days there is a 40% increase in initial stiffness ($= \frac{0.026-0.0155}{0.026}$). Initial stiffness increases under one dimensional consolidation conditions have been reported for stored remolded clay samples as compared to samples loaded immediately following remolding by Mitchell

(1960) using San Francisco Bay mud and by Mesri et al. (1975) who investigated Mexico City Clay. Their results show a greater effect of thixotropy than that observed for resedimented BBC; however, this is to be expected for initially remolded samples.

Beyond the preconsolidation pressure, $\sigma'_p(t)$, the ratio of strain to change in log σ'_{vc} does not show any consistent correlation with length of storage time. Fig. 3.8 presents values of the virgin compression ratio ($CR = \Delta\varepsilon/\Delta\log\sigma'_{vc}$) for all the consolidation tests in Table 3.3. The range of reasonable values of CR is between 0.153 and 0.182. As can be seen in Fig. 3.6, the nearly parallel but displaced virgin compression curves result in CR being independent of storage time.

Because samples of BBC tested in one dimensional compression all started at essentially the same initial void ratio, nearly parallel but displaced virgin compression lines (VCL) will also be apparent in void ratio, e, vs. log σ'_{vc} space. In contrast, secondary compression-induced quasi-preconsolidation pressures change the precompression void ratio, e_o, of the sample and hence samples which have differing virgin compression curves in ε_v-log σ'_v space can follow a unique VCL in e-log σ'_{vc} space.

Mitchell (1960) reported nearly parallel e-log σ'_{vc} curves following yield in his work on the thixotropy of remolded San Francisco Bay Mud. These samples yielded at stress levels in the vicinity of 0.2 ksc. However, at higher stress levels (σ'_{vc}

≈ 10 ksc) Mitchell noted that there is a slight tendency towards convergence of the virgin compression curves. The highly plastic (I_p ≈ 350%) Mexico City Clay ($\sigma'_p \approx 0.4$ ksc) actually converged at much lower stress levels ($\sigma'_v \approx 2$ ksc) according to Mesri, et al. (1975). Inspection of Fig. 3.6 reveals the same slight convergence at $\sigma'_{vc} \approx 10$ ksc with a σ'_{vc}/σ'_p ratio of about 10.

The effect of thixotropy on the time rate of consolidation, as demonstrated by the coefficient of consolidation, c_v, is only to raise the stress level at which the normally consolidated rate of consolidation is reached. Fig. 3.9 presents c_v data for the consolidation tests. The scatter for the overconsolidated values is partially due to the very small times to primary (generally less than three minutes) and the consequent difficulty in obtaining precise estimates because of the small number of readings and the rapidity with which they had to be taken. The average normally consolidated value of c_v for resedimented BBC is approximately 3.5×10^{-3} cm^2/sec. Based on the data in Fig. 3.9, there may be a slight trend towards increasing c_v(NC) with storage time but any effect is small compared to the accuracy of the measurements.

Mesri, Rokhsar and Bohar (1975) contend that the coefficient of secondary compression, C_α, is increased by thixotropy. They report a doubling of C_α (defined by Mesri et al. as $\Delta e/\Delta \log t$) in the low stress range for "aged" remolded Mexico City Clay which merges with the nonaged sample at stress levels greater than the yield stress. As can be seen in Fig.

3.10, the coefficient of secondary compression, C_α (defined as $\Delta\varepsilon/\Delta\log t$ in this research) is unaffected by thixotropy, except that the stress level at peak C_α is raised due to the change in $\sigma'_p(t)$ with time of storage. There is only a constant multiplication factor of $(1 + e_o)$ to change $\Delta\varepsilon/\Delta\log t$ to $\Delta e/\Delta\log t$ and, as mentioned previously, e_o values for all resedimented BBC are essentially the same.

3.2 DEVELOPMENT OF METHODS TO CORRECT UNDRAINED SHEAR DATA AFFECTED BY THIXOTROPY

Having established the effect of thixotropy on consolidation parameters, it is now important to assess the degree to which the undrained shear behavior of resedimented BBC at OCR 4 is affected by extended storage. The investigation is performed using standard triaxial equipment and the Direct Simple Shear device with all samples consolidated under K_o-conditions (i.e., no lateral strain).

3.2.1 K_o-Consolidated Triaxial Compression and Extension Results for Resedimented BBC at OCR=4

Since the "sampling" process for the resedimented BBC batches allows some absorption of water (considered to be the cause of the decreased measured initial effective stress (Germaine, 1982)) and therefore an increase in the overconsolidation ratio, the value of K_o on reconsolidation to the final batch consolidation stress (σ'_{vc}=0.25 ksc) is less than one. K_o values for BBC are discussed in Section 2.2. Refer to Fig. 2.6 for variation of K_o with OCR.

Measurement of the variation of the ratio of horizontal effective stress to the vertical consolidation stress, $\sigma'_{hc}/\sigma'_{vc}$, with changing vertical stress (multiple unload and reload cycles) using the Lateral Stress Oedometer (LSO) has revealed that drained unloading to an OCR between eight and ten results in a reload K_o value equal to approximately 0.73 at OCR=4. The entire K_o-consolidated triaxial testing program for OCR=4 behavior, however, was performed assuming K_o=1.0 and hence the tests were isotropically consolidated. The difference in the true K_o and applied K_c=1 condition should be kept in mind.

3.2.1.1. Variation in Stress-Strain Relationships with Elapsed Storage Time

Stress-strain results for BBC samples tested in triaxial compression and triaxial extension at OCR=4 and K_o=1.0 are presented in Figs. 3.11 and 3.12 respectively. (Tabulated data from these tests are contained in Appendix H). "OCR=4" refers to nominal value based on the resedimentation stress history (σ'_p=1 ksc and σ'_{vc}=0.25 ksc) and not $\sigma'_p(t)$. The reason for this is that values of average effective stresses at low shear stress levels (i.e., $q < q_y$) are not affected by storage time, as discussed in Section 3.2.4).

Given the low stress levels at which the BBC samples exist (σ'_p=1.0 ksc) and eventually fail ($q_f \approx$0.15 to 0.30 ksc), accurate estimation of the correction for both the uplift force of the cell pressure on the piston and the weight of the piston are important. Figs. 3.11 and 3.12 include separate estimates

of the possible range of variation in the shear stress measurement due to uncertainty in the area and weight of the piston for the triaxial cells used. These bands were based on multiple cell calibration exercises over the past two years at MIT and a cell pressure of 2.0 ksc. (Based on values of backpressures plus σ'_{vc}=0.25 ksc used during these tests (Table 3.4), σ_c=2.0 ksc is an average value). It is likely that the actual deviation of the measured stresses is not as extreme as these bands would indicate.

Temperature fluctuations in the laboratory ($\Delta T = \pm 5°C$) led to further difficulties in data reduction due to variation in transducer readings. Corrections were made to the raw data based either on simultaneous relative thermistor readings or on variation in the cell pressure transducer (since $\Delta\sigma_c$=0 throughout shear). Table 3.4 identifies the three triaxial compression tests which required temperature corrections. The only triaxial test considered of very poor quality is TC-5. This sample had been stored for 326 days wrapped only in one layer of saran wrap and a light coating of wax, unlike all the other samples which were sealed according to the method described by Germaine (1982). The preyield stress-strain curve for this sample (Fig. 3.11) indicates that the sample behaves substantially softer than both "young" and "old" samples. Therefore, the results of TC-5 are disregarded.

The triaxial compression data in Fig. 3.11 show a general trend toward increasing undrained strength with increasing elapsed storage time. The yield stress values, q_y, (as

determined using the strain energy method (Tavenas et al. 1979), evaluated for use on BBC by Bensari (1984)) and the peak strengths, q_f, are plotted versus storage time in Fig. 3.13. The triaxial extension tests (Fig. 3.12) demonstrated similar trends with time; these yield and peak strengths are also plotted in Fig. 3.13.

There are two important issues which merit further attention before discussing the effect of thixotropy on the shear strength of resedimented BBC:

1) the consolidation method, i.e., recompression vs. SHANSEP type; and
2) use of the yield stress rather than the peak stress to assess the magnitude of the storage effect.

The first issue, regarding the reconsolidation procedure, is the most fundamental as far as thixotropy is concerned in that the hardening effect survives recompression type consolidation and is destroyed by SHANSEP type consolidation. SHANSEP (an acronym for Stress History and Normalized Soil Engineering Properties) is a method requiring consolidation in the testing device beyond the preconsolidation pressure experienced "in situ" by the sample (Ladd and Foott, 1974).

All triaxial compression and extension tests performed at values of t_s greater than one day were consolidated in the recompression mode. This means that once in the triaxial cell, they were subjected to a vertical consolidation stress equal to the final σ'_{vc} in the resedimentation process (i.e., σ'_{vc}=0.25

ksc). Hence, not only does the structure attributable to batch consolidation remain unaltered, but any additional strengthening incurred during the elapsed storage time should remain intact.

In order to compare the effect of recompression type vs. SHANSEP type consolidation on undrained shear behavior, a triaxial compression test was performed on a sample consolidated according to the SHANSEP method. Comparison between and problems associated with the two consolidation methods are elaborated upon in Section. 6.2. Within Chapter 3, however, the SHANSEP type test (TCSHAN-1) is utilized to simulate behavior unaffected by thixotropy (i.e., "t_s=0" which is plotted as t_s=0.5 days since according to the remolded clay fall cone test series a half a day is approximately the time when thixotropy begins to become evident).

The TCSHAN-1 test sample had been stored for 186 days and hence had an estimated $\sigma'_p(t)$=1.62 ksc (from Fig. 3.5). K_o-consolidation was carried to σ'_{vc}=2.46 ksc so as to go 1.5 times beyond the thixotropically gained preconsolidation pressure. It is assumed that, during consolidation sufficiently beyond $\sigma'_p(t)$, thixotropic hardening effects are removed. Following four days consolidation at 2.46 ksc, the sample was unloaded to σ'_{vc}=0.619 ksc and hence its preshear stress history resulted in an OCR=4. Shearing commenced three days subsequent to application of the final consolidation stress, rendering t_s=0.5 days reasonable given the method for determining storage time (Section 3.1.3).

As mentioned above, problems associated with comparing SHANSEP type tests with their recompression type counterparts are discussed in Section 6.2 as well as in Section 2.3.3 of Jamiolkowski et al. (1985). The most significant differences are found in shear-induced pore pressures, while undrained shear strengths, although occurring at lower strains in the case of recompression (as also found by Sambhandharaksa, 1977) are basically the same. It is this similarity in undrained shear strength and an assumed small difference in yield stress which is utilized in generating the curve illustrating the effect of thixotropy on shear strength.

The second issue, use of yield stress rather than peak stress to assess the effect of thixotropy, is primarily in recognition of the fact that the Directional Shear Cell shears in a stress controlled fashion which precludes measurement of strain softening. Under these conditions, identification of the shear stress at failure, when a rupture surface does not develop rapidly, is difficult. Therefore, any corrections of strength behavior must revolve around a parameter which is consistently exhibited by the clay for any inclination of σ_1 (i.e., the δ angle).

In other words, although $\delta=0°$ and $\delta=20°$ tests demonstrate failure stress levels by the development of failure planes along which immediate displacement is very obvious, tests performed at higher values of δ (i.e., tests in the passive region) do not develop failure planes rapidly, but instead strain uniformly until the kinematic constraints of the DSC

device become of concern. Therefore, the stress level at which the samples yield was chosen as a more consistent parameter.

The yield stress is obtained via the strain energy method which involves determining the work done at specific stress levels as suggested by Tavenas et al. (1979). This strain energy is plotted vs. shear stress level. The method is somewhat arbitrary as post-yield work per unit volume values do not necessarily fall on a straight line. The method was standardized somewhat by choosing particular ranges of energy levels over which a straight line was approximated, a standardization especially useful for the anisotropic DSC test data wherein the character of the curves differed so radically.

Fig. 3.13 presents the normalized shear stress results for all the TC and TE tests performed at OCR=4 on the resedimented BBC (except TC-5). Since the only SHANSEP type OCR=4 test was in compression, an estimate had to be made for a "t_s=0 days" (nonthixotropic) strength in extension since it is considered valuable to correct all test data "down" to the "no storage" value, particularly for purposes of comparison with other published data. Inspection of Fig. 3.13 reveals that the difference between the yield stress levels for TC and those for TE remains essentially constant regardless of the elapsed storage time. Using the results of tests with t_s<100 days having a slower rate of increasing strength with time, an estimate of the yield stress difference was made:

$$\frac{q_y(TC)}{\sigma'_{vc}} - \frac{q_y(TE)}{\sigma'_{vc}} \simeq 0.735.$$

This difference was then subtracted from $\frac{q_y}{\sigma'_{vc}}$ for TCSHAN-1 to arrive at an estimate for a TE yield stress at "t_s=0";
$\frac{q_y(TE)}{\sigma'_{vc}} \simeq 0.99 - 0.735 \simeq 0.255$.

In order to evaluate the reasonableness of the "nonthixotropic" yield stress chosen for TE, the anisotropy inferred from this value in terms of K_s ($= \frac{q(TE)}{q(TC)}$) at peak stress levels is investigated. The q_f/σ'_{vc} for triaxial extension was estimated by adding the average difference between q_f and q_y for the triaxial extension tests to the previously estimated TE yield stress. Therefore:

$$\frac{q_f(TE)}{\sigma'_{vc}} = 0.255 + 0.32 = 0.575$$

$$\text{and } K_s = \frac{q_f(TE)}{q_f(TC)} = \frac{0.575}{0.99} = 0.58$$

at "t_s=0."

Figure 3.14 plots this triaxial OCR=4 anisotropy ratio with triaxial data at OCR=1 and results from plane strain tests. There are no reliable triaxial data at OCR=4 for resedimented BBC other than that produced by this research. Based on Fig. 3.14, the "t_s=0" value of q_y/σ'_{vc} chosen for TE is considered reasonable.

Based on the results presented in Fig. 3.13, it is considered reasonable to assume that the increase in q_y with increasing storage time is independent of whether the sample is tested under TC or TE conditions. The hypothesis that thixotropic effects are isotropic (assuming that thixotropy does not affect the effect of σ_2) leads to the following

important conclusions:

1) The relationship, presented in Fig. 3.15, between Δq_y and storage time, derived from the data in Fig. 3.13, can be used to correct both TC and TE test results for thixotropic hardening effects.
2) The same relationship can also be applied to the DSC test results regardless of the angle of shear.
3) The thixotropic correction to the yield stress will also be applied to the post yield strength since changes in peak strengths vs. t_s (Fig. 3.13) appear to be parallel to changes in yield stress vs. t_s.
4) The ratio of TE to TC yield stresses increases with storage time leading to an apparent reduction in anisotropy. From the data regarding q_f presented in Fig. 3.13, it appears that q_f vs t_s for TC and TE tests are also parallel. Therefore K_s $(= \frac{q_{f(TE)}}{q_{f(TC)}})$ will also increase with time.

Figure 3.15 contains all information available on the effect of storage on the shear stress at which samples yield and hence will ultimately act as the shear stress correction curve to be discussed in Section 3.2.3. The reason that Direct Simple Shear test data are not included to ascertain the effect of thixotropy on intermediate values of δ will be discussed in Section 3.2.2.

The effect of thixotropy on initial stiffness is investigated in terms of Young's secant modulus, E, in Fig. 3.16. Since yield stresses and undrained shear strengths

increase with time, it was considered more informative to evaluate the value of E at a given stress level rather than at a given percentage of the peak stress. These data are presented in Fig. 3.16 as open symbols. TC moduli (at $q/\sigma'_{vc}=0.60$) indicate a slight trend toward increasing stiffness with increasing t_s. TE values of E (at $q/\sigma'_{vc}=0.30$), on the other hand, do not show a consistent trend due to the fact that some of samples have begun to yield at this stress level and hence their moduli decrease radically. Calculation of stiffness at lower stress levels for TE tests is not viable since strain levels are less than 0.1% and hence tend to be inaccurate.

Normalized secant moduli, also plotted in Figure 3.16, indicate a trend only for the TE condition. The trend is due to the proximity of the yield stress level to the level at which the sample reaches 50% of its q_f. As storage time increases, yield stress and q_f increase by essentially equal amounts (Fig. 3.13). Therefore, 50% of the undrained shear strength becomes increasingly less than the yield stress and hence the modulus becomes greater.

3.2.1.2 Variation of Shear-Induced Pore Pressure with Elapsed Storage Time

The effect of thixotropy on pore pressure behavior during shear is a bit more elusive than the effect of storage on shear stress levels at yield. Figs. 3.17 through 3.20 present normalized effective stress paths, and pore pressure ch[illegible]s,

stress ratio and pore pressure parameters versus axial strain for triaxial compression and triaxial extension tests on resedimented BBC at OCR=4. For TC tests, it is difficult to identify any consistent variation in the stress paths with storage time. Normalized pore pressure changes, $\Delta u/\sigma'_{vc}$, however, do indicate a change in behavior with increasing storage time: the maximum $\Delta u/\sigma'_{vc}$ increases with increasing storage time (Fig. 3.18a). The same is true for the stress ratio, q/p' (Fig. 3.18b). Although the essential trend is present, it is difficult to analyze these data, particularly because the effect seems apparent over such a small span of strain ($0.5\% < \varepsilon_a < 1.0\%$).

It is apparent, also from Figs. 3.17 and 3.18, that the effective stress path of the SHANSEP type test is radically different from those of the recompression type tests. Such a difference in average effective stresses for a given shear stress was noted by Sambhandharaksa (1977) in his investigation of the effect of consolidation method on the undrained shear behavior of varved clays (discussed in further detail in Section 6.2). Hence, TCSHAN-1 cannot be used to simulate "t_s=0" (or nonthixotropic) pore pressure behavior.

The effect of elapsed storage time on ESP's for triaxial extension is very obvious (Fig. 3.19). Because yielding occurs at such low strain and stress levels, whereas peak strengths are not reached until large strains, pore pressures generated due to post-yield structure breakdown and particle reorientation (see Fig. 3.20a) are manifest early in the ESP

and are maintained until the undrained shear strength is reached. For triaxial compression, on the other hand, yielding occurs at relatively large strains, closely and consecutively followed by the peak shear stress and strain softening. This perhaps explains why the effect of thixotropy on Δu behavior is not readily evident in ESP's or Δu vs ε_a for shear in triaxial compression.

Having established the similarity of the storage effect on the values of q_y and q_f for both TC and TE, the pore pressure effects are assumed to be equivalent as well (a contention which will be supported by the consistent manner by which the data compare). In order to study these effects for both TC and TE, it is necessary to first separate changes in pore pressure due to shear stress from pore pressure changes due to changing the octahedral stress, σ_{oct} $(= \frac{1}{3}(\sigma_1 + \sigma_2 + \sigma_3))$, since the magnitudes of normal stress changes differ between the two types of triaxial tests. Therefore, the shear-induced pore pressure, Δu_s $(= \Delta u - \Delta\sigma_{oct})$, will be evaluated. By separating the influence of the intermediate principal stress, σ_2, results from the triaxial test program can hopefully be used to correct the plane strain DSC test data for the effects of thixotropy.

Shear-induced pore pressure results for the triaxial test series are presented in Figs. 3.21 and 3.22 for TC and TE tests, respectively. Δu_s has been normalized to the preconsolidation pressure for the recompression-type tests and to the maximum past pressure for the SHANSEP type test, TCSHAN, for comparative purposes. It is evident that removing changes

in the octahedral stress renders the effect of thixotropy on the pore pressure behavior more readily evident.

The results in Figs. 3.21 and 3.22 show that onset of the effect of storage on Δu_s occurs following yield. Subsequently, Δu_s continues to change until attaining either the strain at which q_f is reached for TC tests or the strain at which the post-yield modulus, G_y, is reached (i.e., when the stress-strain curve has completed the transition from its initially stiff behavior prior to yield to the almost straight line along which the sample strain hardens until q_f is reached) for TE tests. For triaxial compression, Δu_s becomes essentially constant at a maximum shear strain, γ, beyond 5 to 6%, while for triaxial extension a constant value is reached at $\gamma \simeq 2\%$.

These observations are useful for developing a 'universal' method by which to assess the overall effect of thixotropy on shear-induced pore pressure behavior. Since, as yet, there are no available values of Δu_s for tests completely unaffected by thixotropy, the constant values of Δu_s reached at q_f or the strain level at which the post-yield modulus is reached are plotted versus t_s for both TC and TE tests in Fig. 3.23. The scale for triaxial extension (on the right-hand side of the plot) was shifted until the TE Δu_s values corresponded with the TC Δu_s values (in accordance with the assumption that the effect of thixotropy is isotropic). Less scatter is associated with the variation in Δu_s with t_s than with Δq_y vs t_s, probably because of the effect of the error due to the estimated area and weight of the piston on the latter parameter.

Using the Δu_s measurements for t_s > 100 days, linear regression is performed to establish a line. Then, using the ratios of slopes for the variation in $\Delta q_y/\sigma'_{vc}$ vs t_s for t_s > 100 days and t_s < 100 days, the slope of Δu_s vs t_s for t_s < 100 days is obtained and plotted in Fig. 3.23. Using this portion of the Δu_s vs t_s relationship, an estimate of Δu_s for a "t_s=0" test is determined by extending the line to t_s = 0.5 days (which is the time at which yield stress for TCSHAN-1 is located as well as the time at which the remolded BBC began to indicate decreased penetration depths in the fall cone test series). Thus, the "t=0" Δu_s values are -0.095 ksc and 0.089 ksc for TC and TE conditions, respectively. Given the "t_s=0" values, the change in the large strain, constant value of the shear-induced pore pressure attained due to thixotropy, termed $\Delta(\Delta u_s)$, can be obtained.

Figure 3.24 summarizes the increase in Δq_y and the decrease in $\Delta(\Delta u_s)$ with time of storage. The scale refers both to the non-normalized change in yield stress and the shear-induced pore pressure, although the scale is opposite in sign to the value of the latter parameter, i.e., $\Delta(\Delta u_s)$ actually becomes more negative with time. Note the fact that all the engineering parameters affected by thixotropy (σ'_p, q_y, q_f and Δu_s) exhibit a significant increase in slope at t_s=100 days.

3.2.2 K_o-Consolidated Direct Simple Shear Test Results for Resedimented BBC

Several Direct Simple Shear (DSS) tests were performed on

resedimented BBC for this research in both overconsolidated (OCR = 4) and normally consolidated states. The series of DSS tests at OCR = 4 was intended to establish the effect of storage time on strength for intermediate angles of orientation of σ_1. DSS tests were conducted on normally consolidated BBC in order to ascertain the minimum reconsolidation stress necessary to obtain truly normally consolidated behavior. Pertinent summary data are presented in Table 3.5. Appendix I contains tabulated data for the individual tests.

The overconsolidated test series includes both recompression and SHANSEP as methods of consolidation. Recompression, wherein the sample is directly reconsolidated to the "overburden" stress (σ'_{vo}=0.25 ksc for this research), is the method of consolidation necessary for measurement of any thixotropic hardening. An important factor involved in the performance of DSS recompression type tests is the use of pins, fixed to the top and bottom porous stones, which are ultimately embedded in the top and bottom surfaces of the sample in order to prevent slippage. An earlier series of recompression type DSS tests on overconsolidated BBC without pins consistently resulted in slippage of the top cap (Germaine, 1982). Because of initial trepidation with regard to the effect of the pins on behavior, SHANSEP type DSS tests were also performed in order to ascertain OCR=4 BBC behavior.

Stress-strain curves for the DSS tests on overconsolidated BBC are presented in Fig. 3.25 and horizontal shear versus vertical normal stress behavior is presented in Fig. 3.26. The

recompression type tests (DSS-14 and 15, which are normalized using σ'_p = 1.0 ksc, not $\sigma'_p(t)$), do not indicate increased shear strength with increased storage time when compared with one another (t_s = 101 and 184 days for DSS-14 and 15, respectively) or when compared with the SHANSEP type tests (DSS-7, 9 and 15A), contrary to the triaxial recompression and SHANSEP results of Section 3.2.1. In addition, the effective stress behavior remains essentiallv unaffected. Whereas increasing storage time results in smaller pore pressures (and hence, greater effective stresses) at a given shear strain level under triaxial conditions (Figs. 3.21 and 3.22 for Δu_s vs. γ for triaxial compression and extension, respectively), the two recompression DSS tests exhibit, if anything, the opposite trend (Fig. 3.27).

It is considered likely that the pins (3.9 mm long, 1 mm in diameter and spaced such that there are 5 pins per square centimeter of porous stone) destroy the structure of the clay, at least in their immediate vicinity which constitutes approximately 30% of a 2.54 cm thick sample. Although difficult to measure due to the presence of the pins, the strain during reconsolidation to the batch overburden stress (σ'_{vc}=0.25 ksc) was estimated at about 2.7% for the case where the pins were forced in (under K_o conditions) during trimming. (Both consolidation and shear strains for the tests with pins involve use of the entire sample height, including the pin infiltrated zone). This vertical strain is about three times greater than the ε_v measured in nine tests without pins in the

same device at σ'_{vc}=0.25 ksc (the average strain was equal to 0.85% (Germaine, 1982)).

In order to conclude whether the lack of a measurable undrained DSS strength increase is due to the dependency of the direction of σ_1 on the thixotropic hardening phenomena or to the testing techniques (i.e., the use of pins to abrogate top cap slippage), it is necessary to investigate the effect of the method of consolidation on undrained shear behavior. As mentioned previously, a detailed discussion of the effect of SHANSEP vs. recompression consolidation techniques is provided in Section 6.2. Therefore, only effects pertinent to the validity of DSS recompression tests using pins are discussed at present.

Data from a recompression test successfully performed on resedimented BBC at OCR = 4 without the use of pins is supplied by Ladd and Edgers (1972). DSS test No. 1002A involved reconsolidating the sample to σ'_{vm} = 4.0 ksc, swelling to σ'_v = 0.5 ksc and recompressing to σ'_v = 1.0 ksc. (The batch from which the sample was taken had a preconsolidation pressure between 1.0 and 1.5 ksc). The stress-strain curve and stress path for this test are presented in Fig. 3.28. For comparative purposes, three SHANSEP-type DSS tests, also provided by Ladd and Edgers (1972), are plotted. The shaded portions of the plot represent the superposition of the overconsolidated DSS results from this research. It is evident that the recompression test performed without the aid of pins (open symbol) developed lower effective stresses than SHANSEP type

tests. However, recompression tests employing pins gave even lower effective stresses.

The DSS tests performed by this research are stiffer and, for the most part, have slightly greater strength than those of Ladd and Edgers. Taking this into account in comparing the effective stress behavior, it can be pointed out that prior to yield (at $\tau_h/\sigma'_{vc}=0.4$) Test No. 1002A exhibited no tendency to contract but rather had a slight tendency to dilate. The tests with pins, however, which yield at τ_h/σ'_{vc} between 0.52 and 0.6, exhibit a definite tendency to contract followed by dilation after yield. Fig. 3.27 better illustrates this effect when particular notice is paid to pore pressure behavior at shear strains of less than 2%.

Since behavior prior to yield is of prime importance when considering the effects of thixotropy, as concluded by investigation of one dimensional consolidation and triaxial compression and extension behavior, it is concluded that DSS recompression type tests using pins fail to produce valid results regarding thixotropic effects.

It is hypothesized that the thixotropic strength gain, assumed to affect undrained shear strength equally regardless of the direction of σ_1 during shear, is obliterated by the disturbance inflicted by the pins. This contention is supported by the tendency of the samples to contract in a manner in excess of that of the recompression test (No. 1002A) performed without pins (refer again to the stress paths in Fig. 3.28). However, use of the pins does not sufficiently disturb the

material to remove the effects of structure accorded the material during resedimentation as is attested by coincidence of the stress-strain curves with the SHANSEP-type results.

In addition, it is to be noted that recompression tests with pins achieved relatively high shear strengths at substantially lower effective stresses. Inspection of Fig. 3.26 reveals that even the SHANSEP-type test using pins (DSS-15A) achieved higher horizontal shear stresses at given vertical effective stresses following yield. The recompression tests, DSS-14 and 15, meet the effective stress path of DSS-15A. The pins seem to strengthen the material at large shear strains.

A second series of DSS tests (performed without pins) did reveal an effect of thixotropic hardening on strength behavior. The original purpose of this normally consolidated program was to establish the minimum reconsolidation stress necessary to obtain true normally consolidated behavior. These data are presented in Figs. 3.29 to 3.31. (Note: $\sigma'_{vc} \equiv \sigma'_{vm}$). Inspection of the stress-strain curves presented in Fig. 3.29 and the data in Table 3.5 shows that DSS-16, consolidated to a vertical stress of 1.70 ksc, has an approximately 10% greater maximum normalized horizontal shear stress as compared to DSS-10 with σ'_{vm} = 2.10 ksc. The suggested reason for this behavior is that although the σ'_{vm} used in the DSS device was in excess of the 1.00 ksc to which the batches were reconstituted, the reconsolidation stress was not sufficiently larger than $\sigma'_{p}(t)$ reached during storage to result in normally

consolidated behavior.

Figure 3.32 illustrates this point graphically: the peak horizontal shear stress, normalized to the consolidation stress, σ'_{vm}, shows a consistent decreasing trend as the ratio of the consolidation stress to the thixotropically increased preconsolidation stress, $\sigma'_p(t)$ increases. Plotted for comparative purposes are the normally consolidated DSS strengths provided by Ladd and Edgers (1972). Although the storage time for these samples is unknown, the DSS consolidation stresses caused sufficient vertical strains ($14\% \leq \varepsilon_{vc} \leq 17\%$) to show that a sufficiently high $\sigma'_{vm}/\sigma'_p(t)$ was obtained. That the thixotropically increased preconsolidation pressure can govern shear behavior is most significantly demonstrated by DSS-12 which was consolidated to 1.32 ksc in the DSS device but had attained $\sigma'_p(t) \approx 1.36$ ksc. Not only was the normalized undrained shear strength increased by 15% over that of DSS-10 and the tests performed by Ladd and Edgers (1972), but the stiffness was also greater.

The effect on the normally consolidated stress paths (Fig. 3.30) appears to be confined to an increase in normalized horizontal shear at a given σ'_v/σ'_{vc} rather than a change in character of the curve. The lower portion of Fig. 3.32 reveals a general decrease in the normalized vertical effective stress with increasing $\sigma'_{vm}/\sigma'_p(t)$ or, in other words, as a truly normally consolidated state is approached. There is no apparent effect on the pore pressure vs strain behavior as presented in Fig. 3.31.

Considering σ'_{vm} in relation to $\sigma'_p(t)$ rather than σ'_p=1.0, it appears that a consolidation stress equal to at least 1.3 times $\sigma'_p(t)$ must be used to generate normally consolidated behavior (as demonstrated by Fig. 3.32). These data prove that the increase in $\sigma'_p(t)$ caused by thixotropy cannot be ignored as it can affect shear results. In addition, these results support (but do not prove) the hypothesis that thixotropy should increase (τ_h)max as measured in the DSS and that the pins are the cause of the lack of any measured strength increase in the recompression DSS tests.

3.2.3 Correction of Stress-Strain Curves to Remove Storage Effects

In order to minimize consolidation strains in the Directional Shear Cell, all tests were performed in an overconsolidated state. The preshear state of stress was achieved by simply reconsolidating the samples to the final batch stress of 0.25 ksc, which led to a theoretical OCR=4. As discussed in Sections 2.2.1 and 2.2.2, K_o was assumed to be approximately equal to 1.0 and, hence $\sigma'_{hc}=\sigma'_{vc}$. The data presented in Sections 3.1, 3.2.1 and 3.2.2 conclusively demonstrate, however, that the resedimented BBC material is vulnerable to the effects of thixotropy. This hardening effect is quite pervasive and is evident in drained 1-D compression curves as well as in numerous undrained recompression-type strength tests on "undisturbed" samples.

Any precise quantitative use of the DSC results presently available must therefore consider the fact that the strength of

the clay changes with time. Comparisons between DSC tests, including both those performed in the isotropic plane for proof testing and those run to determine the anisotropic strength character of the clay, must be corrected based on the time elapsed between the last batch consolidation increment application and recompression in the DSC device (as explained in Section 3.1.3.2). In addition, comparison between DSC results and those from other devices which have also been performed according to the recompression method requires that not only must the DSC results be adjusted but so must the results from the other devices.

Since the thixotropic phenomenon is not well enough understood to develop a theoretical model which will predict the degree to which a material will harden and the effect this will have on the various parameters, experimental information must be relied upon. Initially, it was considered adequate to utilize the thixotropically affected yield stress, $\sigma'_p(t)$, that one would expect after a particular storage time, as determined from Fig. 3.5, to correct recompression strength data. The rationale was that since Boston Blue Clay showed normalizable behavior with respect to a mechanically obtained preconsolidation pressure, σ'_p, then the same might be true for $\sigma'_p(t)$, especially since the consolidation curves (Fig. 3.6) appeared to show no anomalous behavior beyond the increased $\sigma'_p(t)$. Moreover, research at Laval University on natural, highly structured clays (e.g., Lefebvre et al., 1983) indicates that the yield envelope of these materials can be normalized to

σ'_p. Section 2.2 of Jamiolkowski et al. (1985) came to the same conclusion. It became obvious, however, after normalizing both DSC and triaxial test results by $\sigma'_p(t)$ that the method overcompensated for the hardening effect.

Recompression type strength tests were subsequently considered as the basis for the time correction. Since it is necessary that any tests attempting to measure a thixotropic gain in strength be performed in the recompression mode, the DSS test results were disregarded because of cap slippage and/or disturbance due to the use of stabilizing pins (Section 3.2.2). Therefore, triaxial tests in compression and extension were relied upon to establish the effect of extended periods of storage.

Since the thixotropic strength increase is relatively small ($\Delta q_y \simeq 0.06$ ksc for t_s=250 days) the effect of error due to piston friction and temperature fluctuations could affect the accuracy with which the hardening effect is predicted. This problem can be reasonably dealt with, however, by generating a large data base and thereby better establishing the mean effect.

The series of triaxial tests relied upon are presented in Figs. 3.11 through 3.23 and are tabulated in Table 3.4. Fig. 3.24 plots the variations in the data of greatest concern, i.e. Δq_y and Δ (Δu_s) vs. time of storage, t_s, for triaxial compression and extension tests performed on BBC at OCR=4.

The first correction for thixotropically affected shear data for OCR=4 resedimented BBC to be discussed is that for the

stress difference, q (= $(\sigma_1-\sigma_3)/2$). As illustrated by the post-yield moduli presented in Fig. 3.33 (CR from 1-D consolidation and G_y from TC and TE tests), there is no consistent change in stress-strain behavior following yield. Therefore, the full thixotropic strength gain is assumed to be reached when the sample first yields and then is assumed to remain constant at larger strains. Thixotropic strength gain is determined for a given time of storage from Fig. 3.24 according to the curve labelled Δq_y.

The yield stress time correction was applied to the various strength tests in as consistent and reasonable a manner as possible taking the following steps:

1) Determine the elapsed storage time, t_s, for a given test as explained in Section 3.1.3.2;
2) Refer to Fig. 3.24 to estimate the strength increase, Δq_y, due to thixotropy;
3) Determine the measured yield stress, q_y, from the uncorrected stress-strain curve using either the Strain Energy Method (Tavenas, et al., 1979) or another suitable construction;
4) Calculate q_t (i.e., q at "t_s=0") for all shear stress levels less than or equal to q_y ($t=t_s$) as follows:

$$q_t = \left(\frac{q}{q_y}\right) \cdot \left(q_y\ (t=t_s) - \Delta q_y\right) = q - \Delta q_y \left(\frac{q}{q_y}\right);$$

5) Calculate q_t for all shear stress levels greater than q_y ($t=t_s$) as follows:

$$q_t = q - \Delta q_y.$$

These corrections are presented in Table 3.6 along with additional corrections to be discussed in the next section. Of note is the fact that the correction to the shear stress is independent of the type of shear test performed. Examples of corrections are contained within the tabulated data for each recompression type shear strength test in the appropriate Appendices.

3.2.4 Correction of Stress Paths to Remove Storage Effects

Assessment and subsequent correction for the effect of thixotropy on the effective stress path followed during undrained shear of an undisturbed sample is more complex than for the storage effect on the shear stress. Fig. 3.24 presents the change in the shear-induced pore pressure, $\Delta(\Delta u_s)$ to be expected for a given elapsed storage time. This value of $\Delta(\Delta u_s)$, however, must be converted to a change in the value of the average effective stress, $\Delta(\Delta p')$, so as to account for the test loading system.

In order to calculate $\Delta p'$ for plane strain type tests such as the DSC, some estimate of the intermediate principal stress (the stress parallel to the no-strain direction) had to be made. Since no measurements of σ_2 were made in this research, the ratio of σ_2' to the sum of the major and minor principal stresses, $m \left[= \sigma_2'/(\sigma_1'+\sigma_3') \right]$ was assumed to be constant and to be equal to 0.35. These assumptions with regards to the value

of m are substantiated as follows:

1) Gens (1982) measured σ_2 in the Imperial College Plane Strain Compression device (which combines rigid and flexible loading elements) during tests performed on Lower Cromer Till (a low plasticity clay simulating sediments found in the North Sea) anisotropically consolidated to an OCR=4.0 according to a method similar to SHANSEP. Although m varied from 0.5 to 0.3 during the first one percent axial strain, it remained essentially constant for the rest of the test. Arthur (personal communication, 1984) measured σ_2 in the DSC by replacing part of the bottom rigid platen of the DSC with a specially designed pressure bag. Using this system to measure the anisotropy of Leighton Buzzard Sand he noted that once a small amount of strain had occurred the value of m remained almost constant.

2) Although measurements of σ_2 made during the performance of plane strain tests on resedimented BBC at OCR=4 using the MIT device (Ladd et al., 1971) are suspect, analysis of tests PSA-5 and 7 gave m = 0.31 to 0.37.

3) Bishop (1966) discusses a method to estimate m at failure using two semiempirical criteria: (1) $K_o=1-\sin\phi'$ as suggested by Jaky (1944) and (2) $\sigma_2'=K_o\sigma_1'$ as noted by Wood after performing plane strain tests on compacted moraine at Imperial College.

The expression Bishop obtained for m at failure is $m=1/2\ \cos^2\phi'$. Assuming $\phi'=33°$, $m\simeq 0.35$.

Assuming a constant value for m facilitated the conversion of $\Delta(\Delta u_s)$ to $\Delta p'$ for the DSC results. The conversion is carried out as follows:

$$\Delta u_s = \Delta u - \Delta\sigma_{oct}$$

$$\Delta\sigma_{oct} = \left[\frac{1}{3}\ (\Delta\sigma_1 + \Delta\sigma_2 + \Delta\sigma_3)\right]$$

$$\Delta\sigma_{oct} = \left[\frac{1}{3}\ (\Delta\sigma_1' + \Delta\sigma_2' + \Delta\sigma_3' + 3\Delta u)\right]$$

$$\Delta\sigma_2' = m\ (\Delta\sigma_1' + \Delta\sigma_3') = 0.35\ (\Delta\sigma_1' + \Delta\sigma_3')$$

$$\Delta\sigma_{oct} = \left[\frac{1}{3}\ (\Delta\sigma_1' + \Delta\sigma_3' + 0.35\ (\Delta\sigma_1' + \Delta\sigma_3'))\right] + \Delta u$$

$$\Delta u - \Delta\sigma_{oct} = -\left[\frac{1}{3}\ (1.35\ (\Delta\sigma_1' + \Delta\sigma_3'))\right]$$

$$\Delta u_s = -\frac{1}{3}\ (1.35 \times 2)\frac{(\Delta\sigma_1 + \Delta\sigma'_3)}{2} = -\frac{2.7}{3.0}\ \Delta p'$$

and, therefore, for DSC testing conditions:

$$\Delta(\Delta p') = -1.11\ \Delta(\Delta u_s) \approx -1.1\ \Delta(\Delta u_s) \quad [\text{Eq. } 3.1]$$

For triaxial testing situations, the intermediate principal stress is known. However, as the following equations will reveal, the effect of thixotropy on $\Delta p'$ is partially dependent on the effect of storage on the shear stress, Δq. The expression for triaxial compression are presented first:

$$\Delta\sigma_{oct} = \left[\frac{1}{3}\ (\Delta\sigma_1 + \Delta\sigma_2 + \Delta\sigma_3)\right] = \left[\frac{1}{3}\ (\Delta\sigma_1' + \Delta\sigma_2' + \Delta\sigma_3')\right] + \Delta u$$

$$\Delta u - \Delta\sigma_{oct} = -\left[\frac{1}{3}\ (\Delta\sigma_1' + \Delta\sigma_2' + \Delta\sigma_3')\right]$$

$$\Delta\sigma_2' = \Delta\sigma_3'$$

$$\Delta u_s = -\left[\frac{1}{3}\left(\Delta\sigma_1' + 2\Delta\sigma_3'\right)\right] = -\left[\frac{1}{3}\left(3\Delta p' - \Delta q\right)\right]$$

$$\Delta u_s = -\Delta\left(p' - q/3\right)$$

and therefore for TC conditions:

$$\Delta(\Delta p') = -\Delta(\Delta u_s) + (\Delta q)/3 \qquad \text{[Eq. 3.2]}$$

The equations relating the effect of storage on Δu_s to the effect on $\Delta p'$ for triaxial extension conditions are as follows:

$$\Delta\sigma_{oct} = \left[\frac{1}{3}\left(\Delta\sigma_1' + \Delta\sigma_2' + \Delta\sigma_3'\right)\right] + \Delta u$$

$$\Delta u - \Delta\sigma_{oct} = -\left[\frac{1}{3}\left(\Delta\sigma_1' + \Delta\sigma_2' + \Delta\sigma_3'\right)\right]$$

$$\Delta\sigma_2' = \Delta\sigma_1'$$

$$\Delta u_s = -\left[\frac{1}{3}\left(2\Delta\sigma_1' + \Delta\sigma_3'\right)\right] = -\left[\frac{1}{3}\left(3\Delta p' + \Delta q\right)\right]$$

$$\Delta u_s = -\Delta\left(p' + q/3\right)$$

and for TE conditions:

$$\Delta(\Delta p') = -\Delta(\Delta u_s) - (\Delta q)/3 \qquad \text{[Eq. 3.3]}$$

The above expressions for the effect of thixotropy on the average effective stress for the various testing systems are presented in Table 3.6.

The method by which p' is corrected for the effect of thixotropy is also slightly more complicated than that required to correct the shear stress. At maximum shear strains less than those at which yield occurs ($\gamma_y \simeq 2\%$ for TC tests and $\gamma \simeq 0.5\%$ for TE tests) there is no consistent effect of storage on the character of the Δu_s vs γ curve (Figs. 3.21 and 3.22) and, therefore, no correction is applied until yield occurs. Conversely, at some strain well beyond yield ($\gamma \simeq 5.5\%$ for TC

tests and $\gamma \simeq 2.5\%$ for TE tests) the maximum effect has been realized and, hence, although the magnitudes achieved by Δu_s are different for different lengths of storage, the character of the curves are the same. It is at this strain and at any greater strains that the entire correction for storage is applied.

In order to maintain consistency in applying the correction, the following steps were developed in accordance with the behavior (noted above) presented in Figs. 3.21 and 3.22:

1) Determine the shear stress level at which the stress-strain curve first deviates from its initial shear modulus. Refer, then, to the accompanying stress path to ascertain the p' associated with this level of shear stress. Call these values q_e and p'_e, respectively, using the subscript e to refer to elastic behavior.

2) For the given shear test, the full correction effect is applied at the shear strain levels at which essentially constant Δu_s values are reached (as mentioned previously $\gamma(TC) \simeq 5.5\%$ and $\gamma(TE) \simeq 2.5\%$ from Figs. 3.21 and 3.22, respectively). The shear stress level for these strains are determined from the appropriate stress-strain curves and, subsequently, one can obtain the pertinent value of p' from the effective stress path for the test. Call these values q_p and p'_p respectively, in this case using the

subscript p to refer to the more plastic behavior at this point in the test. There is slightly greater difficulty in determining q_p and p'_p for stress-controlled type tests, such as the DSC tests, since nearly constant values of Δu_s are not so readily achieved (see Fig. 4.19a). For these cases, the stress-strain curve is once again consulted for the shear stress level, q, at which the yielded modulus, G_y, is reached.

3) Determine $\Delta(\Delta u_s)$ from Fig. 3.24 based on the same time of storage, t_s, used to determine Δq_y. Convert $\Delta(\Delta u_s)$ to the $\Delta(\Delta p')$ relevant to the test condition under consideration using Equation 3.1, 3.2 or 3.3.

4) For values of $q<q_e$ do not alter p' (therefore $p_t'=p'$).

5) For values of $q>q_p$, subtract $\Delta(\Delta p')$ from p' to obtain the corrected value, p'_t.

6) For intermediate values of q (which are also intermediate values of p', i.e., $p'_e<p'<p'_p$ and $q_e<q<q_p$) subtract a proportional amount of $\Delta(\Delta p')$ from p' according to the following equation:

$$p' - \Delta(\Delta p') \cdot \left[\frac{p' - p'_p}{p'_p - p'_e}\right] = p'_t$$

Table 3.6 presents an overview of the correction for the effect of storage on the effective stress path. Corrected versions of the triaxial tests presented in Figs. 3.11 through 3.23 can be found in Figs. 6.3 to 6.13 where they are compared to corrected DSC tests performed on anisotropic samples.

Chapter 4 contains uncorrected and corrected DSC tests performed on isotropic BBC samples.

It is necessary to emphasize at this point that the correction curves supplied in Fig. 3.24 are perhaps somewhat crude, based as they are on data which exhibit considerable scatter in light of magnitude of the thixotropic effect. In addition, factors which may effect the rate of thixotropy (such as temperature and external load application) are not well understood and hence can not be accounted for. There is also no information to indicate whether this strength gain is a normalizable feature, i.e., whether a batch having a preconsolidation pressure other than 1.0 ksc would demonstrate the same percentage increase in either strength or one dimensional yield stress, or if the absolute change in these parameters would be the same.

Due to these uncertainties, the data discussed and analyzed in this chapter should be confined to use only with resedimented BBC subjected to similar stress histories as the batches from Germaine (1982) and Appendix A until additional research further clarifies the thixotropic effect. Finally, future performance of recompression type tests would best be constrained to testing of samples stored for no more than 100 days and, preferably, efforts should be made to minimize the times of storage spanned by the test series (i.e., $50<t_s<80$ days).

BATCH No.	t_s (days)	Atterberg Limits (%)			Base Material for w_L device	Salt Concentration (gram/liter)	Organic Matter (% by wt)	Specific Gravity (based on H_2O @ 20°C)
		w_L	w_P	I_P				
Powder	~ 0	41.8	21.6	20.2	?	~ 9 (@ w=40%) (3.5g/kg)		2.779
100	366					15.7 ± 0.7SD	0.4	
102	327					15.5 ± 1.0SD	0.4	
103	36					Nominal 16		2.782
104	192 1150					16.7 ± 0.3SD 19.5 ± 0.6SD*	0.6	
105	94 366 1094	40.2 41.6	22.0 21.0	18.2 20.6	? Hard Rubber	Nominal 16		2.766
106	155 950					18.3 ± 0.4SD* 20.9 ± 0.3SD*		
111	250 470	41.5 42.4	25.3 ** 21.6	16.2 ** 20.8	Micarta Hard Rubber	Nominal 16		
112	151	40.8	20.6	20.2	Hard Rubber	Nominal 16		

* Salt concentration measured following centrifugation of sample slurry.
** Questionable plastic limit determination.

Table 3.1: Index Properties for Resedimented BBC

Consolidation Test	t_s (days)	$\sigma'_p(t)$ (ksc)		
		(1) Casagrande	(2) Butterfield	Strain Energy
OED-1	8	1.08	1.09	1.04
OED-2	126	1.39	1.35	1.26
OED-4	567	1.88	1.62	1.70
OED-6	9	1.13	1.10	1.07
OED-G	139	1.50	1.40	1.38

(1) Construction based on ε vs log σ'_{vc} curve

(2) Construction based on $\ell n(1+e)$ vs $\ell n\ \sigma'_{vc}$ curve using a recompression line beginning at $\sigma'_v = 0.15$ ksc

Table 3.2: Comparison of Preconsolidation Pressures for Resedimented BBC Using Three Methods

Test	Batch No.	Storage Time t_s (days)	w_N (%) Batch[1]	w_N (%) Sample (initial)	$\sigma'_p(t)$ and range (ksc)	RR ($\times 10^3$) Initial Reload[2]	RR ($\times 10^3$) Unload Reload Cycle	CR	c_v ($\times 10^3$) (cm^2/sec) NC	C_α ((%)ε/logt) NC	$\frac{C_\alpha}{CR}$ (%) NC	Remarks (Test Quality)
OED-1	107	8	41.76	41.10	1.09 1.06-1.12	24.3 [19.9]		0.153	3.1	0.59	3.86	(Very good)
OED-2	106	126	40.73	40.23	1.39 1.37-1.41	16.4 [20.2]		0.165	4.0	0.60	3.64	(Very good)
OED-3	102	610	39.56	40.27	1.90 1.87-1.98	15.8 [20.9]	11.0 (OCR=10)	0.181	5.0	0.60	3.31	(Very good)
OED-4	103	567	39.78	40.28	1.88 1.80-1.92	16.0 [20.9]	11.8 (OCR=10)	0.166	4.7	0.58	3.49	(Very good)
OED-5	107	87	41.76	41.26	1.32 1.30-1.38	19.4 [19.4]		0.178	4.8	0.62	3.48	(Very good)
OED-6	109	9	41.6	41.53	1.13 1.11-1.18	27.5 [22.6]		0.171	2.4	0.66	3.86	(Very good)
OED-7	109	26	41.6	41.99	1.22 1.20-1.26	23.5 [21.6]		0.167	3.3	0.55	3.29	(Very good)
OED-PO	104	280	40.14	39.89	1.84 1.79-1.89	25.4 [28.5]		0.175	4.6	0.61	3.49	(Fair):connected to falling head k test; flushed @ σ'_v= 0.5 ksc
OED-G	101	139	39.85	39.05	1.50 1.48-1.58	24.3		0.178	4.7	0.57	3.20	(Fair)
OED-UG	104	59	40.14	39.92	1.30 1.24-1.35	24.3 [23.4]	12.2 (OCR=4)	0.160	3.0	0.76	4.75	(Very good)
DSS-13	107	96	41.76	41.48	1.33 1.28-1.40	24.9		0.146	2.7	0.49	3.35	(Fair)
K_oOED-1	102	267	39.76	--	1.73 1.70-1.79	24.3 [25.6]		0.156	--	--	--	(Fair)
K_oOED-2	105	54	40.99	39.44			10.3 (OCR=7)	0.169	--	--	--	(Fair): unload-reload cycle before $\sigma'_p(t)$
K_oOED-3	105	233	40.99	40.70	1.65 1.60-1.66	27.9 [31.1]		0.176	--	--	--	(Fair)
CK_oUC-NCI	107	114	41.76	41.31	1.43 1.41-1.49	18.2 [19.9]	--	0.156	--	--	--	(Very good)
CK_oUE-NCI	106	195	40.73	40.90	1.64 1.64-1.67	15.8 [18.1]	--	0.154	--	--	--	(Very good)
TCSHAN	107	186	41.76				--		--	--	--	(Very good)
OED-8[3]	110	40		40.93	1.30 1.28-1.32	18.3 [17.8]		0.167	2.8	0.63	3.77	(Very good)

(1) Based on DSC water contents, because largest amount of clay used.
(2) σ'_v = 0.15 to σ'_v = 1.0 ksc; values in brackets: from σ'_v = 0.15 to 0.75 $\sigma'_p(t)$
(3) Batch 110 was maintained at σ'_{vc} = 0.25 ksc for 25 more days than all other batches.

Table 3.3: Summary of Consolidation Test Data for Resedimented BBC

Test No.	(BATCH) t_s (days)	$\sigma'_p(t)$ (ksc)	(Cell No.) u_b (ksc)	W_i W_f (%)	σ'_{vc} (B%)	ε_{con} [log(t/t_p)]	$\dot{\varepsilon}_a$ (%/hr)	@ $(\sigma_1-\sigma_3)_{max}$ ε_a (%)	$\frac{q}{\sigma'_{vc}}$	$\frac{p'}{\sigma'_{vc}}$	q/p'	$\frac{\Delta u}{\sigma'_{vc}}$ A	$\frac{q_y}{\sigma'_{vc}}$ (ε_y%)	G_y	$\frac{\Delta q_y}{\sigma'_{vc}}$	$\frac{\Delta q_y}{\sigma'_{vc}}$ (from Fig. 3.15)	REMARKS
TC-1	(102) 29	1.23	(WFE-3) 0	40.2 39.8	0.250 (103)	0.34 [0.96]	0.46	5.87	1.171	1.919	0.610	0.248 0.11	1.072 (2)	1.09	0.083	0.072	
TC-2	(104) 78	1.32	(WFE-6) 1.68	40.5 40.9	0.250 (93)	0.19 [1.08]	0.47	5.24	1.179	--	--	-- --	1.055 (1.8)	0.83	0.066	0.089	wax paper over base
TC-3	(102) 225	1.70	(WFE-4) 2.18	38.7 40.5	0.258 (100)	0.18 [1.26]	0.48	4.29	1.355	2.123	0.638	0.201 0.075	1.271 (2.2)	1.12	0.282	0.230	
TC-4	(106) 112	1.40	(WFE-7) 1.30	40.3 40.9	0.243 (100)	0.23 [1.03]	0.46	3.02	1.179	1.938	0.609	0.254 0.106	1.065 (1.4)	0.89	0.076	0.117	Temp Corr
TC-5	(105) 326	1.82	(WFE-7) 1.63	41.4 40.7	0.246 (102)	0.33 [0.96]	0.46	5.62	1.169	1.882	0.621	0.295 0.13	--	1.31	--	--	Test NG
TC-6	(107) 65	1.30	(WFE-6) 1.51	41.5 41.5	0.250 (101)	0.23 [1.10]	0.45	4.26	1.249	1.897	0.659	0.357 0.142	1.092 (1.6)	1.09	0.103	0.086	Temp Corr Temp corr
TC-7	(106) 150	1.52	(WFE-4) 1.81	40.0 40.9	0.250 (102)	0.15 [1.29]	0.46	5.66	1.308	1.934	0.676	0.384 0.15	1.175 (1.7)	0.83	0.186	0.164	
TCSHAN	(107) 0	σ'_{vm}= 2.455	(WFE-7) 1.22	41.7 37.9	0.619 (102)	6.7 Last load 2.8 days	0.48	2.46	0.998	1.782	0.561	0.105 0.058	0.989 (1.2)	2.68	--	--	
TE-1	(103) 36	1.25	(--) 0	39.0 40.2	0.254 (-)	0.56 [1.09]	0.49	-10.0	0.653	0.638	1.02	-0.292 0.78	0.355 (0.9)	0.39	0.102	0.075	
TE-2	(104) 24	1.22	(WFE-6) 1.98	39.4 40.0	0.259 (-)	0.06 [-]	0.47	-10.0	0.681	--	--	--- ---	0.335 (0.5)	0.78	0.082	0.068	Poor pore pressure response
TE-5	(104) 62	1.30	(WFE-6) 1.40	38.0 40.6	0.251 (104)	0.07 [1.56]	0.49	-10.3	0.608	0.671	0.907	-0.271 0.78	0.320 (0.9)	0.67	0.067	0.084	
TE-6	(103) 180	1.60	(WFE-7) 2.90	39.7 40.4	0.252 (101)	0.35 [1.26]	0.46	-5.24	0.548	0.751	0.730	-0.302 0.73	0.440 (0.75)	0.42	0.187	0.194	Ext. Adapter slipped prior to failure
TE-7	(103) 257	1.75	(WFE-7) 2.17	39.9 -	0.247 (101)	0.61 [1.43]	0.46	-11.8	0.860	0.989	0.870	-0.815 0.52	0.530 (0.85)	0.57	0.277	0.252	
TE-10	(103) 359	1.85	(WFE-7) 1.90	39.9 41.6	0.247 (100)	0.31 [1.54]	0.48	-12.4	0.841	1.025	0.821	-0.870 0.51	0.508 (0.4)	0.63	0.255	0.307	

(*) values based on parabolic area correction for high strains (ε_a>7%)
and on cylindrical area correction for low strains (ε_a<7%)

Table 3.4: Summary of Triaxial Compression and Extension Test Data for Resedimented BBC (OCR=4)

Test	STRESS HISTORY						DATA @ τ_{hmax}				$\frac{E_{50}}{c_u}$	DATA @ END OF TEST					W_i (%)	W_f (%)	REMARKS	
	σ'_{vc}	σ'_{vm} or σ'_p	OCR	tc (days)	H_i (cm)	ε_{cf} (%)	γ (%)	$\frac{\tau_h}{\sigma'_{vc}}$	$\frac{\sigma_v}{\sigma'_{vc}}$	$\frac{\tau_h}{\sigma'_v}$		γ (%)	$\frac{\tau_h}{\sigma'_{vc}}$	$\frac{\sigma_v}{\sigma'_{vc}}$	$\frac{\tau_h}{\sigma'_v}$	ψ (deg)			t_s (days)	$\sigma'_p(t)$
DSS-7	0.496	1.999	4.0	1.1	2.20	5.4	10.5	0.672	1.335	0.503	450	23.3	0.435	0.725	0.599	30.9	40.7	38.8	97	1.34
DSS-9	0.496	1.984	SHANSEP	3.0	2.14	7.8	4.8 to 6.7	0.660	1.543	0.428	750	22.6	0.472	0.856	0.551	28.9	39.2	38.5	62	1.30
DSS-15A	0.504	2.007		1.0	1.97	5.6	11.7	0.700	1.224	0.563	370	28.0	0.416	0.556	0.749	36.8	--	39.6	-- (reshear with pins)	--
DSS-14	0.250	1.00	4.0	0.8	1.95	2.7	4.1	0.669	1.044	0.641	500	37.9	0.326	0.342	0.954	43.7	41.4	42.5	100 (pins)	1.36
DSS-15	0.250	1.00	RECOMP.	1.0	Preshear H=1.98cm		7.5	0.648	0.977	0.663	400	13.1	0.600	0.849	0.707	35.3	40.7	--	184 (pins)	1.62
DSS-10	2.104	2.104	1.0	1.0	2.46	6.0	4.2	0.201	0.635	0.316	500	16.0	0.140	0.340	0.410	22.3	39.0	38.0	198	1.63
DSS-11	1.501	1.501	1.0	1.3	2.75	5.4	4.2	0.210	0.565	0.371	960	24.2	0.124	0.167	0.746	36.7	39.7	38.9	61	1.30
DSS-12	1.318	1.318	1.0	1.5	2.18	4.0	3.0	0.233	0.726	0.320	920	31.6	0.086	0.115	0.748	36.8	40.6	40.4	101	1.36
DSS-16	1.702	1.702	1.0	0.6	2.15	4.5	3.3	0.222	0.607	0.365	455	28.7	0.112	0.148	0.753	36.9	40.7	41.6	187	1.61

1. Nominal strain rate for DSS tests: $\dot{\gamma}$ = 5%/hr (displacement rate = 0.769 mm/hr)
2. All stresses in ksc.

Table 3.5: Summary of CK_oUDSS Test Data for Resedimented BBC (OCR's 1 and 4)

CORRECTION FOR THIXOTROPIC EFFECT		TRIAXIAL COMPRESSION $\sigma_1>\sigma_2=\sigma_3$	TRIAXIAL EXTENSION $\sigma_1=\sigma_2>\sigma_3$	DSC (PLANE STRAIN) $\sigma_1>\sigma_2>\sigma_3$, $\sigma'_2=0.35(\sigma'_1+\sigma'_3)$
CORRECTION OF SHEAR STRESS, $q=(\sigma_1-\sigma_3)/2$	GENERAL	• Determine elapsed storage time, t_s [t_s(days) = date test recompressed - date batch unloaded to 0.25 ksc - 5] • Find Δq_y using t_s and Fig. 3.24		
	$q \leq q_y$	$q_t = q - \Delta q_y(\frac{q}{q_y})$		
	$q > q_y$	$q_t = q - \Delta q_y$		
CORRECTION OF AVERAGE EFFECTIVE STRESS, $p'=(\sigma'_1+\sigma'_3)/2$	GENERAL	• Using t_s, find $\Delta(\Delta u_s)$ from Fig. 3.24		
	CONVERT $\Delta(\Delta u_s)$ to $\Delta(\Delta p')$	$\Delta(\Delta p') = \frac{\Delta q_y}{3} - \Delta(\Delta u_s)$	$\Delta(\Delta p') = -(\frac{\Delta q_y}{3}+\Delta(\Delta u_s))$	$\Delta(\Delta p') = -1.1\ \Delta(\Delta u_s)$
	$q < q_e$	$p'_t = p'$		
	$q > q_p$	$p'_t = p' - \Delta(\Delta p')$		
	$q_e < q < q_p$ and $p_e < p' < p_p$	$p'_t = p' - \Delta(\Delta p')\ [\frac{p' - p'_e}{p'_p - p'_e}]$		

Table 3.6: Correction Method for Effect of Thixotropy on Undrained Shear Strength Tests

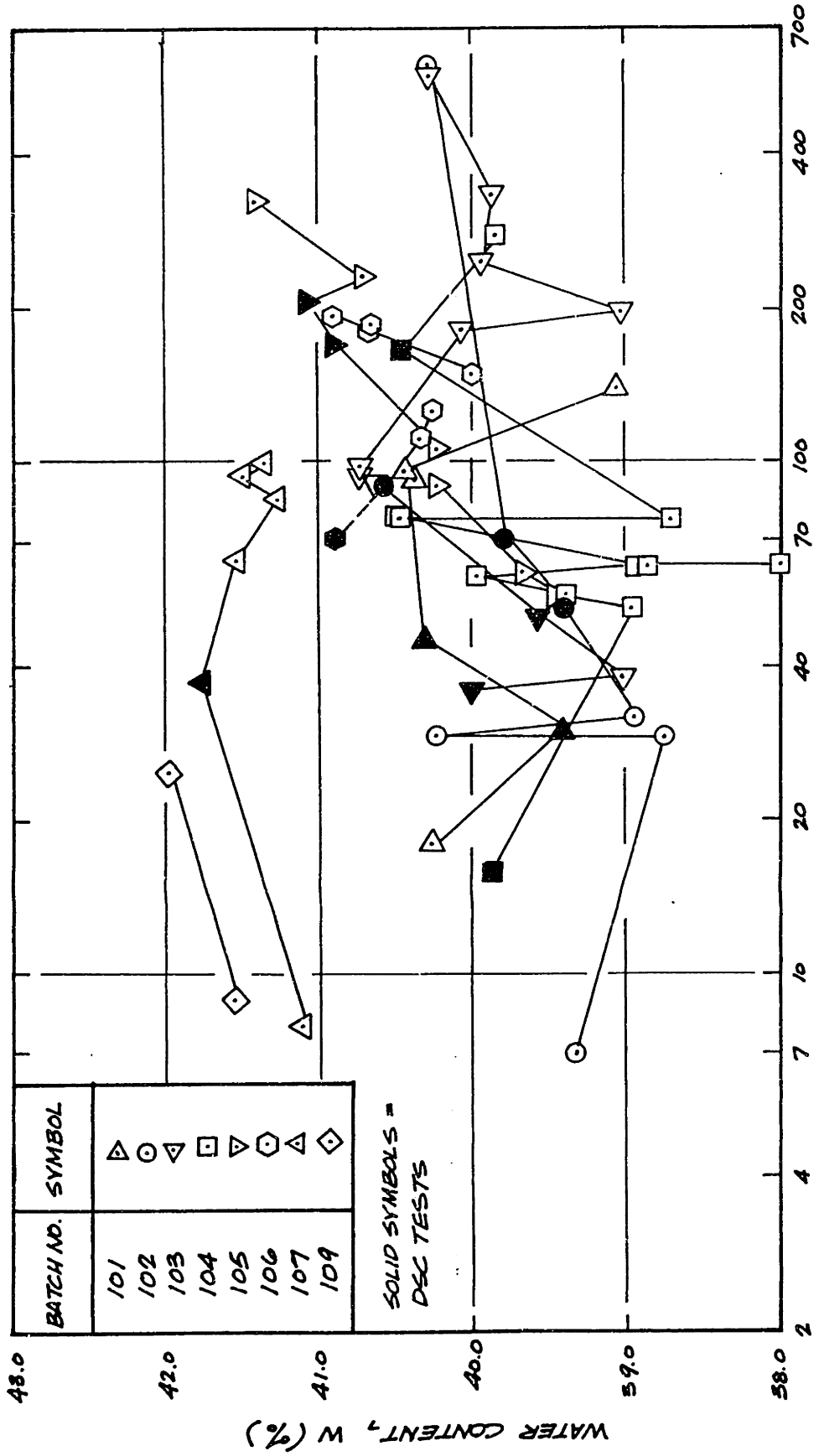

Figure 3.1: Initial Water Content vs. Storage Time for Samples of Resedimented BBC from Several Different Batches.

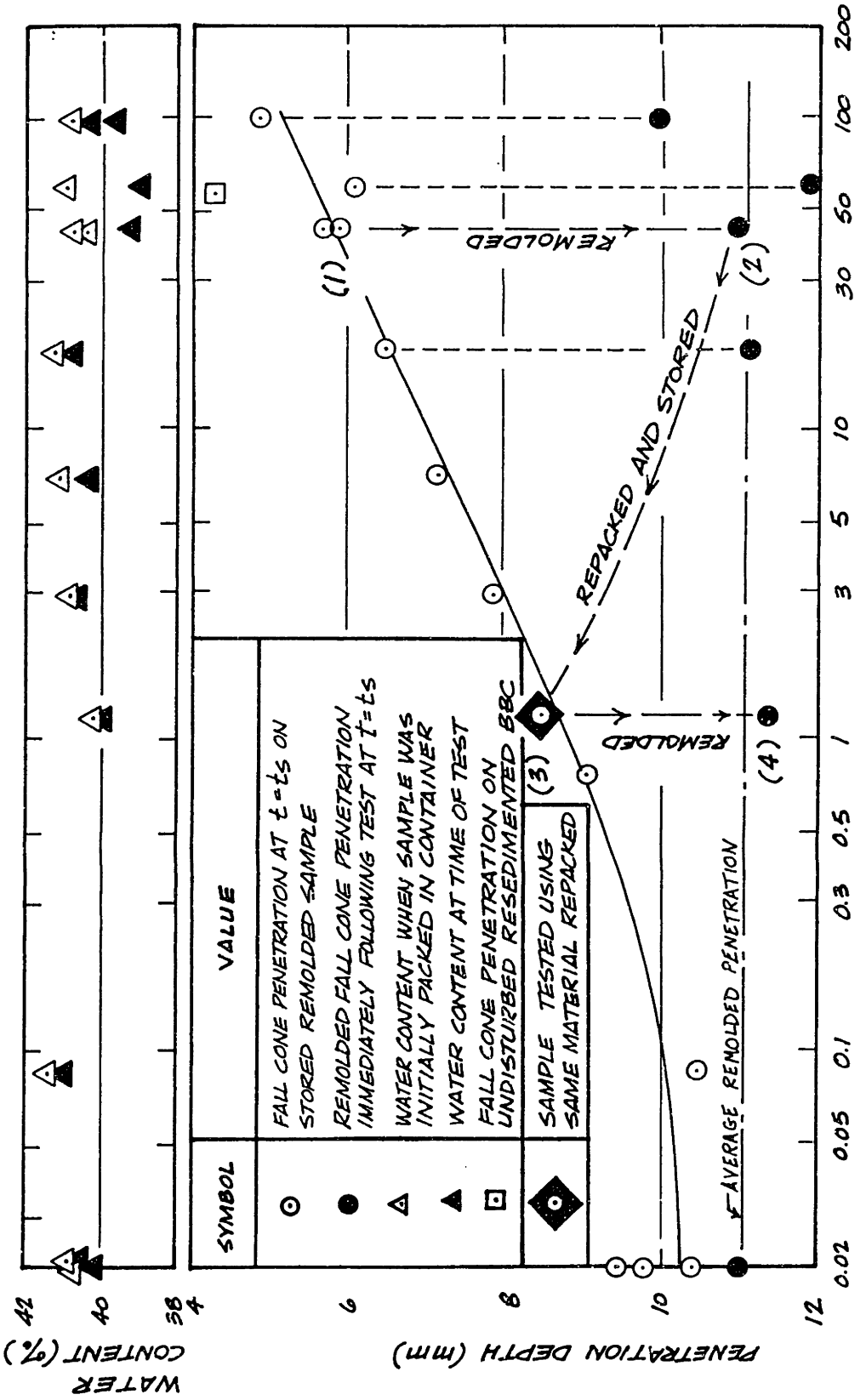

Figure 3.2: Effect of Thixotropy on Fall Cone Penetration Depths for Remolded Resedimented BBC.

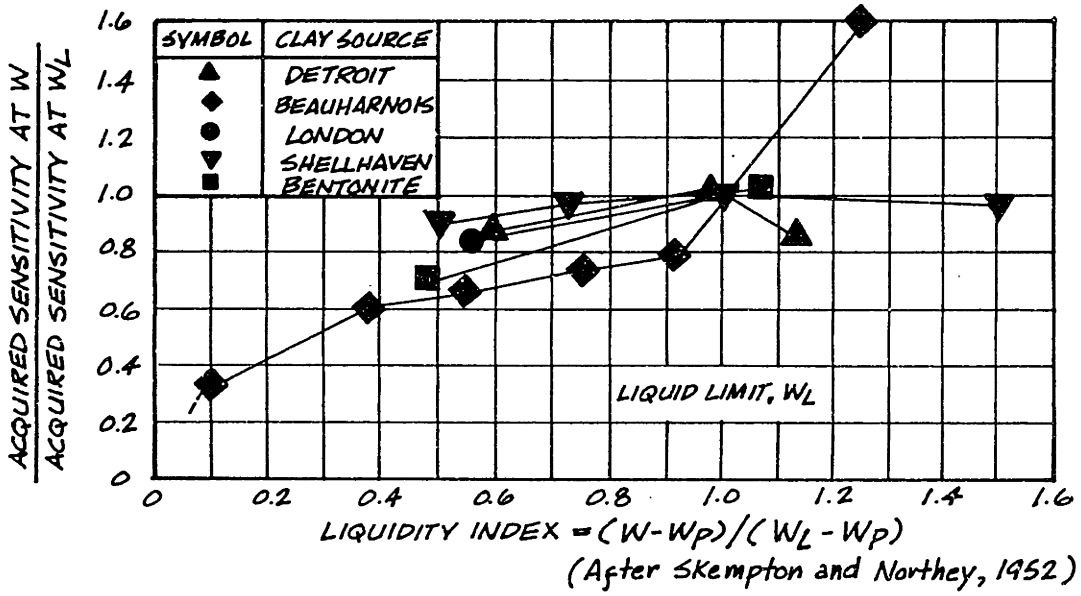

(a.) SAMPLES PREPARED BY REMOLDING AND PACKING IN CONTAINERS; STRENGTH MEASURED BY LAB VANE

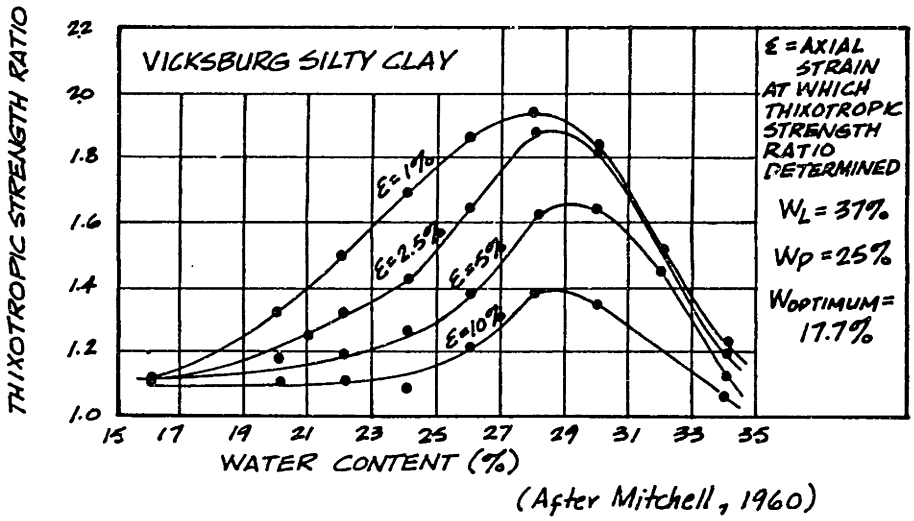

(b.) SAMPLES PREPARED BY KNEADING COMPACTION; STRENGTH MEASURED BY UU TEST (σ_c = 1.0 kg/cm²)

Figure 3.3: Effect of Water Content on Thixotropic Regain of Strength in Clay.

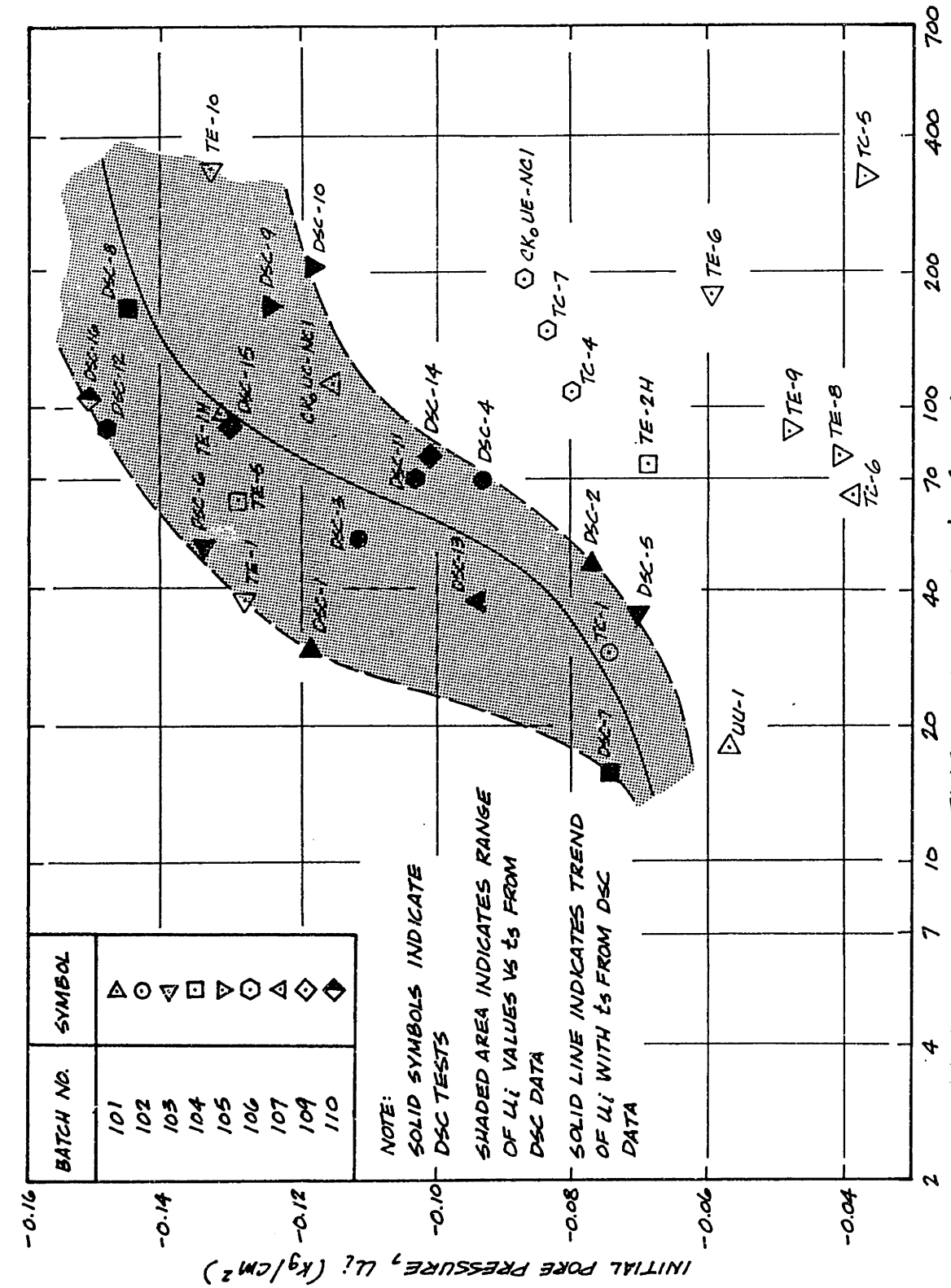

Figure 3.4: Initial Pore Pressure vs. Elapsed Storage Time for Resedimented BBC (Sampling OCR=4).

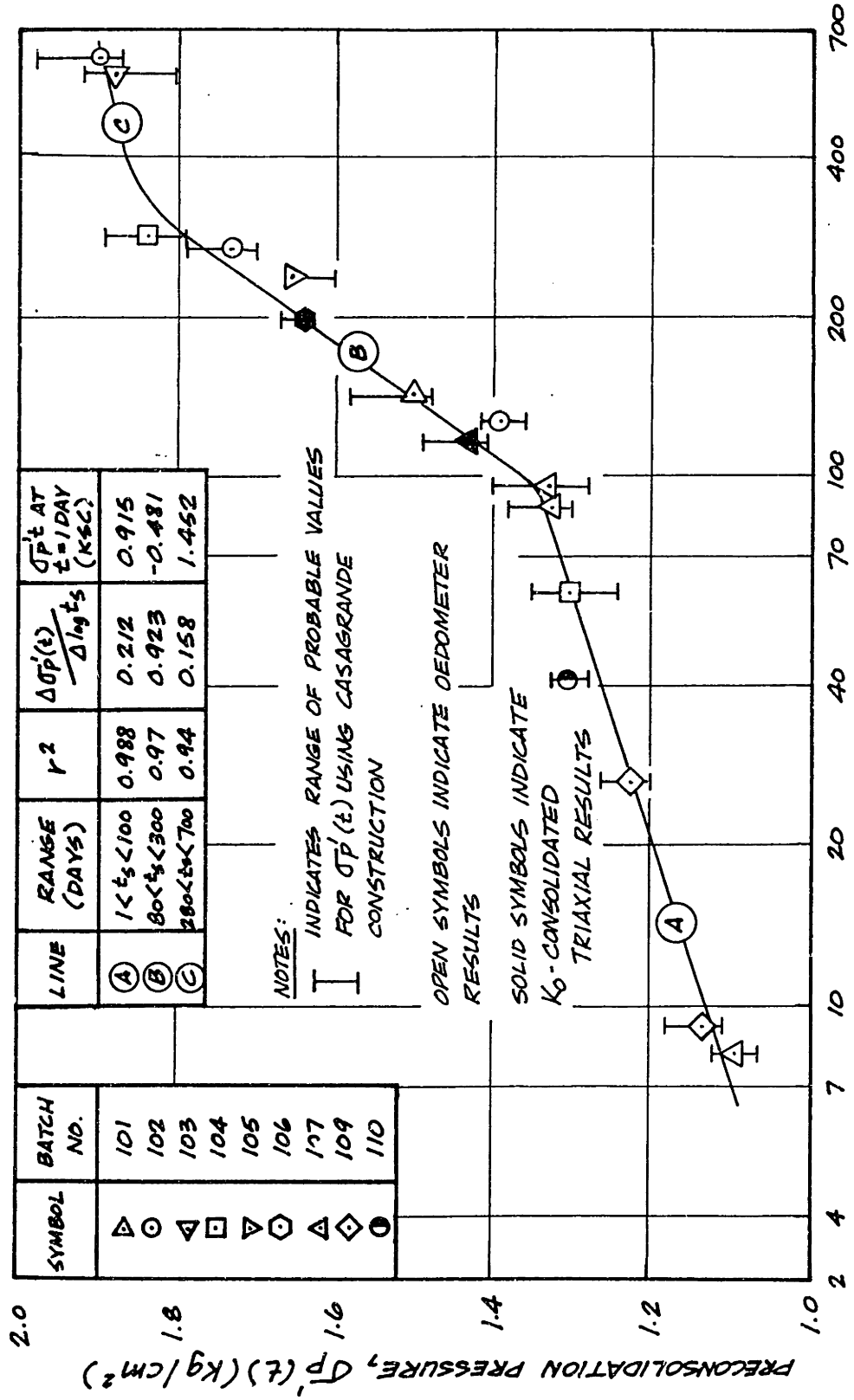

Figure 3.5: Effect of Thixotropy on Measured Preconsolidation Pressure for Resedimented BBC.

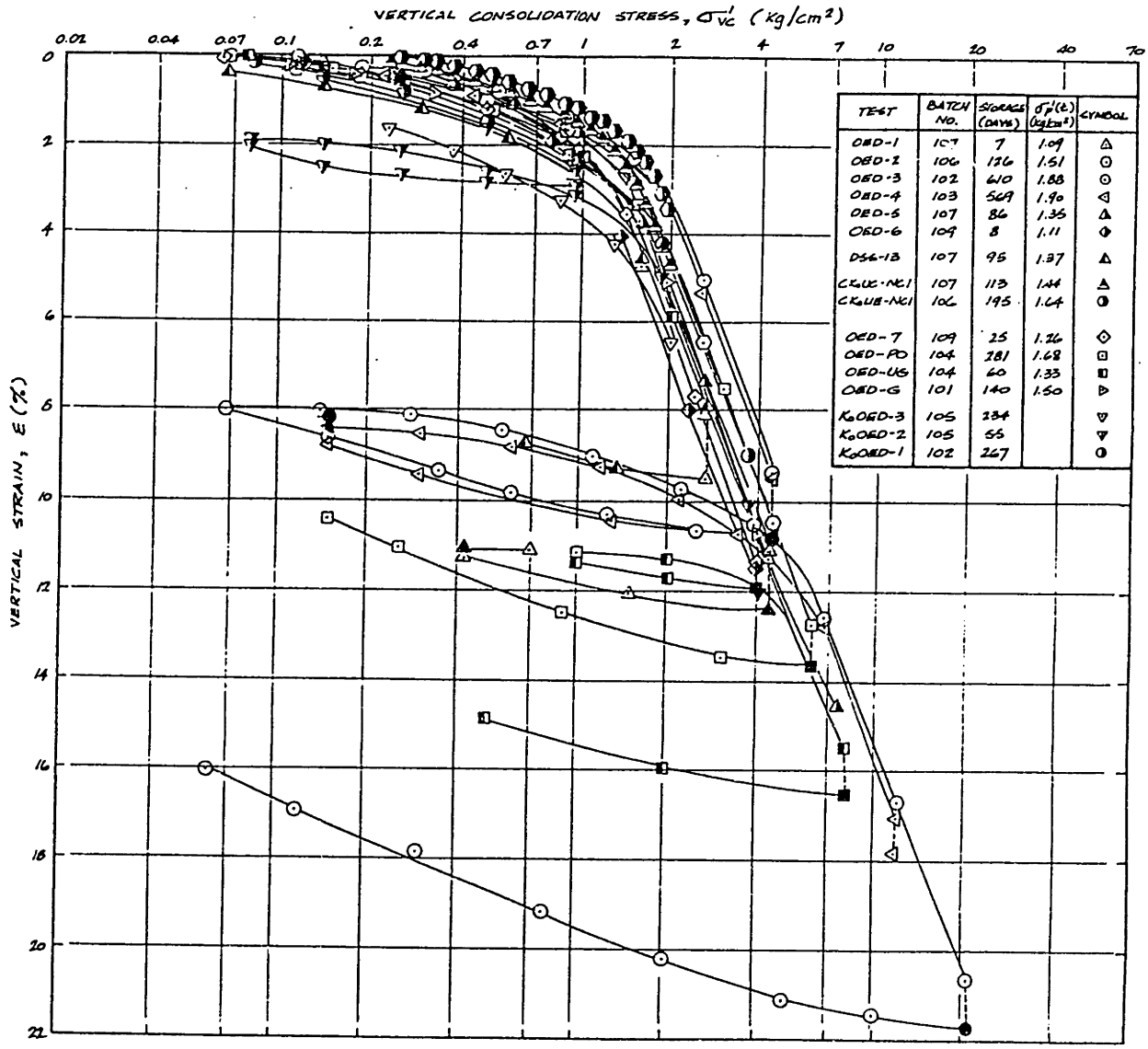

Figure 3.6: Consolidation Stress-Strain Results for Resedimented BBC.

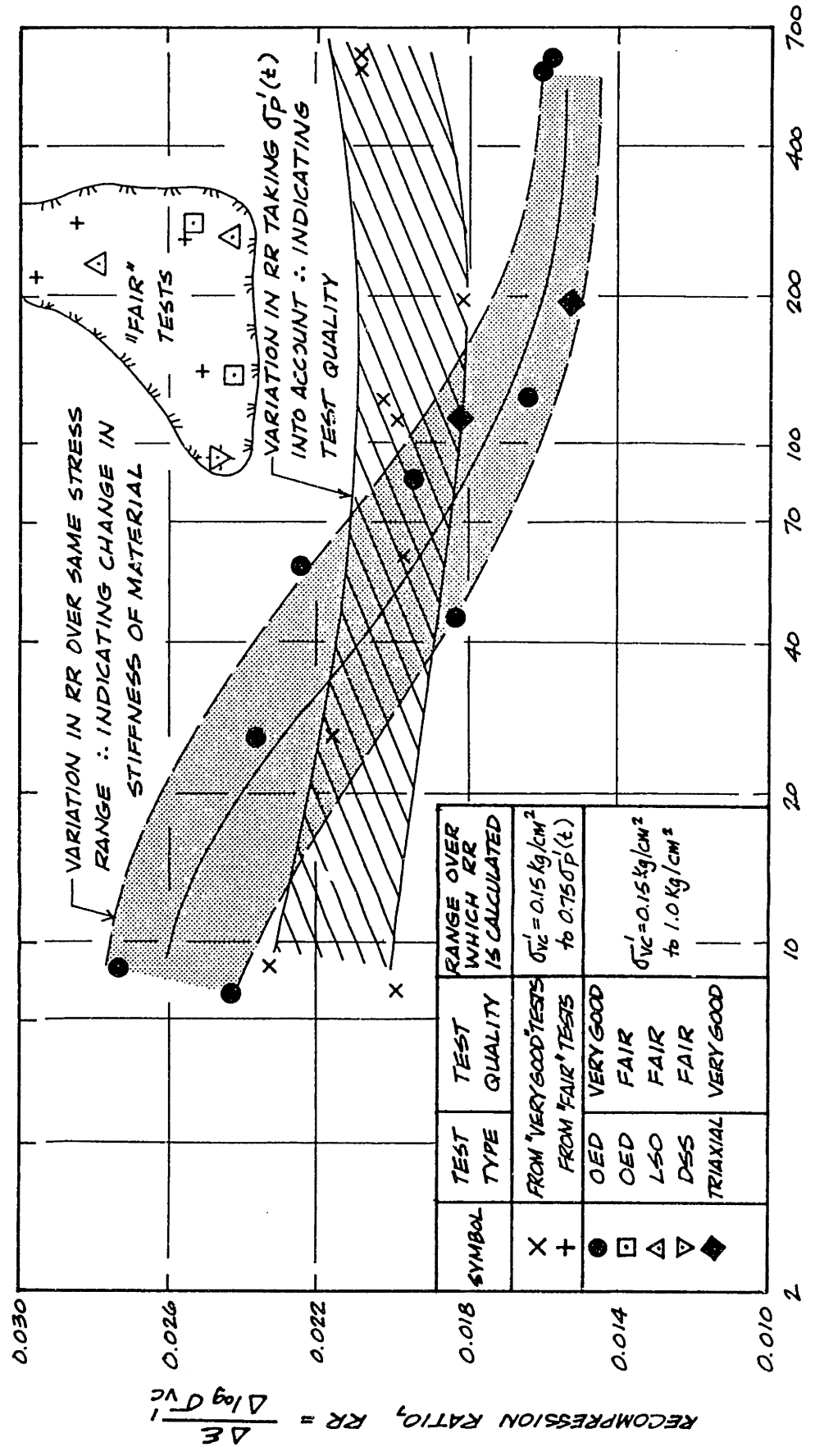

Figure 3.7: Effect of Storage Time on Recompression Ratio upon Initial Recompression of Resedimented BBC

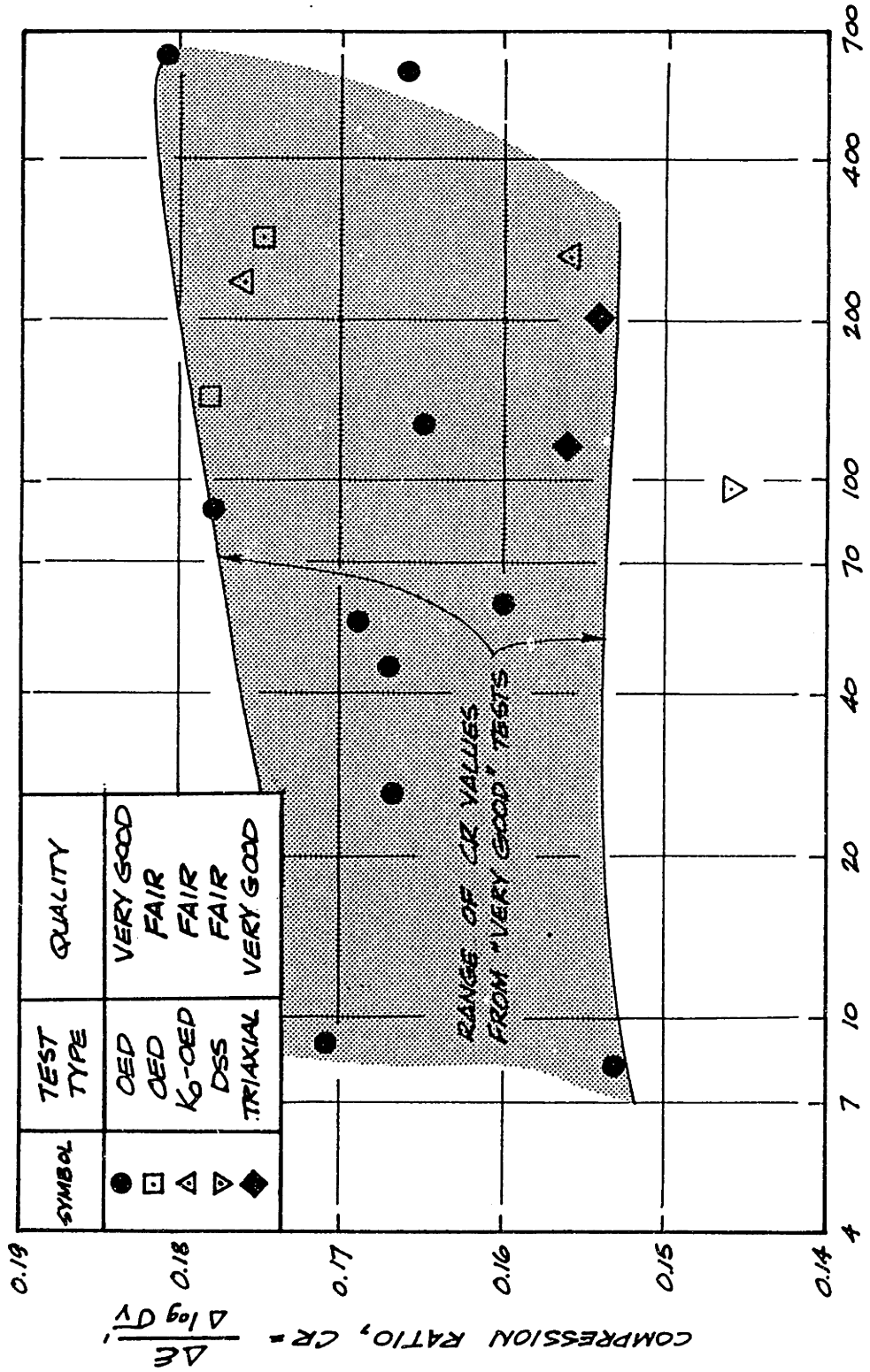

Figure 3.8: Effect of Storage Time on Compression Ratio of Resedimented BBC.

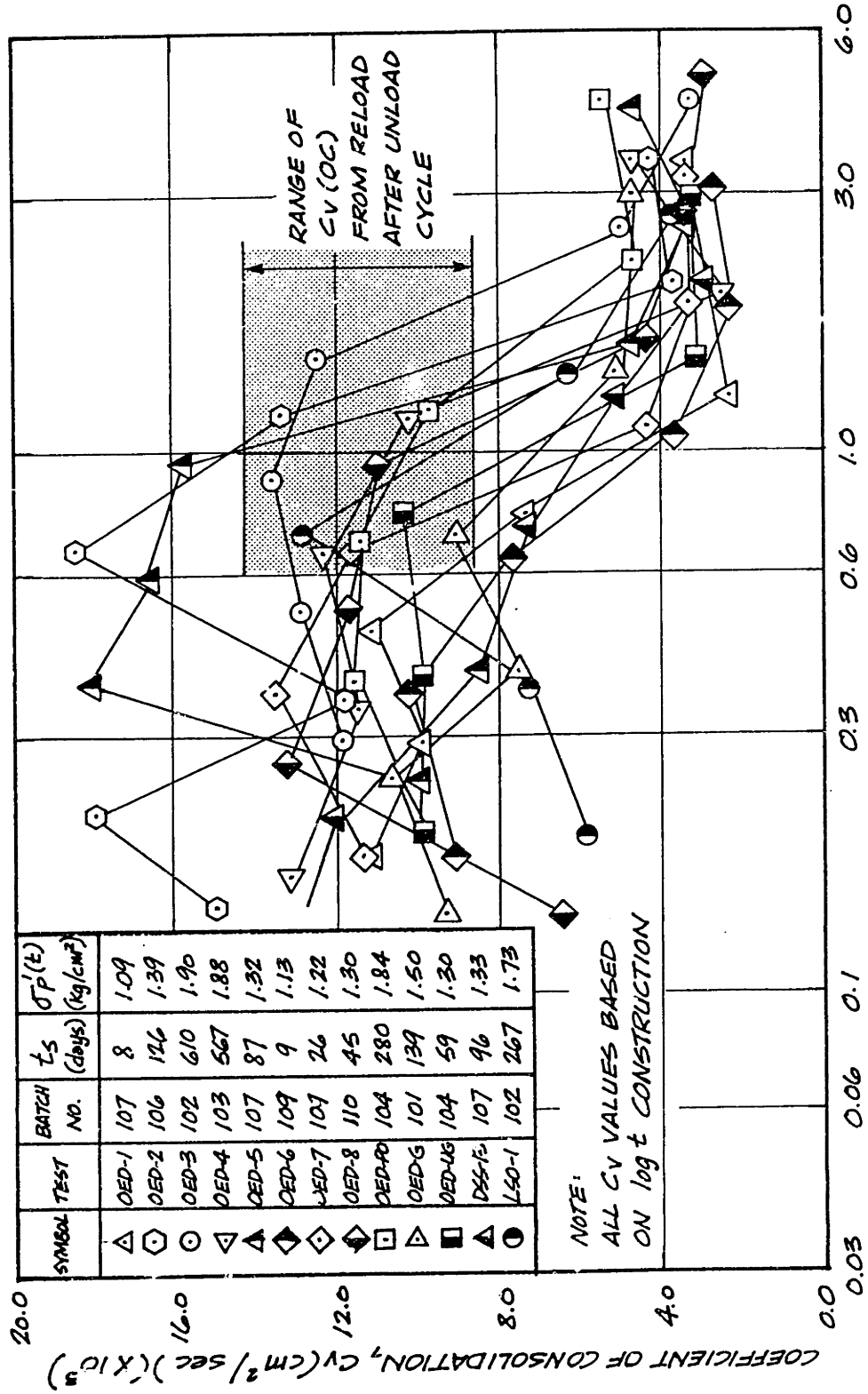

Figure 3.9: Coefficient of Consolidation for Resedimented BBC.

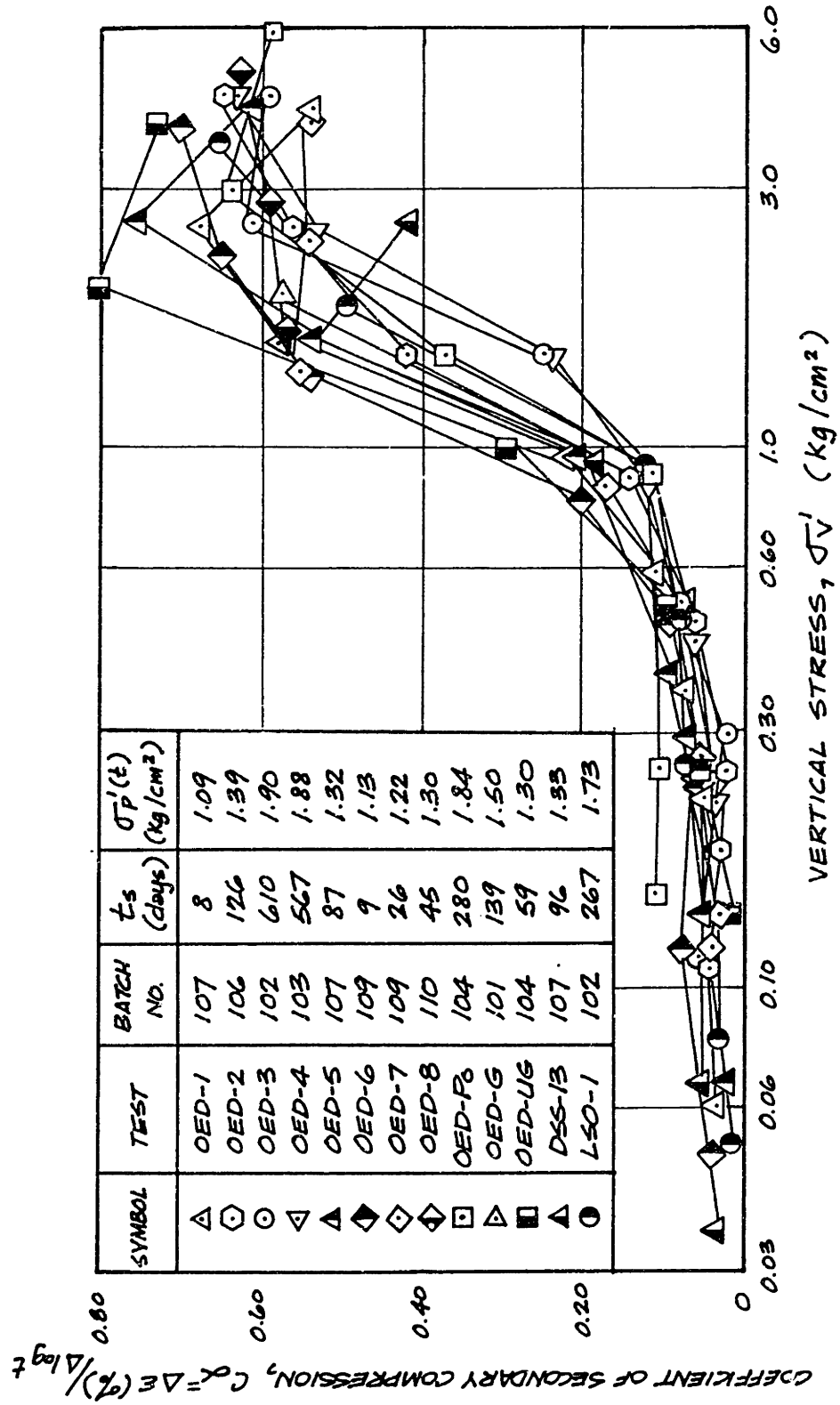

Figure 3.10: Coefficient of Secondary Compression for Resedimented BBC.

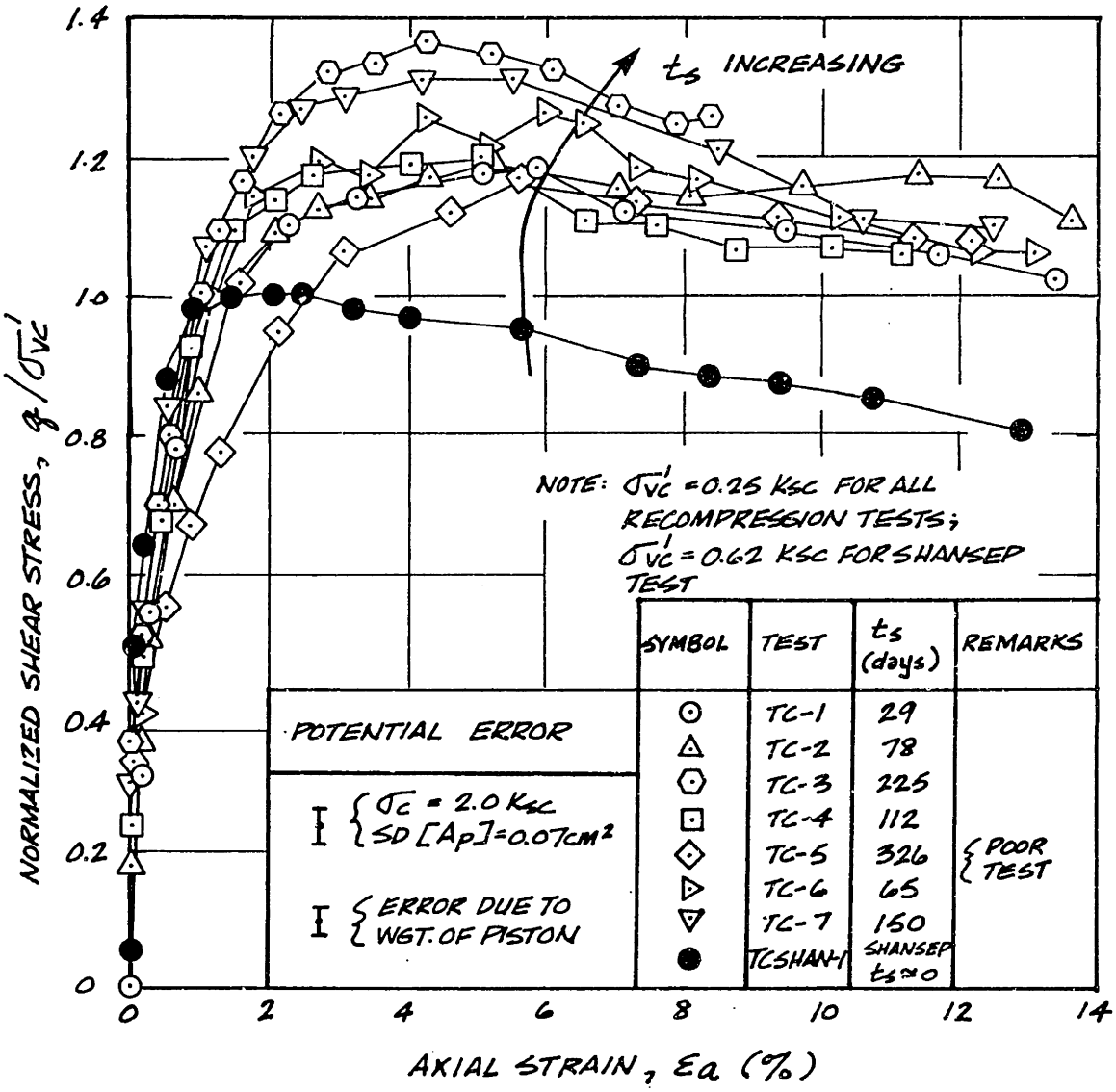

Figure 3.11: Stress-Strain Curves from $\overline{CK_oU}$ Triaxial Compression Tests on Resedimented BBC (OCR=4).

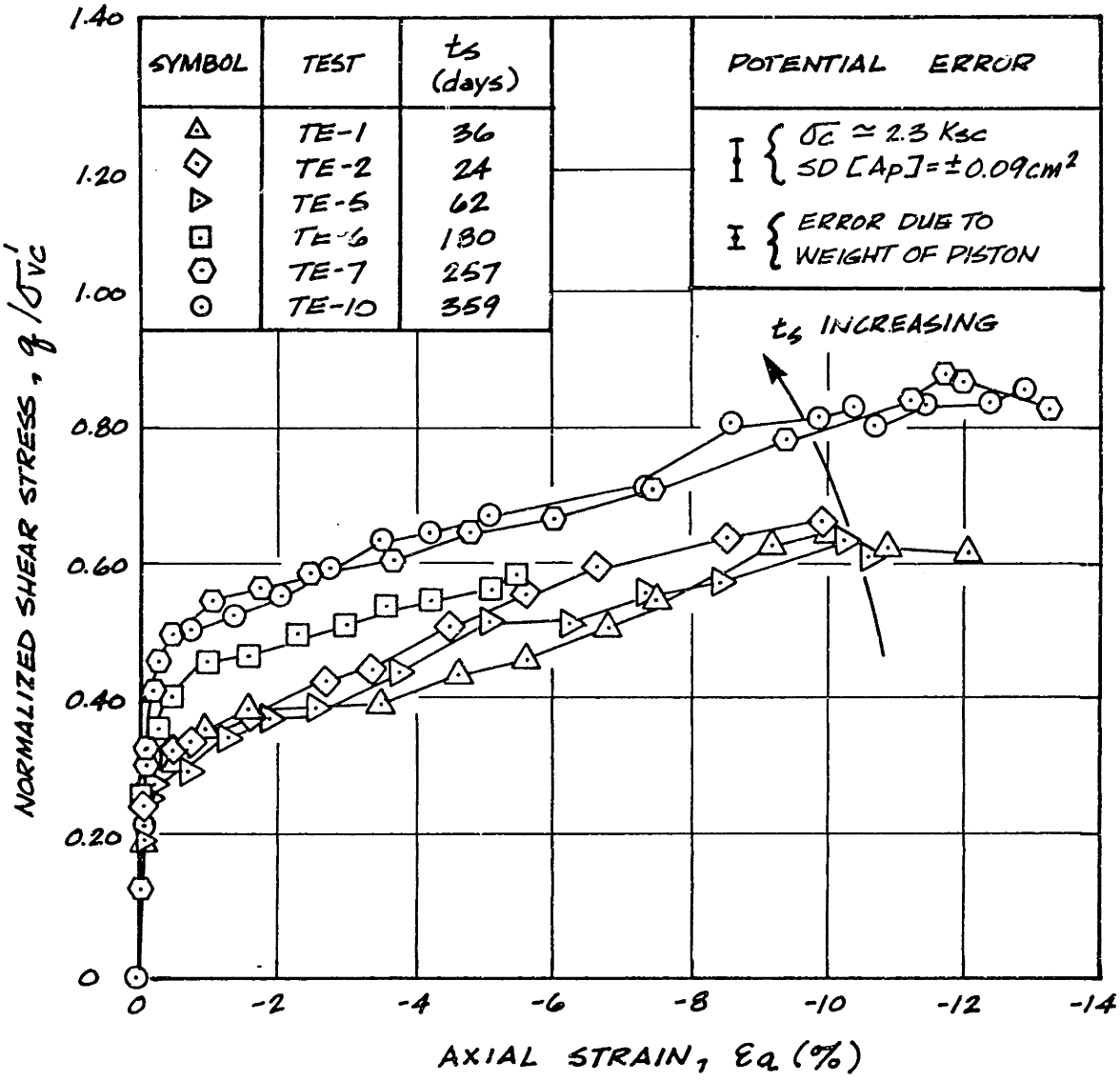

Figure 3.12: Stress-Strain Curves from $\overline{CK_oU}$ Triaxial Extension Tests on Resedimented BBC (OCR=4).

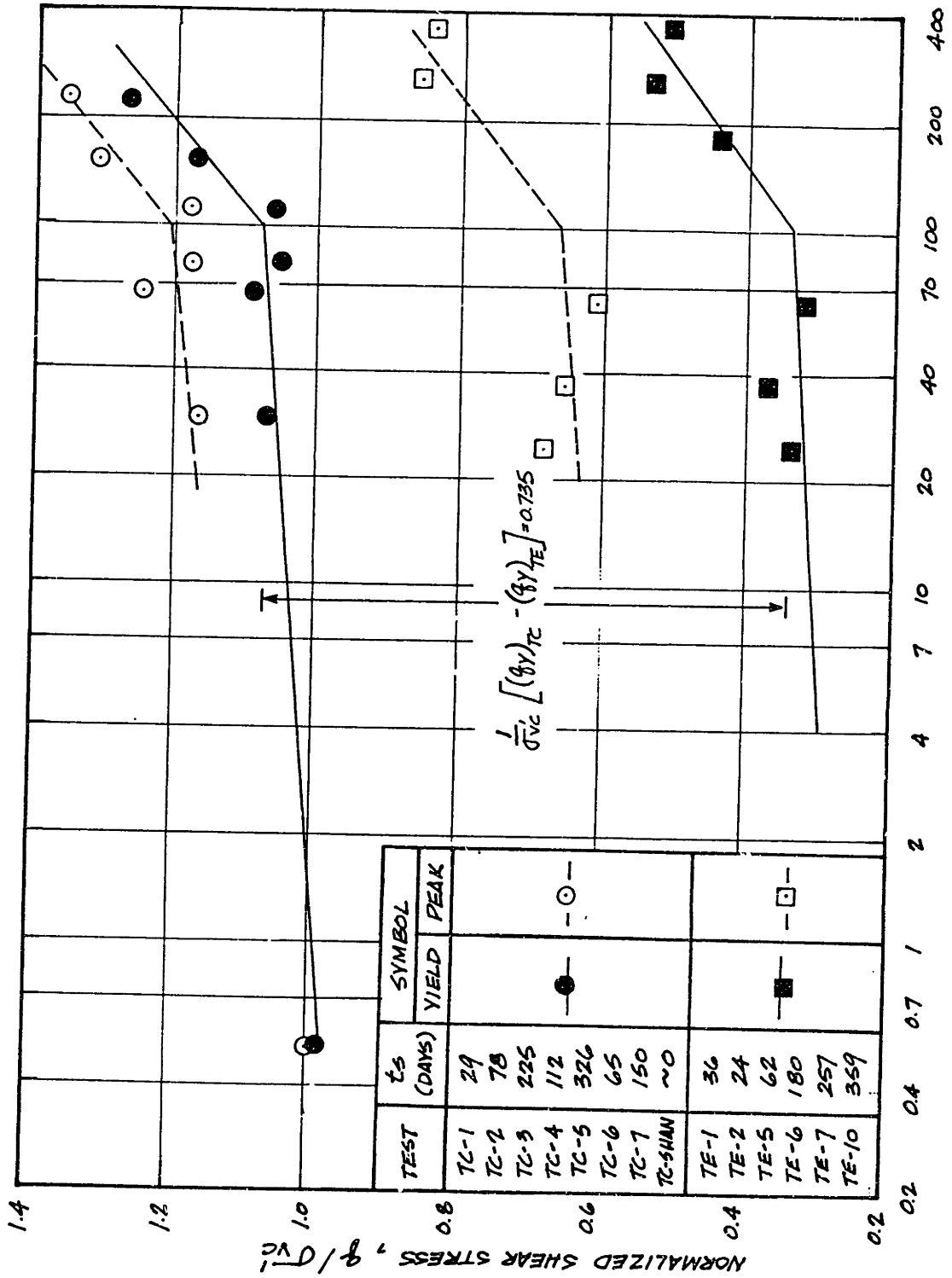

Figure 3.13: Changes in Strength of Resedimented BBC (OCR=4) in Compression and Extension between Samples with Different Storage Times.

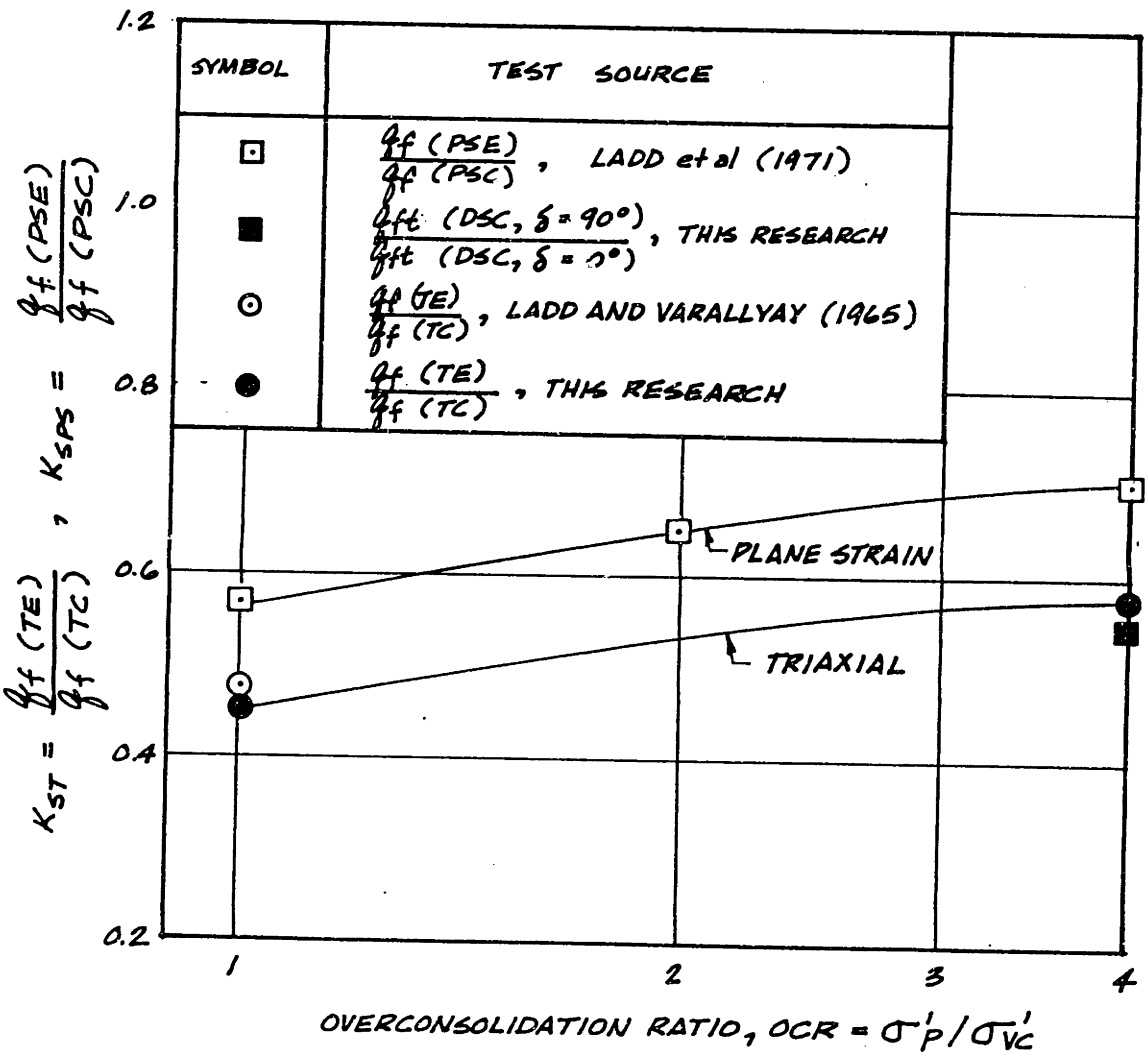

Figure 3.14: Anisotropy Ratio from Triaxial and Plane Strain Tests on Resedimented BBC.

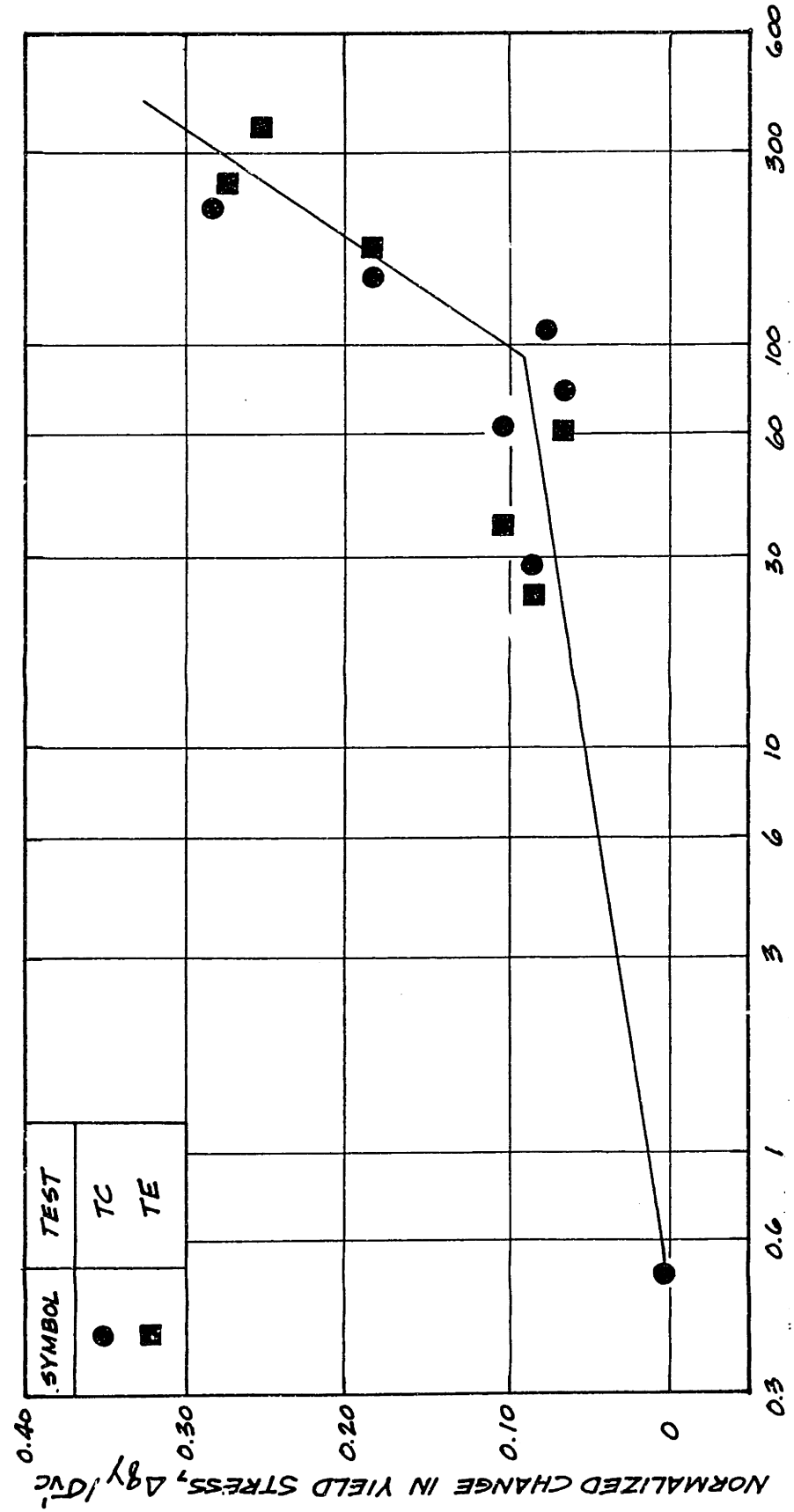

Figure 3.15: Effect of Storage Time on Undrained Shear Yield Stress for Resedimented BBC (OCR=4, σ'_p=1.0 ksc).

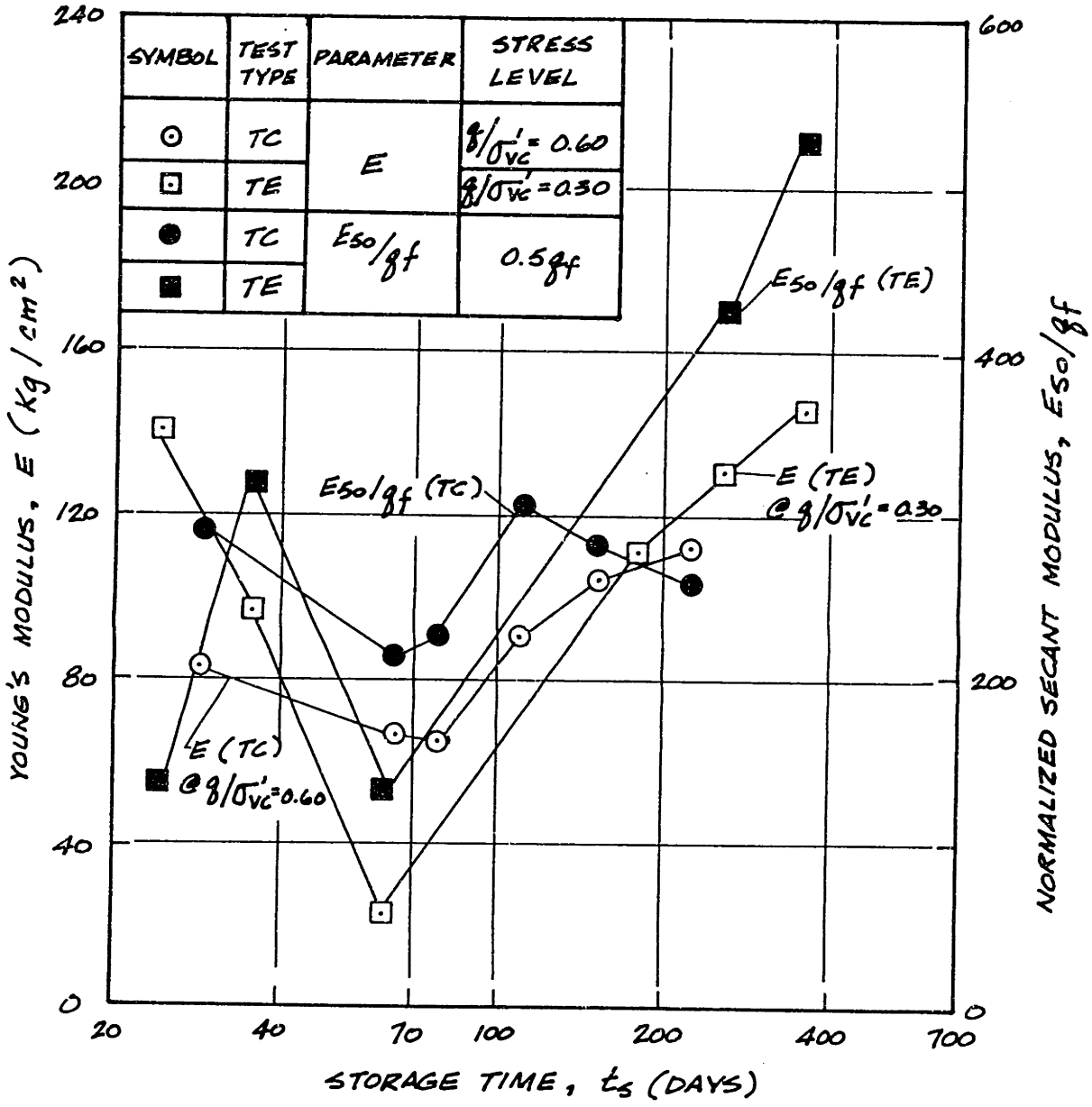

Figure 3.16: Effect of Storage Time on Initial Stiffness under Undrained (Triaxial) Shear for Resedimented BBC (OCR=4).

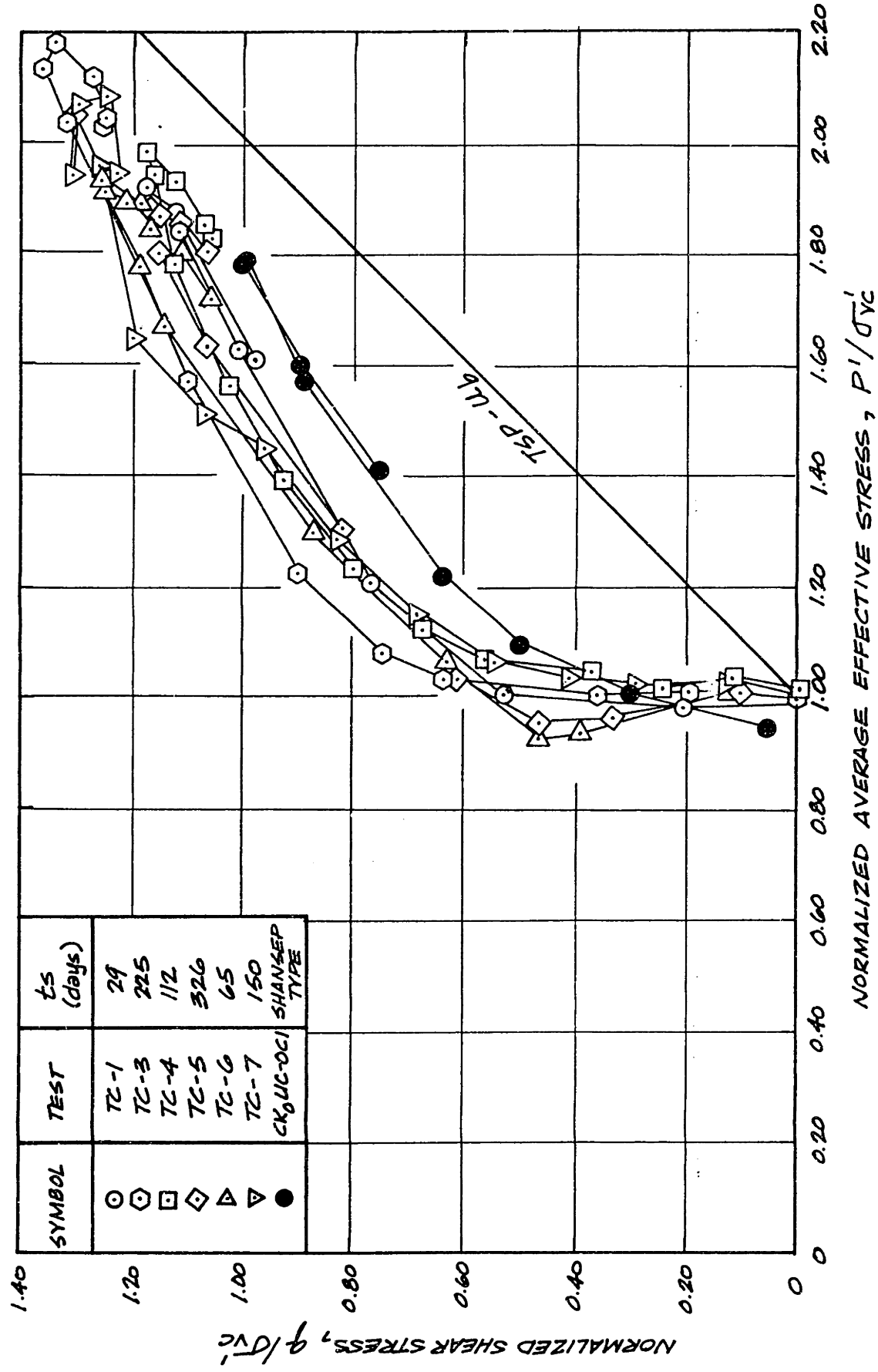

Figure 3.17: Normalized Stress Paths from $\overline{CK_oU}$ Triaxial Compression Tests on Resedimented BBC (OCR=4).

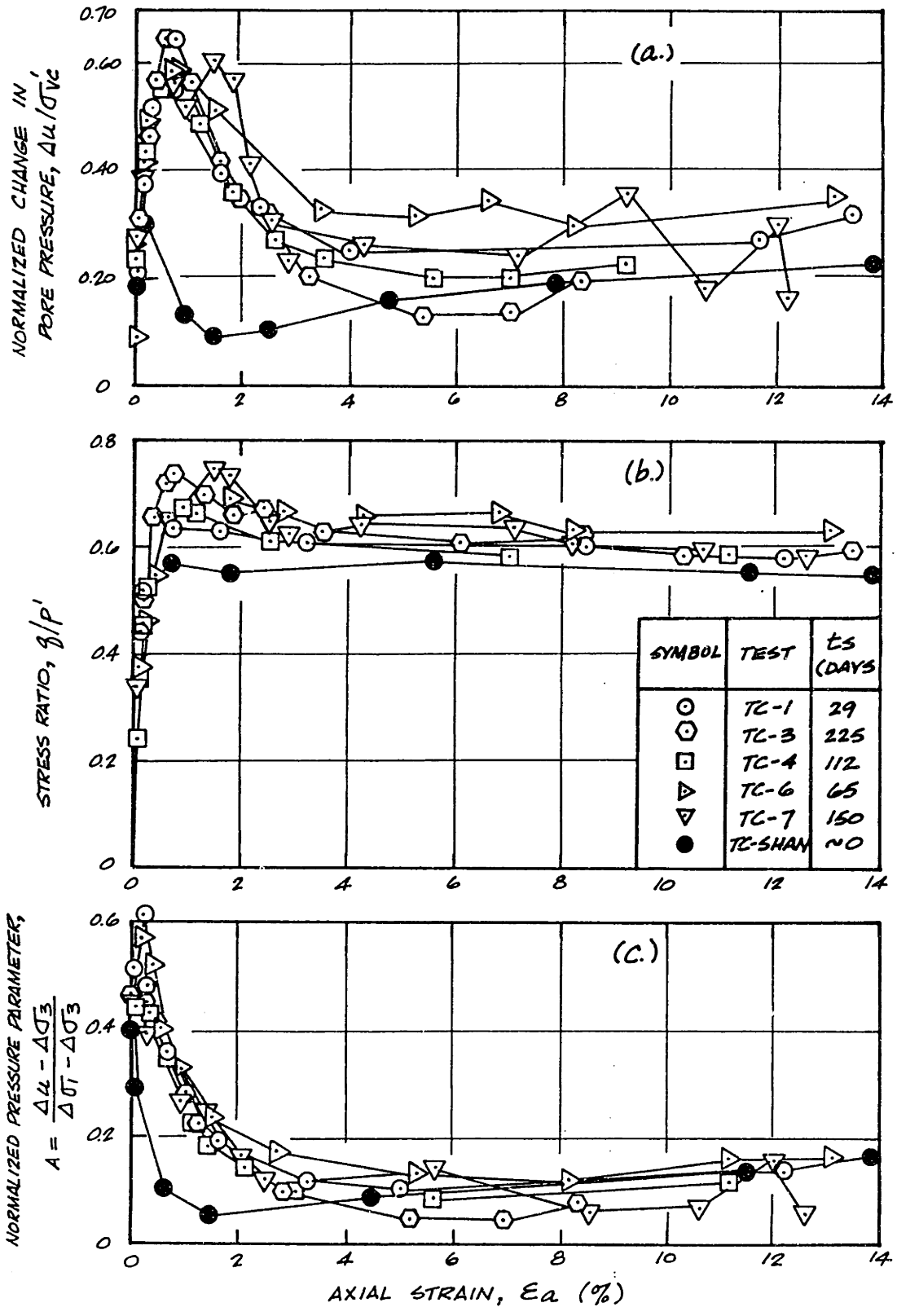

Figure 3.18: Normalized Pore Pressure, Stress Ratio and A Parameter from CK_oU Triaxial Compression Tests on Resedimented BBC (OCR=4).

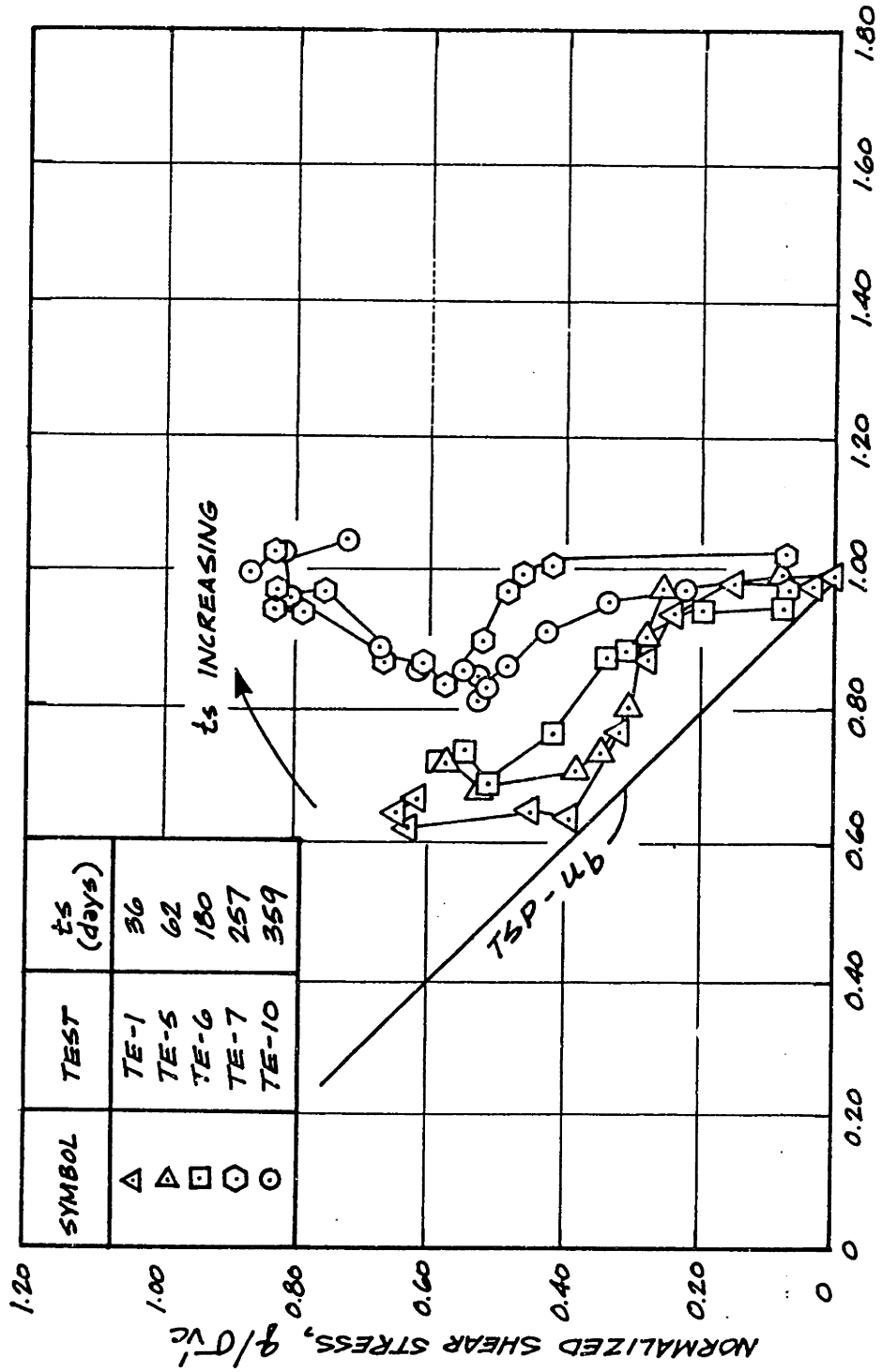

Figure 3.19: Normalized Stress Paths from $\overline{CK_oU}$ Triaxial Extension Tests on Resedimented BBC (OCR=4).

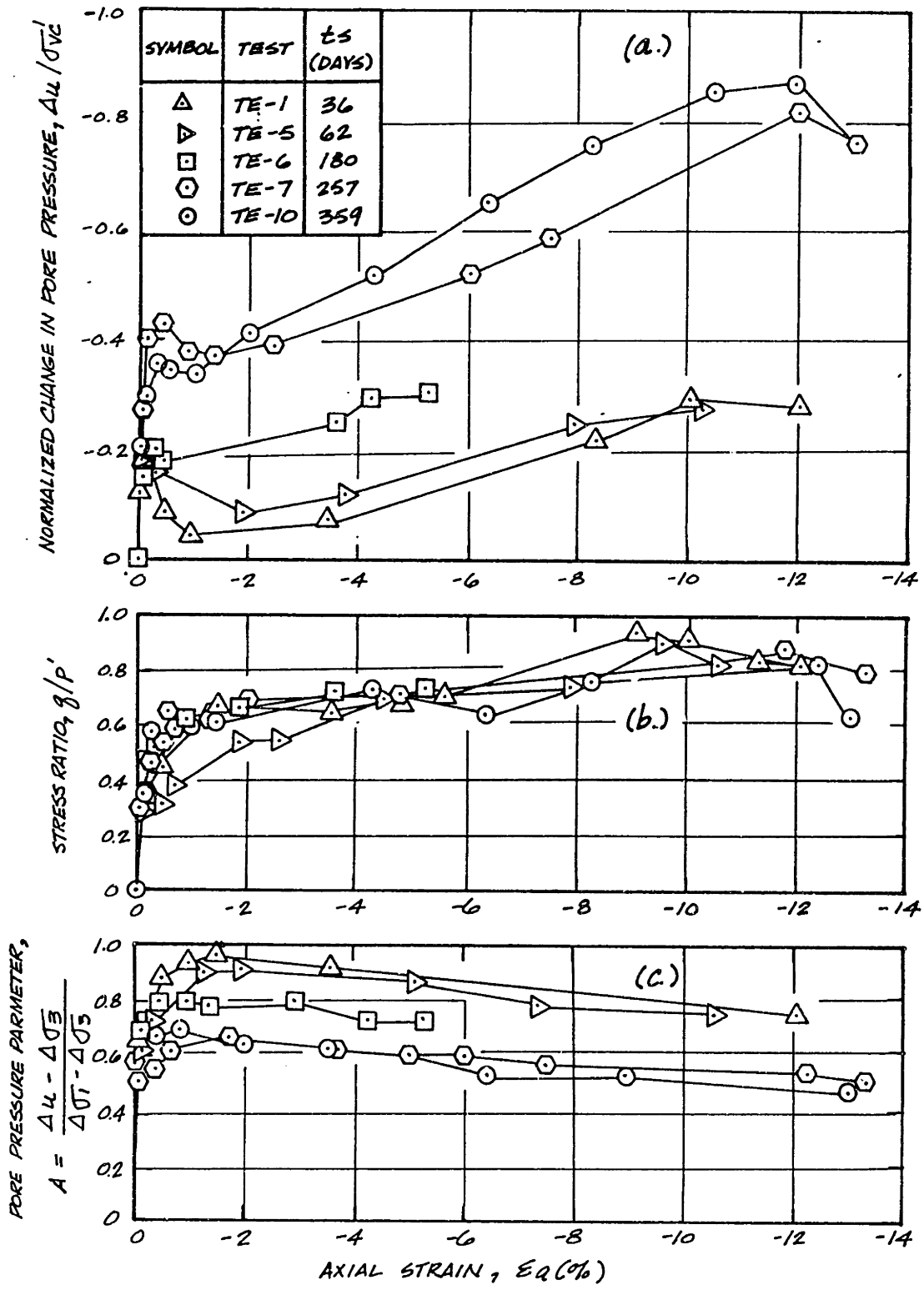

Figure 3.20: Normalized Pore Pressure, Stress Ratio and A Parameter from CK_oU Triaxial Extension Tests on Resedimented BBC (OCR=4).

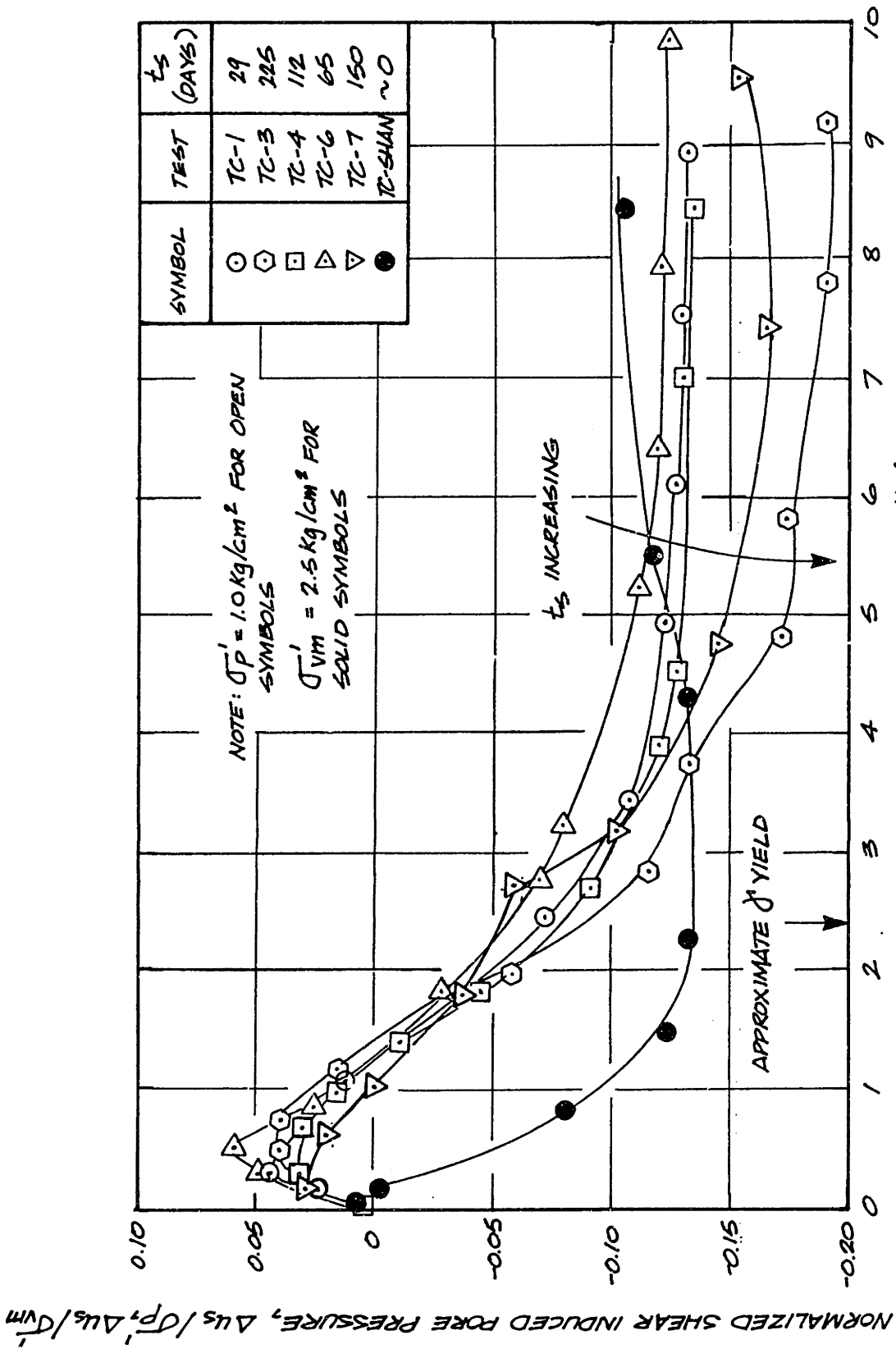

Figure 3.21: Normalized Shear-Induced Pore Pressure vs. Maximum Shear Strain from CK_oU Triaxial Compression Tests on Resedimented BBC (OCR=4).

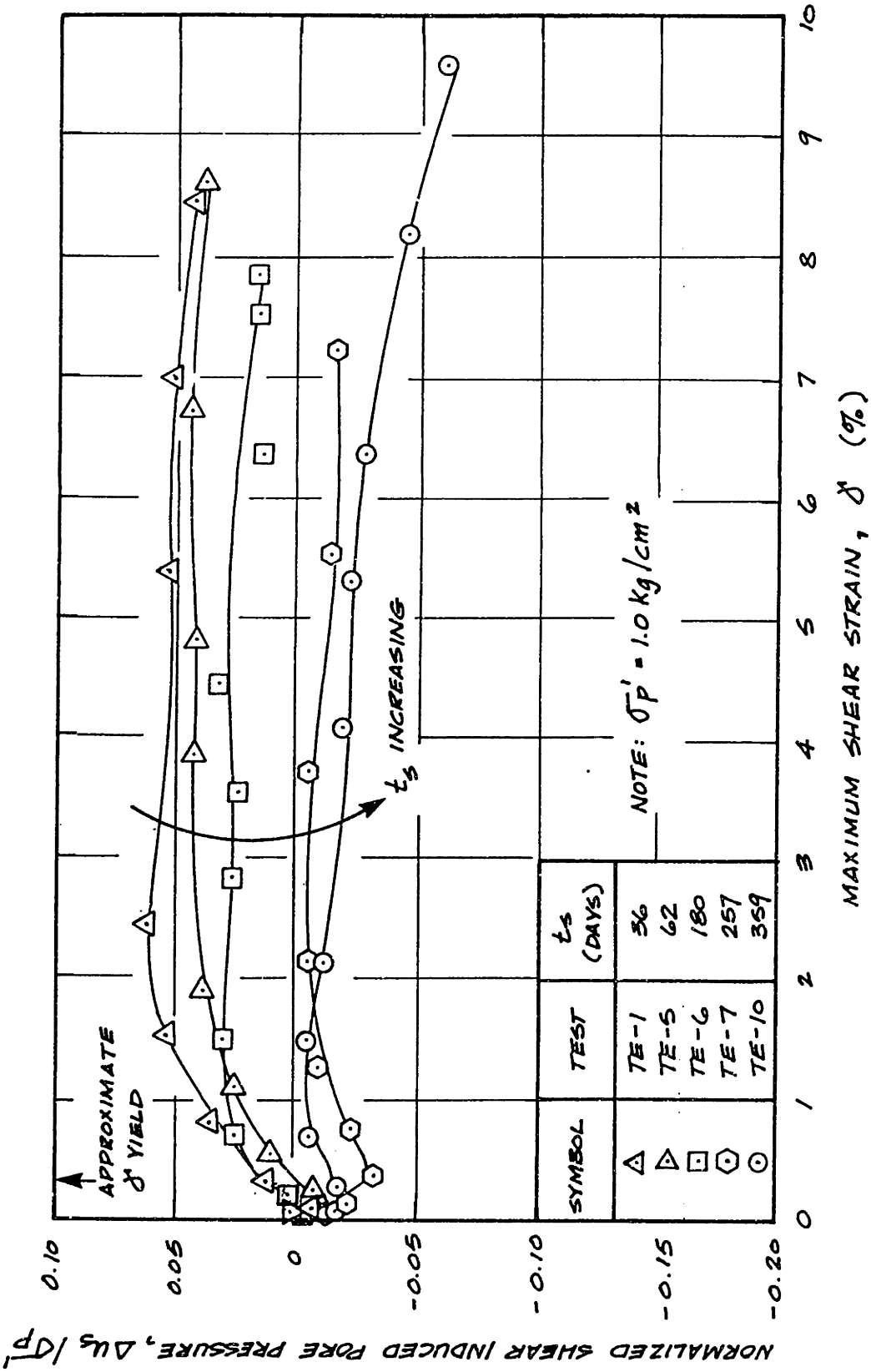

Figure 3.22: Normalized Shear-Induced Pore Pressure vs. Maximum Shear Strain from CK_oU Triaxial Extension Tests on Resedimented BBC (OCR=4).

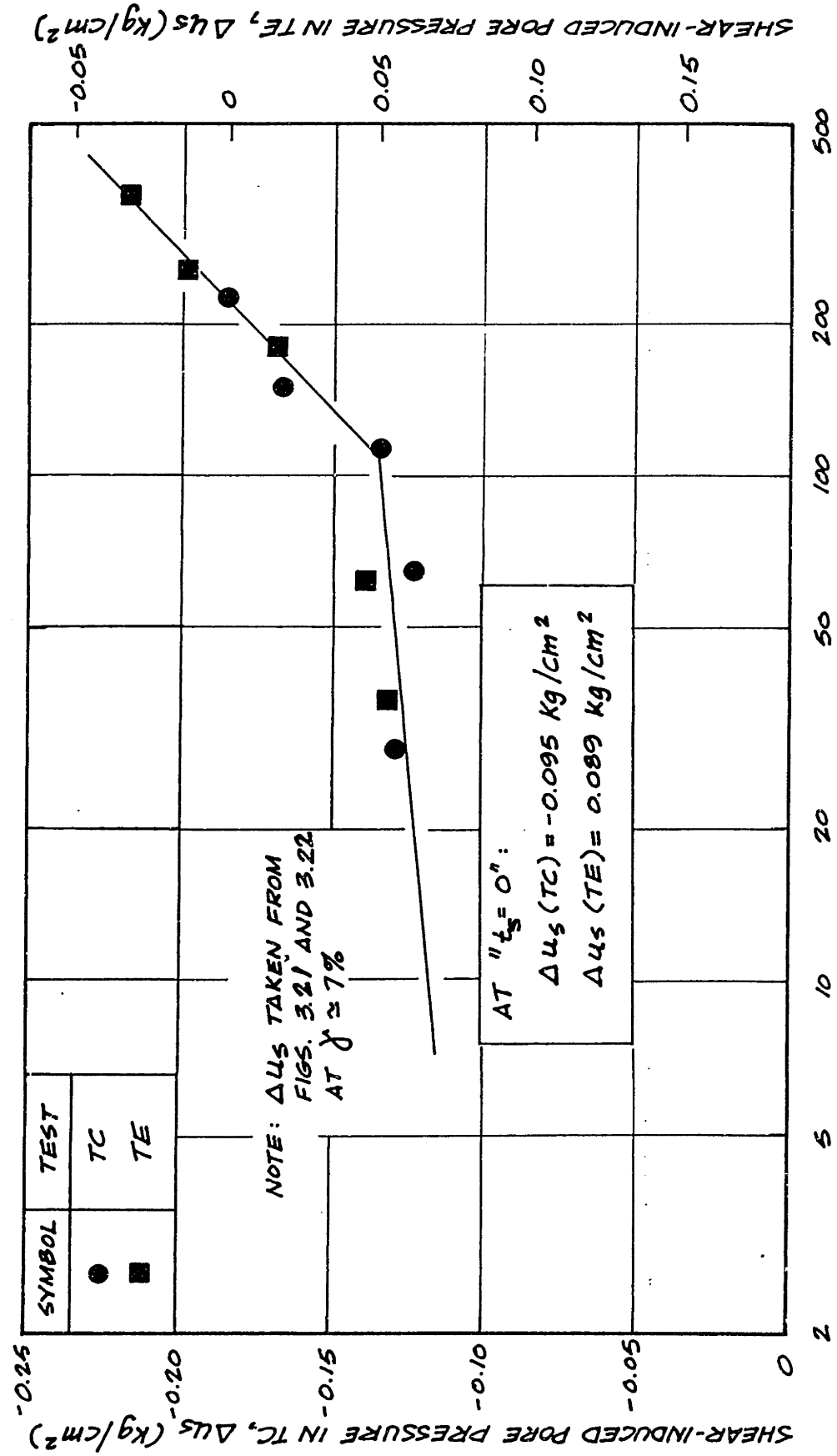

Figure 3.23: Effect of Storage Time on Undrained Shear Induced Pore Pressure for Resedimented BBC (OCR=4).

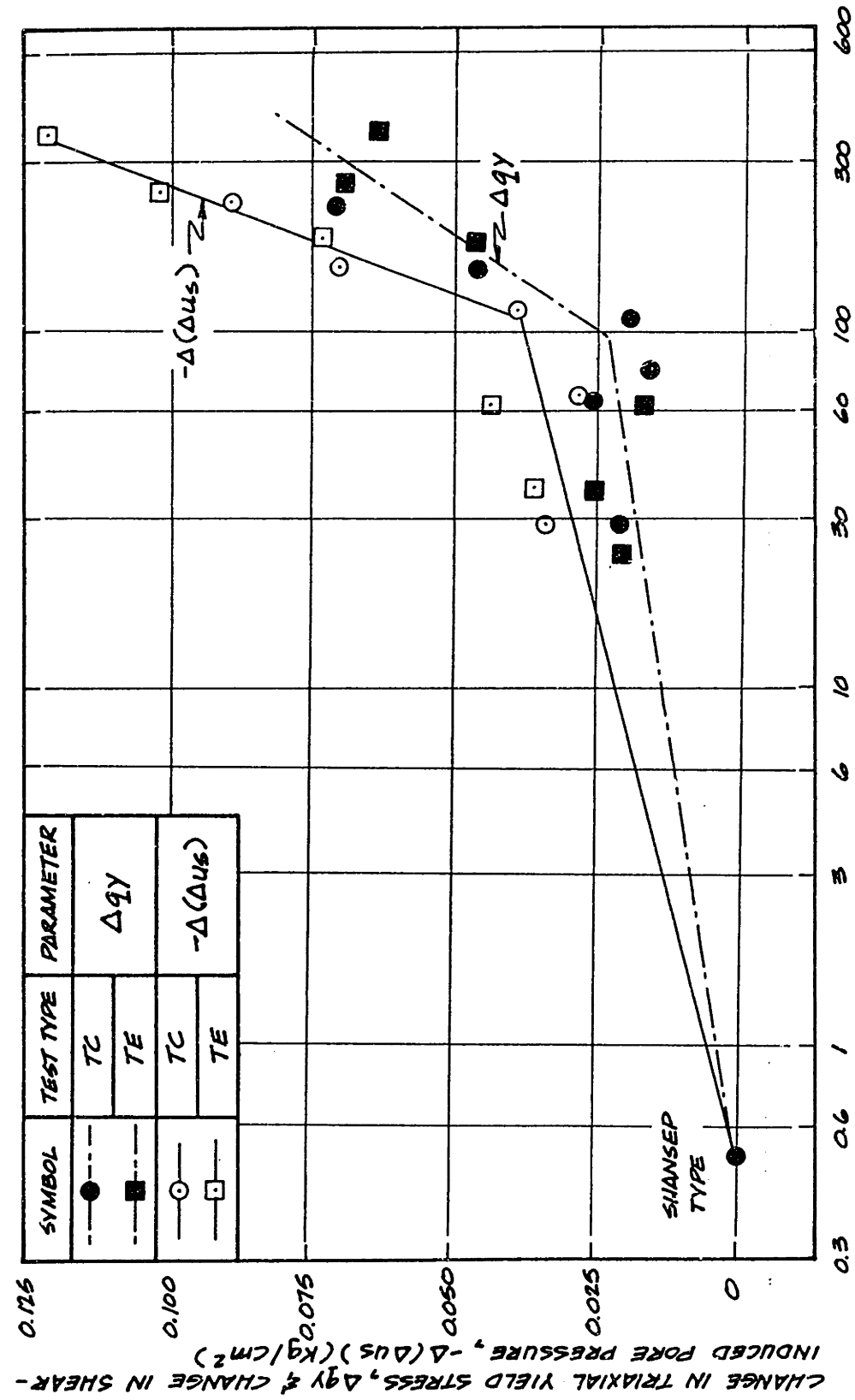

Figure 3.24: Summary Plot of Effect of Storage Time on Undrained Shear Yield Stress and Shear Induced Pore Pressure for Resedimented BBC (OCR=4, σ'_p=1.0 ksc).

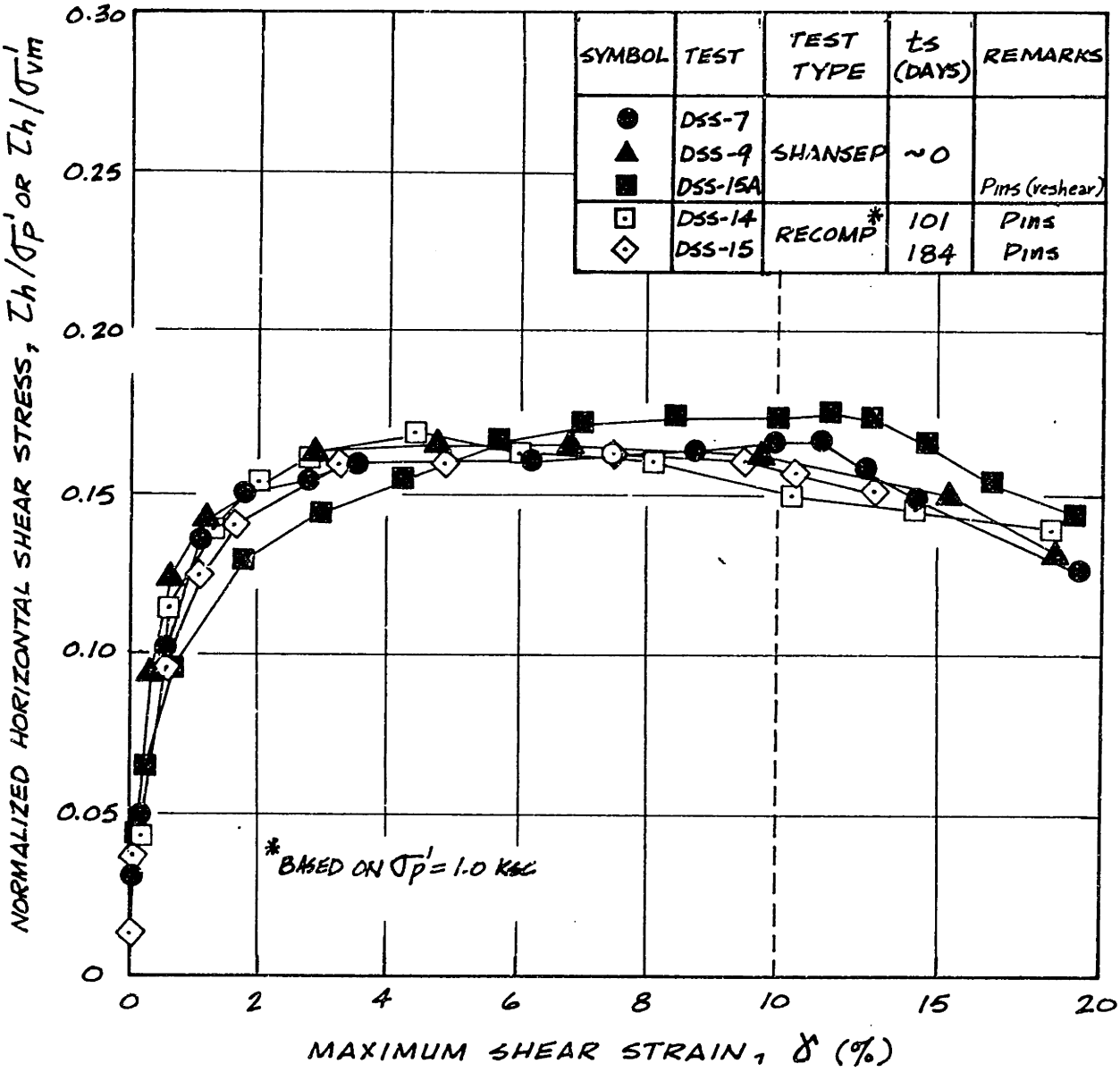

Figure 3.25: Normalized Stress-Strain Relationships from CK_oUDSS Tests on Resedimented BBC (OCR=4).

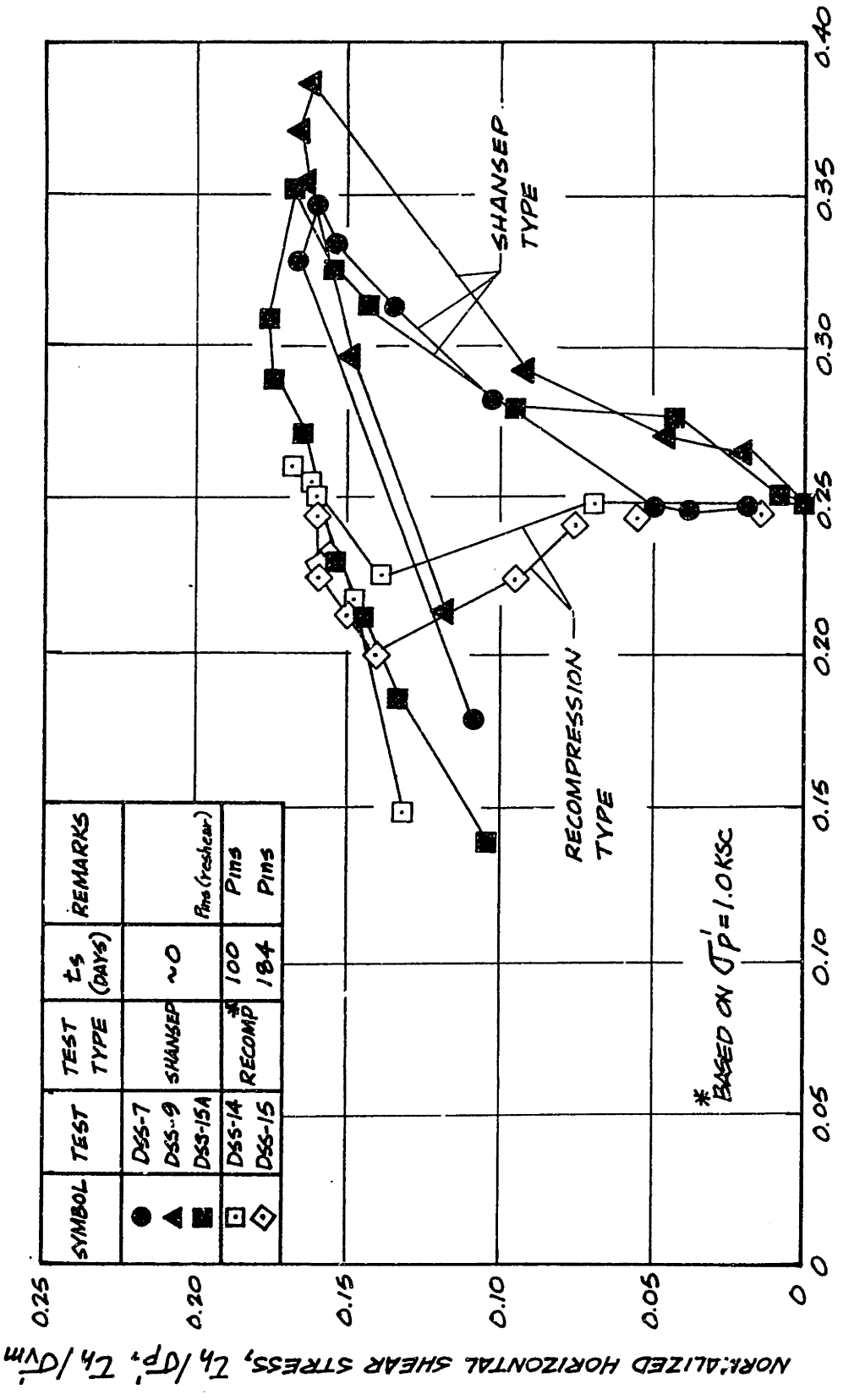

Figure 3.26: Normalized Horizontal Shear Stress vs. Vertical Normal Stress from CK_oUDSS Tests on Resedimented BBC (OCR=4).

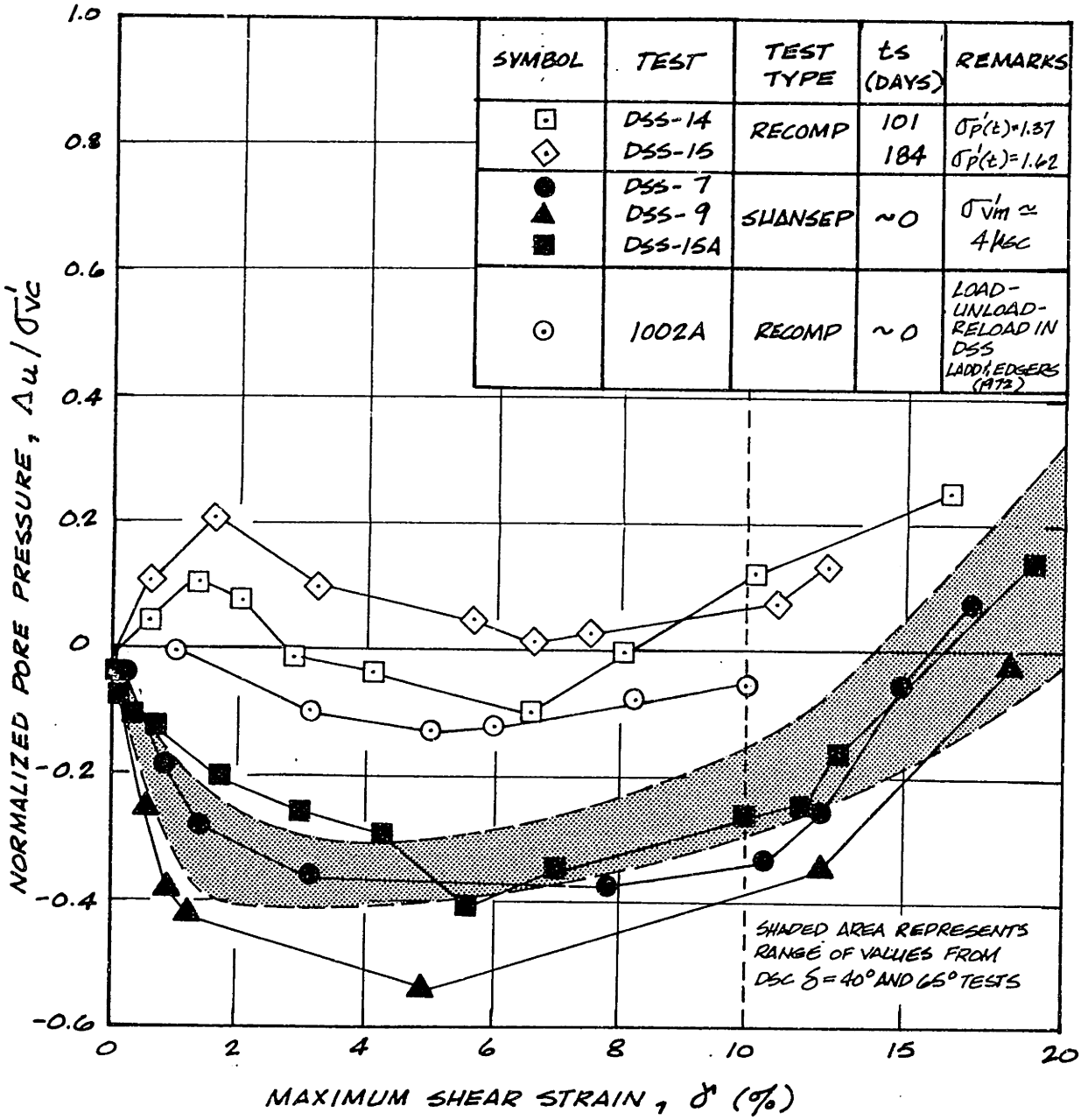

Figure 3.27: Normalized Shear-Induced Pore Pressures from CK_oUDSS Tests and Anisotropic DSC Tests (δ=40° and 65°) on Resedimented BBC (OCR=4).

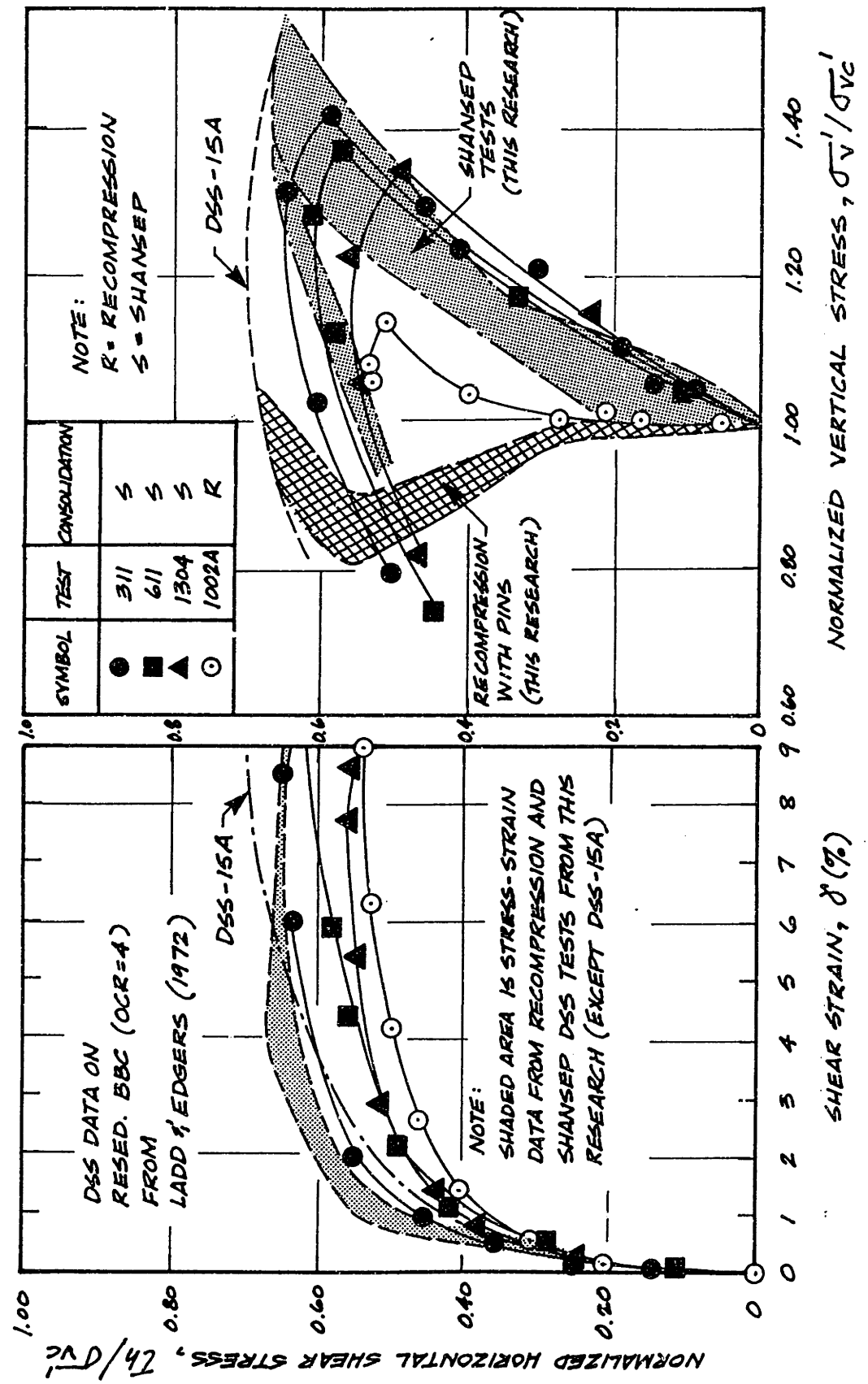

Figure 3.28: Normalized Stress-Strain Relationships and Stress Paths from CK_oUDSS Tests following Recompression and SHANSEP type Consolidation on Resedimented BBC (OCR=4).

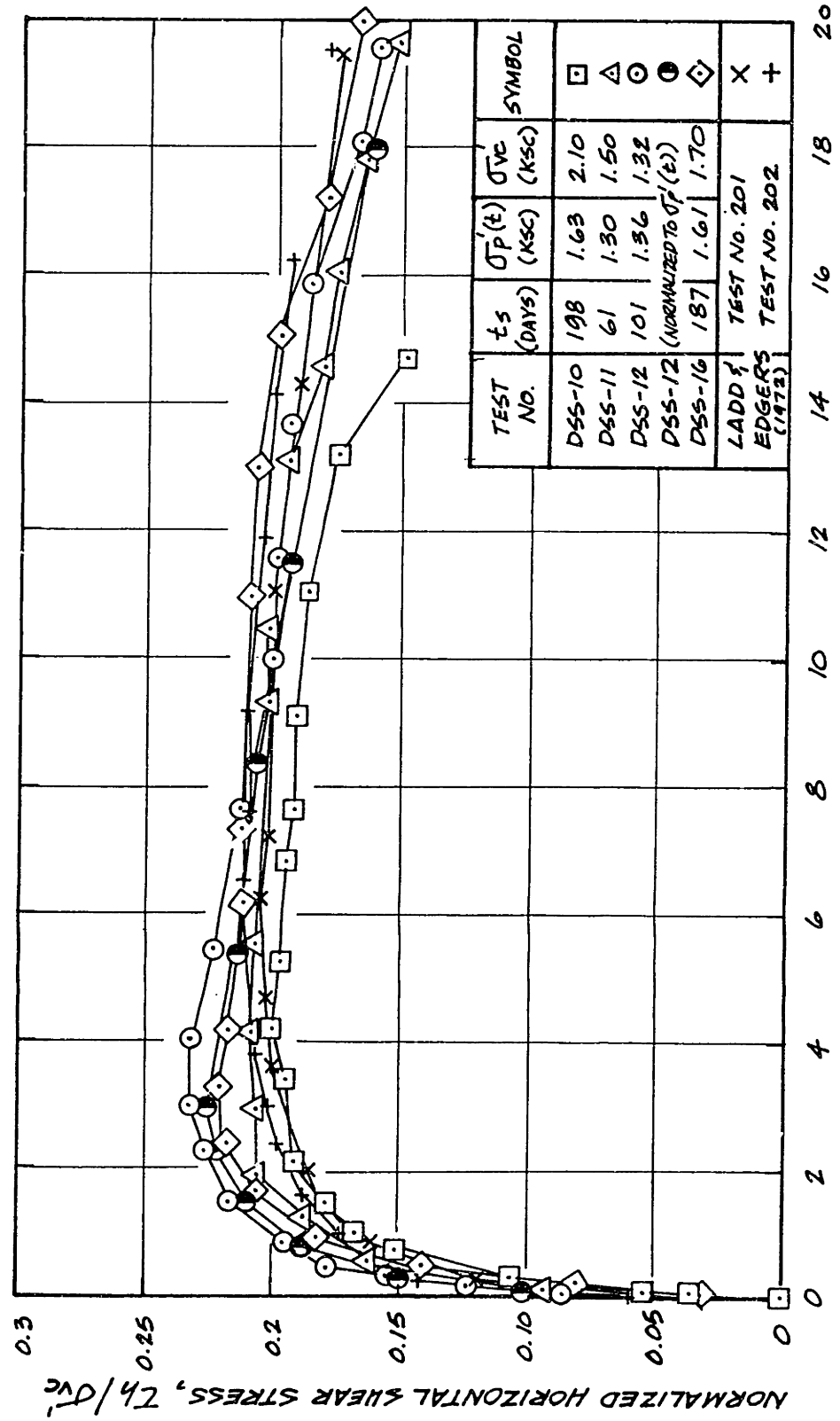

Figure 3.29: Normalized Stress-Strain Relationships from CK_oUDSS Tests on Resedimented BBC (OCR=1).

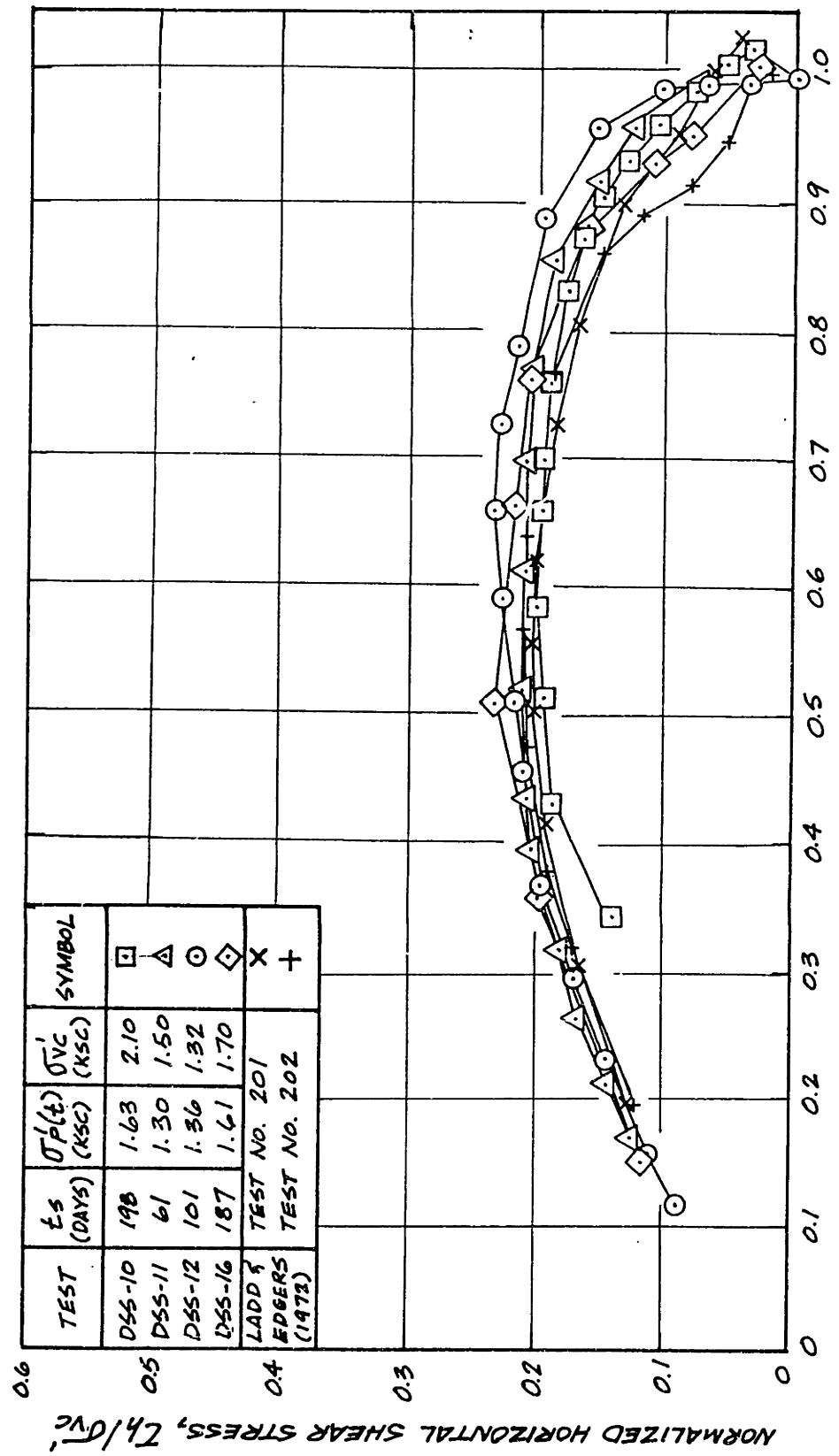

Figure 3.30: Normalized Horizontal Shear Stress vs. Vertical Normal Stress from CK_oUDSS Tests on Resedimented BBC (OCR=1).

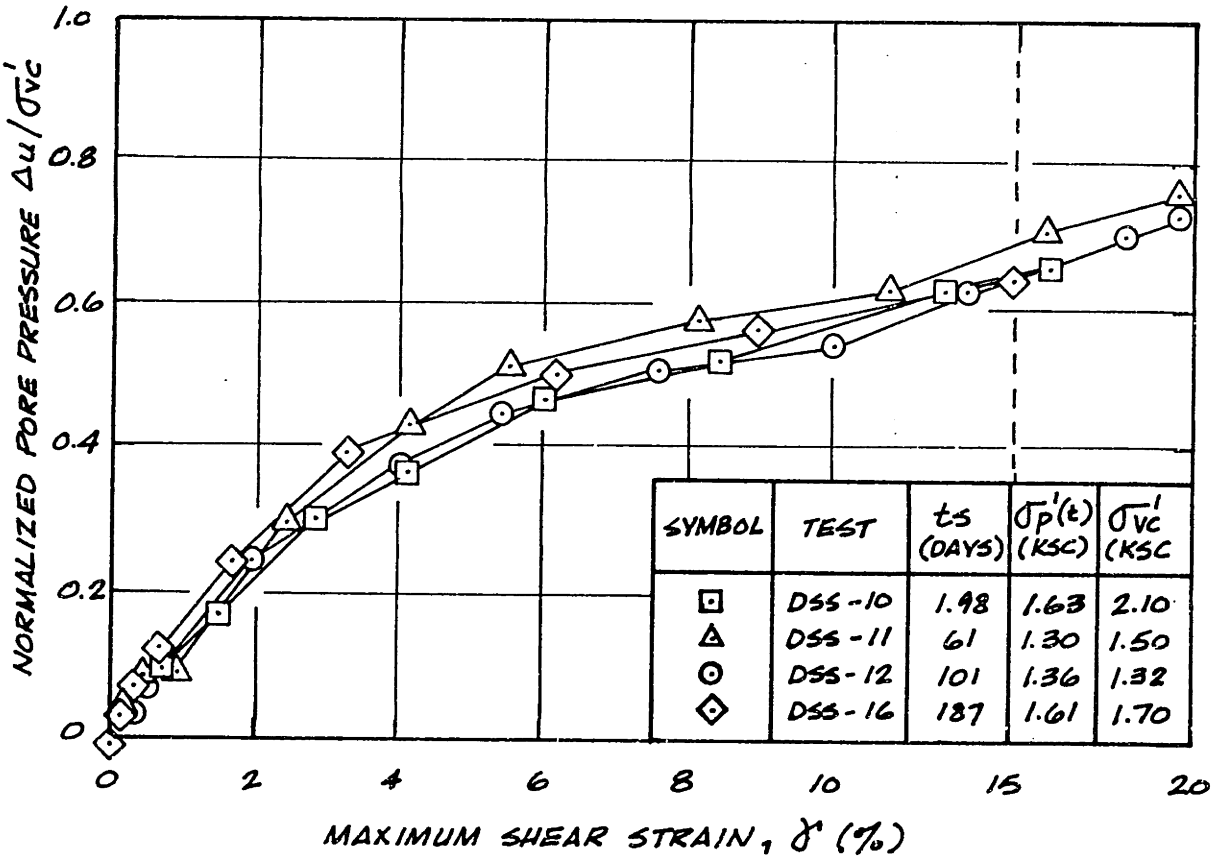

Figure 3.31: Normalized Pore Pressure vs. Maximum Shear Strain from CK_oUDSS Tests on Resedimented BBC (OCR=1).

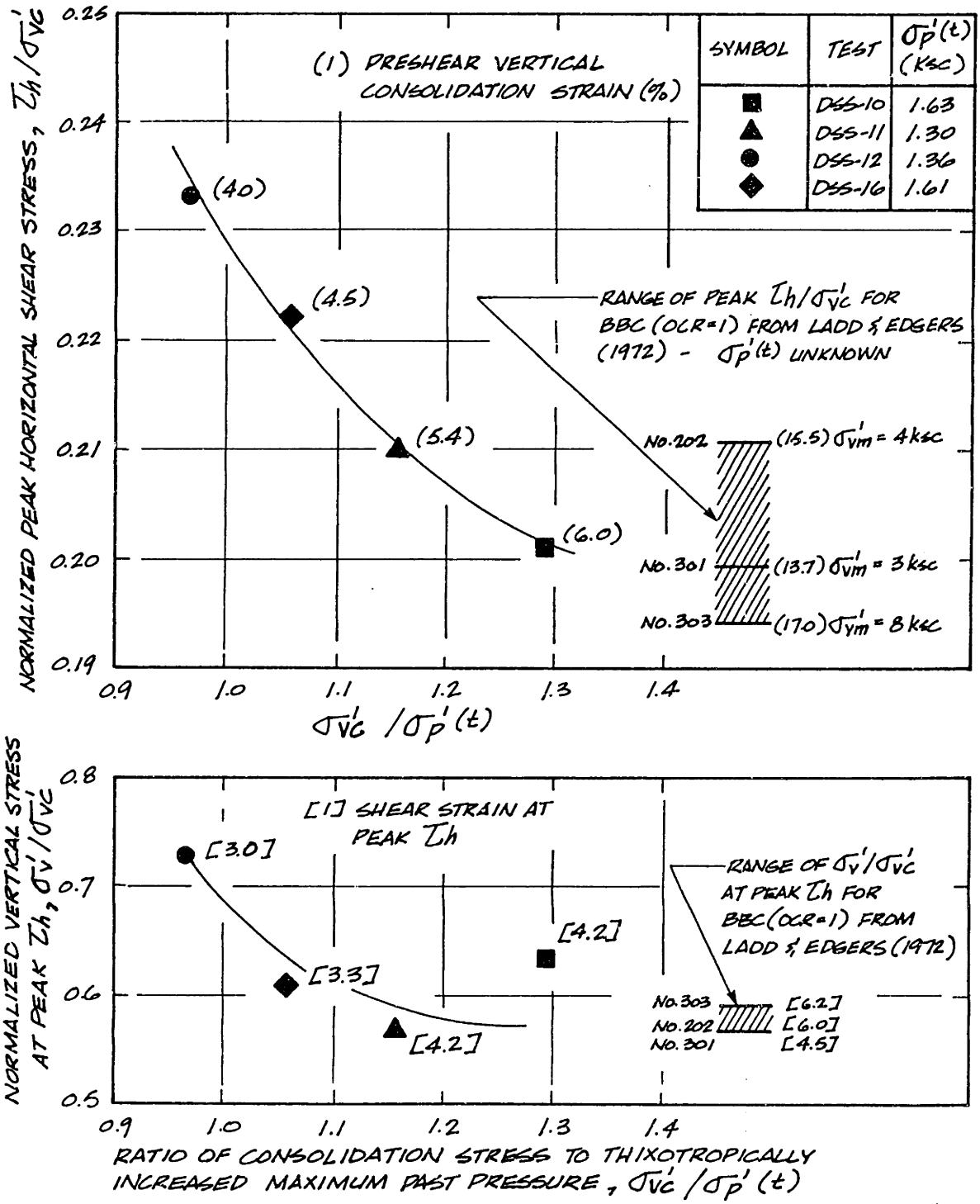

Figure 3.32: Effect of Ratio of Vertical Consolidation Stress to Thixotropically Increased Maximum Past Pressure on Horizontal Shear Strength and Vertical Effective Stress on Resedimented BBC (OCR=1).

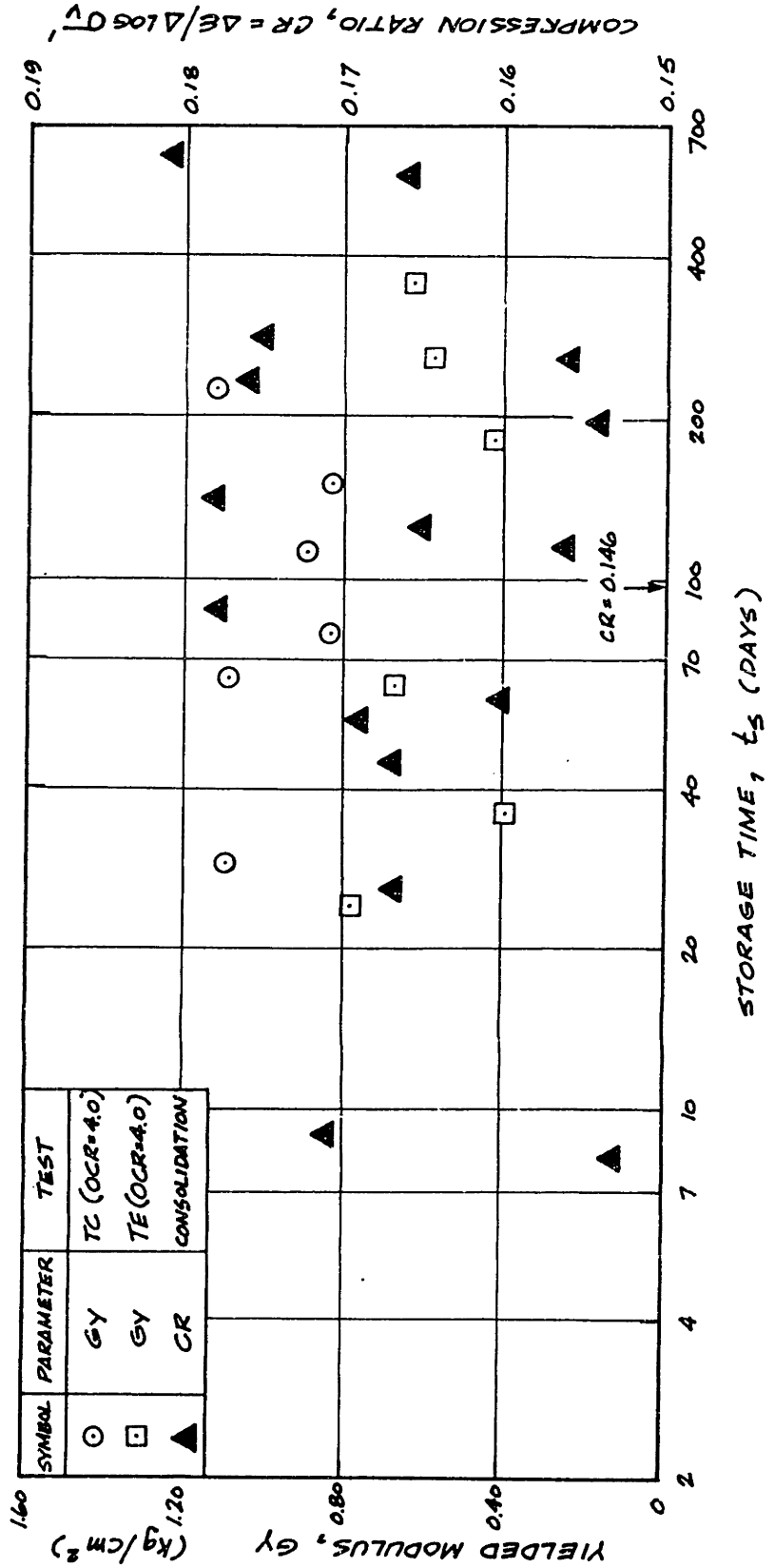

Figure 3.33: Effect of Storage Time on Post-Yield Moduli from Tests Performed on Resedimented BBC (OCR=1 and 4).

CHAPTER 4

EVALUATION OF AND IMPROVEMENTS TO DSC TESTING TECHNIQUES

4.1 OVERVIEW OF DSC TEST EVALUATION PROCEDURE

Performance of a Directional Shear Cell (DSC) test on cohesive samples demands operator skill considerably more advanced than those necessary for triaxial or Direct Simple Shear tests. Application of the desired stresses to the sample, very much a function of proper positioning of pressure bags and shear sheets for normal and shear stresses, respectively, has improved during the period of this research. In addition, new experimental techniques (to be discussed in Section 4.2) serve to mitigate the potential for errors due either to zones of stress concentration or to unacceptable interaction between the shear sheets and the pressure bags. Given that improvement of DSC testing techniques evolved during this research, measurable standards are desired in order to determine whether or not individual DSC tests are satisfactory.

Since sample pore pressures are monitored during performance of a test, measurement of pore pressure response to applied total stresses can assist in determining the correct orientation of the loading elements. This fact was not fully appreciated, however, until a significant number of DSC tests had been performed. Therefore, as with the strain distribution

standard established by Germaine (1982), the effective stress path followed during shear can be used as an independent means to evaluate the quality of DSC tests.

4.1.1. Strain Distribution Standard

The strain distribution standard involves inspection of the strains in elements of the grid, grouping elements in such a manner as to form "rings" following the borders of the sample (Fig. 4.1). The 81 elements within the 9 x 9 grid on the top square surface of the sample are divided into five rings: the largest ring follows the outline of the sample and contains 24 elements; the interiormost ring, located at the center of the sample face, contains only one element. Of interest, for purposes of determining test quality, are the strains in the three outermost rings, γ_r, in relation to the average maximum shear strain, γ, of the entire sample. This parameter ($= \frac{\gamma_r - \gamma}{\gamma}$) has been termed the normalized ring strain, NRS (Germaine, 1982).

An NRS greater than approximately 40% for one or more of the three outer rings is considered indicative of a testing problem. For example, in an early test DSC-4 (δ=45°) the sample, without the aid of prisms in the corners where the shear sheets intersect, succumbed to extensive progressive yielding. NRS values for the three outermost rings are presented in Fig. 4.2 for DSC-4 along with the range of NRS values for acceptable DSC tests.

Progressive failure due to stress concentrations at

vulnerable corners, even though reinforced with prisms, can also occur although to a lesser extent. Should a sample fall victim to such premature failure, it is unlikely that stress-strain-strength data generated by the test would be characteristic of clay behavior at that particular value of δ and hence the test should be discarded.

If, however, the progressively failed area remains relatively isolated, i.e., restricted to a corner of the sample and does not extend through a large portion of the sample, excessively strained elements can be removed from calculation of NRS. In so doing, a more representative strain distribution for the sample can be obtained. This approach is particularly useful when the corners containing triangular plexiglass pieces (i.e., see Fig. 2.4 where the shear sheets from adjacent sides interweave) deform excessively with respect to the rest of the sample but the deformations do not lead to development of sample-wide progressive failure surfaces. As will be seen, the plexiglass-supported corners were susceptible to excessive deformation during both isotropic tests sheared at intermediate Ψ values and anisotropic tests sheared at intermediate angles of δ in the "active" zone (i.e., $\delta<45°$). The strengths of BBC samples tested anisotropically at $\delta>45°$, on the other hand, appear to be low enough such that either the stress levels at which stress concentrations lead to excessive corner deformations are not reached or strains are so significant by the time these stress levels are reached, that excessive corner deformations cannot be identified.

4.1.2 Stress Application Standard

From the number of DSC tests performed on both isotropic and anisotropic planes of resedimented BBC at OCR=4, sufficient data are now available regarding the expected "correct" stress paths to be followed. Since experimental technique is a very important variable affecting the effective stress path followed during shear, especially for intermediate values of ψ or δ which require the use of shear sheets, it is easy to unwittingly generate erroneous results. Therefore, the bank of data established from all the tests is used to delete, or at least question, tests deviating from the norm. Such an "in-house" standard is necessary due to the lack of published data concerning anisotropic plane strain behavior of lightly overconsolidated clays.

The two most common problems manifested by the measured effective stress paths are: (1) an apparent increase in the average effective stress during the initial stages of shearing; and (2) a decrease in the average effective stress during the latter stages of shearing wherein the tendency of the sample to strain significantly (and, in the case of OCR=4, further dilate) is inhibited by shear sheet restriction.

The former problem is addressed first, using DSC-7 (ψ=45°) as an example (Fig. 4.3). The following is a possible explanation for the "knee" of high p' at low shear stress levels. After the sample pore pressure has equilibrated with respect to the consolidation stress, shearing is initiated. At

Ψ or δ angles of 40 to 50 degrees most of the shear stress is applied by the shear sheets (all of the shear is applied by the shear sheets for δ or ψ=45°). When the first few shear stress increments are applied, adhesion between the pressure bags and the sheets due to the finite shear resistance of the silicon-teflon grease (Appendix B) causes the pressure bags to be shifted slightly off of and away from the sample. Shifting of the bags was possible in the early stages of this research, as samples sheared at intermediate δ or ψ angles had only one retaining vane on each pressure bag, leaving the side of the bag closest to the pulling strips attached to the shear force piston unconfined as pictured in the inset of Fig. 4.3. Since the pressure bag loading system has an "accordion-like" shape (it is composed of three flexible bags glued to one another), the pressure bag is fairly flexible in both the plane parallel as well as that normal to the loading direction.

Shifting of the pressure bags causes partial unloading of the sample and when the normal pressure is slightly reduced, the sample, which has no access to water, reacts by developing a negative pore pressure. This negative pore pressure is measured, but the reduction in normal stress experienced by the sample is not. In other words, the total stress path, and consequently the actual effective stress path, are unknown. The TSP thought to be applied is greater than that actually felt by the sample because of the "unloading" caused by the shifting of the bags. Applying the measured negative pore pressure (value too low) to the presumed total stress (value

too high) leads to an overestimate of the actual average effective stress, p' (see Fig. 4.3).

Based on results such as shown in Fig. 4.3, the amount of unloading is estimated to be approximately 10% of the consolidation stress during the initial phases of shearing. New, thinner retaining vanes were designed to provide bag confinement on both sides during tests involving shear sheets, thus preventing shifting of the pressure bag by reducing the pressure bag flexibility in the direction of the shear force. DSC-14 (ψ=40°) was performed using these vanes, resulting in the same ESP as the other isotropic DSC tests (see Fig. 4.12 and Section 4.2).

Tests manifesting the high p' problem were all performed at δ or ψ near 45°. The preceding discussion and data suggest, but do not conclusively prove, that shifting of the pressure bags is responsible for increasing p' (the worst possible case is δ or ψ=45° since the shear sheets apply all the stress difference to the sample). It may be possible that slight differences in the degree to which shear stresses are transferred to the sample lead to rigid body rotation of the sample. Since the pore pressure probe extends from the bottom of the sample cube and through an opening between two pressure bags, it is likely that there would be relative movement between the clay and the probe which might lead to a negative pore pressure measurement. In cases where some shear is applied by differential normal stresses, rotation would be inhibited. Of note is the fact that this ESP problem,

regardless of its cause, would not be immediately recognizable in either the resulting stress-strain curve (except that the sample appears to behave stronger than would be expected possibly because the actual stress difference is unknown) or the strain distribution analyses. Therefore, it is necessary to evaluate the effective stress path during shear in the DSC in order to adequately assess the applied stress state.

The second problem associated with stress application in the DSC and demonstrated by an anomalous effective stress path is the restriction of sample strain by shear sheet confinement. Although strain data are not available during actual testing (due to film development, digitization and reduction, etc.), pore pressure behavior during an increment can often be used to identify confinement problems as illustrated in Fig. 4.4, which can then be immediately corrected. This fact was noted during tests performed by Germaine (1982) and was subsequently employed to aid in shear sheet adjustment during all tests of intermediate ψ and δ. The restriction problem, therefore, was generally corrected during shearing of the sample thus maintaining the validity of the results, unlike the pressure bag shift problem which was recognized only prior to DSC-14 (ψ=40°). (DSC-13 (δ=40°) was performed with vanes attached to both sides of the pressure bags, however, to maintain integrity of the aging pressure bags hence unwittingly alleviating the pressure bag shift problem.).

In order to establish a method by which to judge individual DSC tests on the basis of applied stresses, it was

considered reasonable to study shear induced pore pressure, Δu_s, (= $\Delta u - \Delta \sigma_{oct}$) vs. shear strain. As discussed in Section 3.2.4, it is necessary to first correct the DSC average effective stresses for storage effects prior to comparison with one another. Anomalous Δu_s vs γ curves can then justify elimination of certain test results. For shear in the isotropic plane, the curves should all be identical. For the anisotropic case, however, shearing produces a changing pattern of Δu_s vs γ curves with varying δ such that anomalies are more difficult to identify (see Sections 4.3 and 5.1 for further discussion of the isotropic and anisotropic cases, respectively).

4.1.3 Silicon-Grease Resistance Correction

As discussed by Germaine (1982), stresses applied by the pressure bags and the shear sheets are subject to some resistance before actually loading the sample. The sources of this resistance are the finite adhesive strength of the silicon-teflon grease, the membrane resistance and the shear sheet/pressure bag/sample interaction. Because comparison of test results involving various directions of the major principal stress during shear is the ultimate purpose of the DSC test series, it is necessary to assess the relative effects of the aforementioned problems on the stress state to which the sample is subjected. Furthermore, when the applied stresses are affected to different extents, the angle between σ_1 and the direction of deposition, δ or ψ, is also affected. Therefore,

in order to assess both the overall capabilities of the device (via the isotropic "proof" tests) as well as the anisotropy of the stress-strain-strength behavior of resedimented BBC it is essential to evaluate the difference between the stresses in the loading elements (i.e., pressure bags and shear sheets) and those actually applied to the sample.

Reference to the DSC test procedures (Appendix D) reveals that all faces of the sample have a parallel layer of silicon-teflon grease either in immediate contact with them or displaced by a set of shear sheet pulling strips. Given such exposure, evaluation of the sample's stress environment requires assessment of the effect of the grease resistance. The recipe for the grease used in this research is 70% (by weight) Dow Corning No. 111 and 30% Dow Corning No. 7 to which 10% teflon powder is added.

The silicon-teflon grease effect can be divided into two categories:

1) direct reduction of the applied shear sheet stress due to relative movement between the shear sheet and the pressure bag (i.e., the shear sheet correction); and
2) reduction of both normal and shear stresses due to the resistance of the grease on the two plane strain faces of the sample.

The first category, easiest both to assess and to apply, is addressed first. The series of tests performed on the silicon-teflon grease (see Appendix B) are relied upon to ascertain the minimum shear resistance of the grease. The

resistance has been determined to be a direct function of the thickness of the grease layer; the thinner the layer, the greater the resistance, as illustrated in Fig. 4.5. The limiting condition which exists at the thicker end of the spectrum is the minimum resistance obtainable using this grease recipe. Considering the particulate nature of a portion of the grease formula and the consequent need to increase the thickness of the grease layer to provide a lubricating layer, the results are reasonable. That the behavior is truly adhesive (as opposed to frictional) is proven by the fact that tests at low values of σ_v yield grease strengths comparable to those at higher normal vertical stresses with similar preshear grease thicknesses (e.g., tests GE and GF; tests GB and GC; and tests GJ and GK, Fig. 4.5).

The pertinence of the measured grease behavior discussed above to reduction of the shear sheet applied shear stress is that the silicon-teflon grease layer between the shear sheets and the pressure bags, although not a measured quantity, is on the order of one millimeter in thickness. (The limiting condition in the above grease investigation was reached at a grease thickness of about 0.60 mm). In addition, there is a thin layer of unattached rubber sandwiched within the grease layer further ensuring the mobilization of the minimum grease resistance (Arthur, 1983). Hence, the limiting shear stress of the silicon-teflon grease, equal to 0.007 ksc is employed as the amount by which the shear sheet applied stress is directly reduced.

Inspection of Fig. 4.5 indicates that approximately one half millimeter of displacement is necessary to reach the maximum shear resistance. As the working design of the shear sheets involves the lengthening of the 120 small unreinforced pulling strips during stress application, the exterior reinforced pulling sheet is drawn past the pressure bag, generally incurring 2 to 5 cm of displacement by the end of a test. The required displacement of 0.5 mm is most likely met by the time the shear sheets have become taut, usually at approximately τ(shear sheet) $\cong$0.05 ksc. According to Fig. 4.6, this assumption is essentially in agreement with the experimental results of Rodriguez del C. (1977), which indicate that full adhesional resistance is mobilized in the grease when the piston pressure is about equal to 0.35 ksc (equal to the uncorrected calculated shear sheet stress of 0.05 ksc (Germaine, 1982 in Fig. 4.6).

Knowing the maximum grease adhesion ($\Delta\tau_g$=0.007 ksc from the grease behavior test series) and the stress level at which it is fully mobilized (τ(shear sheet)$\cong$0.05 ksc) the correction is as depicted in Fig. 4.6. It has already been accepted that the force applied to the piston divided by the original area of the sample face - less any adhesional correction - constitutes the shear sheet stress (Germaine, 1982) and hence that is how the shear sheet stress is calculated. Prior corrections suggested by both Beckenstein (1980) and Rodriguez del C. (1977)(also shown in Fig. 4.6) result from a calibration technique which fails to separate the direct shear sheet

correction due to sliding past the pressure bags (i.e., stresses lost by individual shear sheets which do not involve the sample or its subsequent deformations for mobilization of resistance) from the adhesional shear resistance due to the platens. These corrections, therefore, incorporate accumulated adhesional forces on the sample and are difficult both to interpret and to apply (Germaine, 1982).

Adhesional resistance developed between the two plane strain greased platens and the sample constitutes the second, more complex category of the silicon-teflon grease effect. It is unclear, in this case, how the corrections should be distributed between the individual applied shear and normal stresses. In addition, the manner in which the shear stress experienced by the sample is affected is not only unclear but is also nonuniform. Furthermore, because of the "end restraint" type of effect imparted by the rigid greased platens onto the sample, the strains will be inhibited at the top and bottom plane strain sample surfaces and, hence, the normal stress distribution will be affected (Germaine, 1982).

The grease thickness on the plane strain surfaces was applied carefully for each DSC test for this research using an initial thickness of 0.50 mm. The grease strength at this thickness is approximately 0.007 ksc (Fig. 4.5). There was no evidence of extensive squeezing out of the grease during shear and, hence, no reason to seriously question this estimate. Unfortunately, the only purpose this information serves is to support the conclusion that the effect is sufficiently small to

neglect and is reasonably consistent between tests. To fully assess the effect of the platen grease strength on the sample stresses one could simulate all the stress applications and boundary conditions associated with the DSC shear environment in a 3-dimensional finite element analysis. Even then, it is likely one would gain only insight rather than a quantitative correction. (Note: Wong and Arthur (1985) do show that photography underestimates linear strains by about 15% due to restraint along the top platen).

4.1.4 Membrane Correction for the DSC

(DSC tests on BBC discussed in this section have been corrected for the effect of storage time by the methods presented in Chapter 3. Detailed discussion of the application of this correction is contained in Section 4.3.2).

The sample membrane correction is derived in Appendix C. Basically, the derivation follows the approach taken in Bishop and Henkel (1957), although further assumptions had to be relied upon to incorporate the fact that pressure is applied in a flexible manner rather than as a force through a rigid end cap. The governing assumption was that since the sample was fully encased by the latex membrane, the force required to strain the membrane sides parallel to a given normal stress direction would uniformly reduce the normal stress imparted by the pressure bag to the sample by an amount equal to the sum of the membrane reaction forces divided by the area of the sample face. The portion of the membrane parallel to the pressure bag

was assumed to unite the peripheral membrane reactions and hence distribute the reactions over the sample face parallel to the pressure bag. The membrane correction, assumed to primarily affect the applied normal stresses, is fully described by the equations presented in Appendix C. The shear sheet applied stresses are affected by the membrane resistance only when the sample distorts and the sample faces are no longer perpendicular to the pressure bags.

The modulus, M, of the rubber, assumed to apply to both compression and extension (Bishop and Henkel, 1957), is expressed in terms of force per unit strain per unit width. M for the white latex DSC membrane material was experimentally determined in tension to be 0.74 kg/cm for a rubber thickness of 0.737 mm. Rubber moduli, as defined in units of force/length, are directly proportional to the thickness of the sheet of interest since the M value is obtained by multiplying Young's modulus ($E = \frac{\sigma}{\varepsilon}$)by the thickness. Therefore, the experimentally determined M is adjusted to account for the fact that membrane thicknesses for the DSC tests are about 0.22 mm (See Table 4.1) resulting in a modulus for the worst case equal to 0.55 kg/cm ($= \frac{0.254}{0.737}$ (0.74)).

Whether or not the shear sheets and glued sand layer have a stiffening effect on the membrane has not been directly measured. Indirectly, however, the results of two isotropic tests performed on BBC at $\psi=0°$, DSC-12 with shear sheets and a sanded membrane and DSC-6 with neither shear sheets nor sand on

the membrane, suggest that there is no strengthening effect associated with the presence of the shear sheets (Fig. 4.7b). Beckenstein (1980) concluded that presence of the shear sheets (in the unstressed state) during isotropic tests on dense Leighton Buzzard Sand (LBS) caused an increase in the strength at failure by inhibiting the formation of rupture surfaces although the stress-strain curves were identical until failure, as presented in Fig. 4.7a. Rodriguez del C. (1977), whose results are also presented in Fig. 4.7a, concludes that there is no difference between the results of tests performed with unstressed shear sheets and those without on loose LBS.

The tests performed by Rodriquez del C. included a test (Test BD) with shear sheets greased to prevent adhesion to the sample membrane thereby producing results which might show a shear sheet effect due only to their finite flexibility and hence capability to inhibit natural sample deformation such as failure surfaces. Test BD did not show any measurable shear sheet stiffening effect on the membrane or "column-like" normal stress reduction.

Since the effect of the membrane has been ascertained to cause an increased measured stress difference as compared to that applied to the sample (i.e. the latex membrane serves to reduce the larger applied normal stress and to increase the smaller applied normal stress) one would expect to see "stronger" behavior if the sheets were indeed stiffening the membrane. One would also expect stronger behavior if the shear sheets were carrying part of the normal stress. Aside from

scatter associated with the DSC device reproduceability, there is no strengthening trend demonstrated by the presence of the shear sheets in any tests performed in isotropic planes of either BBC or LBS.

There are anisotropic data on BBC, however, which might suggest a strengthening effect due to the presence of the shear sheets. DSC-1 and DSC-3 were both performed at δ=0°. Fig. 4.7b plots the stress-strain curves which show DSC-3 (performed with shear sheets but no sand on the membrane) to be approximately 6% stronger than DSC-1 (performed without shear sheets or sand). It should be kept in mind, however, that:

1) the quality of DSC-3 is slightly compromised by the fact that this δ= 0° test followed an aborted attempt to shear at δ=45° and
2) the increase in strength is within the range of reproduceability for the DSC.

A question, as yet unaddressed, is whether or not the membrane reactive forces are transferred directly to the face of the sample as shear forces when a sand layer is present. The previous evaluation assumes that all membrane reactions are absorbed at sample edges as normal forces.

The isotropic ψ=0° DSC tests shed some insight on the effect of sanding the membrane. Theoretically, the glue with which the sand is fixed essentially serves to increase the effective thickness and, thereby, the stiffness of the membrane. However, the fixed sand particles allow some transfer of the strain-induced force in the membrane as shear

to the sample face. DSC-12 (ψ=0°) was performed with both shear sheets and a sanded membrane. Compared with DSC-6 (ψ=0°)(no sand and no shear sheets), these two tests completely encompass the variability of all the proof tests (as will be seen in Fig. 4.21).

As the test of lower strength (DSC-12) was performed with the sanded membrane, there seems to be some justification in claiming that some of the membrane reaction is transmitted to the sample as shear stress and that if the sand and rubber glue coating as well as the adhered shear sheets do have a stiffening effect, it is apparently compensated for by the transfer of shear to the sample. Since neither the magnitude of the proposed sand transmitted shear stresses nor their true distribution are known, in addition to the fact that the membrane effect will probably be less than 5% of the final strength in the worst case (see Table 4.2), the most reasonable conclusion was to neglect these shear stresses as well as any changes in membrane stiffness. Therefore determination of the membrane correction for any combination of sanded or smooth membranes in conjunction with or without shear sheets is the same and is detailed in Appendix C.

To fully evaluate the combined impact of the proposed grease and membrane corrections, Table 4.2 presents the corrected as well as the uncorrected values of the stresses at failure (as defined by the formation of a failure plane and/or excessive deformations) for all DSC tests performed in the isotropic plane of the BBC as well as the test incurring the

maximum normal strain in the x and z directions in the anisotropic plane (DSC-2). The maximum combined membrane and grease correction effect is on the order of 5 to 6% of the shear stress at failure, with the most significant effect being experienced by tests sheared predominantly with the shear sheets (i.e., δ, ψ = 40°, 45°). The membrane correction for δ=90°, expected to be most severe due to large linear strains and low final strength, is only on the order of 1% ($= \frac{0.002}{0.138}$). Therefore it is concluded that the membrane contributes negligible resistance to the applied stresses and hence, the grease resistance on the shear sheets is the only device correction applied to all DSC tests presented hereafter.

4.2 IMPROVED DSC TESTING TECHNIQUES

Changes in DSC testing techniques presented in this section were developed in an attempt to improve both application and distribution of normal and shear stresses as well as the accuracy with which strains are determined. The DSC test procedures put forward by Germaine (1982) form the original DSC testing technique for overconsolidated clay to which the following modifications are applied.

4.2.1 New Pressure Bag Retaining Vanes

Previous to this research, tests performed at intermediate values of δ or ψ involving use of shear sheets required that the pressure bag vane immediately adjacent to the pulling strips of the shear sheets be removed. If the vanes were left

in place, the shear sheet strips would be displaced by 3.18 mm (the thickness of the thinnest vanes) disrupting both the shear stress application at the corner of the sample as well as the sighting line used to locate the adjustable shear sheet pistons such that the pulling force is parallel to the distorting sample face. The stressed reinforced pulling strips were considered sufficient to at least partially restrain the pressure bag during shear.

Due to the "unloading" phenomenon explained in Section 4.1.2, in addition to the fact that future normally consolidated DSC tests would require substantially higher normal stresses, thus necessitating full confinement of the pressure bags, new vanes were designed as illustrated in Fig. 4.8. Stiffness and resistance to bending in the vicinity of the grooves where the attaching screws are located were maintained, although the thickness of the vane was greatly reduced (from 3.18 mm to 1.59 mm) by changing the material from aluminum to stainless steel. In the interest of minimizing possible interference due to the protruding screw heads, the grooves were recessed. The new vanes were employed successfully in tests following and including DSC-14. (DSC-13 (δ=40°) employed the "old" vanes on both sides of the pressure bags during shear). As discussed in Chapter 7, it is believed that use of the new vane will not be sufficient to allow testing in the normally consolidated range and further modifications to the pressure bag construction will most likely be necessary to prevent leaks.

4.2.2 New Corner Prisms

In order to strengthen the two zones of the sample located at the intersections of the interweaving reinforced pulling strips of the shear sheets, the soil at these two corners is replaced by plexiglass prisms of triangular cross section (Fig. 4.9a). Although the prisms were successful in preventing the excessive corner deformation for which they were originally designed (Arthur et al., 1977), it became apparent after several DSC tests on BBC that there was considerable relative displacement between the prisms and the adjacent soil. It is believed that irregularities in the stress application (both normal and shear) at these corners results in forces which tend to push the prisms away from the soil, resisted only by the sample membrane.

In order to enlist some shear resistance from the contact of the prism with the soil, the prisms were redesigned in the shape of chevrons as depicted in Fig. 4.9b. DSC-16 (δ=75°), the only test employing the new prisms, exhibited much less corner "twist," as illustrated in Fig. 4.10, commonly seen in the DSC tests employing the triangular prisms. Hence, the chevron-shaped prisms are considered successful and should be used in future DSC research.

4.2.3 Photographic Improvements

Reduction of strain data resulting from undrained shear in the DSC is explained in detail in Germaine (1982). Ilford FP4 was the plate film used to photograph the 9 by 9 element grid

inked onto the top plane strain surface of the latex membrane encased cubical (104 mm) DSC sample. Analysis of the error associated with film shrinkage and digitizing accuracy yielded an estimated 0.15 to 0.2% standard deviation as the best measure of strain obtainable.

Most of the error is due to the minimal targetability of the image itself, a result of the following:

1) photographing through a thin (0.5 mm) slightly opaque grease film which consequenced a low contrast image which, in turn, led to significant loss of sharpness on magnification during digitization; and
2) attempting to target the grid intersections, difficult because of their irregular and distorting shapes as the sample strains.

As further incentive to improve the photographic film contrast, future research, intended to involve DSC testing in the normally consolidated range, will require a silicon-teflon grease of even greater opacity (necessary to ensure a greater normal stress capacity before squeezing of the grease). Kodalith Ortho Film Type 3 was employed, providing a final black and white extremely sharp image. An Estar base and film thickness of 0.10 mm were chosen to reduce film shrinkage. Appendix D details the filming procedure and film development technique.

Although Kodalith film proved a vast improvement with regards to image clarity over Ilford FP4 film, the standard deviation, as calculated between two films of the same image,

remained essentially the same; standard deviations of shear strains were 0.119% and 0.131% for Ilford FP4 and Kodalith films, respectively. Even though the grid was easier to focus using Kodalith film, the grid intersection target was still difficult to mark in a consistent manner. The solution to this problem was a solid round marker (Letroset dots 0.8 mm in diameter) which neither require a particular orientation to target nor change shape during shear. The dots were affixed to the membrane with a small film of Elmer's glue using the inked grid as a guide in placement.

Table 4.3 lists various standard deviations of strain (or measurements of error) with their sources. It is evident from these data that use of Kodalith film with Letroset dots as targets reduces the combined shear strain error associated with readability and film shrinkage (i.e., two films of identical image) by 50% (from 0.14% to 0.07%). The most accurate method is still that involving radiographs of the tungsten carbide balls ($SD[\varepsilon_{xy}] = 0.047\%$). Given the extreme differences in density between the tungsten balls and the rest of the medium x-rayed, nothing affects the radiographic ball image. In the case of surface-fixed Letroset dots, however, a small amount of excess grease or a slight withdrawal of the dot from the top plate leads to a less round image even when the high contrast film is used. It is assumed that this fact in conjunction with the lesser dimensional stability of the thinner plate film as compared to the x-ray film leads to greater error associated with the photographic technique.

4.3 RESULTS OF PROOF TESTING

Utilization of the DSC testing device requires differing relative magnitudes of applied normal and shear stresses in order to rotate the major principal stress direction. This section seeks to assess whether or not the device is capable of subjecting the sample to various orientations of the principal stresses without inducing any anomalous behavior due to changing boundary conditions. Given the plane strain nature of the DSC, proof testing can be accomplished by using a sample that is isotropic in at least one plane. As the resedimented BBC is consolidated under K_o conditions, DSC tests performed in the isotropic X-Y plane (Fig. 2.5) should produce identical results for various values of the angle of shear, ψ.

Two isotropic DSC tests were performed by Germaine (1982) on resedimented BBC at OCR=4. As discussed in Chapter 2, however, the two samples were not identical since they experienced different periods of storage and hence the test data must first be corrected for the thixotropic effect. Furthermore, in the interest of more firmly evaluating the ability of the DSC to measure the true stress-strain-strength anisotropy of overconsolidated BBC, the following isotropic DSC test program was undertaken:

- a test at $\psi=25°$ to assess the device at intermediate angles (i.e., where the principal stress difference results from both applied normal stress differences and applied shear stresses);

- a test at $\psi=40°$ to illuminate the problem with the $\psi=45°$ effective stress path reported by Germaine (1982); and, finally,
- a test at $\psi=0°$ with a set of unstressed shear sheets in place around the sample to quantify possible shear sheet effects (as partially discussed in section 4.1.4).

The results of all DSC tests on isotropic BBC, prior to adjustment for the thixotropic effect, are presented in Figs. 4.11 and 4.12 in the form of stress-strain curves and effective stress paths, respectively. These data have been corrected for adhesive resistance of the silicon-teflon grease to the shear stress applied by the shear sheets as set forth in Section 4.1.3. (Membrane resistance is neglected due to its negligible magnitude). Pertinent isotropic DSC test data are given in Table 4.4, along with time corrected values of the strength parameters, discussed later in this section. Both measured and time corrected isotropic DSC test data are contained in Appendix E.

4.3.1 Pore Pressure Response

Of note in Table 4.4 and in Table 5.1 which presents summary data for DSC tests in the anisotropic plane of the BBC samples are the very low and very variable values of Skempton's pore pressure parameter, B. Germaine (1982) also addressed this problem after having established that the pore pressure probe could be relied upon to yield accurate pore pressure measurements. Germaine concluded that it was unlikely that the

variable B values were caused by variations in plate separations and this research investigated and confirmed this conclusion (plate separations are listed in Table 2.3).

One approach adopted by Germaine (1982) to evaluate both the test to test B value variation as well as its low magnitude was to study the uniformity of consolidation stress application as demonstrated by nonuniform consolidation strains at the corners of the prismatic sample. Corner volumetric consolidation strains ($\varepsilon_{vol_{corner}}$) are normalized with respect to the volumetric strain of the entire sample ($\varepsilon_{vol_{AI}}$) for the isotropic tests and are plotted versus measured B values in Fig. 4.13. The corners studied were those which were not fitted with plexiglass supports. Fig. 4.13 demonstrates that there is no unique trend relating the pore pressure parameter B with the strains incurred by the corner elements. Ultimately, Germaine concluded the low values of B were due to short term end effects (i.e., due to grease adhesion) over the 30 seconds of application of the stress, and that in the long term, (that is, during shear) the proper stresses would be applied.

This research, however, has revealed a very important factor which does affect pore pressure behavior: thixotropy. Although the thixotropic phenomenon has, to date, only very scant empirical data upon which to assess its impact on soil behavior, the data presented in Chapter 3 regarding the increase in the initial effective stress as well as the decrease in shear-induced pore pressure with time for resedimented BBC cannot be ignored (Figs. 3.4 and 3.23,

respectively).

Fig. 4.14 indirectly illustrates the effect of time of storage on the pore pressure response on application of the consolidation stress by comparing B values to the initial negative pore pressure of the sample. There appears to be greater correlation between B and u_i than between B and time of storage, t_s. The reason for this may be either that the initial negative pore pressure is a better indicator than t_s for the degree to which the thixotropic phenomenon has progressed or that it is the more negative initial pore pressure actually causing the lower B value. These hypotheses are addressed in this section.

The reason that storage time may have an effect on the measured B value is not immediately obvious. Reference to the thixotropic effect reveals a marked decrease in shear-induced pore pressures, Δu_s ($=\Delta u-\Delta\sigma_{oct}$), at given levels of shear strain as the phenomenon progresses. According to Bjerrum and Lo (1967), this is due to the change in the strength and or character of the interparticle bonds. The effect on consolidation B values, on the other hand, is not related to the nature of the interparticle bonds since the change in pore pressure on application of an all round stress should not require breaking any bonds.

Inspection of the relationship between Skempton's B parameter and material parameters; $\frac{\Delta u}{\Delta\sigma_c} = B = \frac{1}{1+n(Cw/C)}$ (assuming the compressibility of the soil particles is very small), shows that the ratio between the compressibility of the

pore fluid, C_w, and that of the soil skeleton, C, governs the pore pressure response. Since Mitchell (1976) postulates that thixotropy may alter the water structure such that some of the free water tends to become more ordered, thereby causing an increase in the pore volume that must be occupied by the rest of the free water, the effect of changing the compressibility of the water on the B value was investigated. It was found, using $C = 2.4 \times 10^{-2}$ cm^2/kg and porosity, n, equal to 0.54, that an increase of approximately three orders of magnitude in the compressibility of the pore fluid would be necessary to obtain B=70% if everything else remained constant. As a matter of fact, a decrease in C and an increase in C_w each by an order of magnitude would theoretically only lower the measured B value to 90%. Such a change in either compressibility parameter is unreasonably large and, therefore, the cause of the lower response values with increasing initial effective stresses lies elsewhere.

As the DSC is a plane strain device, it depends on generation of the total intermediate principal stress, σ_2, by preventing strain in that direction. A slight decrease in compressibility of the soil skeleton may lower the normal stress in the $\varepsilon_2=0$ direction immediately after application of the consolidation pressure by decreasing the likelihood that the drained seating load actually caused sufficient strain to bed the sample against the platen. A decreasing trend in the vertical strain obtained from oedometer tests at $\sigma'_v=0.25$ ksc as storage time increases is seen in the consolidation data

presented in Fig. 3.6.

Since the B value is measured upon application of the consolidation stress, dissipation of pore water pressure begins to be measured after approximately one minute. If significant drained strain is required to cause the generation of the plane strain condition, then the maximum pore pressure response will be compatible with a lower octahedral stress increment and hence will yield a low B value. Indeed, because the measure of the initial B value is limited temporally by the imminent dissipation of the pore pressure, any factor which slows the application of the stress increment such as slow pressure bag extension or time dependent end effects such as grease extrusion will lead to apparently lower values of $\Delta u/\Delta \sigma_c$.

If the initial increasingly negative pore pressure itself is causing the lower B values, it only would be because of the limited time available for measurement of the pore pressure response. It is also possible that as pore pressures become lower some air may be coming out of solution. Application of an all round stress may redissolve the air but this takes time and hence the maximum pore pressure response may be masked by the onset of consolidation. (There could not be a serious cavitation problem since we are capable of measuring the initial negative pore pressures). It may be that the change in B value with t_s and/or u_i is a combination of the plane strain seating and redissolution problems.

The hypothesis of insufficient plane strain seating can also be called upon to explain the consistently lower isotropic

DSC postconsolidation B values as compared with the DSC tests in which the direction of deposition does not coincide with the no strain direction (Fig. 4.14). (Note: the same trend also exists upon application of the consolidation stress). Since the direction of deposition is the least compressible direction, it is possible that insufficient strain occurred on consolidation to fully satisfy the plane strain condition. The postconsolidation check on saturation used a small stress increment of 0.1 ksc and was applied for only 30 seconds which is insufficient time to cause significant strain. Therefore it may be that the lower postconsolidation B values measured for DSC tests in the isotropic plane are due to smaller actual total stress increments.

Similarly, the greater postconsolidation B values for the anisotropic DSC tests (as presented in Fig. 4.14) are perhaps due to the greater compressibility of the plane of the clay perpendicular to the direction of deposition leading to better establishment of the plane strain condition. These B values are still fairly low (83%<B<94%) most likely due to both the small stress increment, the short term end effects, and to a smaller degree than above, the difficulty in generating the full out-of-plane stress.

In conclusion, the most likely explanation for the low B values appears to lie in $\Delta\sigma_{oct}$ being less than the pressure applied to the pressure bags due to short term grease resistance and/or lack of full confinement in the σ_2 direction.

4.3.2 Evaluation of Quality of Isotropic DSC Tests using Established Standards

4.3.2.1 Evaluation of Strain Distribution

Since the DSC device uses flexible elements which are capable of rotation to load the sample, strains resulting from the imposed stresses are not necessarily uniform. Further, the directions of the principal strains do not necessarily coincide with the orientation of the principal stresses even though they should for an isotropic test specimen. Hence, use is made of the inked grid to analyze strain distributions in the plane of major and minor principal stresses and strains, a capability lacking in most strength testing devices. These data, in the form of the normalized ring strain, NRS, the coefficient of variation ($= \frac{SD[\gamma]}{\bar{\gamma}}$) of the maximum shear strain, COV[γ] and the angular difference between the direction of σ_1 and ε_1, Δ, are presented versus the maximum shear strain for Area No. 2 for the isotropic tests in Figs. 4.15, 4.16 and 4.18, respectively.

Although meaningful DSC test comparisons require correction for thixotropy, it must not be inferred that uncorrected test data are defective. As long as they pass the strain distribution and stress application standards established in Sections 4.1.1 and 4.1.2, the recompression-type DSC tests may be considered individually as representative of shear behavior particular to the length of storage which the samples experienced.

Since the strain distribution analyses remain as they are, unaffected by the storage effect correction, the strain standard with regards to evaluation of test quality shall be applied first. It is important to note that the strain distribution data for DSC-9 and 14 (ψ=25° and 40°, respectively) have been calculated after the removal of the two six-element corners as mentioned in Section 4.1.1 and as illustrated by the inset in Fig. 4.15. Referring to Fig. 4.15, it is evident that the normalized ring strains remain within the bounds of ± 40% (as set forth in Section 4.1.1) with the exception of the outside ring of DSC-9 (Ψ=25°). However, violation of the 40% NRS standard is not severe ($|NRS|_{max}$=53%) nor does it extend to the more relevant Area No. 2 of the sample since Ring No. 1 (as defined in Fig. 4.1) nowhere exceeds $|NRS|$= 30%. Hence it is concluded that all the isotropic tests are acceptable with respect to the normalized ring strain standard.

Further evaluation of the uniformity of the shear strains involves inspection of the coefficient of variation , COV[γ] (= $\frac{SD[\gamma]}{\bar{\gamma}}$), as it varies with maximum shear strain level, as presented in Fig. 4.16 for the DSC tests in the isotropic plane. Both Areas No. 1 and 2 are plotted, although the former are used more for determining the impact of the end effects while Area No. 2 (open symbols) provides information most representative of sample behavior.

Tests performed at intermediate angles (i.e., Ψ=25°, 40° and 45°) demonstrate significantly greater variation when Area

No. 1 is considered. This is believed attributable to the tendency of shear sheet applied stresses to not only cause excessive distortion of Ring No. 0 elements before actually 'seating' the sanded membrane but also to distort the corners located where the shear sheets interweave. DSC-9 (Ψ=25°) is a good example of the former "seating" problem. At a maximum shear strain of 1.4%, the COV[γ] for DSC-9 rose to 0.75. Inspection of Fig. 4.17a reveals that the increase in strain variation is due to the sudden slippage between the membrane and the left hand side of the sample, to which the lower normal bag pressure is applied. This apparent slippage does not increase with shear stress level indicating adequate "seating" following the slippage. The opposite side of the sample began to undergo similar slippage at γ=4.1% which led to the second rise in COV[γ] for DSC-9 Area No. 1. This rise is smaller, however because the rest of the sample has achieved greater strain levels as well.

DSC-7 and 14 (Ψ=45° and 40°, respectively), also demonstrate greater variation for Area No. 1 than for Area No. 2 although gross membrane slippage was not the problem. The slight rise in COV[γ] for DSC 14 at γ=3.7% is due to initiation of failure surfaces as indicated in Fig. 4.17b.

That the middle portion of the sample, Area No. 2, can escape unscathed by such end effects as membrane slippage is indicated by the low magnitude and uniform nature of the COV[γ] for Area No. 2 for DSC-9 (Fig. 4.16). In addition, although the other isotropic tests were not as severely affected by

boundary conditions, the Area No. 2 variation is also lower in magnitude and more uniform. Except for DSC-6 (ψ=0°) coefficients of variation for the maximum shear strain for Area No. 2 fall between 0.22 and 0.33 before failure surfaces send it higher. Scatter due to the measurement technique at these strain levels is about 0.10 to 0.05. DSC-6 (ψ=0°) was even more uniform with a COV[γ] of approximately 0.12.

Bekenstein reports a similar range of COV[ε_1] = 0.13 to 0.30 for isotropic loose and dense sands although the areas under consideration are slightly different. Wong and Arthur (1985) report an essentially similar variation (COV[ε_1] = 0.15 to 0.25) in their tests on LBS in the isotropic plane, considering an area of the sample similar to Area No. 2 of this research.

It is still not known whether one would expect less or more variation in strains when investigating clays as opposed to sands. An independent study was performed at MIT by Ms. Mary McCartney on commercially packed Roka clay (w_L=35%, I_p=15% and w_N =28%) under unconfined compression conditions wherein uniform states of normal strain were imposed at the ends of the sample by rigid top and bottom loading elements. End effects were minimized by interlayering silicon-teflon grease with two thin latex sheets and placing this sandwich between the sample and each of the loading elements. Hence, variations in normal strains midheight in the sample should be due to material behavior alone. Strains were calculated based on the digitized displacements of 1.2 mm diameter tungsten carbide balls

embedded in the center of a 76.2 mm cube in a vertical 8 x 8 square array spaced at 10 mm.

The strains of the Roka clay in response to unconfined compression performed at an axial strain rate of 1.6%/hr until $\varepsilon_1 \approx 0.5\%$ then at 8%/hr, indicated $COV[\varepsilon_1]=0.22$ to 0.12 considering all 64 tungsten carbide balls at $\varepsilon_1=1.0\%$ and the inside 36 balls at $\varepsilon_1=1.2\%$, respectively. The $COV[\varepsilon_1]$ indicative of the scatter in strain due to strain measurement and reduction techniques, is approximately equal to 0.13 at these strains. For $\varepsilon_1<1\%$, $COV[\varepsilon_1]$ is approximately equal to this scatter and hence the variation in strain due to the material must be measured in a more accurate manner. At axial strains greater than 1%, where the measurability of $COV[\varepsilon_1]$ falls below 0.10 to approximately 0.02 at $\varepsilon_1 \approx 8\%$, $COV[\varepsilon_1]$ for the Roka clay is about 0.10 to 0.14. Such values for $COV[\varepsilon_1]$ are similar to the lower end of the range reported for Leighton Buzzard Sand by Arthur above and are slightly lower than those reported for LBS by Bekenstein (1980).

An additional study was performed by Ms. McCartney on the effect of repeated digitization of two films on the error of the final averaged results. (The films were images of the DSC grid from an anisotropic DSC test on resedimented BBC). It was determined, on the basis of five runs, that the mean strain remained basically unchanged, although the standard deviation was reduced by about 60% thus reducing the $COV[\varepsilon_x]$. Therefore, although $COV[\gamma]$ = 20 to 30% is fairly significant, we can be confident in the relevance of the average value and attribute

the variation to the following: measurement and reduction techniques; the effects of boundary conditions; the use of surface membrane targets as opposed to embedded markers; and, finally, actual material variability. Improvements such as the filming techniques of Section 4.2 will serve to further evaluate true sample strain nonuniformities.

An important, potentially device dependent parameter is the angular difference between the direction of the major principal stress and the direction of the major principal strain, Δ. Fig. 4.18 presents these data versus maximum shear strain level for the DSC tests performed in the isotropic plane of resedimented BBC. The values of Δ shown have been calculated taking into account changes in the applied Ψ due to reductions in the shear sheet applied stress due to grease resistance as well as any initial misorientation of the membrane grid with the sample edge.

Since the clay is being sheared in the isotropic plane the principal strains should coincide with the direction of the principal stresses, that is $\Delta=0°$. As measurement accuracy is approximately $\pm$ 1°, DSC's 6, 7 and 12 all appear to strain in the appropriate direction. (Values of Δ for $\gamma \lesssim 0.75\%$ are fraught with error and hence should be disregarded). DSC-9 and DSC-14, however, vary slightly about $\Delta \simeq -3.5°$; the minus sign means that ε_1 trails σ_1, hence indicating a tendency to strain more in the direction of the applied normal stress.

4.3.2.2 Evaluation of Stress Application

Investigation of the effect of thixotropy on the behavior of resedimented BBC during shear at OCR=4 following recompression-type consolidation revealed an effect on both the stress difference (q) and the average effective stress (p') (see Chapter 3). Therefore, in order to apply the stress application standard (Section 4.1.2) which involves a measure of the shear induced pore pressure, Δu_s (= $\Delta u - \Delta\sigma_{oct}$), the tests must first be adjusted to similar times of storage. The correction detailed in Chapter 3 corrects the tests to time of storage, t_s, equal to approximately zero. A general outline of the steps followed in adjusting the DSC test values is as follows:

(1) Stress difference correction:

- establish yield stress of uncorrected data, q_y
- determine Δq_y from Fig. 3.24 based on time of storage for test;
- preyield $t=t_s$ values of q are corrected by subtracting percentage (equal to q/q_y) of Δq_y to obtain q_t;
- postyield $t=t_s$ values of q are corrected by subtracting Δq_y to obtain q_t.

(2) Average effective stress correction:

- determine q (and then p' from stress path) at which stress-strain curve first veers from its initial shear modulus, G (call these values q_e, p'_e,

respectively);

- due to the stress controlled nature of the DSC test, it is more difficult to assess when the full correction, $\Delta p'$, is to be applied (in a triaxial situation, Δu_s vs γ reached an almost constant value over a range of approximately $\Delta\gamma$=7%, Figs. 3.21 and 3.22). Therefore, it is suggested that one determine the p' at which the stress-strain curve first attains the vielded modulus level (call these values q_p and p'_p, respectively).
- determine Δ (Δu_s) from Fig. 3.24 based on the time of storage for the test. Convert this to $\Delta(\Delta p')$ by assuming $\frac{\sigma'_2}{\sigma'_1+\sigma'_3} = 0.35$ (see section 3.2.4) and using the following equations:

$$\Delta u_s = \Delta u - \Delta\sigma_{oct}$$

$$\Delta\sigma_{oct} - \Delta u = \frac{2.7}{3.0}\,\Delta p'$$

$$\Delta(\Delta p') = \frac{3.0}{2.7}\,\Delta(\Delta\sigma_{oct} - \Delta u) = \frac{3.0}{2.7}\,(\Delta(-\Delta u_s))\ ;$$

- for values of $q < q_e$ do not alter p' ($\therefore$ $p'=p'_t$);
- for values of $q > q_p$ subtract $\Delta(\Delta_p')$ from p' to obtain p'_t;
- for intermediate values of p' ($p'_e<p'<p'_p$) subtract from p' a proportional amount of $\Delta(\Delta p)$ based on $\frac{p'-p'_e}{p_{p'}-p'_e}$ to obtain p'_t.

The stress application standard involves assessment of

the stress paths for "normal" behavior (Section 4.1.2). This is achieved by studying shear-induced pore pressure versus maximum shear strain for Area No. 2 after these data have been adjusted for thixotropy (see Fig. 4.19). Given the present data base, the best that can be done in establishing a "normal" shear-induced pore pressure vs γ pattern for the isotropic tests is to rely on the quantity of tests performed. As Fig. 4.19b demonstrates, four of the tests follow basically the same pattern, while DSC-7 (Ψ=45°) appears to be anomalous. Fig. 4.20 further illustrates the irregularity of the DSC-7 pore pressure behavior. On the basis of these data, DSC-7 stress-strain-strength behavior is deleted from consideration.

In summary, all the DSC tests performed in the isotropic plane on resedimented BBC at OCR=4 demonstrated acceptable strain distributions. DSC-7 (Ψ=45°), however, behaved anomalously when the time corrected shear-induced pore pressure vs γ pattern was investigated. Therefore all isotropic DSC tests, except for DSC-7 (Ψ=45°) are considered valid.

4.3.3 Presentation of Time Corrected Results

Time adjusted results for DSC tests performed in the isotropic plane of resedimented BBC at OCR=4 are presented in Figs. 4.21 and 4.22. The stress-strain curves (Fig. 4.21) are identical until approximately 50% of the undrained shear strength is reached. At greater levels of shear stress, the tests incur slightly different values of shear strain at given stress difference levels. The variation in stress levels at

γ=4% is q_t/σ'_p = 0.162 ± 0.005 SD which leads to a COV[q]=3.3% ($= \frac{0.005}{0.162}$). The two DSC tests performed by applying differential normal stresses only (i.e., DSC-6 and 12 (Ψ=0°)) form the bounds of the stress-strain variation. The weaker Ψ=0° DSC test was that performed with unstressed shear sheets in place, although, as discussed in Section 4.1.4, there does not appear to be a consistent correlation between decreased strength and the presence of the shear sheets based on several clay and sand DSC test comparisons.

Both the stresses and shear strain levels at failure vary. As mentioned by Germaine (1982), failure is a difficult phenomenon to pinpoint in a stress-controlled testing device. During tests which predominantly use the normal stress pressure bags (i.e., Ψ=0°), one can depend on the flow rate of water into the bags to indicate failure. But this method cannot be used for tests sheared using the shear sheets since the direction of strain does not coincide with the bag applied stress direction. Therefore, in order to maintain a failure criteria consistent with all values of Ψ, failure in the isotropic tests was determined by the onset of a discontinuity in the grid of the sample (see Fig. 4.17b, for example). Often this failure plane extended not through the center of the sample but along a side. For tests which employed the shear sheets the failure strains were approximately 4.5%, while the Ψ=0° tests failed at about $\gamma \approx 7\%$ (all for Area No. 2). The different levels of $(q_t)_f$ are more easily explained following review of the effective stress paths (Fig. 4.22).

It is evident from the effective stress paths that the lower shear stresses at failure are associated with lower average effective stresses. In the case of shear sheet applied shear, latter stage restriction of strain close to failure may lead to less dilational tendencies and hence lower values of p'_t when the "failure envelope" is reached. Nevertheless, The consistency exhibited by the effective stress paths from the four DSC tests performed in the isotropic plane is indeed remarkable given the extreme differences in imposed boundary conditions as Ψ varies from 0° to 40°.

Fig. 4.23 presents the normalized Young's modulus at various shear stress levels during shear of BBC in the isotropic plane. The negligible effect that correction for storage time has on the normalized stiffness of the BBC samples is demonstrated by DSC-6 Ψ=0° which has values of the normalized secant modulus for both $t=t_s$ values and those corrected to t=0. The modulus values at shear stress levels less than 0.4 are somewhat suspect because at these stress levels, shear strains are in the vicinity of 0.1% which, for tests reduced based on digitization of grid intersections, are associated with a COV[γ]≈2.0. (The mean shear strain is not as fraught with error as a COV=200% would lead one to believe, however, as it was shown in Section 4.3.2 that significant reduction of the measurement standard deviation by repetitive digitization did not severely alter the average strain).

Due to the stress controlled nature of the DSC, it is important to ascertain whether or not the samples were

subjected to significantly different strain rates. Strain rates which differ by orders of magnitude could conceivably be the cause of a variety of strength and stiffness anomalies. Fig. 4.24 reveals that although each isotropic test experiences strain rates ranging over almost two orders of magnitudes, all the isotropic tests were subjected to similar rates of shear strain at given normalized shear stress levels. Stress levels were calculated using uncorrected stress values because the strain rate experienced by the sample at the applied stress levels is the parameter which would be expected to lead to changes in strength. Since the procedure for shearing DSC samples involves application of a total stress path at slightly lower average stress levels than the ESP (i.e., a negative pore pressure equal to about 0.006 ksc is maintained) without allowing access to water, the DSC tests are undrained (Germaine, 1982). Therefore, no volume change should occur during shear. Germaine (1982) addressed the problem of measuring negative volumetric strains (i.e., sample expansion) and concluded that they were attributable to bowing of the non-plane strain sides of the sample. Fig. 4.25 presents the volumetric strains calculated from Area No. 2 strain values.

Isotropic tests DSC-6, 7 and 12 all remain within insignificant levels of volumetric strain ($-0.2\% < \varepsilon_{vol} < 0\%$) given film shrinkage error, non-plane strain bowing and access to what little water may have been stored in the sanded membrane following consolidation.

Both DSC-9 and 14 ($\Psi=25°$ and $40°$, respectively) show a

slight sample contraction. Both of these tests also exhibited negative values of Δ, the deviation in the direction of ε_1 from that of σ_1. It is possible that slight adhesion of the grease in the top platen, which leads to an approximate 15% underestimate of ε_1 (Wong and Arthur, 1985), has a greater effect on samples sheared at intermediate values of Ψ due to the greater length over the direction of ε_1 upon which the adhesion acts. In other words, for $\Psi=0°$, ε_1 is parallel to the side of the sample, hence the adhesion acts over a length of $\frac{4.0 \text{ in.}}{2}=2.0$ in. However, for $\Psi=45°$, for example, ε_1 is approximately parallel to the diagonal of the sample face and for one portion of the sample, the adhesion acts over a length equal to about 2.8 in. ($\simeq \frac{\sqrt{2}(4.0 \text{ in.})}{2}$).

In addition, DSC-14 ($\Psi=40°$) was the only isotropic test which employed Kodalith film. This was the first time the high contrast film was used and inexperience led to complications during film development. Variable times of immersion of the individual films in the developing solutions is believed to lead to differential isotropic shrinkage, a problem which would be doubled in the calculation of the volumetric strain. This hypothesis is supported by the extremely erratic nature of the volumetric contraction plotted in Fig. 4.25 for DSC-14. Hence it is concluded that the sample itself did not experience all of the 'measured' volumetric strains. (The film shrinkage, even at its extreme in the case of DSC-14, should not affect the maximum shear strain calculations because of its nearly isotropic nature).

4.4 EVALUATION OF THE DSC AS A TESTING DEVICE FOR MEASUREMENT OF ANISOTROPY

The DSC isotropic test program covers the range of possible DSC testing situations involved in the rotation of the principal stresses from 0° to 90°. In assessing the device, it is necessary to study the isotropic results as a function of the angle of shear, ψ. Fig. 4.26 shows the stress-strain-strength parameters vs the angle Ψ, while Fig. 4.27 demonstrates the effect of Ψ on the strain distributions.

4.4.1 Variations in Strength Behavior with Ψ

The method by which shear is applied (i.e., shear sheets vs differential normal pressures) as defined by the angle Ψ does not affect the shear stress at yield nor the strain at which yield occurs (Fig. 4.26). The failure stresses are all within a ± 3.5% band but maximum shear strains at failure appear to be reduced when shearing with the help of shear sheets. As discussed previously in Section 4.3, this may be the result of restriction of strain by the sheets and hence should be preventable if monitored closely. In any event, the change in strain at failure appears to have a very small effect on strength.

Skempton's pore pressure parameter, A, at failure is fairly consistent for the isotropic tests performed at various angles of Ψ. The failure obliquity, R (= σ_1'/σ_3') on the other hand, varies such that DSC-9 (Ψ=25°) has the greatest value. Since BBC is overconsolidated, there is a cohesive intercept,

c'>0 (further detailed in Chapter 6). This fact, plus the low p' levels, mean that slight changes in q or p' cause large changes in R. Hence the higher R for DSC-9, which had the lowest p'_f, is not considered significant.

4.4.2 Variations in Strain Distribution with Ψ

DSC-7 (Ψ=45°) was eliminated from the pool of valid isotropic DSC tests on resedimented BBC due to its anomalous shear-induced pore pressures. However, since the desired angle of shear, ψ=45°, was such that shear stresses were applied via the shear sheets alone, it is unlikely that Ψ itself was changed significantly even though the normal stress was thought to have been reduced. As the "unloading" phenomenon had equal likelihood of occurring at all four pressure bags, it is possible that the average stress levels were reduced but the direction of ψ remained constant. Assuming Ψ remained constant, it is possible to use the strain distribution patterns to assess additional problems with shearing with the major principal stress located at the apex of a corner of the prismatic sample.

Fig. 4.27 illustrates the effect of the shearing angle in the DSC device on the resulting COV[γ] for Area No. 2. The lowest degree of scatter is associated with tests sheared only with pressure bags (Ψ=0°), although the presence of unstressed shear sheets seemed to increase the scatter to the level existing in tests where Ψ>0°. At low strains (i.e. γ≈1%), regardless of the direction of shear, scatter appears to be on

the order of 40% of the mean. There does appear to be a slight trend toward greater scatter with increasing dependence on the shear sheets which can be seen at levels of $\gamma>4\%$. In summary, there appears to be a 50% and 100% increase in the COV[γ] as ψ is varied from 0° to 25° and 0° to 40°, respectively, at the larger maximum shear strains. At lower shear strains, however, all angles of shear appear to yield similar degrees of scatter.

It must be remembered that the calculated COV[γ] is not completely device-induced. Any increase in COV[γ] beyond the smallest measured value (i.e., from DSC-6) can be attributed to the device but it is still not known how much of the minimum scatter is due to true material behavior.

A significant portion of the minimum COV[γ] is due to the method of strain measurement; at low strain levels the error is significant. The measurement method has a particular standard deviation associated with the strains it reports -regardless of the mean strain level. (For Ilford FP-4 film SD [γ] was on the order of 0.20%; for Kodalith film in conjunction with the grid SD [γ] was about 0.15%; and for Kodalith film with dots, SD[γ] is about 0.09%). The hatched area in Fig. 4.16 illustrates the portion of the COV[γ] attributable to the strain measurement process. The effect of scatter due to the reduction process decreases from approximately 40% of the measured COV[γ] at $\gamma=1\%$ to about 15% of measured COV[γ] by $\gamma=4\%$. Research with respect to material strain nonuniformities is elaborated upon in Section 4.3.2.

The DSC device appears to have a large impact on the global variation in strain experienced by the sample. Fig. 4.27 presents the variation in the normalized ring strain for Ring No. 2 (interiormost) and Ring No. 0 (outermost) as a function of Ψ. Basically, when shear sheets are relied upon to contribute to the shear stress, the edges of the sample will incur the greatest shear strain. Removing portions of the sample vulnerable to boundary effects reveals that Ring No. 2 still strained less than Ring No. 1 although there is less of a difference between the two values. (Referring back to Fig. 4.15 it can be seen that regardless of the direction of shear, the strain for Ring No. 1 remains approximately equal to the strain for the entire sample and hence these values were not plotted in Fig. 4.27).

For tests sheared by differential normal stresses (i.e., $\Psi=0°$) the interior of the sample strains more than the exterior as well as slightly more than Ring No. 1. These trends, possibly masked in the case of the tests performed using shear sheets due to the excess strains at the sample boundaries, may result from the grease restraint along the top platen, based on the radiography (interior) versus photography (top surface) comparison given by Wong and Arthur (1985). These results are definitely a device induced phenomenon and must be borne in mind when studying anisotropic strain distributions.

There is approximately a 3° lag between the direction of ε_1 and σ_1 for tests sheared with the aid of shear sheets and normal pressure bags. For $\Psi=0$ or $\Psi=45°$ the principal strains

are essentially coincident with the principal stresses (allowing approximately ± 1° for initial orientation error). The bottom portion of Fig. 4.27 illustrates this variation in Δ. A possible explanation for this effect on Δ is that the finite pressure bag flexibility, when compromised by the addition of the shear sheets of about 3 to 5 mm in effective thickness, tends to force the direction of strain slightly (in the way a rigid end cap forces the direction of the principal strain to coincide with the principal stress although to a much lesser degree). The reason that $\Delta \approx 3°$ is not observed in the $\Psi = 45°$ test is because the pressure bags are all at the same normal stress, thus there is no incentive for the principal strain to either trail or lead the principal stress direction. It is also possible that the error due to photographic measurement of surface strain rather than radiographic measurement of interior strains (Wong and Arthur, 1985) is affected by the prismatic shape of the sample and hence will result in differing underestimates of linear strains with varying angle of shear. The degree to which this problem occurs is important when assessing the angle Δ for anisotropic soils where Δ is not necessarily zero.

TEST NO.	SHEARING ANGLE (deg)		MEMBRANE THICKNESS (mm)	
	δ	Ψ	SIDES	TOP
DSC-12		0	0.232	0.174
DSC-13	40		0.234	0.254
DSC-14		40	0.195	0.236
DSC-15	20		---	0.195
Combined	Average =0.22 ± 0.03 SD			

Table 4.1: Measurements of Membrane Thicknesses from Recent DSC Tests

TEST (ψ,δ)	Stresses at q_f		Membrane Correction							Grease Correction		Correction Impact		
	σ_A σ_B (ksc)	τ_A τ_B (ksc)	ε_{aAl} ε_a (%)	ε_a^{RO} ε_{ar} (%)	ε_b^{RO} ε_{br} (%)	α(deg) ε_{am} (%)	β_1,β_2 (deg) ε_{bm}(%)	$\Delta\sigma_A$ $\Delta\sigma_B$ (ksc)	$\Delta\tau_A$ $\Delta\tau_B$ (ksc)	$\Delta\tau_A$ (ksc)	$\Delta\tau_B$ (ksc)	$\frac{\Delta q}{q_t}$ (%)	$\frac{\Delta p'}{p'_t}$ (%)	ψ,δ (deg)
DSC-6	0.468	--	2.949	2.387	-2.577	--	-,-	0.003	--					
(ψ=0°)	0.062	--	2.949	2.387	-2.577	2.387	-2.577	-0.001	--	--	--	-1.1 (=- 0.002/0.183)	-0.4 (=- 0.001/0.229)	0
DSC-7	0.270	0.212	-0.049	-0.432	-1.256	2.000	1,1	0.000	0					
(ψ=45°)	0.270	0.212	-0.110	-0.493	-1.318	-0.509	-1.333	-0.001	0	0.007	0.007	-4.1 (=- 0.007/0.170*)	0 (=- 0.001/0.208*)	45
DSC-9	0.408	0.158	1.689	1.463	-3.388	1.3	-,-	0.002	0					
(ψ=25°)	0.143	0.170	1.635	1.409	-3.445	1.409	-3.445	-0.002	0	0.007	0.007	-5.9 (=- 0.010/0.169)	-2.2 (=- 0.006/0.272)	25
DSC-12	0.438	--	2.855	2.152	-2.742	--	-,-	0.002	--					
(ψ=0°)	0.058	--	2.855	2.152	-2.742	2.152	-2.742	-0.001	--	--	--	-1.2 (=- 0.002/0.169)	-0.2 (=- 0.001/0.210)	0
DSC-14	0.287	0.191	0.514	-0.207	-1.323	1.9	--	0	0					
(ψ=40°)	0.220	0.193	0.459	-0.262	-1.379	-0.262	-1.379	-0.001	0	0.007	0.007	-4.6 (=- 0.008/0.173)	0.4 (=- 0.001/0.242)	40
DSC-2	0.377	--	4.130	2.724	-2.384	--	3,3	0.003	0					
(δ=90°)	0.057	--	4.130	2.724	-2.384	2.591	2.591	-0.001	0	--	--	-1.4 (=- 0.002/0.138)	-0.5 (=- 0.001/0.188)	90

* Values for q_t and p'_t at failure averaged from four good isotropic tests since DSC-7 did not pass Stress Application Standard.

Table 4.2: Membrane and Grease Corrections Applied to Isotropic DSC Tests and δ=90° Anisotropic DSC Test on Resedimented BBC (OCR=4)

TYPE OF DATA	FILM, TARGET	DATA SET	ε_x(%)		ε_y(%)		ε_{xy}(%)	
			$\bar{x}$	SD	$\bar{x}$	SD	$\bar{x}$	SD
Repeat of same film	ILFORD FP4, GRID	Average from Germaine (1982)	-0.006	0.191	0.002	0.151	-0.005	0.122
		Preshear (DSC-12)	-0.004	0.220	-0.007	0.187	-0.004	0.140
	X-RAY, SPHERES	Germaine (1982)	0.001	0.071	-0.012	0.066	-0.010	0.047
	KODALITH ORTHO, GRID	Preshear (DSC-14)	-0.009 0.008	0.211 0.178	0.009 -0.034	0.157 0.216	-0.004 -0.003	0.151 0.127
		Setup (DSC-15)	-0.008	0.187	0.005	0.224	0.003	0.143
	KODALITH ORTHO, DOTS	Setup (DSC-16) Preshear (DSC-16)	0.007 0.001	0.094 0.111	-0.005 0.013	0.082 0.094	-0.005 -0.005	0.075 0.078
Two films of identical image	ILFORD FP4, GRID	Average from Germaine (1982)	0.035	0.178	0.030	0.180	-0.002	0.119
		Average from this research (6 sets)	0.054	0.236	0.052	0.239	0.011	0.163
	KODALITH ORTHO, GRID	Preshear (DSC-15)	0.186 0.155	0.207 0.265	0.195 0.133	0.189 0.243	0.039 0.062	0.131 0.163
	KODALITH ORTHO, DOTS	Preshear (DSC-16)	-0.006 -0.016	0.126 0.097	-0.017 0.004	0.122 0.095	-0.003 -0.014	0.074 0.071

Table 4.3: Effect of Film Type and Target on Scatter Associated with Strain Measurement

1	2		3	4	5	6	7	8			9	10		11						REMARKS
	THIXOTROPIC EFFECT													@q_{tf} and $[(\sigma_1-\sigma_3)_f$max]						
TEST (BATCH)	t_s(days) / Δq_y (ksc)	σ'_{pt}(ksc) / $\Delta p'$(ksc)	w_i / w_f (%)	ψ (deg)	shear sheets/ prisms	u_i (ksc)	B ($=\frac{\Delta u}{\Delta \sigma_c}$) (%)	σ'_{vc} (ksc)	ε_x / ε_v (%)	log (t/t_p)	q_y/σ'_p (γ_y,%)	q_{yt}/σ'_p (γ_y,%)	$\frac{G_y}{\sigma'_p}$	γ (%)	$\frac{q_f}{\sigma'_p}$	$\frac{p'_f}{\sigma'_p}$	$(\frac{\sigma_1'}{\sigma_3'})_f$	A_{tf}	Δ (deg)	
DSC-6 (103)	48 / 0.020	1.28 / 0.038	40.2 / 39.6	0	no/no	-0.147	c:84.6 +: 74 +: 80	0.250	0.27 / 0.24	1.26	0.163 (1.7)	0.144 (1.7)	0.67	6.9	0.183	0.227	9.32	0.56	-0.2	
DSC-7 (104)	15 / 0.015	1.17 / 0.023	39.6 / 39.9	45	yes/yes	-0.074	c:91.3 +: 73 +: 76	0.252	0.43 / 0.40	1.78	0.163 (1.5)	- -	--	--	--	--	--	--	0.7	Poor pore pressure behavior
DSC-9 (105)	169 / 0.046	1.58 / 0.079	40.9 / 40.8	25	yes/yes	-0.122	c:83.5 +: 78 +: 78	0.250	0.51 / 0.52	1.92	0.166 (1.0)	0.122 (1.2)	1.0	4.4	0.163	0.193	11.9	0.68	3.5	strain calculations did not include corners with plexiglass prisms
DSC-12 (106)	91 / 0.023	1.34 / 0.043	40.6 / 40.8	0	yes/yes	-0.148	c:76.2 +: 71 +: 73	0.250	0.33 / 0.15	1.93	0.155 (1.6)	0.132 (1.5)	0.67	7.0	0.169	0.210	9.24	0.62	-0.2	
DSC-14 (109)	79 / 0.022	1.32 / 0.041	42.1 / 42.1	40	yes/yes	-0.127	c:70.6 +: +:	0.250	0.203 / 0.302		0.153 (1.5)	0.132 (1.4)	0.87	4.3	0.166	0.202	10.2	0.65	-2.9	strain calculations did not include corners with plexiglass prisms

1 Test designation and Batch No.
2 Thix. effect based on t_s and Chap.3
3 Initial and Final water contents
4 Isotropic angle of shear
5 Physical aspects of DSC test
6 Initial pore pressure
7 Skempton's B parameter, where c= consol. inc. ($\Delta\sigma_c$=0.22 ksc), +=($\Delta\sigma_c$= -0.10 ksc) and +=($\Delta\sigma_c$= +0.10 ksc)
8 Consolidation data
9 Uncorrected yield data
10 Yield results corrected for thixotropy
11 Shear results corrected for thixotropy

Table 4.4: Summary of Isotropic DSC Test Data for Resedimented BBC (OCR=4)

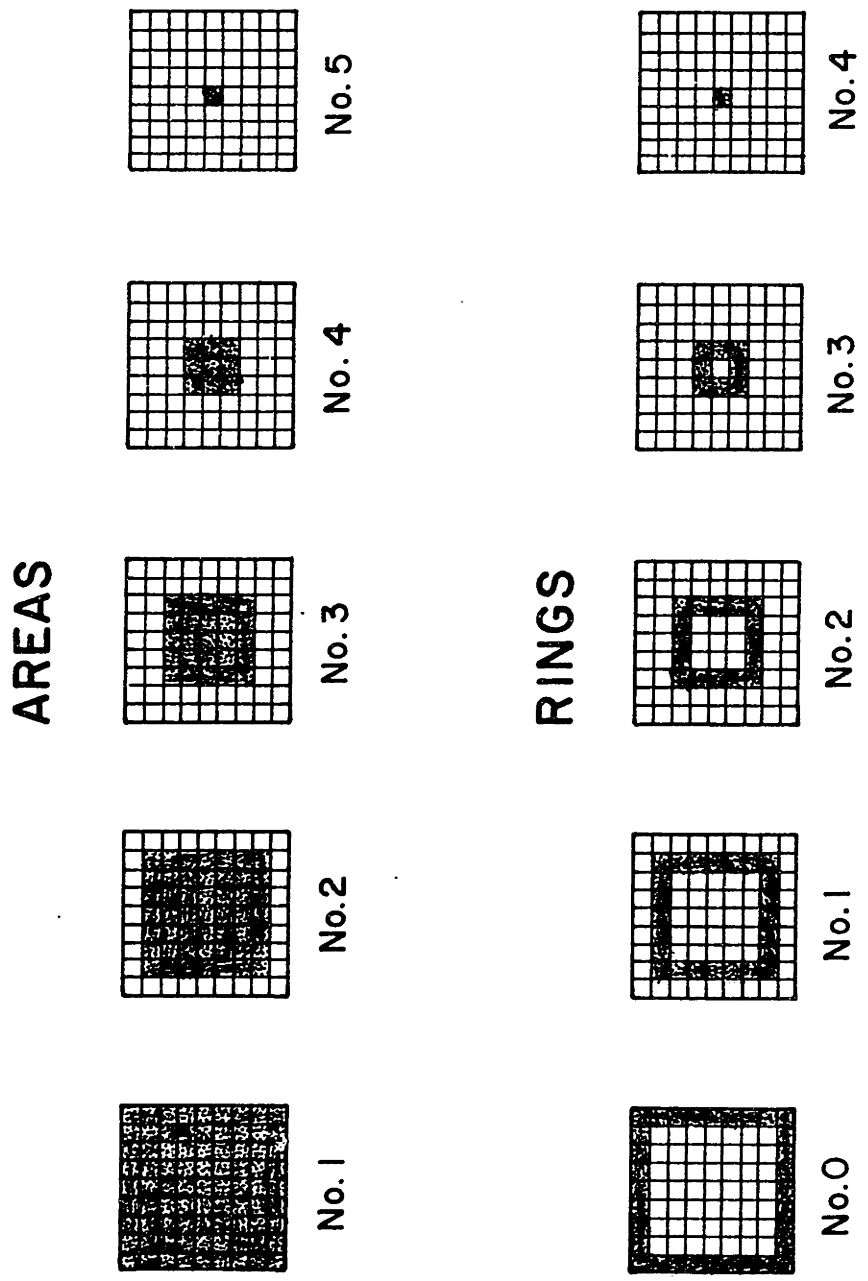

Figure 4.1: Definition of Sample Zones over which Average Strain Values are Computed (from Germaine, 1982).

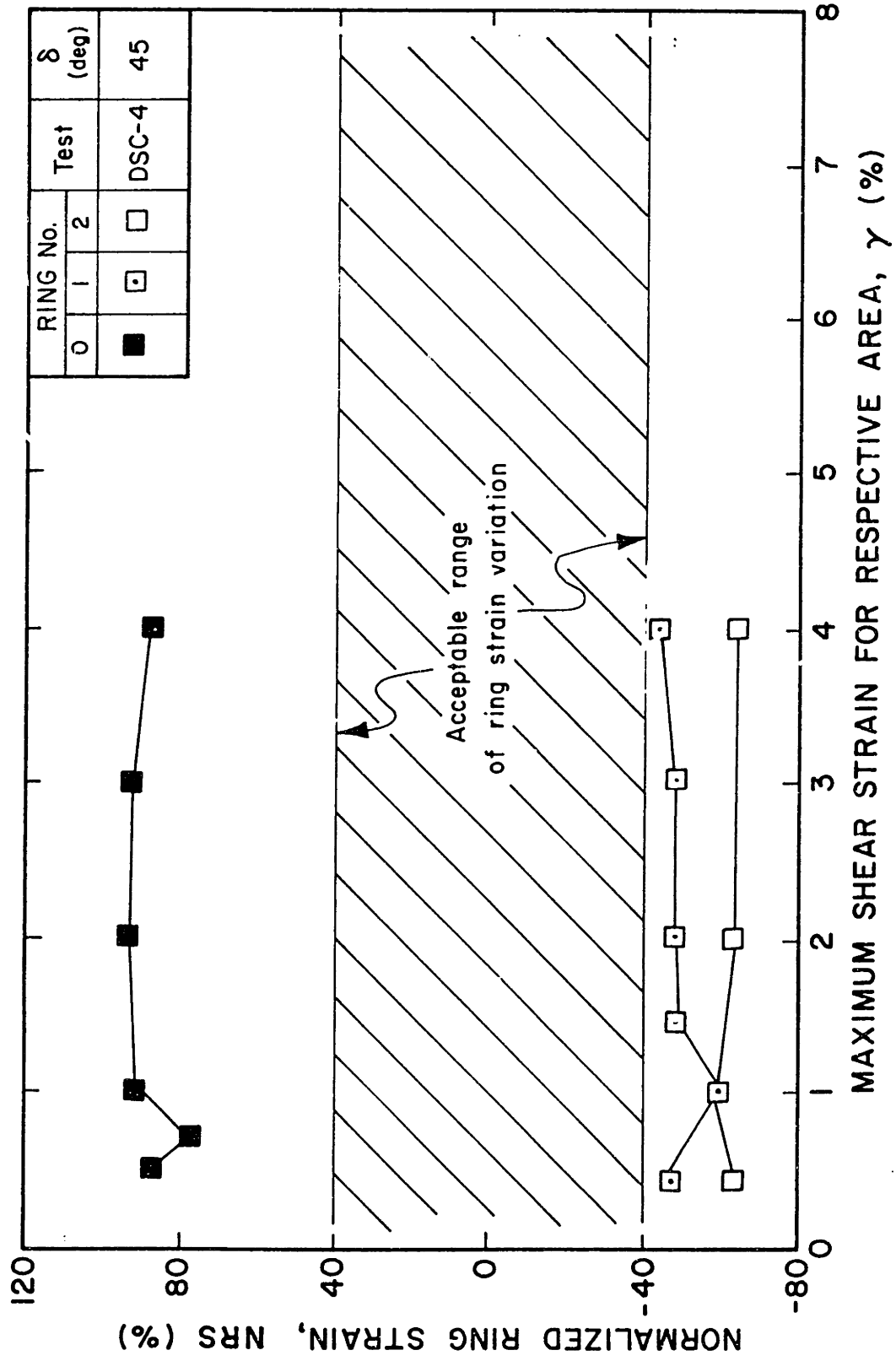

Figure 4.2: Variation of Normalized Ring Strain from DSC-4 (δ=45°) Performed Without Plexiglass Prisms on Resedimented BBC (OCR=4).

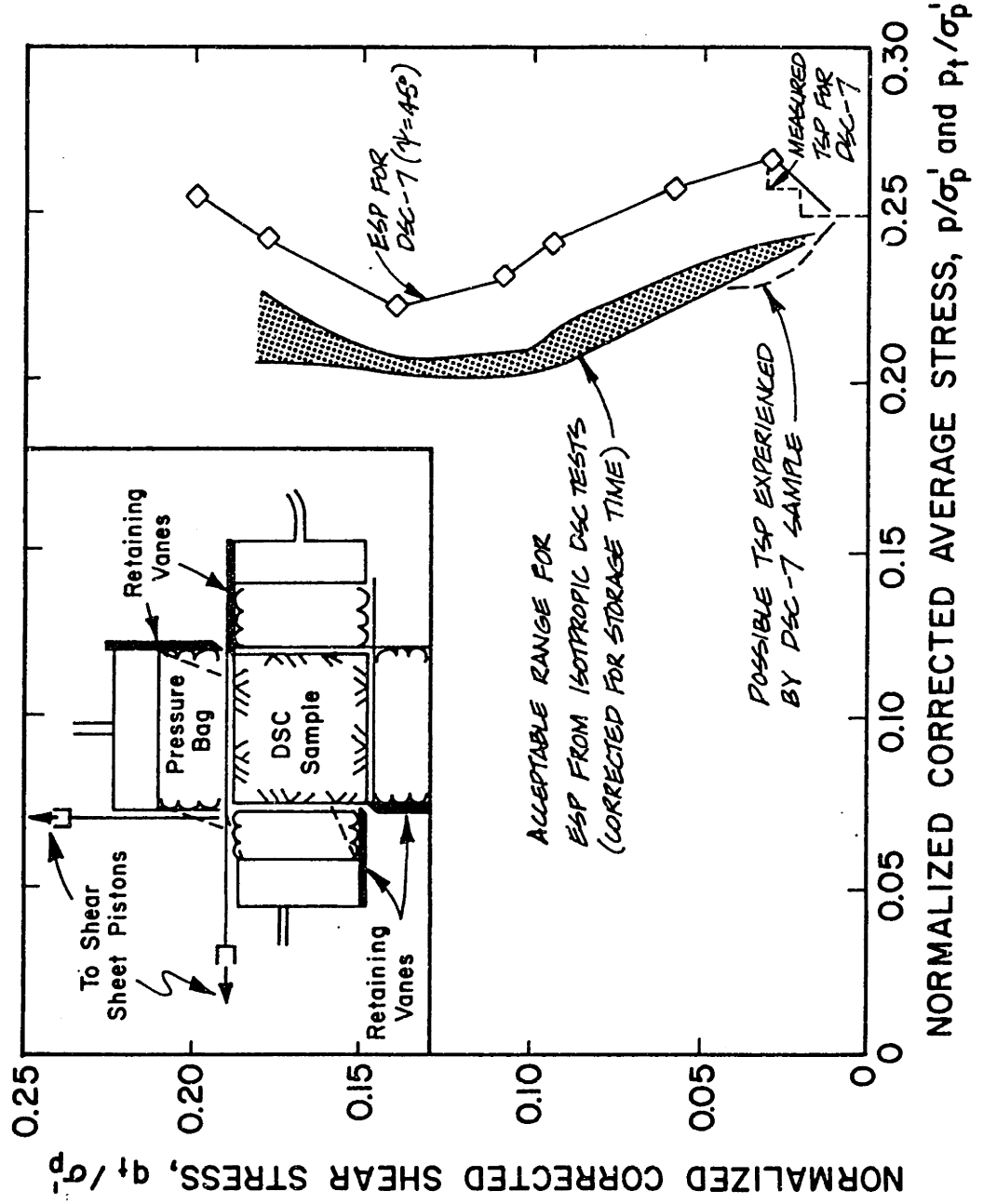

Figure 4.3: Possible Explanation for Anomalous Effective Stress Paths from DSC Tests on Resedimented BBC (OCR=4).

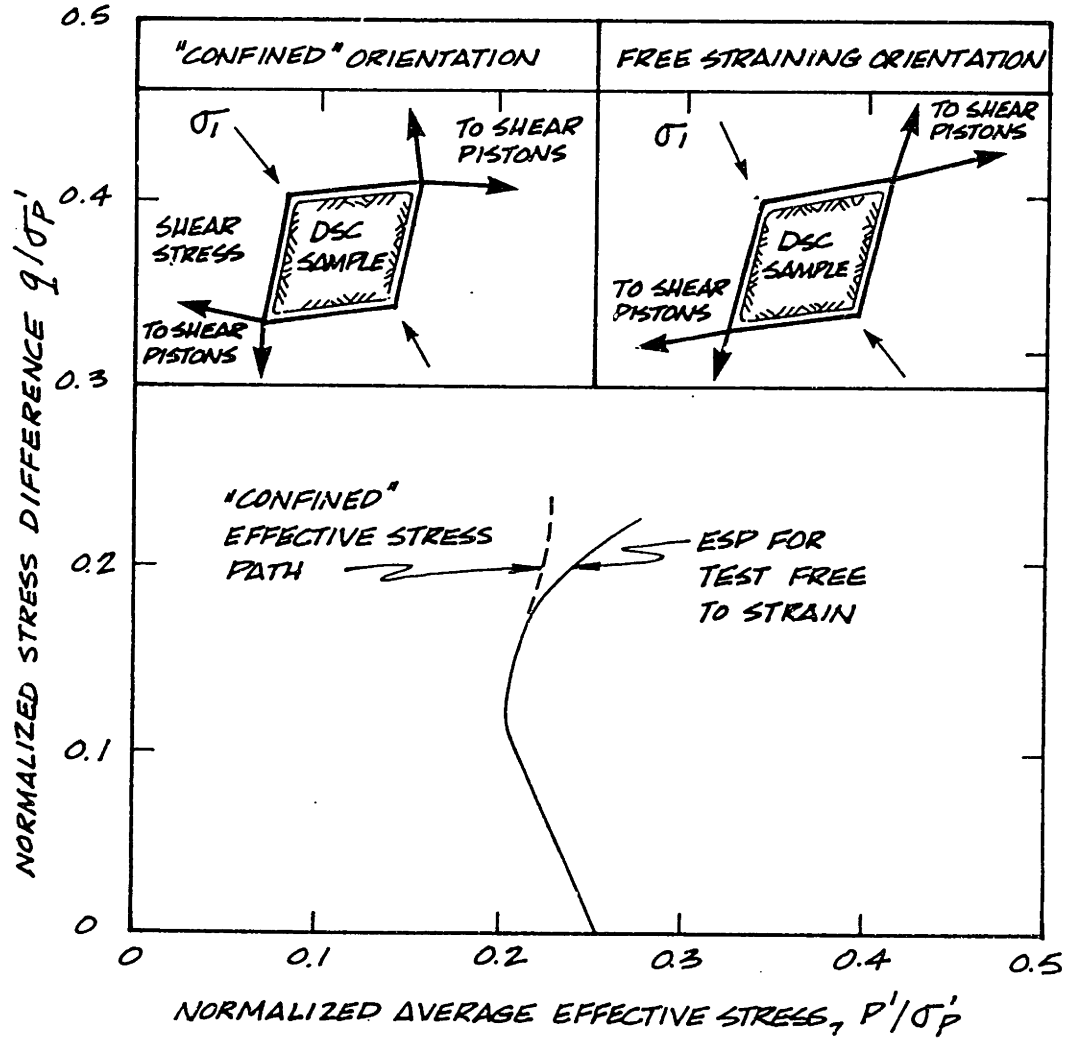

Figure 4.4: Illustration of the Effect of Confinement by Shear Sheets on Effective Stress Paths from Isotropic DSC Tests.

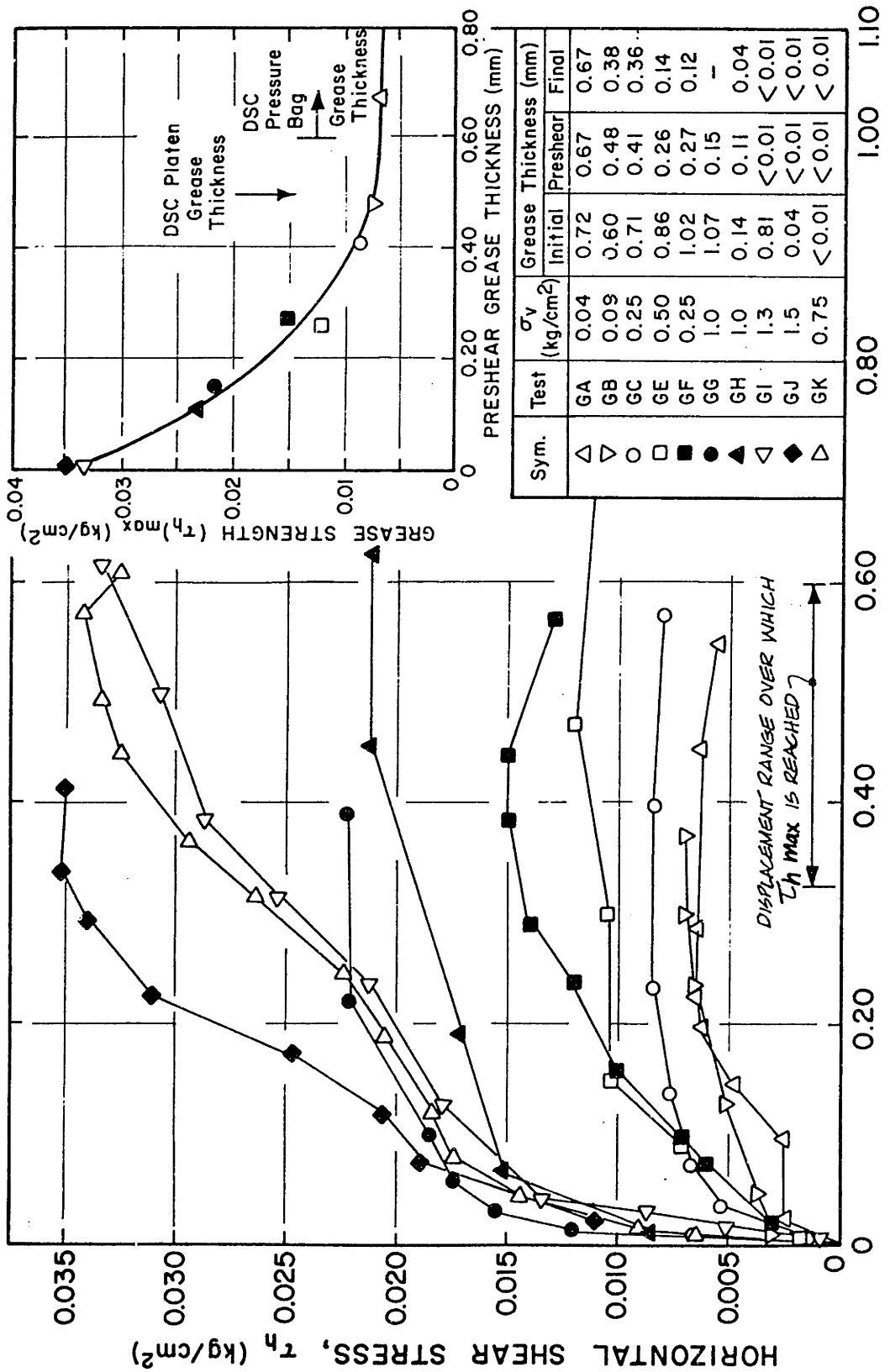

Figure 4.5: Silicon-Teflon Grease Stress-Strain Characteristics.

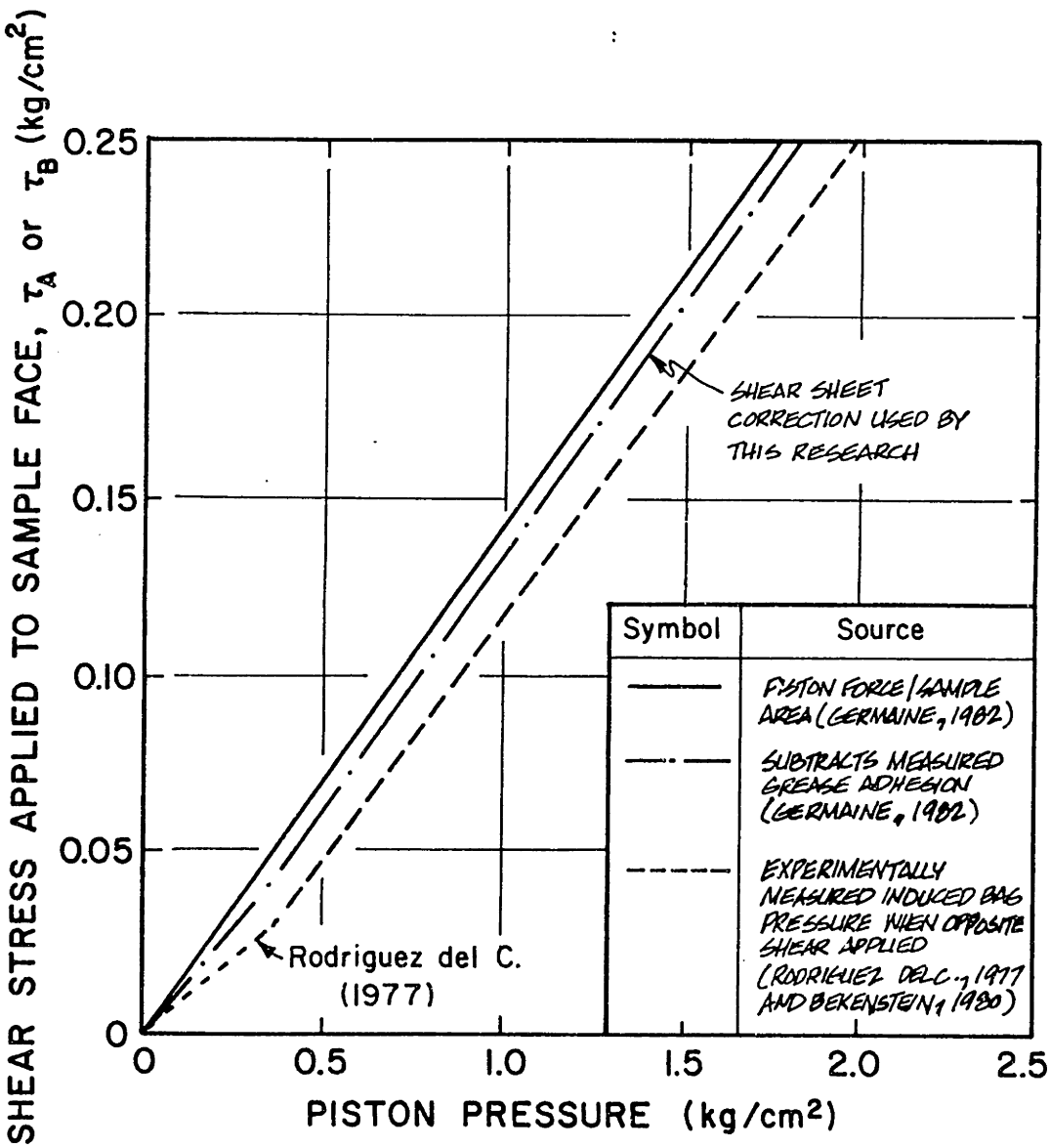

Figure 4.6: DSC Shear Sheet Corrections.

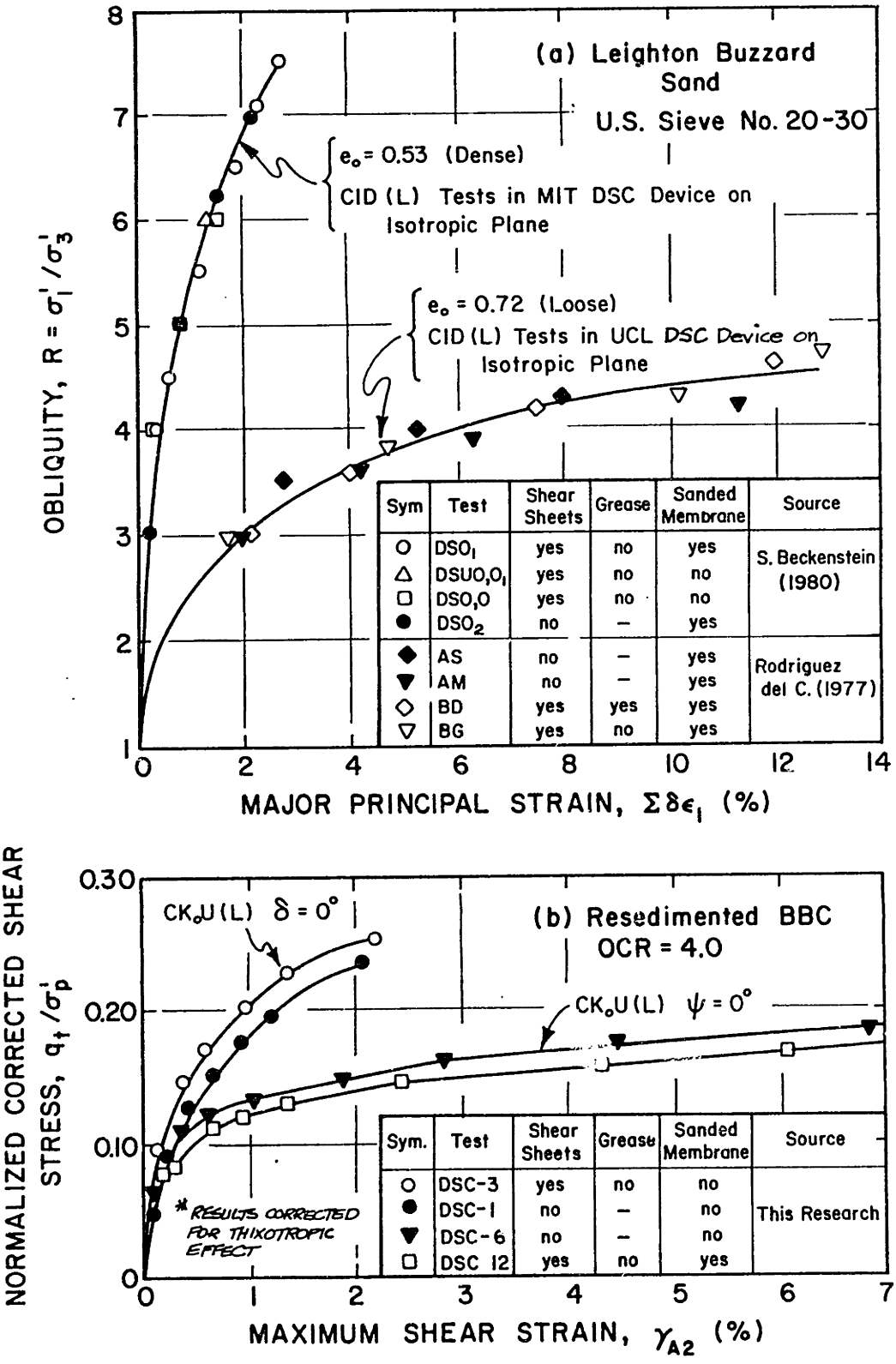

Figure 4.7: Effect of Unstressed Shear Sheets on Soil Behavior as measured by the DSC.

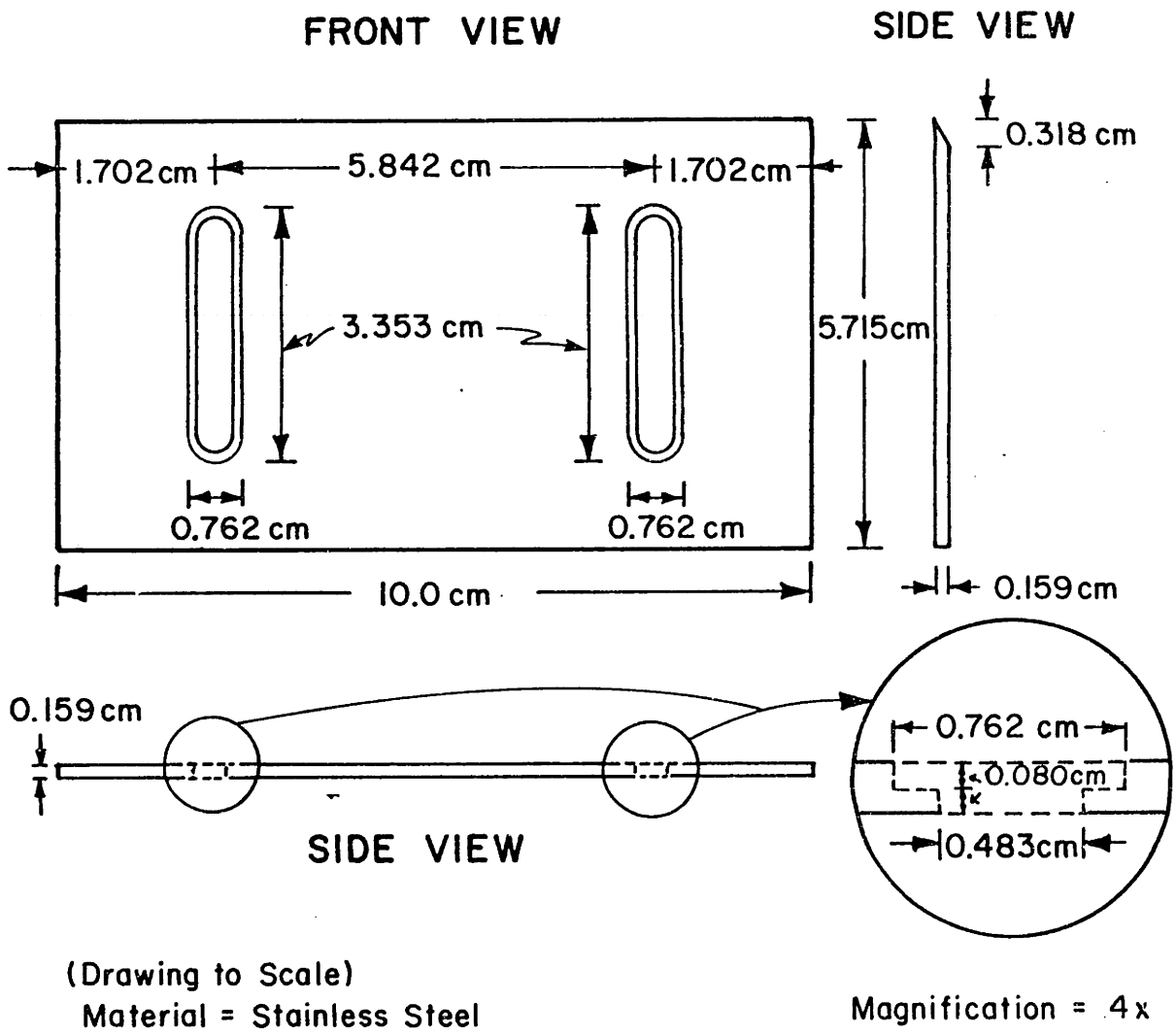

Figure 4.8: New Retaining Vanes for DSC Pressure Bags.

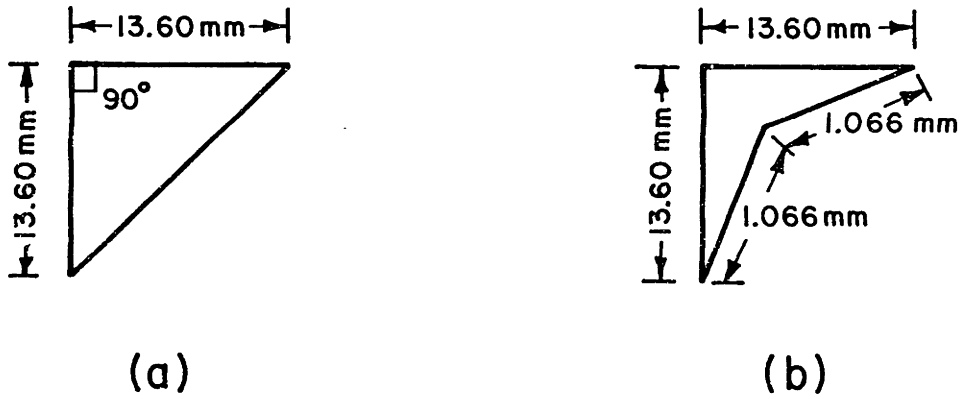

Figure 4.9: Plexiglass Prisms used to Protect DSC Samples from Stress Concentrations.

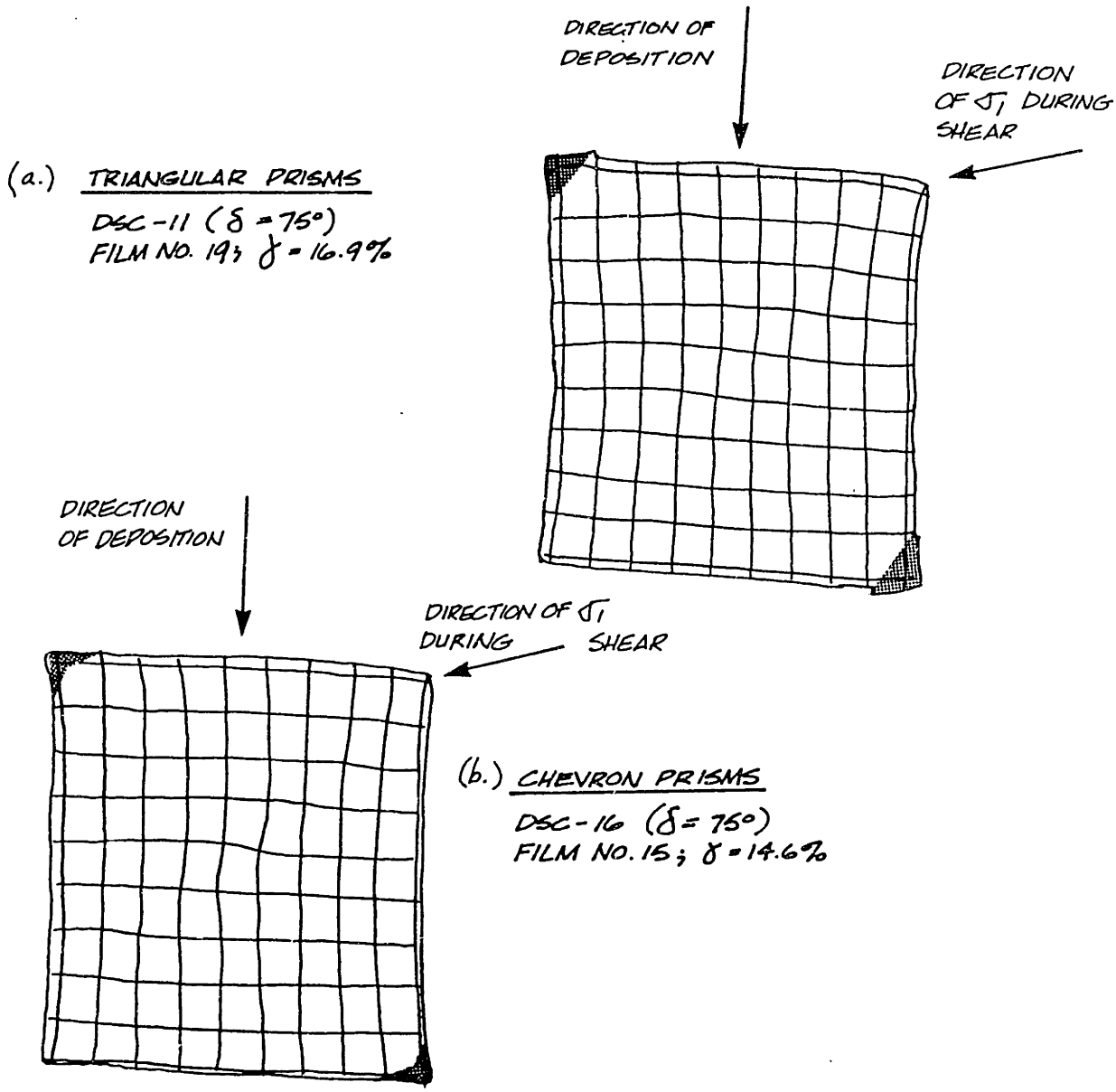

Note that at large shear strains, the chevron-shaped prisms appeared to allow less distortion of the protected corners of the sample.

Figure 4.10: Effect of Prism Shape on the Protection of the DSC Sample Corners during Tests Performed at Intermediate Angles of Shear.

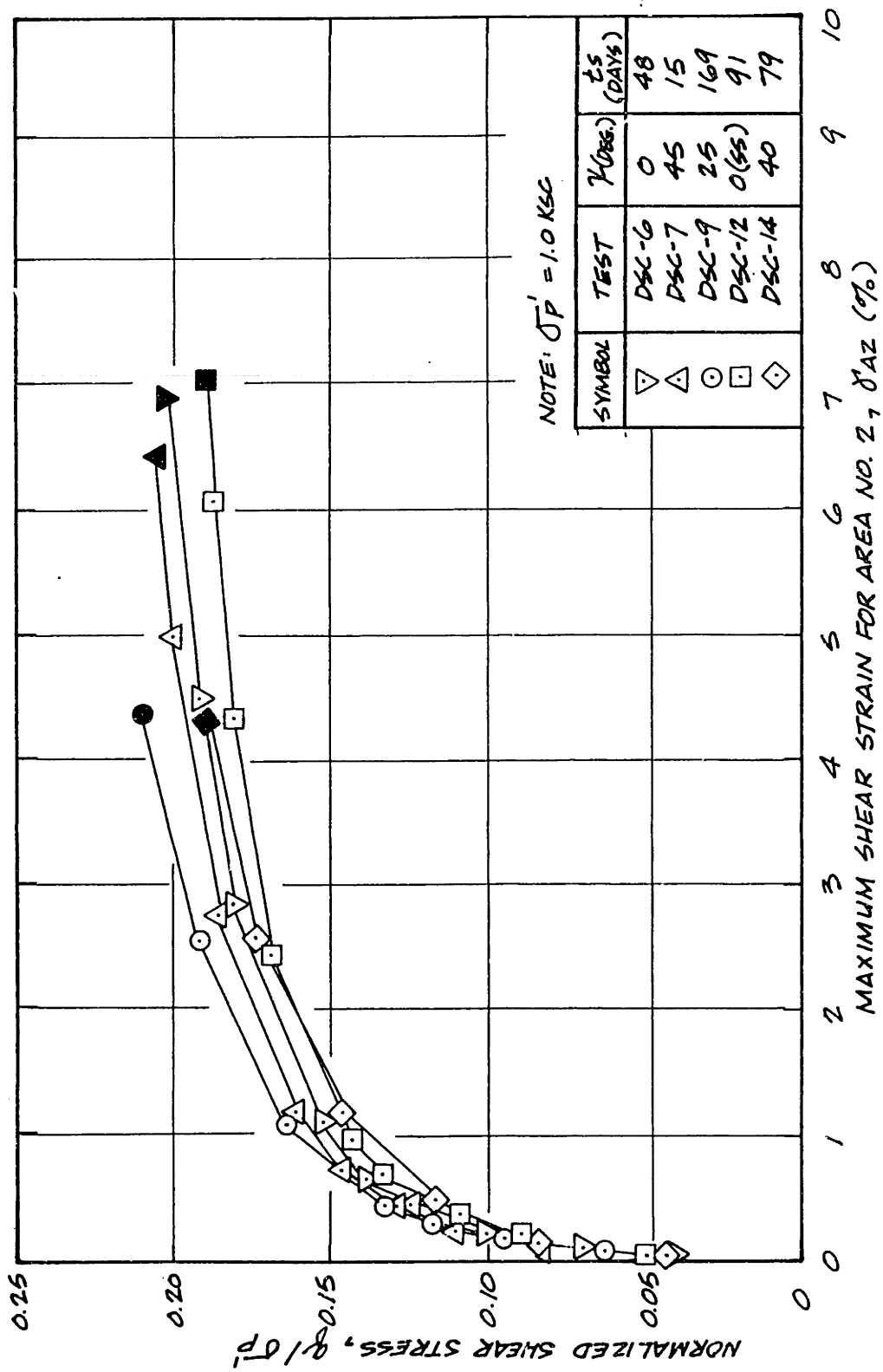

Figure 4.11: Stress-Strain Curves from Isotropic DSC Tests on Resedimented BBC (OCR=4); (not Corrected for Thixotropic Effects).

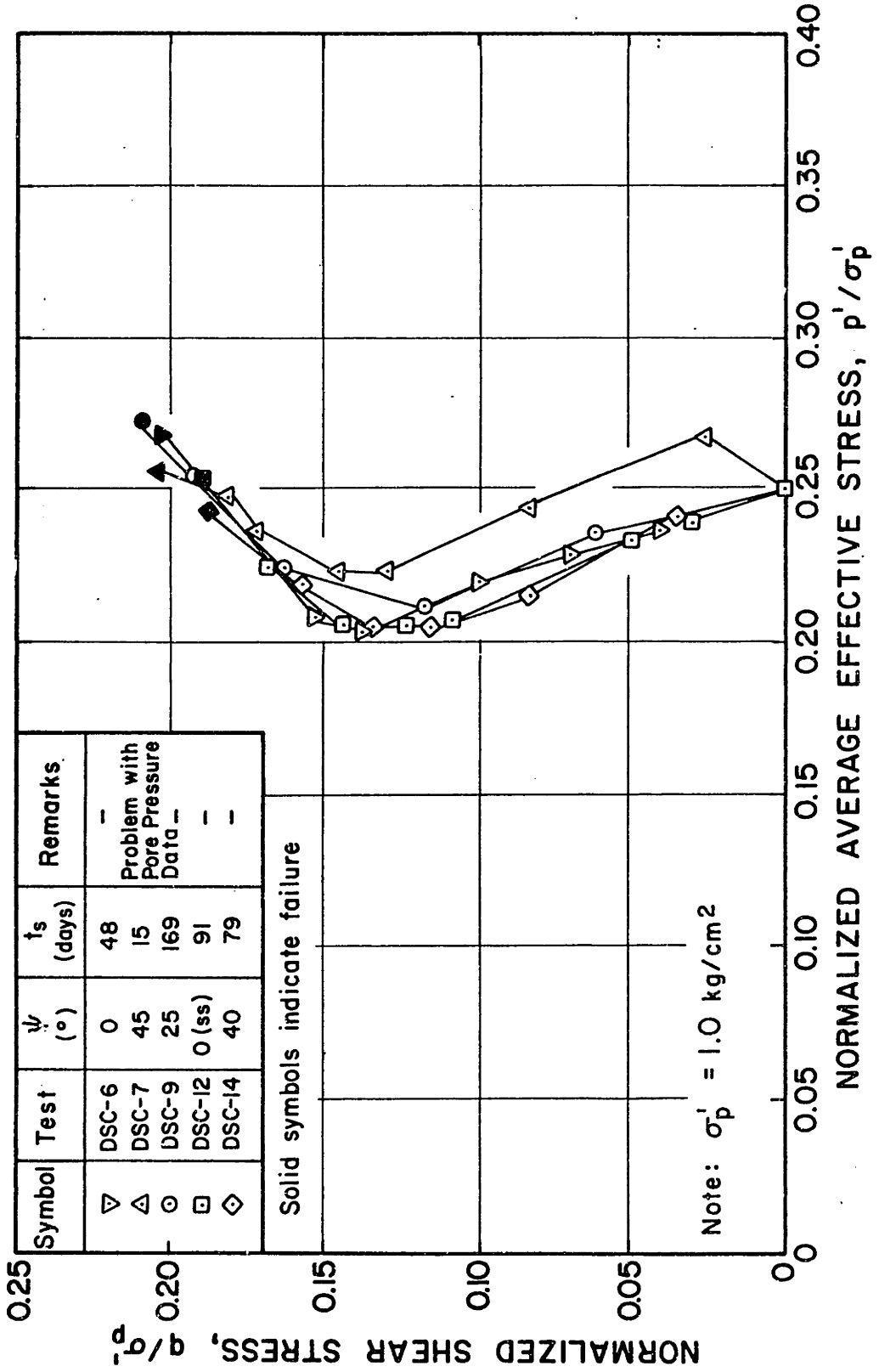

Figure 4.12: Effective Stress Paths from Isotropic DSC Tests on Resedimented BBC (OCR=4); (not Corrected for Thixotropic Effects).

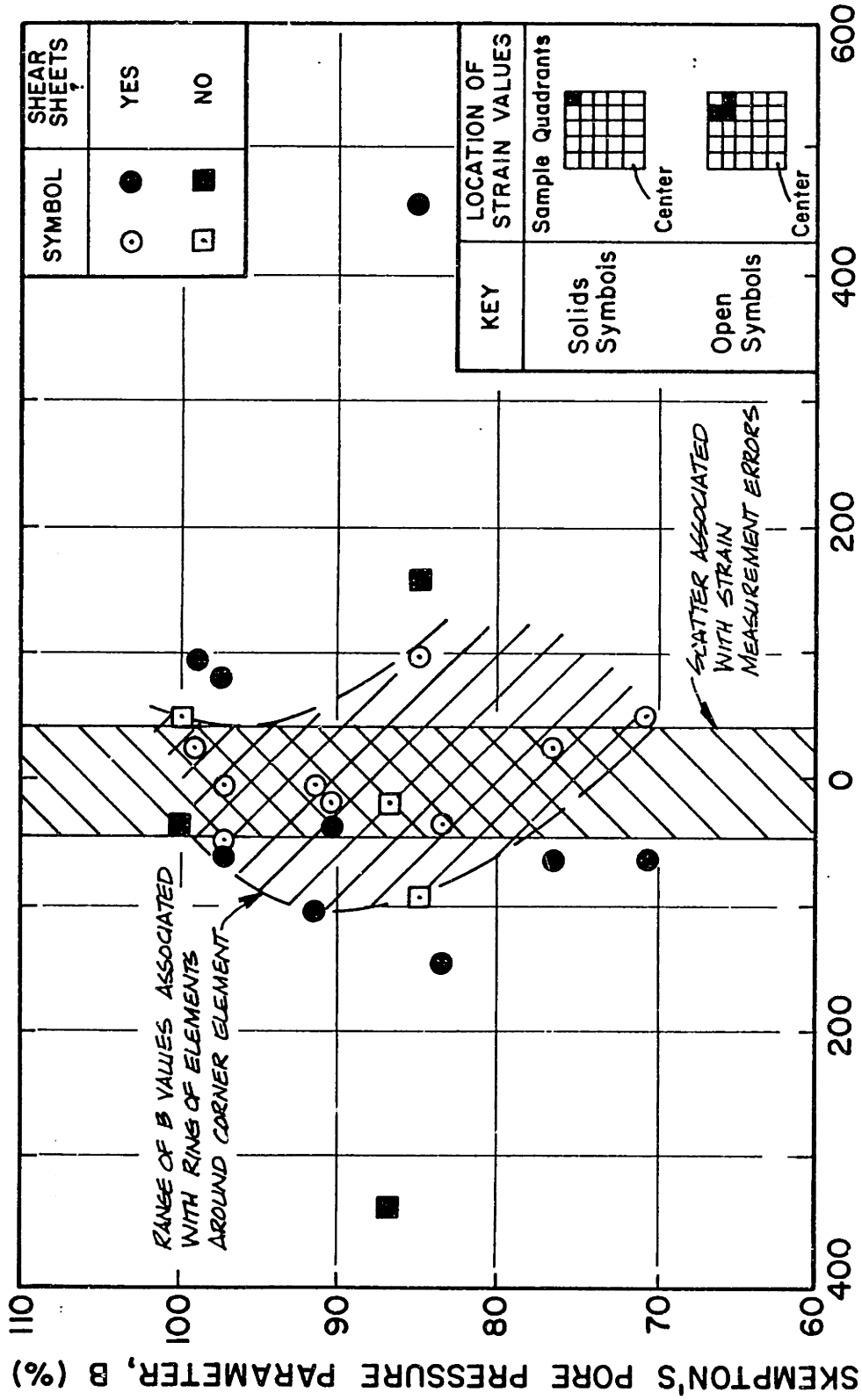

Figure 4.13: Effect of Nonuniform Stress Application at Sample Corners on Pore Pressure Response.

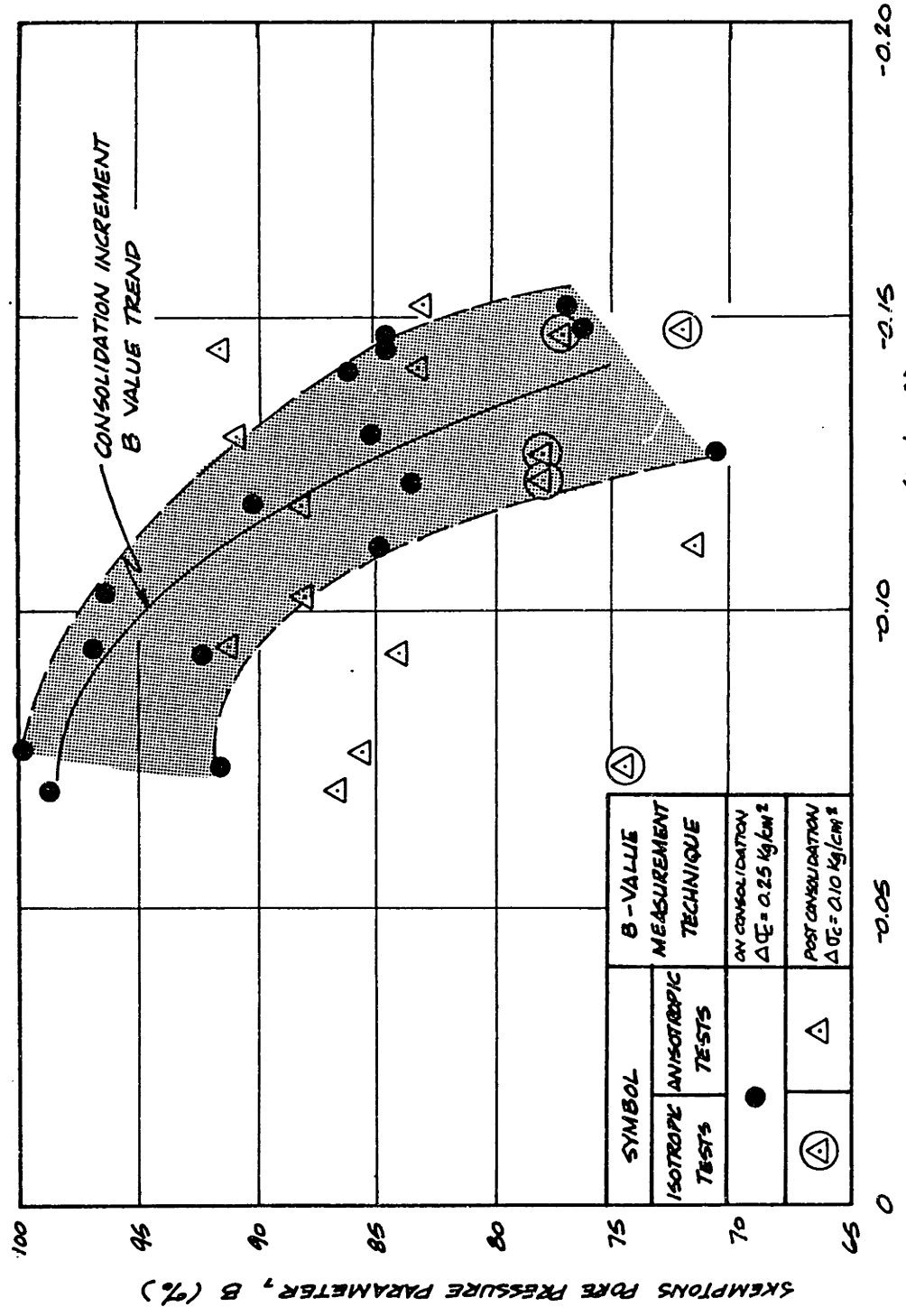

Figure 4.14: Relationship Between Pore Pressure Parameter, B, and the Initial Negative Pore Pressure as Measured in the DSC on Resedimented BBC (OCR=4).

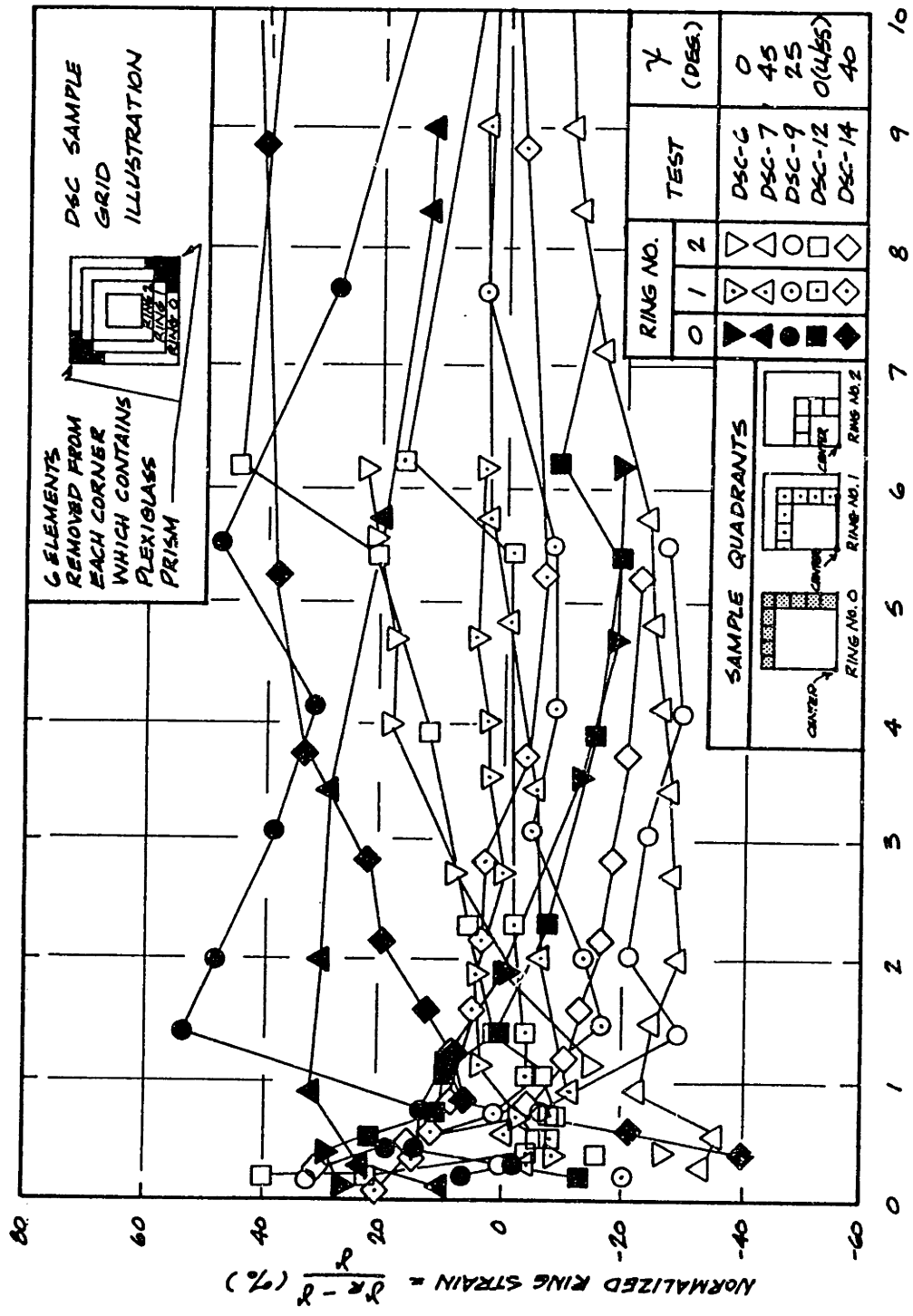

Figure 4.15: Variation of Maximum Shear Strain Distribution (NRS) with Maximum Shear Strain Level from Entire Sample from Isotropic DSC Tests on Resedimented BBC (OCR=4).

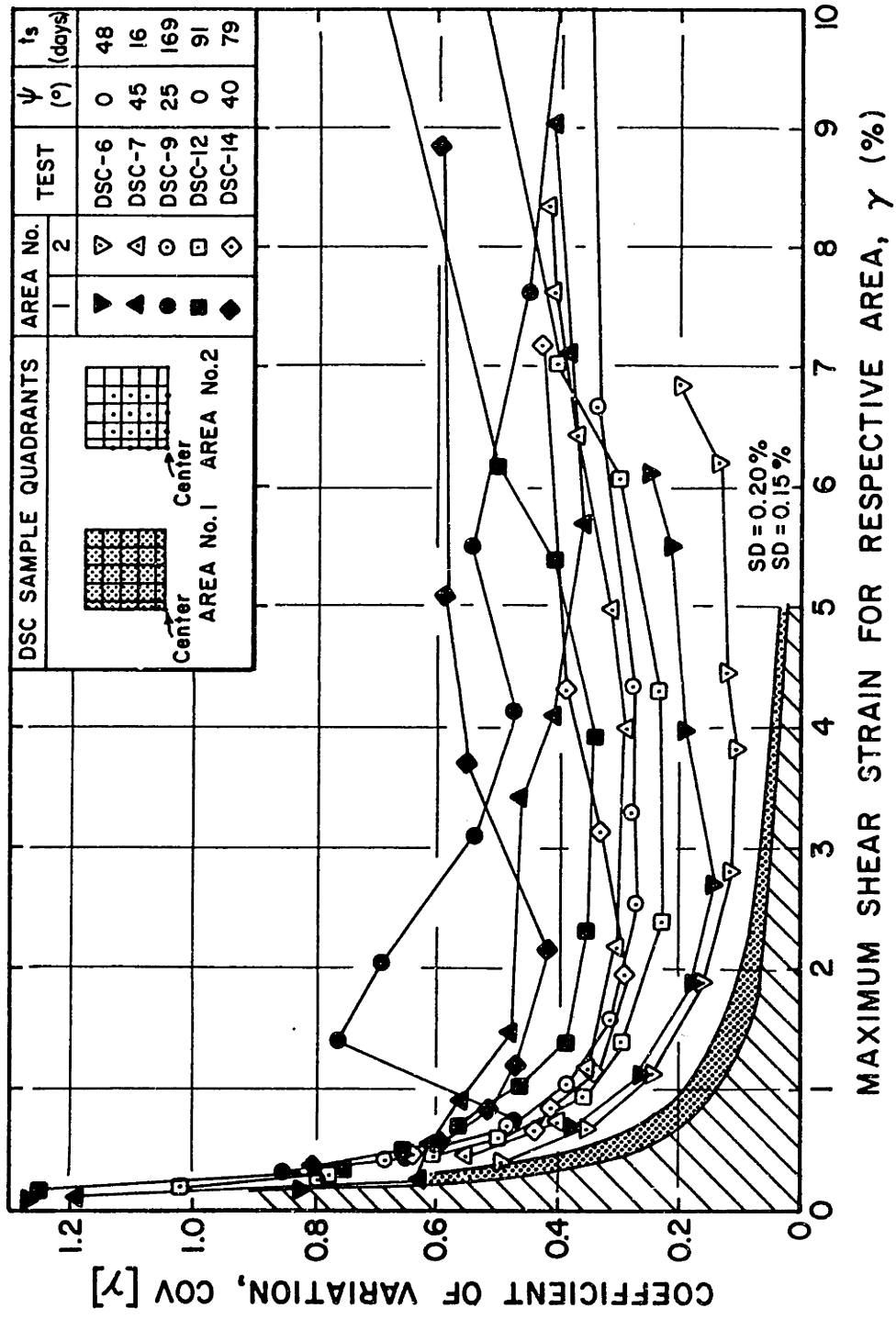

Figure 4.16: Coefficient of Variation vs. Shear Strain from Isotropic DSC Tests on Resedimented BBC (OCR=4).

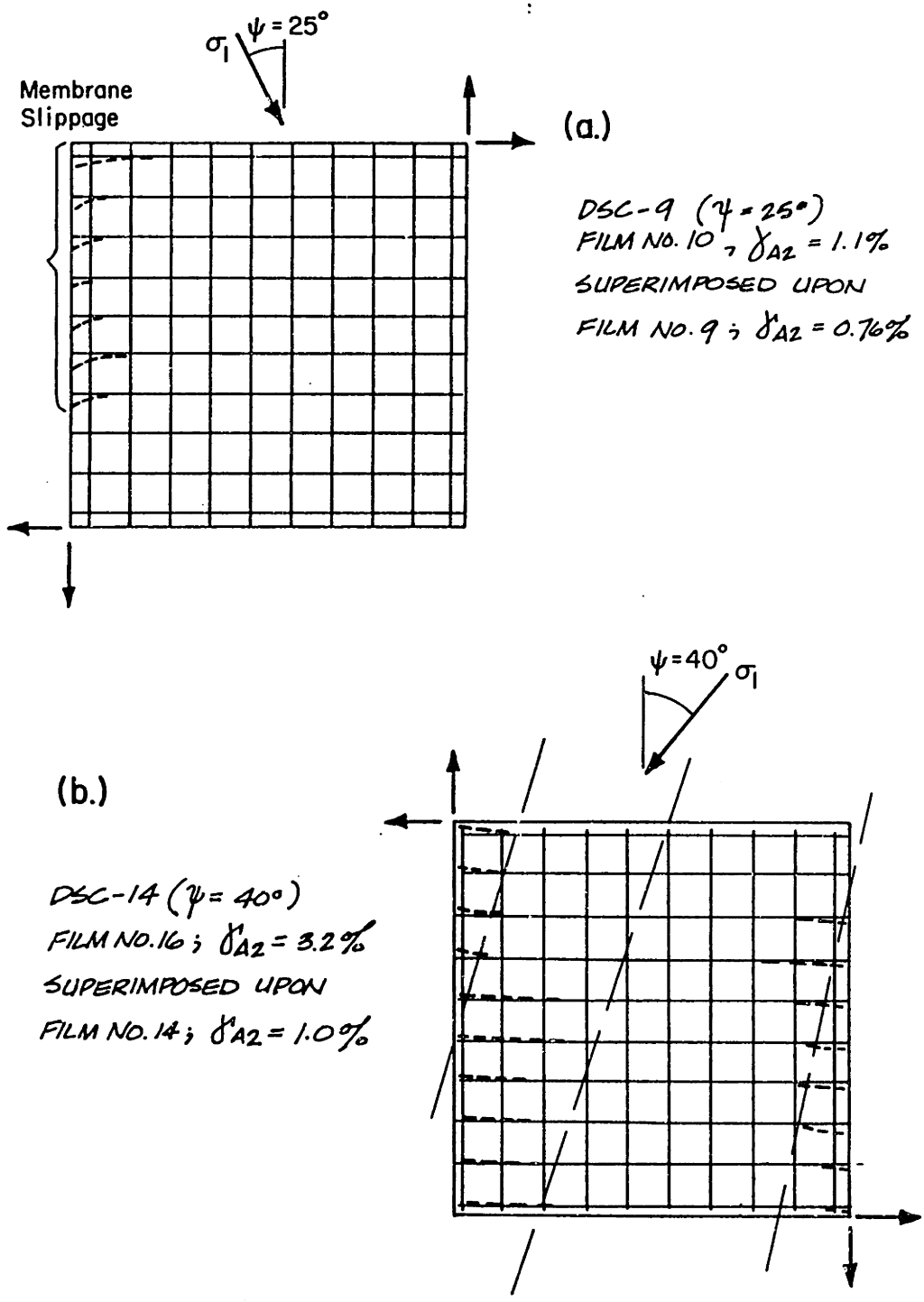

Figure 4.17: Illustration of Grid Deformations which led to Increases in Coefficients of Variation for Maximum Shear Strain.

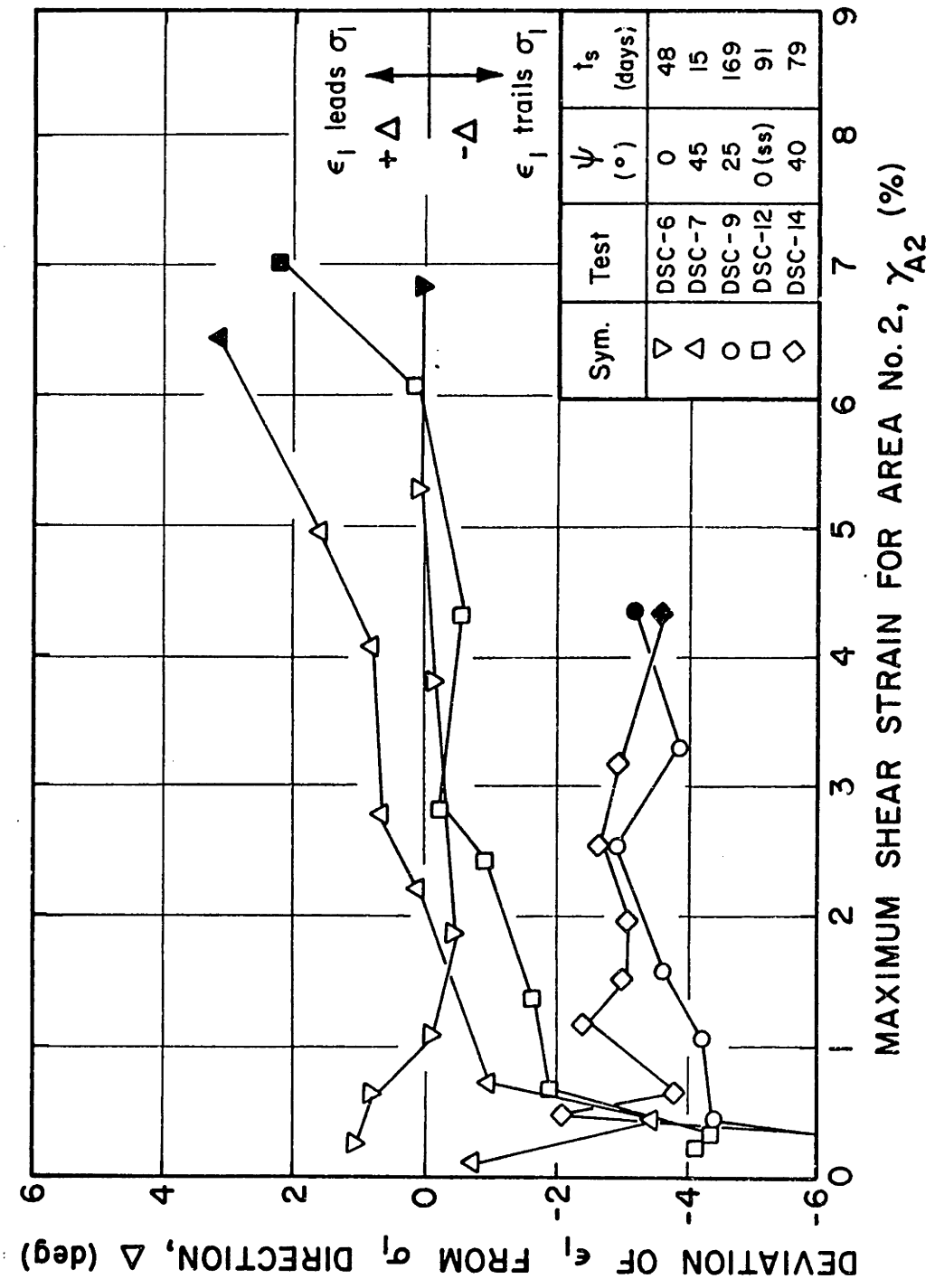

Figure 4.18: Deviation of the Direction of Principal Strain from that of Principal Stress for Isotropic DSC Tests on Resedimented BBC (OCR=4).

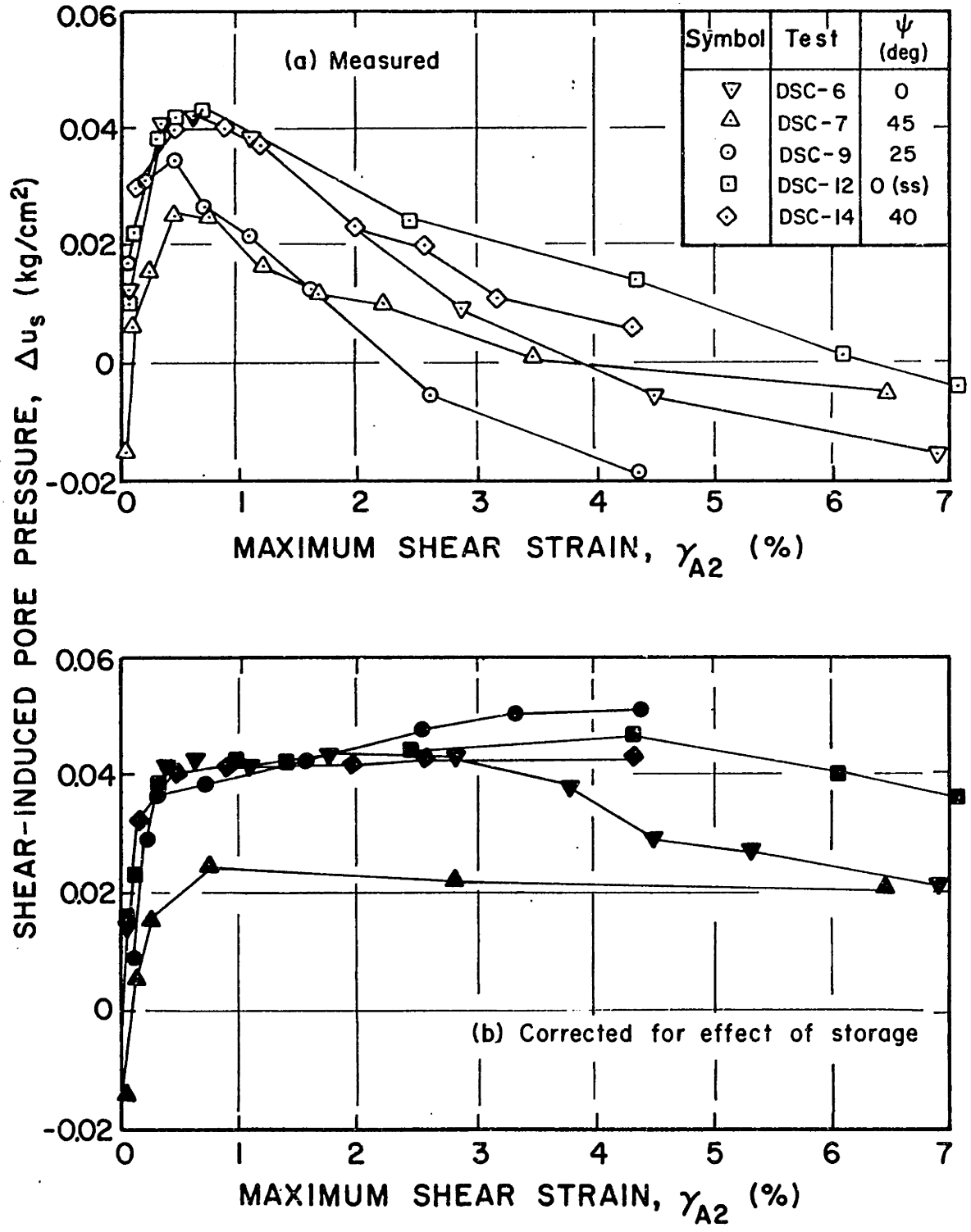

Figure 4.19: Measured and Corrected Shear-Induced Pore Pressure vs. Strain from Isotropic DSC Tests on Resedimented BBC (OCR=4).

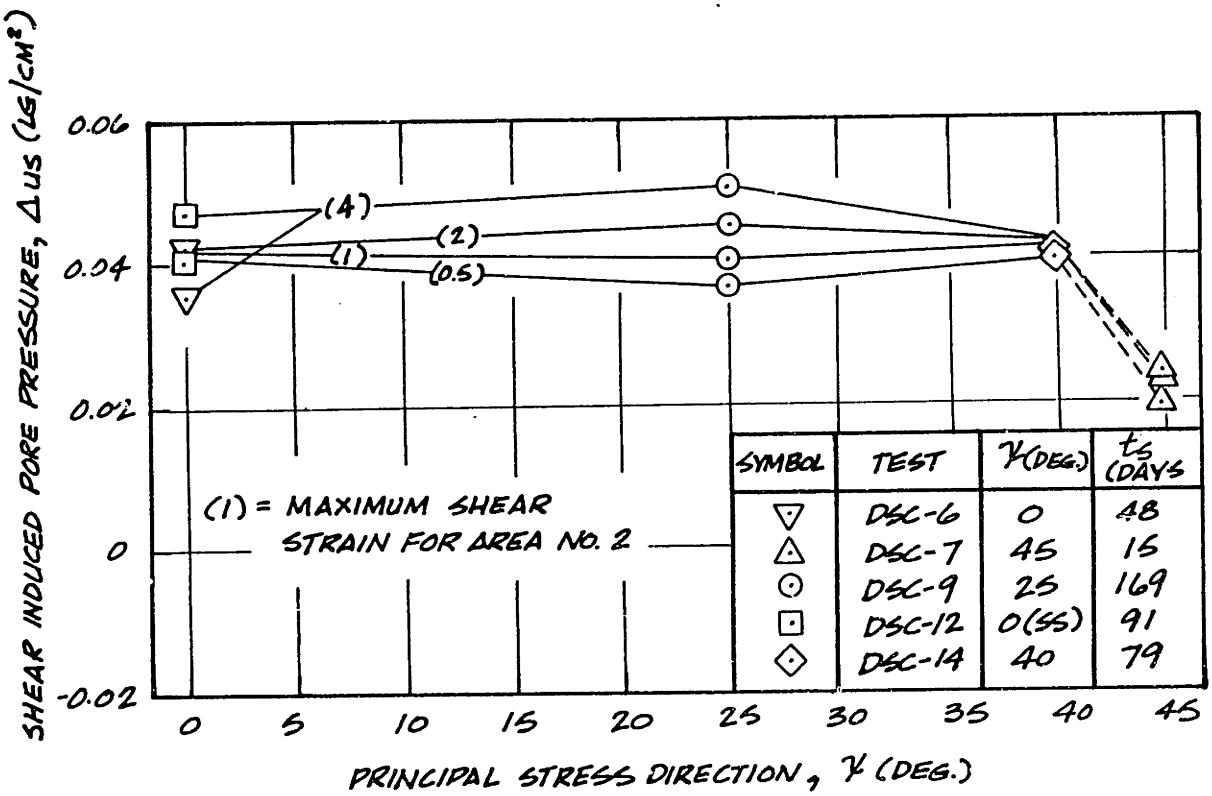

Figure 4.20: Variation of Shear-Induced Pore Pressure with Angle of Shear from Isotropic DSC Tests on Resedimented BBC (OCR=4).

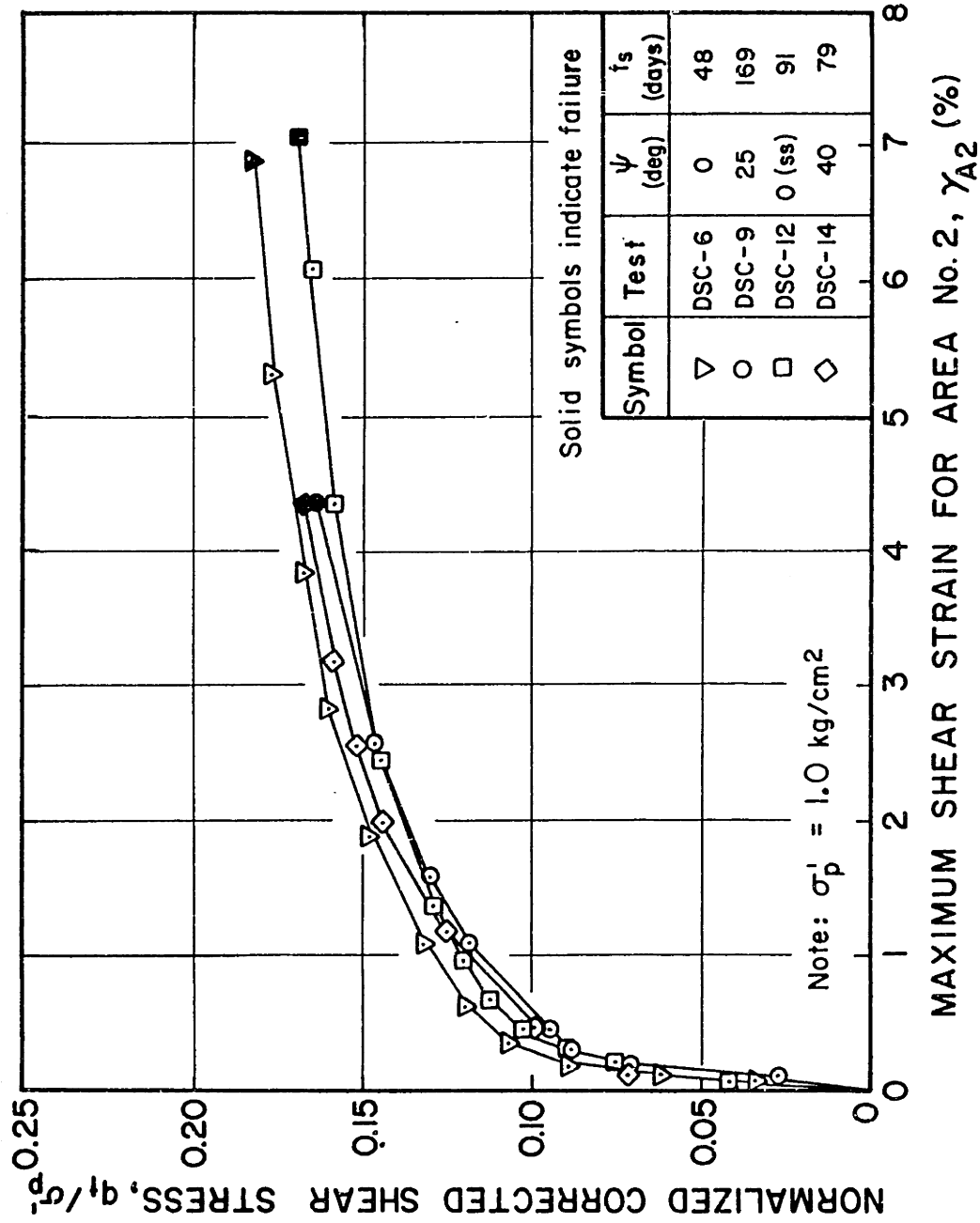

Figure 4.21: Stress-Strain Relationships (Corrected for Thixotropic Effects) from Isotropic DSC Tests on Resedimented BBC (OCR=4).

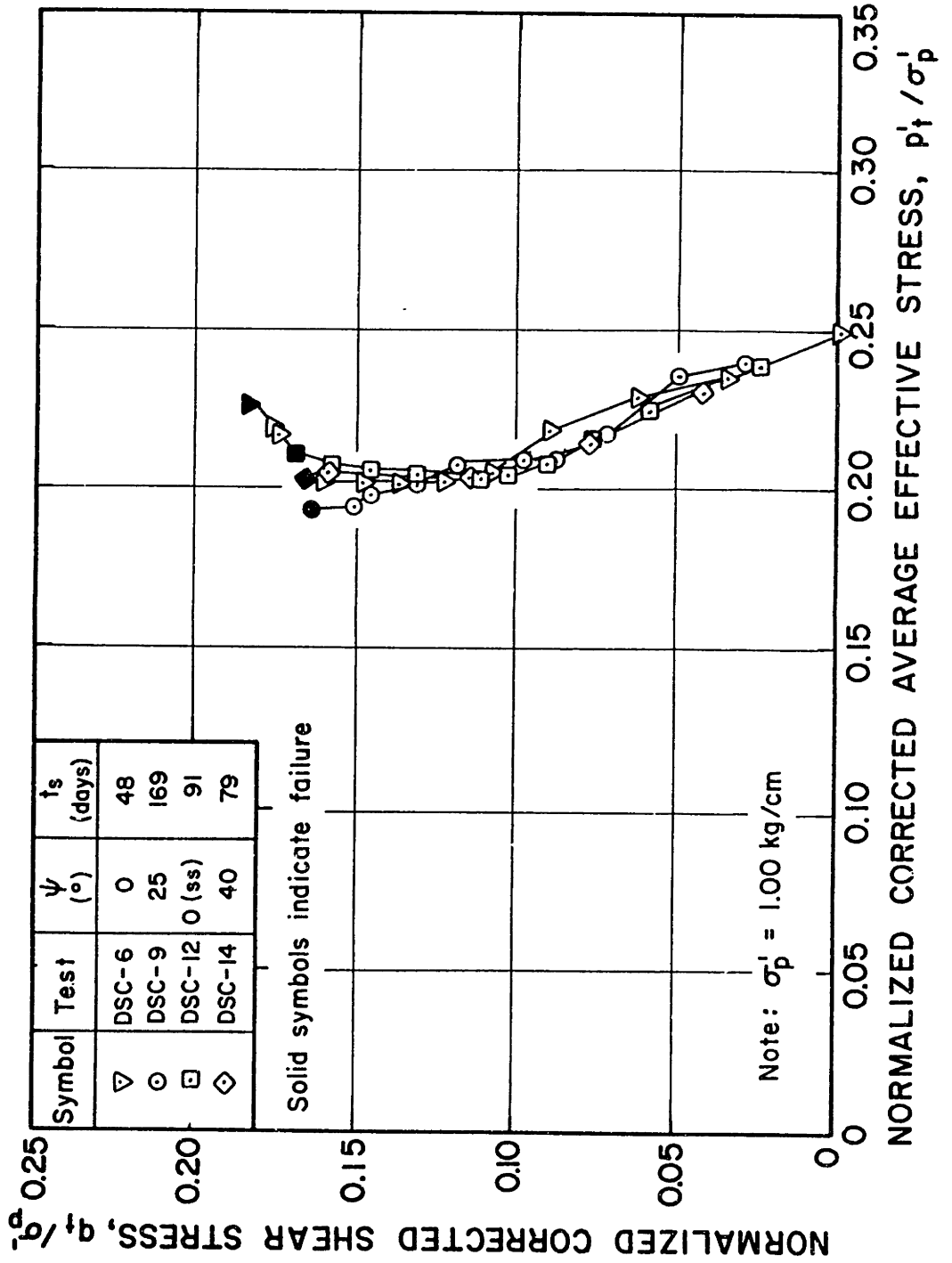

Figure 4.22: Effective Stress Paths (Corrected for Thixotropic Effects) from Isotropic DSC Tests on Resedimented BBC (OCR=4).

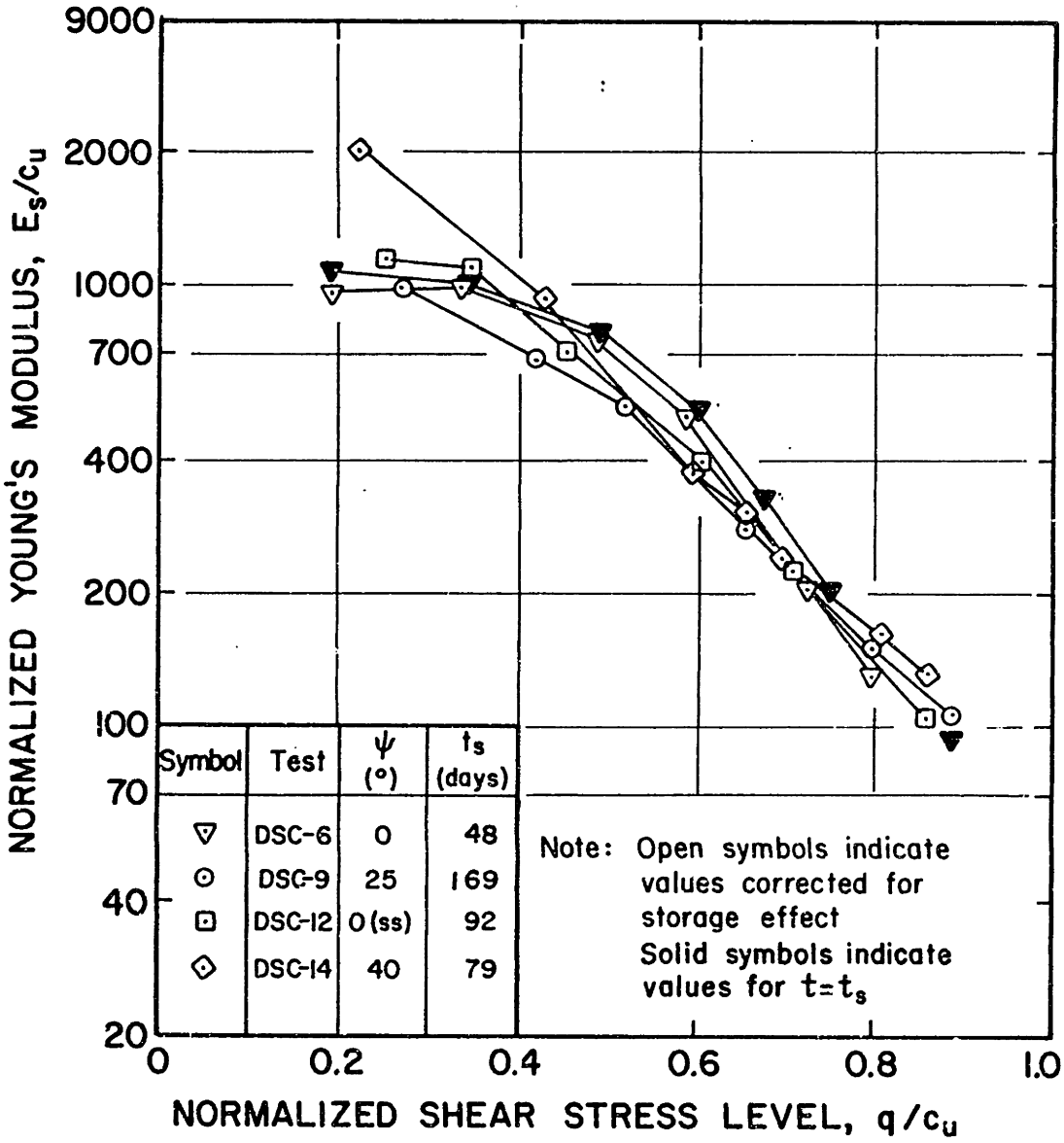

Figure 4.23: Variation in Normalized Young's Modulus with Stress Level from Isotropic DSC Tests on Resedimented BBC (OCR=4).

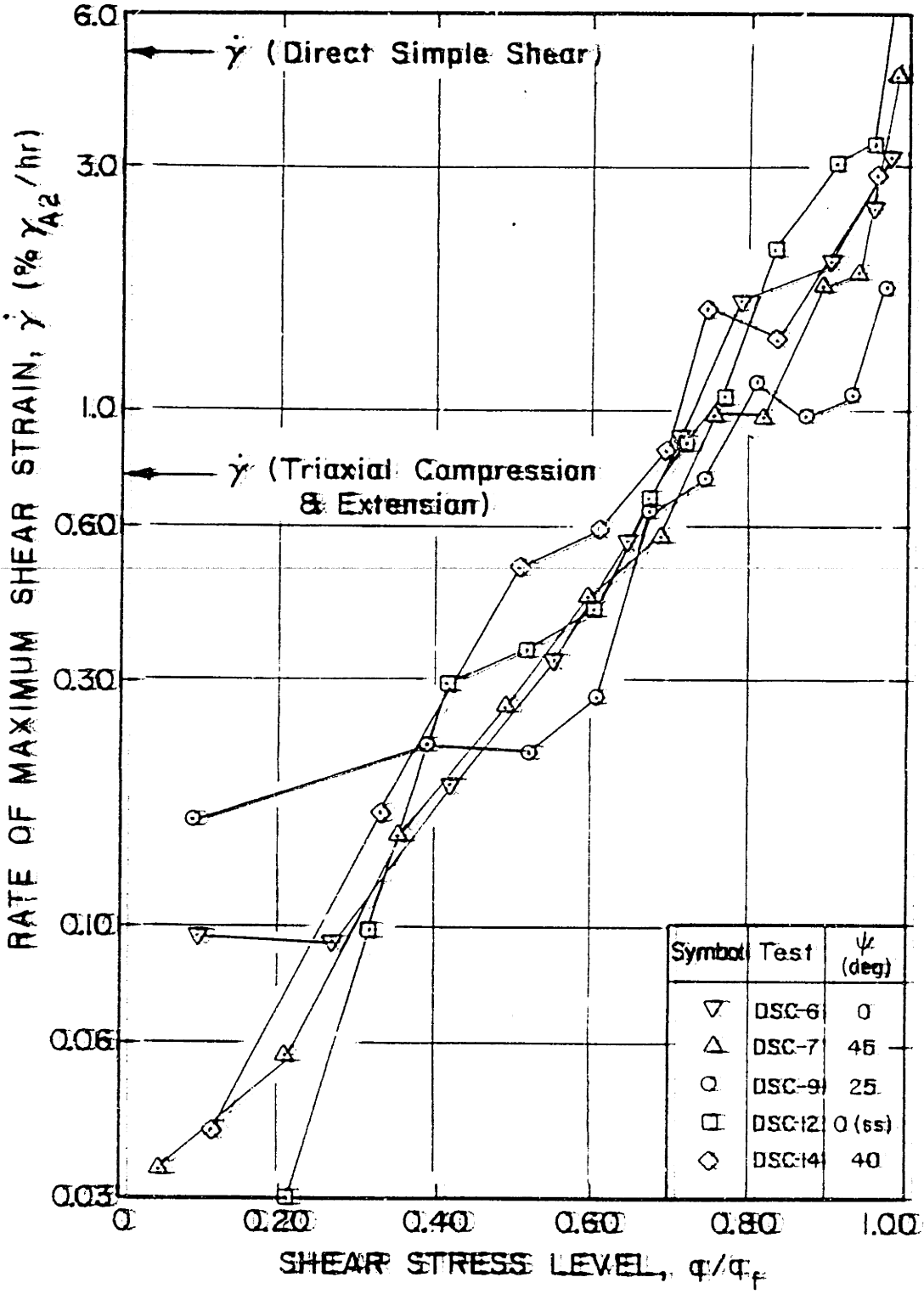

Figure 4.24: Shear Strain Rates from Isotropic DSC Tests on Resedimented BBC (OCR=4).

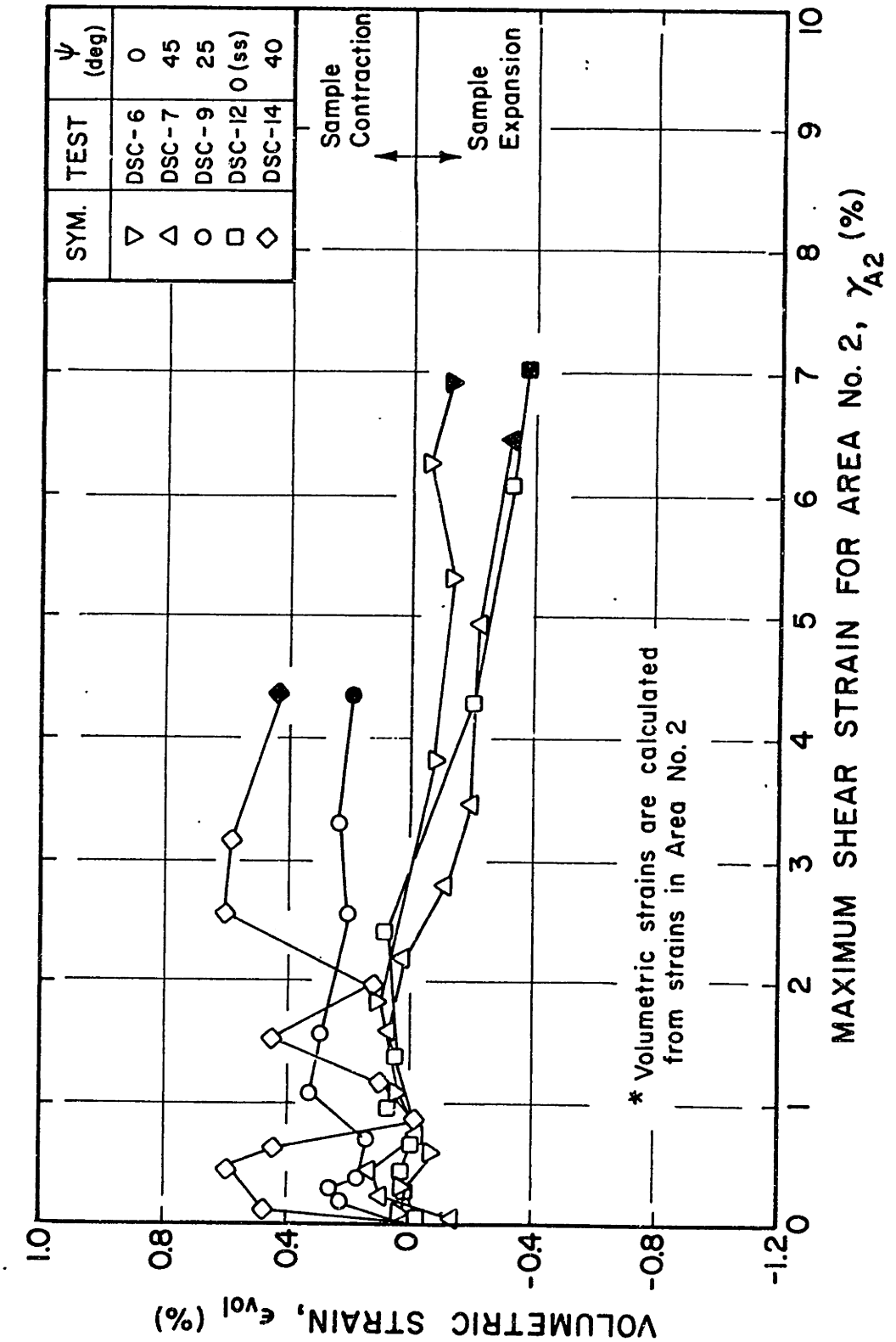

Figure 4.25: Volumetric Strain vs. Maximum Shear Strain from Isotropic DSC Tests on Resedimented BBC (OCR=4).

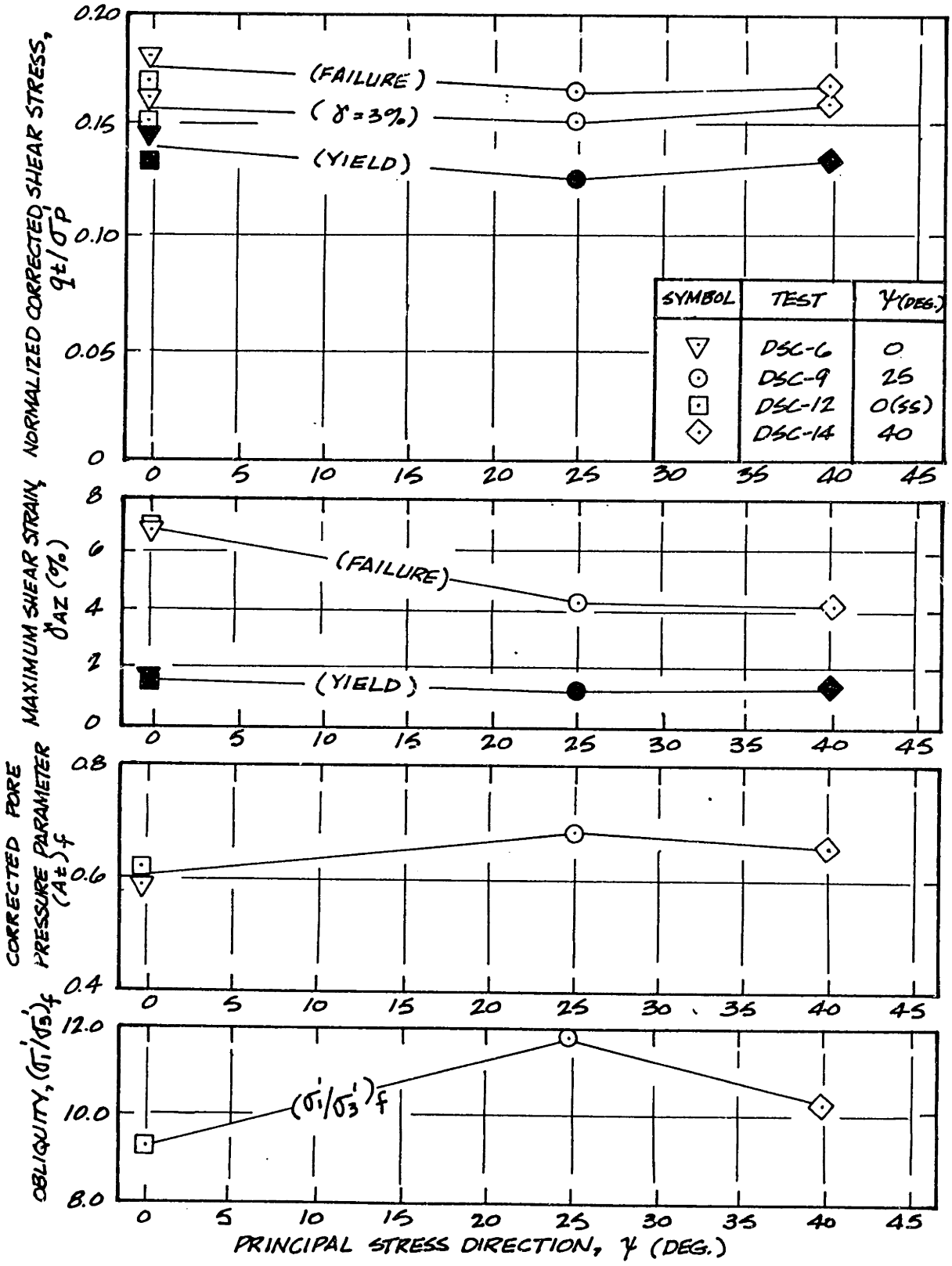

Figure 4.26: Effect of Angle of Shear on Strength Parameters from Isotropic DSC Tests on Resedimented BBC (OCR=4).

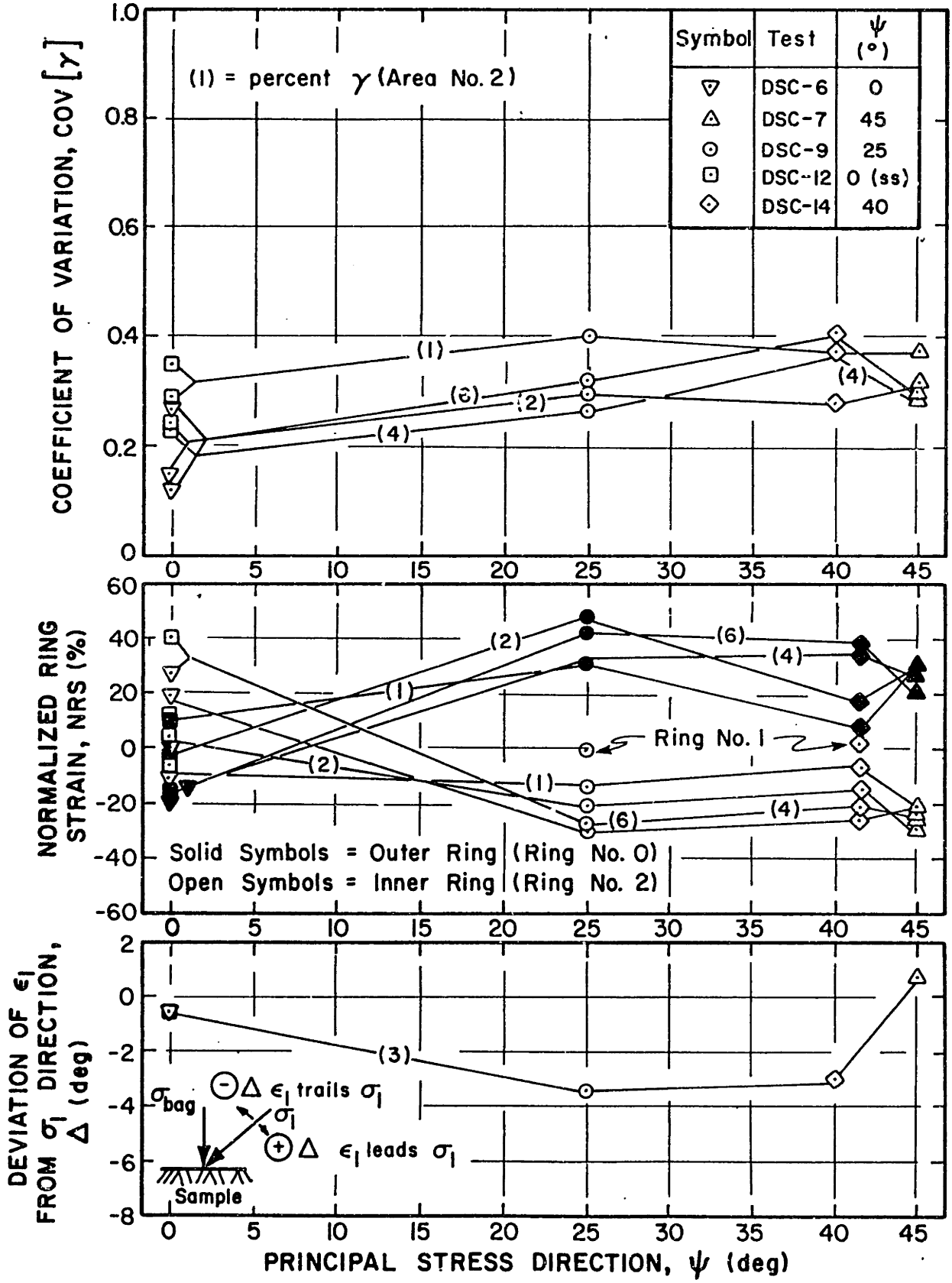

Figure 4.27: Effect of Angle of Shear on Strain Behavior from Isotropic DSC Tests on Resedimented BBC (OCR=4).

CHAPTER 5

MEASUREMENT OF UNDRAINED STRESS-STRAIN-STRENGTH ANISOTROPY OF OVERCONSOLIDATED BOSTON BLUE CLAY IN THE DIRECTIONAL SHEAR CELL

5.1 INTRODUCTION

In order to establish the anisotropic nature of resedimented BBC, a series of Directional Shear Cell tests was performed. The procedures followed with regards to sample preparation, consolidation and shearing were as detailed by Germaine (1982) except for the modifications presented in Section 4.2. Since this series of tests is directed toward the investigation of anisotropy, the direction of deposition of the sample is oriented parallel to the no strain direction (Fig. 2.5). Rotation of the major principal stress is then accomplished by application of varying amounts of shear and normal stress to bring the sample to undrained shear failure.

DSC tests provide an attractive means of ascertaining the degree of anisotropy of particulate media because it enables rotation of the direction of the principal stresses without involving an accompanying variation in the relative magnitude of the intermediate principal stress, $b = [\sigma'_2-\sigma'_3)/(\sigma'_1-\sigma'_3)]$. In the past, for example, the degree of anisotropy of a soil was often determined by performing triaxial compression (TC), direct simple shear (DSS) and triaxial extension (TE) tests which generated data for angles of shear equal to 0°, ~40° to

70° and 90°, respectively. However, these "standard" tests run the gamut of values for the intermediate principal stress ratio with TC, DSS and TE tests having values of b equal to 0, ~0.4 and 1, respectively. Comparison of DSC results with those from such "standard" tests is covered in Chapter 6.

Thixotropy affects many of the measurable strength parameters of resedimented Boston Blue Clay, as discussed in Chapter 3. In order to assess the anisotropic nature of the clay, then, it is necessary to either test samples of very similar age or to correct the results of tests on samples which span a range of storage times. As the effect of extended storage times was quantified during the DSC test program, the latter approach is dictated for this research.

The anisotropic DSC tests performed on resedimented BBC during this research are presented in Table 5.1. A brief list of these tests is as follows:

δ (deg)	Number of Tests	Test Quality
0	2	Both good
20	2	One poor
40,45	3	Two poor
65,75	3	All Good
90	1	Good

Total Number of Tests = 11

5.2 RESULTS OF ANISOTROPIC DSC TESTING

5.2.1 Evaluation of Test Quality

The standards developed in Chapter 4 (strain distribution and stress application, Sections 4.1.1 and 4.1.2, respectively) using the DSC tests performed in the isotropic plane of BBC samples are applied to the results of DSC tests in the anisotropic plane. Such an approach should maximize the objectivity used to select "good" tests. All anisotropic DSC tests are evaluated first on the basis of the strain distribution standard and then on the basis of the stress application standard.

5.2.1.1 Evaluation of Strain Distribution

The strain distribution standard involves inspection of the normalized ring straining, NRS (in which the difference between the average maximum shear strain of each ring and the average maximum shear strain of the entire sample is normalized with respect to the average maximum shear strain of the entire sample), as it varies with the increasing average maximum shear strain of the entire sample. Figs. 5.1 and 5.2 present these data for the anisotropic DSC tests performed.

As with the isotropic tests performed at Ψ=25° and 40° (DSC-9 and 14, respectively) NRS values for DSC tests at δ=20° (DSC-10 and 15) and at δ=40° (DSC-13) are calculated after deleting a total of 12 elements from consideration. These

elements, located in two diametrically opposite corners of the grid, represent the behavior of the two unprotected corners of the sample which succumbed to isolated premature failure. Justification for this deletion is detailed in Section 4.1.1; the location of the deleted elements is depicted in the inset of Fig. 5.1. It is evident that the only tests not meeting the strain distribution standard set for the NRS values (i.e., NRS $\tilde{<}$ |40%|) are DSC-4 and 10 in Fig. 5.2.

Additional evaluation of the uniformity of the strain during shear is accomplished by reference to Fig. 5.3. Coefficients of variation of the average maximum shear strain, COV[γ], for both Area Nos. 1 and 2 (see inset Fig. 5.3) are plotted versus the respective average strain of the areas. The largest COV[γ] values occur in the cases of the lowest δ values: 0° and 20°. Rapid formation of a failure plane occurs at relatively low strains in these tests. Disparity in strains created by the failure planes in some of the grid elements, yet not in others, leads to rather large standard deviations.

Assessment of sample strain behavior is more realistic when considering Area No. 2 since Area No. 1 inevitably incorporates a larger percentage of end effects (Fig. 4.1). Prior to the development of failure planes COV[γ] values for Area No. 2 range between 0.2 and 0.9. It may be wise, for the time being, to ignore the large COV[γ] values associated with the low δ tests since the onset of a failure plane seems apparent in the COV[γ] value at lower strains than in visual

assessment of the inked grid. In addition, DSC-5 (δ=45°) has significantly greater COV[γ] than normal for both Area Nos. 1 and 2 over a large range of strains, flagging a potential problem (as will be identified when the stress application standard is applied).

Without considering the DSC tests at δ = 0°, 20° and 45° the pre-failure plane range of COV[γ] values for Area No. 2 is between 0.2 and 0.4. Basically, this range is comparable in extent to that demonstrated by the isotropic DSC test series (COV[γ]=0.12 to 0.33) although the average value is approximately 35% greater in the case of the anisotropic test series. Values of COV[ε_1] given by Bekenstein (1980) for tests in both the isotropic and anisotropic planes of loose Leighton Buzzard Sand exhibit a range similar to that for the isotropic tests on BBC.

Variation in COV[γ] values with increasing γ over a range of δ angles is discussed further in Section 5.2.2. For the time being, it is sufficient to establish that the following DSC tests indicate some aberration in Fig. 5.3:

- DSC-5 (δ=45°); COV[γ] values are anomalously high over a large range of strains. Since this feature is not corrected even upon considering Area No. 2, it is possible that there are some extreme end effects occurring due to the improper application of the shear traction (see the following discussion on stress application standard). Germaine (1982) identifies two zones which yielded prematurely in DSC-5 which cause the

very high scatter.

- DSC-10 (δ=20°); COV[γ] values for Area No. 1 rise rapidly to a value almost double that for DSC-15 (δ=20°). Although this in itself is insufficient to disqualify DSC-10, it does provide a flag to the problem already noted in the NRS distribution for DSC-10. Having an NRS >>|40%| is sufficient to disqualify a test.

For the rest of the anisotropic DSC tests, the strains, particularly when considering Area No. 2, seem acceptably uniform given the range of COV[γ] (= 0.2 to 0.4).

Although study of the direction of major principal strain with respect to that of the major principal stress is a vehicle for evaluation of DSC test quality for the isotropic test series, it cannot be used as such for the anisotropic series. In the case of the isotropic plane, the true value of Δ (the deviation of the ε_1 direction from that of σ_1) is assumed to be zero. For the anisotropic case, however, the true value of Δ is unknown and is one of the parameters which this research will hopefully ascertain for overconsolidated BBC. The strain direction parameter is plotted in Fig. 5.4 as shearing progresses in the form of the deviation of the direction of ε_1 from that of σ_1, Δ, such that a positive value for Δ indicates that the angle between the direction of ε_1 and the direction of disposition is greater than δ.

In assessing the true deviation of the ε_1 direction, some consideration must be made for any potentially device induced

deviations. Section 4.4.2 discusses the variation of Δ with the isotropic angle of shear, Ψ. Since for the isotropic case, Δ should equal zero, any consistently measured value is likely to be due to the mechanical methods of stressing the sample. For example, the isotropic cases reveal that ε_1 tends to trail σ_1 slightly when the shear sheets are involved in the shearing process (Fig. 4.27). (Bear in mind that the measurement techniques allow for a precision of $\pm 1°$).

Fig. 5.4 plots calculated values of Δ, not considering deviation in the direction of ε_1 from that of σ_1 due to the device. Prior to evaluating angular relationship between ε_1 and σ_1 for the anistropic DSC tests, it is suggested that the relationship between Δ and ψ presented in Fig. 4.27 be taken into account. The effect of δ on the deviation angle, Δ, is discussed in Section 5.2.2.

To summarize the results of evaluation of the strain distribution while bearing in mind the quantitative established strain distribution standard, the only anisotropic DSC tests definitely considered of poor quality are DSC-4 ($\delta=45°$) (also considered poor by Germaine (1982)) and DSC-10 ($\delta=20°$). DSC-5 ($\delta=45°$) appears to have possible problems due to fairly high values of COV[γ].

5.2.1.2 Evaluation of Stress Application

As with the isotropic DSC test series, the anisotropic tests surviving the strain distribution standard must be corrected for the thixotropic effects of extended dissimilar

storage times prior to evaluation of test quality under the established stress application standard (Section 4.1.2). The method for correcting the measured DSC data is presented in Chapter 3 (Sections 3.2.3 and 3.2.4) and a general outline of the steps followed is provided in Section 4.3.2. Uncorrected stress-strain curves and stress paths for the anisotropic DSC test series are provided in Appendix F along with the tabulated data for these tests.

The stress application standard involves assessment of the character of the shear-induced pore pressure, Δu_s (= $\Delta u - \Delta \sigma_{oct}$) vs shear strain curve and the effective stress paths. This standard is somewhat more ambiguous in its application to anisotropic tests compared with isotropic tests. In the latter case, one is interested only in ascertaining whether or not the shear-induced pore pressure behavior and the stress paths coincide with one another, regardless of the shearing angle, Ψ.

But with the presence of anisotropy, the angle of shear, δ, will probably affect the shear-induced pore pressure. Therefore, the approach followed in evaluating anisotropic test quality for the anisotropic cases involves the determination of a pattern as δ varies. This requires, of course, sufficient tests to suitably establish some pattern.

Fig. 5.5 plots time corrected Δu_{st} versus shear strain for the anisotropic test series. Essentially, the pattern which emergences is one of increasing Δu_{st} as the angle of shear, δ,

increases beyond approximately one percent shear strain (as per Area No. 2 of the inked grid). Fig. 5.6 better illustrates the nature of the shear-induced pore pressure behavior with varying δ. For $\gamma \tilde{<} 0.5\%$, where the shear stress level is either less than, or just equal to, the yield stress, Δu_s seems independent of δ. As the sample begins to strain significantly ($\gamma > 1\%$), however, a definite increase in Δu_{st} with increasing δ is apparent.

The only DSC test which does not fit this pattern is DSC-5 ($\delta = 45°$). Although the general shape of Δu_{st} vs. γ for DSC-5 is similar to that for DSC-13 ($\delta = 40°$), it is shifted to much lower levels of pore pressure. As with DSC-7 ($\Psi = 45°$), DSC-5 was sheared solely by application of shear tractions (i.e., the applied normal stresses were equal throughout the test). In addition, DSC-5 was performed prior to use of restraining vanes on both pressure bag sides. In a manner similar to that for the isotropic test at $\Psi = 45°$ (DSC-7, see Fig. 4.3), DSC-5 followed a stress path exhibiting relatively high average effective stresses at low shear stresses well before yielding, however, the average effective stresses drop back to approximately the consolidation stress of 0.25 ksc. Thus, a "knee" is formed at the base of the stress path. The knee, seen in the uncorrected ESP, persists even after correction for storage time effects.

Given the conditions under which both DSC-7 and 5 were performed (i.e., all shear stress applied by shear traction

without sufficient constraint on the pressure bags) it is concluded that the actual stresses in the sample are not equivalent to those applied. Section 4.1.2 discusses the high p' phenomenon exhibited by the two 45° DSC tests in greater detail.

Although Δu_{st} vs γ curves for the two DSC tests performed at $\delta=0$ do not coincide exactly, the character of the plots is very similar. Further, the curve for DSC-3 differs from that for DSC-1 by less than 0.5% shear strain. Careful inspection of Fig. 5.5 reveals that both samples began to dilate (i.e., to generate lower and lower pore pressures as the sample strains) at approximately the same strain ($\gamma\approx0.25\%$). DSC-3 behaved in a stiffer manner than DSC-1 and generated lower pore pressures in the early stages of shear (stress-strain curves are presented in Fig. 5.7). The two tests, DSC-1 and DSC-3, are considered valid and thus offer a measure of reproduceability, as do the two tests performed at $\delta=75°$ (DSC-11 and DSC-16).

In summary, of all the DSC tests considered in light of the quality of stress application, only DSC-5 fails. The probable reason for failure is inadequate transference of shear stress via the shear sheets accompanied by a reduction in the normal stress as the pressure bags were slightly drawn from the sample. This problem, also apparent in DSC-7 ($\Psi=45°$), is solved by the attachment of thin retaining vanes (Fig. 4.9) to the unconstrained sides of the pressure bags. Use of the vanes makes it possible to run high quality tests in the Directional

Shear Cell at angles of shear which dictate predominant use of the shear sheets, without running the risk of normal stress unloading (e.g., DSC-13 (δ=40°)).

The anisotropic DSC tests which met both strain distribution and stress application standards are as follows:

Test	δ (deg)	Thixotropic σ'_{pt}(ksc)
DSC-1	0	1.23
DSC-3	0	1.30
DSC-15	20	1.34
DSC-13	40	1.26
DSC-8	65	1.55
DSC-11	75	1.32
DSC-16	75	1.39
DSC-2	90	1.27

5.2.2 Presentation of Time Corrected Anisotropic DSC Test Results

Having removed the effects of differing storage times as well as having assessed test quality, the best estimate of the anisotropic stress-strain-strength behavior of overconsolidated resedimented Boston Blue Clay as measured in the plane strain environment of the DSC is presented. Measurement techniques and associated errors, sample preparation and storage as well as assessment of the effect of thixotropy are discussed in Chapter 4, Appendix D and Chapter 3, respectively.

Table 5.1 contains the pertinent results of the successful anisotropic DSC tests. Items such as the length of storage, the magnitude of some of the time corrections and testing details (such as whether or not shear sheets and/or plexiglass

prisms were used) are also presented for convenient referral. The figures studied to arrive at these final results are presented in this section.

Shear stress versus maximum shear strain based on the average for Area No. 2 are presented in Fig. 5.7. It is evident from this plot that resedimented BBC displays significant anisotropic characteristics. At one percent shear strain, for example, samples sheared with σ_1 coincident with the direction of deposition (δ=0°) are 100% stronger than samples tested in a plane strain passive manner (δ=90°).

Tests performed at low values of δ behave in a brittle manner and developed failure planes at fairly low shear strains. These tests would have exhibited strain-softening, but such behavior cannot be readily measured in a stress-controlled test. (The solid symbols in Fig. 5.7 signify the onset of failure planes qualitatively identified in photographs taken at the end (i.e., 10 min. after application) of the stress level indicated). As the mode of shear begins the transition to a more passive (extension) state with δ>45°, samples undergo ductile behavior prior to "failure", also identified by the onset of a rupture surface which is, however, much less well-defined. Concurrent with increasing values of δ, failure becomes an increasingly more elusive state to identify.

Two tests were performed at δ=0° (DSC-1 and DSC-3) as well as at δ=75° (DSC-11 and DSC-16). The plane strain active set

of tests demonstrates a fairly consistent difference in normalized shear stresses of $q_t/\sigma'_p \approx 0.02$ throughout the tests with DSC-3 being the stronger. The shapes of the curves, as well as the strains at which failure occurred, are very similar. At failure, DSC-3 is approximately 8% stronger than DSC-1.

The two tests at $\delta=75°$ exhibit stress-strain curves which are essentially identical in shape although DSC-16 yields at a normalized stress level approximately 0.015 greater than that for DSC-11 and maintains this difference to high strain levels. By the time a failure plane is noted ($\gamma_{fp}=14.1\%$ and 13.0% for DSC-11 and 16, respectively), DSC-16 is about 9% stronger than DSC-11. The most disconcerting feature about DSC-11 is its coincidence with the stress-strain curve for DSC-2 ($\delta=90°$). However, reference to Fig. 5.8 as well as Fig. 5.5 reveals a substantial difference in both the stress paths followed by DSC-11 and DSC-2 and their shear-induced pore pressures. Moreover, the two tests at $\delta=75°$ follow similar effective stress paths.

The normalized stress paths of Fig. 5.8 generally fall within a very narrow band such that any effects of anisotropy are not clearly evident. The end (failure) points, however, do vary considerably, as shown by the q_t/σ'_p vs. p'_t/σ'_p failure values plotted in Fig. 5.9, along with those from the four isotropic DSC tests. The following features are noteworthy:

- There is a very consistent decrease in q_{tf} and p'_{tf} with increasing δ except that $\delta=65°$ and 75° plot very

close to one another.

- A straight line drawn through all the anisotropic DSC tests gives a negative shear stress intercept which is totally unrealistic and therefore shows that increasing δ must lead to a significant lowering of the effective stress envelope (ESE).
- The isotropic data plot above the anisotropic data, further proving that anisotropy leads to changes in the ESE.
- ESE's at various angles of shear cannot be defined without data from tests at varying σ'_{vc} for each δ.
- With the available data, there is no way of determining if increasing δ leads to decreasing c' or decreasing ϕ' or both. (Symes et al. (1984) show increasing δ leads to a decrease in ϕ' for Ham River sand, but with resedimented BBC there also exists the possibility for some effect of changing δ on the cohesion.)

It is also quite clear from Fig. 5.5 (but less evident from the shape of the ESP's) that apart from an initial tendency to contract (i.e. generate positive pore pressures) the samples tested at $\delta<45°$ want to dilate at strains greater than 1%. High δ tests on the other hand have a tendency for contraction until reaching much larger strains at which point only a slight reduction in pore pressures occurs.

Reference to Fig. 5.7 shows that all the anisotropic tests exhibit essentially identical initial shear moduli to normalized shear stress levels of approximately 0.05.

Normalized stiffness, as measured by Young's (secant) Modulus, E_s/q_{tf}, appears to be relatively unaffected by anisotropy until approximately 60% of the undrained shear strength, q_{tf}, as shown in Fig. 5.10. At stress levels equal to about half of the strength, E_s/q_{tf} values range from 350 to 600 with no unique relationship to δ. Once higher stress levels have been reached the DSC tests at $\delta>45°$ exhibit a more rapid decrease in the normalized modulus than tests at lower δ values. This feature is due to the large strains developed in the $\delta>45°$ tests at very small increments of stress after yielding has occurred.

Two additional effective stress parameters are presented in Fig. 5.11: obliquity, R ($=\sigma'_1/\sigma'_3$), and Skempton's pore pressure parameter, A, both versus the maximum shear strain. The obliquity decreases at any given strain with increasing angle of shear, until $\delta=75°$. Then the plane strain passive test (DSC-2) exhibits higher obliquity than the two $\delta=75°$ tests. The pore pressure parameter, A, on the other hand exhibits consistently increasing values for increasing angle of shear after approximately 0.5% shear strain. This pattern is maintained until failure. The highest value of A is attained by the $\delta=90°$ test ($A\simeq0.88$) and the lowest by the $\delta=0°$ tests ($A\simeq0.35$).

Due to the stress-controlled nature of the DSC, strain rate is a result of, rather than a driving force for, the application of load unlike most triaxial and Direct Simple Shear tests which are strain-controlled. Because the DSC

testing procedure followed to date does not immediately generate the strains resulting from imposed stresses, some estimate of the stress-strain curve must be made prior to testing so as to maintain reasonable rates of strain throughout shear. The rates of maximum shear strain, $\dot{\gamma}$, for the anisotropic DSC test series are presented in Fig. 5.12. These $\dot{\gamma}$ values are determined based on the differential total maximum shear strain accumulated between films divided by the time which elapsed between shots.

Fig. 5.12 reveals $\dot{\gamma}$ varying from approximately 0.10 to 6.0 %/hr, a range of one and a half orders of magnitude. For purposes of comparison with typical strength tests (triaxial and DSS), this range is well-located since it is in the vicinity of the rates of strain usually imposed by these tests (as identified in Fig. 5.12. However, an ideal situation would have been to maintain a constant rate of strain so as to eliminate strength differences due to varying strain rates.

The values of $\dot{\gamma}$ appear to be randomly distributed with respect to the shear angle, δ, until q/q_f becomes greater than about 0.7 to 0.8. After this point, which approximately coincides with the yield stress level, tests at increasing values of δ experienced greater strain rates. The only test which does not fit this pattern is DSC-11 (δ=75°), which had strain rates that are slightly greater than twice those of DSC-2 (δ=90°).

5.3 DISCUSSION OF EFFECT OF ROTATION OF MAJOR PRINCIPAL STRESS DIRECTION ON STRESS-STRAIN-STRENGTH PARAMETERS OF OVERCONSOLIDATED BOSTON BLUE CLAY

5.3.1 Variations in Strength Behavior with δ

Cross anisotropic strength behavior of resedimented BBC at OCR=4 is presented in Fig. 5.13 and Fig. 5.14. All these data have been corrected according to the procedures detailed in Chapters 3 (for thixotropy) and 4 (for grease and shear sheet resistance). Table 5.1 presents pertinent information related to each test.

At the extreme ends, strength anisotropy of BBC at OCR=4 is such that samples sheared at $\delta=0°$ are 100% stronger at yield than those sheared at $\delta=90°$. Yield stresses were estimated via the intersection between a line through the initial portion of the stress-strain curve and a line through the post yield portion. The decrease in normalized yield stress with increasing δ is essentially linear between $\delta=0°$ ($q_{ty}/\sigma'_p=0.20$) and $\delta=70°$ ($q_{ty}/\sigma'_p\simeq0.11$) as presented in Fig. 5.13. After $\delta=70°$, the decrease in q_{ty}/σ'_p per degree increase in δ is much lower. The character of the yield stress vs δ curve is basically mimicked by the shear stresses obtained at successively greater strains. The strength at failure versus δ curve is parallel to that at yield. Hence the anisotropy ratio at failure in the DSC is $K_s = \frac{q_{tf}(\delta=90°)}{q_{tf}(\delta=0°)} = \frac{0.138}{0.245} = 0.56$.

At low angles of shear, the behavior is brittle and failure plane formation is easily identified. At higher values

of δ, failure planes do form, but at much higher shear strains rendering identification of failure plane occurrence more difficult. Careful visual comparative study of the films resulted in the identification of failure at the values indicated in Table 5.1 and Fig. 5.14. (Since the DSC is stress-controlled, use of the peak q as the failure stress is not practicable. Some of the tests were carried to stresses well in excess of those at which failure planes were formed. Strains did not "run away" in an obvious fashion. Hence, onset of failure planes was used to indicate failure.)

The stress-strain curves of all the anisotropic DSC tests coincide with one another at very low strains ($\gamma \tilde{<} 0.15\%$), as can be seen in Fig. 5.7. The moduli at 50% of q_{tf} decreases as δ increases. However, there is no consistent variation in the normalized Young's modulus with δ until approximately 60% of the undrained shear strength is mobilized (Fig. 5.10). Fig. 5.14 presents the normalized secant moduli at 50% of the shear strength and, although there is significant scatter, it is concluded that the variation is random. (Decreasing E_{50} is accompanied by decreasing q_{tf} leading to constant E_{50}/q_{tf} with increasing δ.)

Strain at yield appears to be unaffected by the direction of the major principal stress during shear. All the anisotropic DSC tests yielded at $\gamma \simeq 1\%$ (Fig. 5.14). The normalized yielded shear modulus, G_y/σ'_p, however, varies with δ in a manner similar to the variation in yield and undrained

shear strengths; i.e., G_y/σ'_p decreases from a value of three almost linearly with increasing δ for $\delta=0°$ to 70° and is essentially constant for $\delta=70°$ to 90°. G_y/σ'_p for $\delta=90°$ is equal to 0.5.

Maximum shear strains at failure are significantly affected by the angle of shear as seen in Fig. 5.14. Strain at failure, especially for the passive type DSC tests is difficult to assess -even more difficult than the undrained strength since the yielded modulus is so low. Furthermore, tests sheared using shear sheets cause extensive distortion of the inked grid, increasing the difficulty of spotting failure. The values of γ presented are the best estimate based on the identification of failure plane formation.

The lowest strain at failure occurs at $\delta=0°$ ($\gamma_f \simeq 2\%$), the maximum γ_f occurs at $\delta=75°$ ($\gamma_f \simeq 13.5\%$). At $\delta=90°$, shear strain at failure decreases to just less than 10%. Assuming that the failure plane forms at an angle equal to $(45°-\phi'/2)$ from the direction of σ_1, a possible explanation for the large γ_f for $\delta=75°$ is that the formation of the failure plane in the case of $\delta \simeq 75°$ is inhibited by the presence of the shear sheets.

The effective stress path followed during shear is also affected by the angle of shear. This is evident in Fig. 5.8 but more easily studied by determining the value of several effective stress parameters such as the obliquity, $R=\sigma_1'/\sigma'_3$, and Skempton's pore pressure parameter, $A=\frac{\Delta u-\Delta\sigma_3}{\Delta\sigma_1-\Delta\sigma_3}$. The large effect of anisotropy on the pore pressure behavior has already

been discussed in relation to the shear-induced pore pressure, Δu_{st}, in order to delete the tests with stress application problems (e.g., DSC-5 (δ=45°)).

Fig. 5.13 presents the variation of A_f and R_f with δ. It is evident from Fig. 5.13 that increasing the angle of shear results in greater values of A_f, although there appears to be a plateau in the vicinity of $\delta \approx 65$ to 75°. This trend is more evident in the Δu_{st} behavior in Fig. 5.6. The obliquity at failure exhibits a minimum ($R \approx 5$) for δ=75° rising linearly with decreasing δ to $R \approx 7$ for δ=0°. The obliquity for δ=90° is approximately the same as that for δ=20°; $R \approx 6.3$.

The location of the failure stress state within q-p' space is completely defined by the values of R_f and A_f. The combination of increasing A_f and essentially decreasing R_f describes a tendency for lower average effective stresses and simultaneously lower shear stresses at failure as the angle between the major principal stress and the deposition direction increases, as depicted in Fig. 5.9.

In order to evaluate the failure envelopes implied by the results of the anisotropic DSC test series (i.e., to determine the effective stress friction angle, ϕ' for each test) cohesion intercepts must be estimated. The plane strain DSC test data are discussed in relation to data from the triaxial and DSS devices in Chapter 6. It is from these data, in particular from the results of the unconsolidated undrained test ($\overline{UU}$-1), that an estimate of the cohesion of the resedimented BBC is

obtained. It is concluded that $a'/\sigma'_p \simeq 0.04$ is an adequate approximation of the cohesion at $\delta=0°$. (This estimate is basically in agreement with the range of data presented by Ladd and Kinner (1967) who performed drained unconfined tests on resedimented BBC). Thus, at $\delta=0°$, the effective friction angle is approximately equal to 39°.

As indicated in Fig. 5.9, the effective stress envelope is affected by anisotropy. Measurements of cohesion at varying angles of shear are not available so, as mentioned previously, estimates of the effect of δ on ϕ' cannot be made. However, reduction in undrained strength with increasing angle of shear is clearly not due solely to increased shear induced pore pressures causing contact with the same envelope at lower shear stresses.

5.3.2 Variation in Strain Distribution Behavior with δ

Fig. 5.15 shows the effect the angle of shear has on the nature of the strain distribution experienced by the sample. The parameters studied are coefficient of variation, COV[γ], for Area No. 2 and Normalized Ring Strain, NRS. Germaine (1982) also investigated the variation of COV[γ] with angle of shear in the DSC. Given the limited number of DSC tests available at that time, it happened that decreasing COV[γ] values coincided with the increasing chronological order in which the tests were performed and hence it was suggested that COV[γ] was not so much affected by δ or Ψ as it was by

increasing operator experience. There exist sufficient data at present (four isotropic DSC tests and eight anisotropic tests, which have passed the established standards), to lay this hypothesis to rest (see Fig. 4.27 for isotropic COV[γ] data). The variation in strain distribution is, rather, considered either a device induced feature (as determined by investigation of strain distribution behavior from the isotropic test series) and/or a feature caused by the anisotropy of the test material.

Because results of the isotropic DSC test series identified strain distribution behavior which is affected by the mode of shear (i.e., shear sheets vs. pressure bags), any conclusions drawn regarding true anisotropic behavior of the BBC sample must take these data (Fig. 4.27) into consideration. Fig. 5.15 includes the range of isotropic strain behavior at the various angles of shear (as depicted by the shaded zones).

The extreme rise in COV[γ] at γ=2% as compared with γ=1% for the tests in the "active" region is caused by the formation, rapid development and subsequent slip along a failure plane. This is true to a lesser degree for δ=40° than it is for δ=0° and 20°, but by γ=8% the failure plane has developed sufficiently to raise the COV[γ] by a small amount. The "passive" tests show a continued decrease in COV[γ] as shear progresses. Although the values at δ=65° and 75° are slightly greater than the maximum level shown by the isotropic tests (COV[γ]≈0.5 vs. 0.35), further strain exhibits less

scatter. Initial high scatter, at γ=1 and 2% may be due to initial seating of the shear sheets. This problem may not be apparent at angles of shear in the active zone because of the higher shear strength and stiffness.

Distribution of strain, as measured by the normalized ring strain, NRS, parameter detects whether the outer portion of the sample or the inner portion experiences the greatest strain. The bottom of Fig. 5.15 presents these data for the anisotropic DSC tests in relation with the ranges from the isotropic tests. It is important to note that the DSC device causes the outer portion of the sample (Ring No. 0) to strain approximately 30% more than the entire sample (Area No. 1) when the shear sheets are employed (as determined from the isotropic test series data). The inner portion of the sample (Ring No. 2) strains approximately 20% less than Area No. 1. As also noted by Germaine (1982), the strain for Ring No. 1 approximately equals the average strain for the entire sample. For tests sheared via application of differential normal stress only, samples sheared in the isotropic plane reveal a tendency to strain less in the outer rings as compared with the entire sample.

That the overall variation of NRS with angle of shear for the anisotropic DSC tests is so similar to that of the isotropic tests indicates that the DSC does affect the strain behavior of the sample. It appears that shear sheets, when stressed, cause more strain in the outer ring of the sample than the interior. The effect of this feature is minimized,

however, by considering the strain in Area No. 2 (see Fig. 4.1), which disregards the exteriormost ring of elements, when evaluating stress-strain behavior.

The angular relationship between the major principal strain direction and the direction of the major principal stress is of particular interest. Most devices involve rigid loading boundaries and thus preclude measurement of this angle. Fig. 5.16 presents the results of both isotropic and anisotropic test series. (Figs. 4.18 and 5.4 plot Δ versus shear strain for the two series). It is evident from the isotropic test data that the DSC device causes a deviation of the strain direction from the σ_1 direction, Δ, reaching approximately 3° at angles of shear involving both shear sheets and pressure bags (see the dotted line in Fig. 5.16). The range of Δ for Ψ=45° to 90° is the mirror image of the range for Ψ=0° to 45°. This device induced deviation always results in the direction of strain being closer to the larger normal stress such that for δ<45° ε_1 trails σ_1 and for δ>45° ε_1 leads σ_1.

Bearing this device related tendency in mind, the anisotropic behavior is studied. As with the isotropic DSC test at Ψ=45°, the anisotropic test at δ=45° (DSC-5) is included, since its strain distribution behavior passed the standards established in Chapter 4.

Given the precision of the angular measurement technique (± 1°), the anisotropic tests which indicate a potential "real" deviation are in the range between δ=25° to 75°. "Real"

deviation is determined by subtracting the values of Δ obtained from the isotropic tests from those measured in the anisotropic tests. Both of these values are provided in Table 5.1 and differences are listed below. (All values of Δ were chosen at shear stress levels greater than the yield stress).

Test No.	δ (deg)	$\Delta_{measured} - \Delta_{isotropic}$ (deg)
DSC-1	0	- 0.4
DSC-3	0	- 0.4
DSC-15	20	+ 1.0
DSC-13	40	+ 4.0
DSC-5	45	+ 6.0
DSC-8	65	+ 1.9
DSC-11	75	+ 1.3
DSC-15	75	+ 2.8
DSC-2	90	- 1.1

In this region of intermediate values of δ, ε_1 appears to lead σ_1 by between 1 and 6 degrees, with the maximum "real" Δ occurring at $\delta=45°$, indicating a dependence of Δ on the angle of shear. Thus, all the anisotropic DSC tests, except those at $\delta=0°$ and 90°, exhibit directions of principal strain which tend slightly toward the weakest plane of the sample. The values of Δ for the tests wherein the direction of σ_1 coincided with an axis of symmetry of the sample (i.e., DSC-1, 3 and 2) are essentially equal to zero, within the accuracy of the measurement.

1	2		3	4	5	6	7	8			9	10		11								
TEST (BATCH)	THIXOTROPIC EFFECT t_s(days) Δq_y (ksc)	σ'_{pt}(ksc) $\Delta p'$(ksc)	w_i w_f (%)	δ (deg)	shear sheets/ prisms	u_i (ksc)	B ($\frac{\Delta u}{\Delta \sigma_c}$)	σ'_{vc} (ksc)	c_v ch (%)	log (t/t_p)	q_y/σ'_p (γ_y,%)	q_{yt}/σ'_p (γ_y,%)	$G_{y,t}$ / σ'_p	γ (%)	q_f/σ'_p	p'_f/σ'_p	$(\frac{\sigma_1}{\sigma_3})_t$	A_t	δ (deg) (measured values @ $q>q_y$)	δ_{device} (deg) (from isotropic tests)	REMARKS
DSC-1 (101)	29 0.018	1.23 0.033	40.6 39.4	0	no/no	-0.141	c:86.2 +: 83 +: --	0.252	0.11 0.15	1.15	0.202 (1.0)	0.190 (1.1)	3.20	2.1	0.237	0.318	6.85	0.357	-1.0	-0.6	
DSC-2 (101)	44 0.020	1.27 0.035	40.8 40.3	90	no/no	-0.077	c:99.8 +: 84 +: 87	0.251	0.32 0.15	1.05	0.116 (1.1)	0.093 (0.90)	0.55	9.5	0.138	0.188	6.52	0.725	-0.5	+0.6	
DSC-3 (102)	60 0.021	1.30 0.038	39.7 39.4	0	yes/no	-0.111	c:84.8 +: 69 +: 74	0.250	0.02 0.05	1.52	0.225 (1.0)	0.208 (1.1)	2.80	2.2	0.254	0.337	7.12	0.329	-1.0	-0.6	Sheared at δ=45° but membrane slipped, resheared at δ=0°
DSC-4 (102)	71 0.022	1.32 0.039	39.8 39.8	45	yes/no	-0.093	c:92.4 +:84 +:84	0.253	- -	2.22	- -	- -	--	--	--	--	--	--	--	--	Lost sides to progressive failure (no prisms)
DSC-5 (103)	34 0.018	1.24 0.033	40.1 40.0	45	yes/yes	-0.070	c:98.8 +: 85 +: 88	0.252	0.27 0.24	1.65	0.156 (1.2)	- -	--	--	--	--	--	--	+6.0	0	Anomalous pore pressure behavior
DSC-8 (104)	167 0.046	1.55 0.075	40.6 40.4	65	yes/yes	-0.145	c:84.5 +:89 +:94	0.250	0.51 0.46	2.30	0.144 (0.60)	0.112 (1.1)	0.79	6.5	0.156	0.223	5.66	0.587	+5.5	+3.6	
DSC-10 (105)	207 0.054	1.66 0.094	41.1 40.9	20	yes/yes	-0.118	c:90.2 +:88 +:88	0.251	1.01 0.97	1.92	- -	- -	--	--	--	--	--	--	--	--	Lost two corners to progressive yield
DSC-11 (106)	71 0.022	1.32 0.039	40.9 40.6	75	yes/yes	-0.103	c:96.7 +:88 +:88	0.251	0.34 0.27	1.80	0.118 (1.5)	0.091 (0.95)	0.54	14.1	0.147	0.224	4.82	0.588	+3.5	+2.2	
DSC-13 (107)	39 0.019	1.26 0.034	40.9 40.6	40	yes/yes	-0.094	c:96.9 +:90.1 +:91	0.250	0.34 0.27	1.94	0.160 (1.0)	0.144 (1.1)	1.48	3.5	0.189	0.260	6.32	0.474	+1.0	-3.0	Reconsolidated due to bag leak
DSC-15 (109)	92 0.023	1.34 0.042	41.6 41.9	20	yes/yes	-0.130	c:85.2 +:90 +:91	0.252	0.08 0.08	1.63	0.188 (1.0)	0.166 (1.0)	1.95	3.6	0.219	0.307	5.98	0.370	-2.0	-3.0	Deleted corners with prisms, from strain calculations
DSC-16 (110)	105 0.027	1.39 0.043	40.3 40.0	75	yes/yes	-0.152	c:76.9 +:83 +:86	0.250	-0.16 -0.16	2.09	0.122 (0.80)	0.108 (1.1)	0.55	13.0	0.160	0.234	5.32	0.550	+5.0	+2.2	New chevron-shaped prisms

1 Test designation and Batch No.
2 Thix. effect based on t_s and Chap.3
3 Initial and Final water contents
4 Anisotropic angle of shear
5 Physical aspects of DSC test
6 Initial pore pressure
7 Skempton's B parameter, where c= consol. inc. ($\Delta\sigma_c$=0.22 ksc), +=($\Delta\sigma_c$= -0.10 ksc) and +=($\Delta\sigma_c$= +0.10 ksc)
8 Consolidation Data
9 Uncorrected yield data
10 Yield results corrected for thixotropy
11 Shear results corrected for thixotropy

Table 5.1: Summary of Anisotropic DSC Test Data for Resedimented BBC (OCR=4)

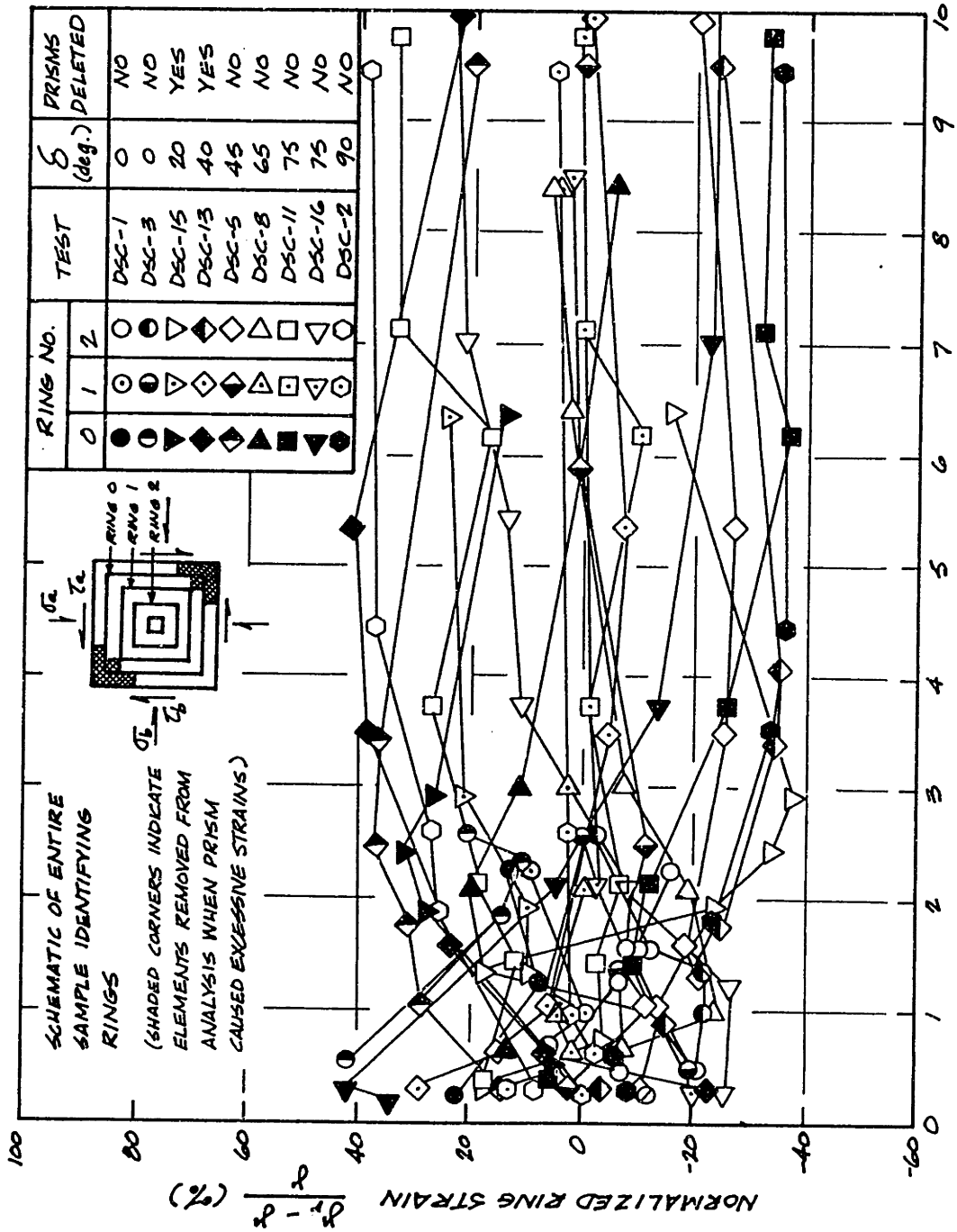

Figure 5.1: Variation of Maximum Shear Strain Distribution (NRS) with Maximum Shear Strain from Entire Sample from Anisotropic DSC Tests on Resedi-mented BBC (OCR=4).

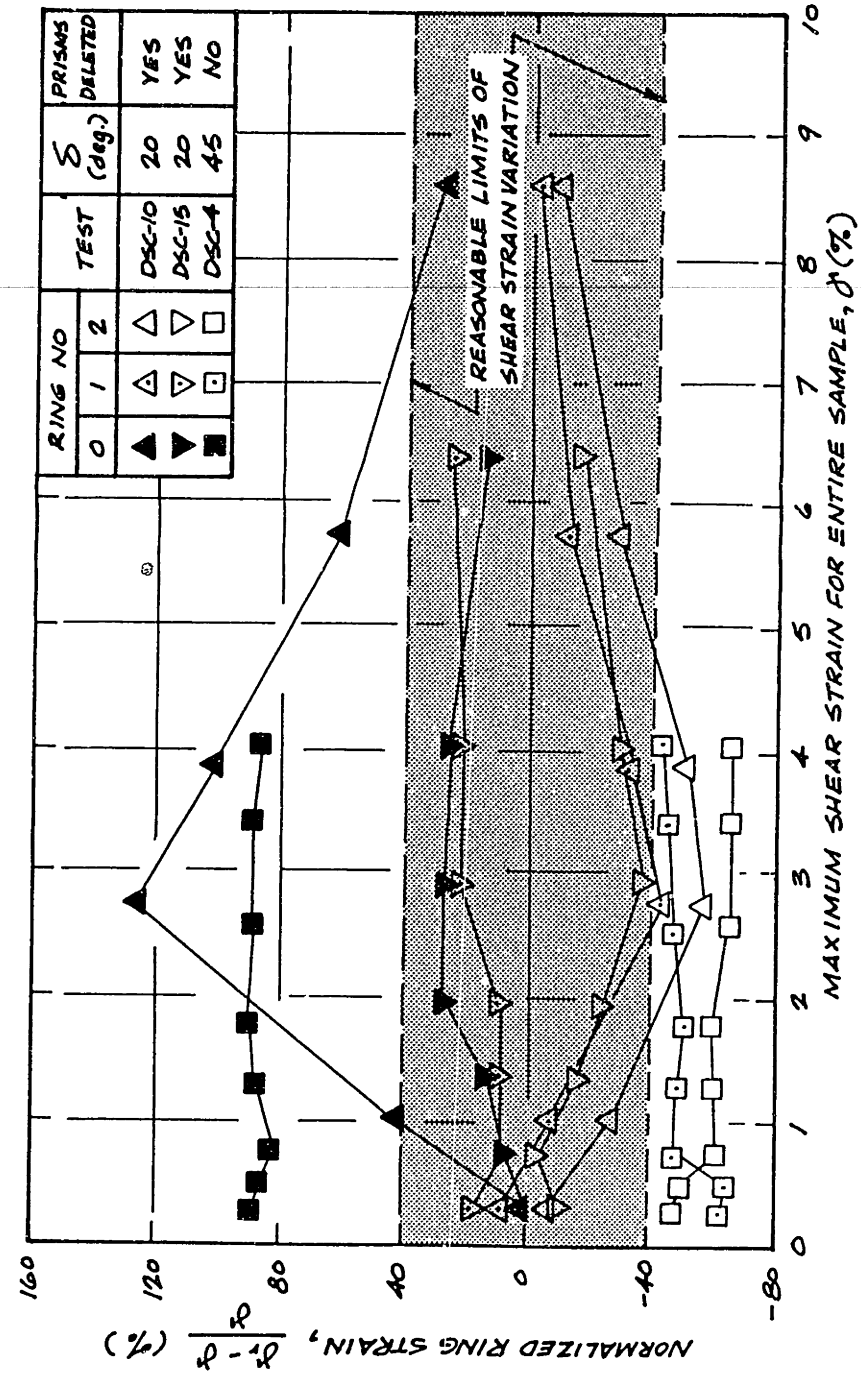

Figure 5.2: Variation of Maximum Shear Strain Distribution (NRS) with Maximum Shear Strain from Entire Sample for Anisotropic DSC Tests on Resedi-mented BBC (OCR=4).

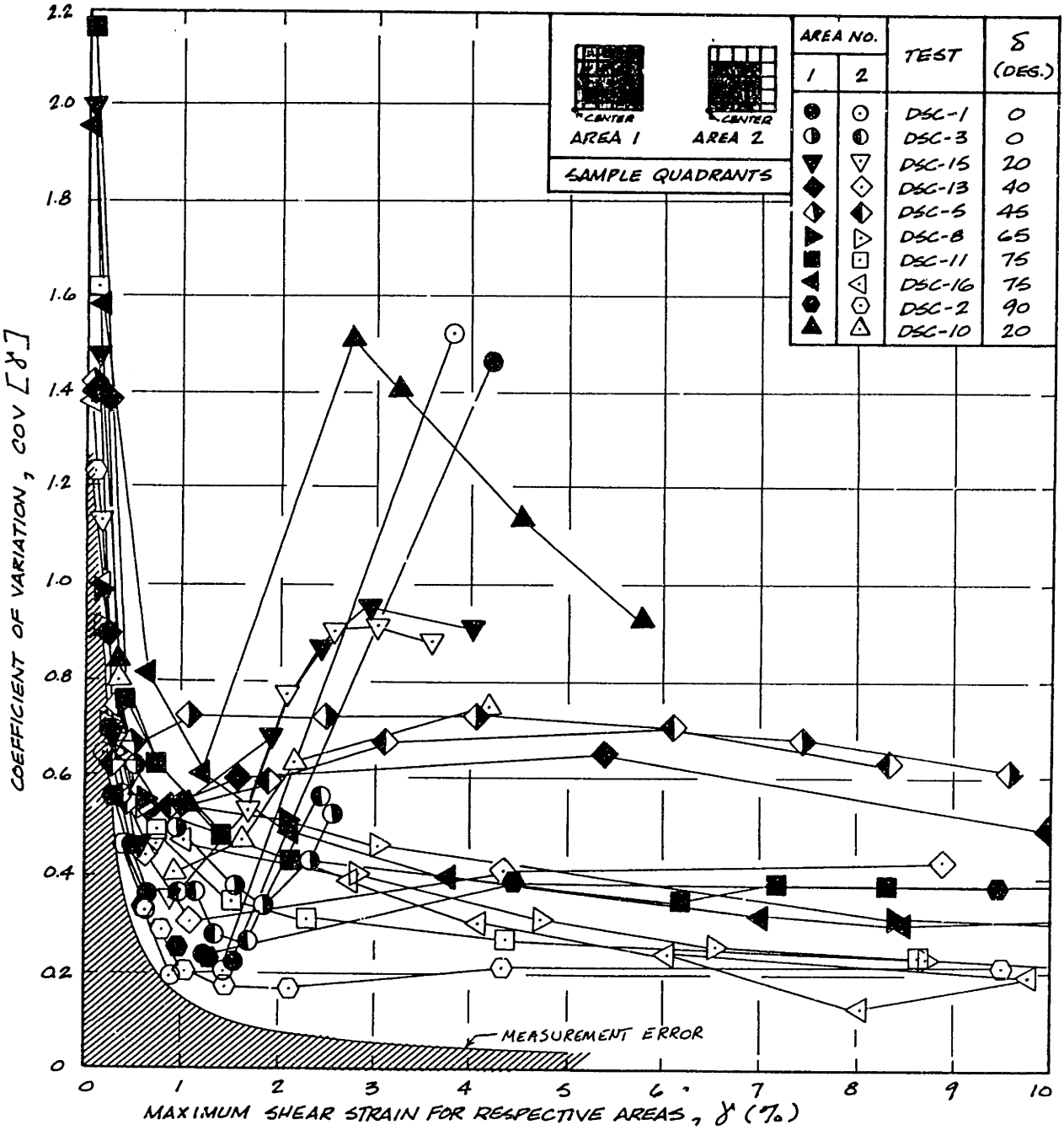

Figure 5.3: Variation of COV[γ] With Maximum Shear Strain from Anisotropic DSC Tests on Resedimented BBC (OCR=4).

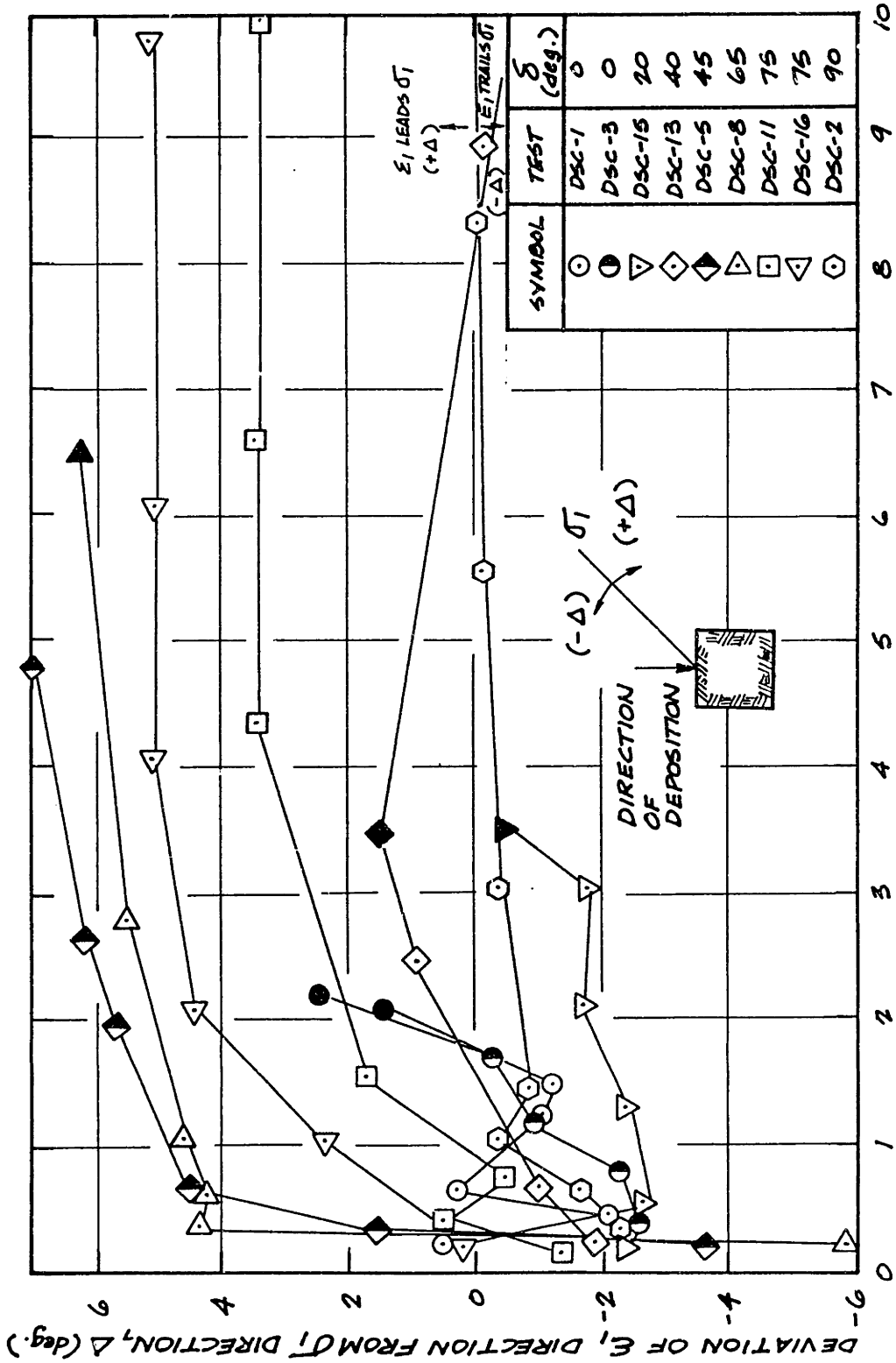

Figure 5.4: Variation of Δ With Maximum Shear Strain from Anisotropic DSC Tests on Resedimented BBC (OCR=4).

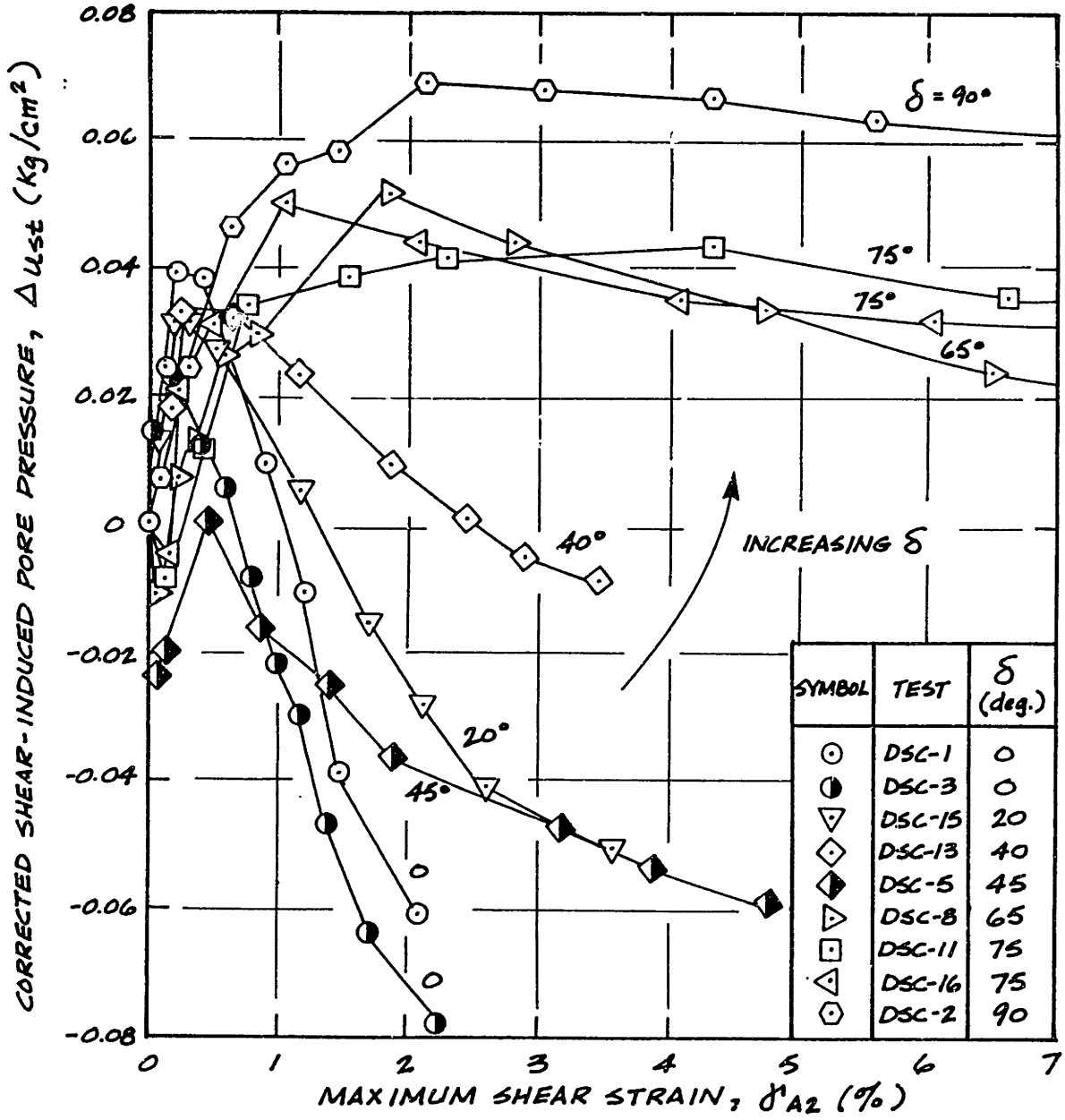

Figure 5.5: Shear-Induced Pore Pressure (Corrected for Storage Time) vs. Maximum Shear Strain from Anisotropic DSC Tests on Resedimented BBC (OCR=4).

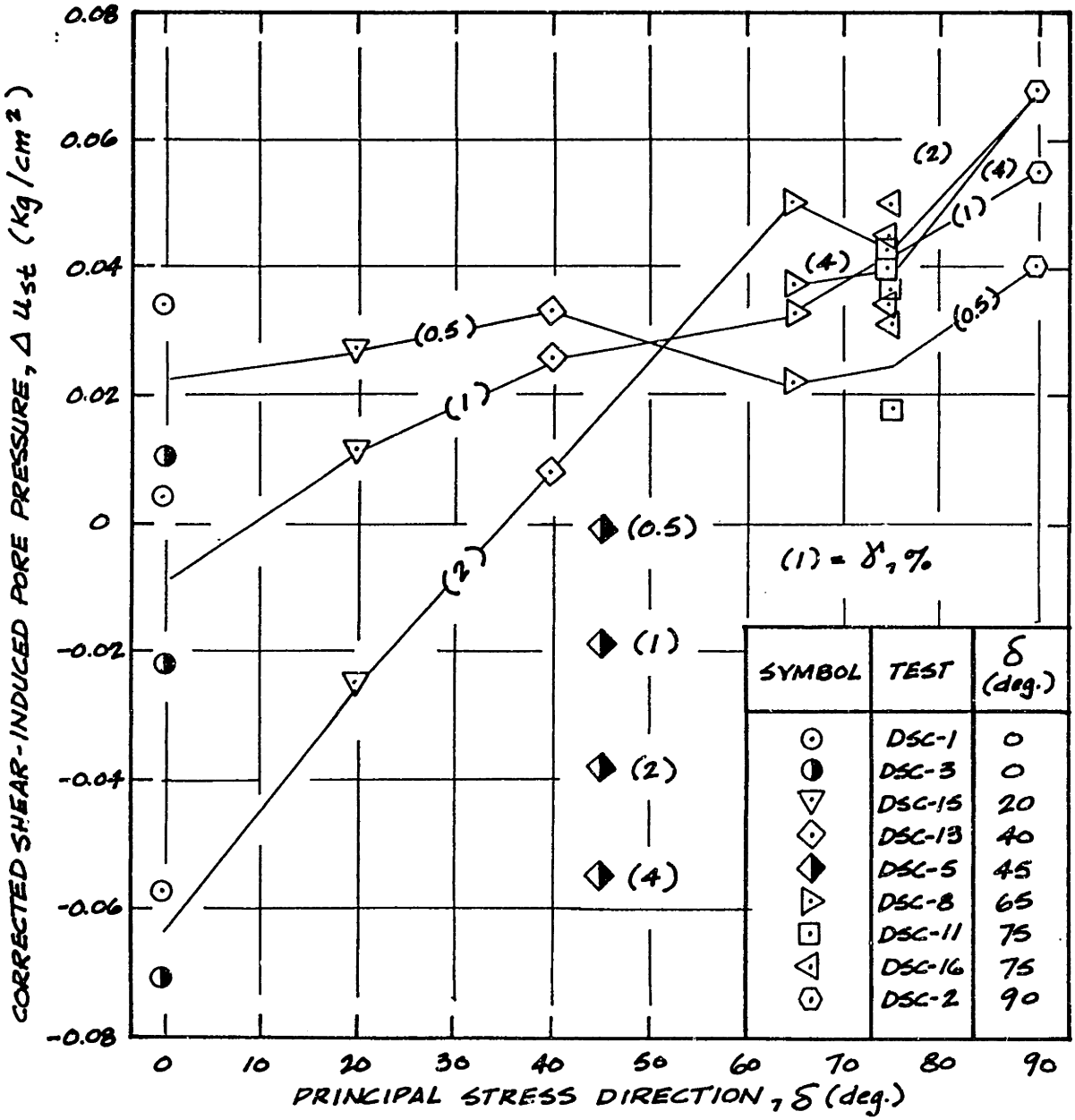

Figure 5.6: Effect of Angle of Shear on Corrected Shear-Induced Pore Pressure from Anisotropic DSC Tests on Resedimented BBC (OCR=4).

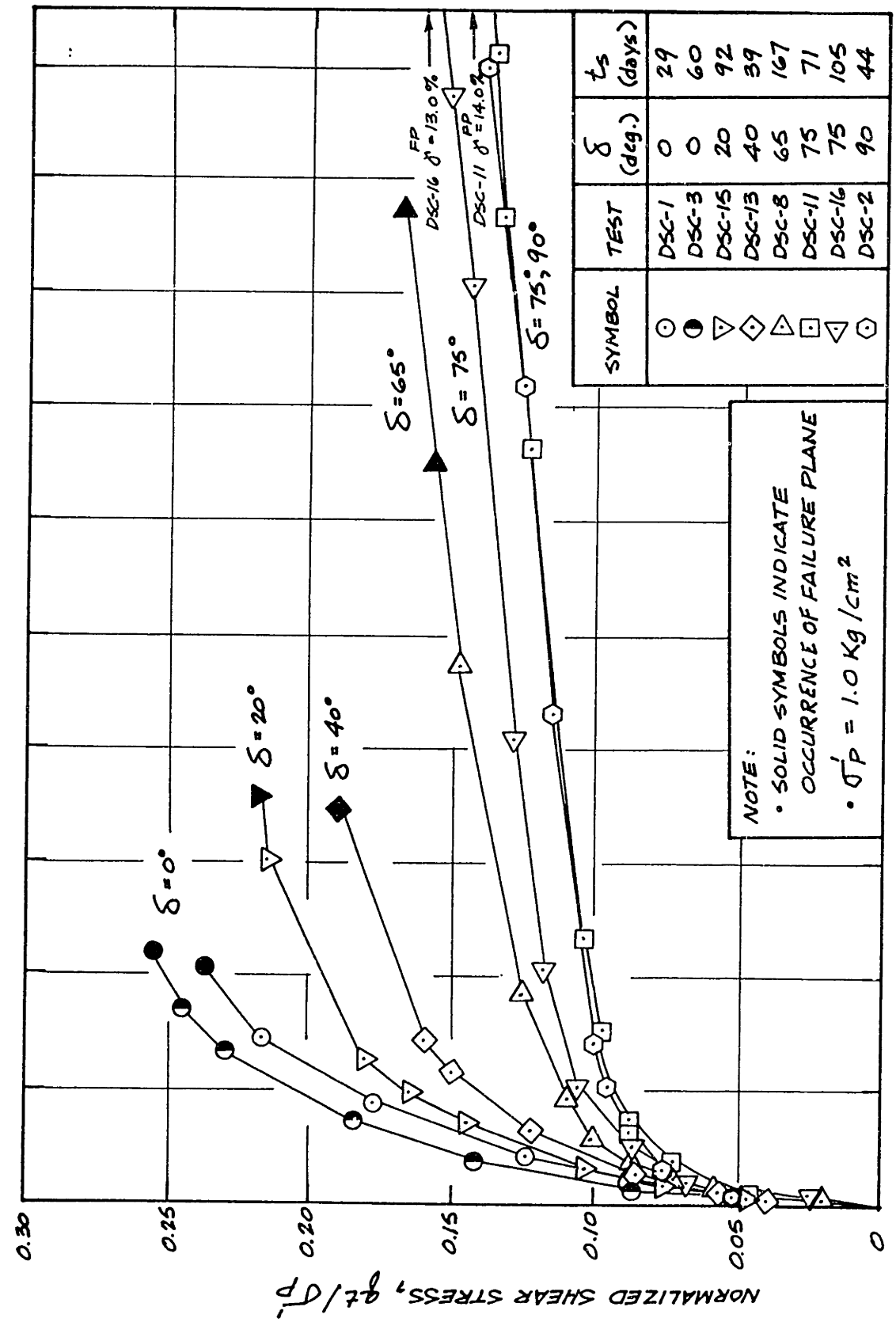

Figure 5.7: Stress-Strain Curves from Anisotropic DSC Tests on Resedimented BBC (OCR=4); (Corrected for Thixotropic Effects).

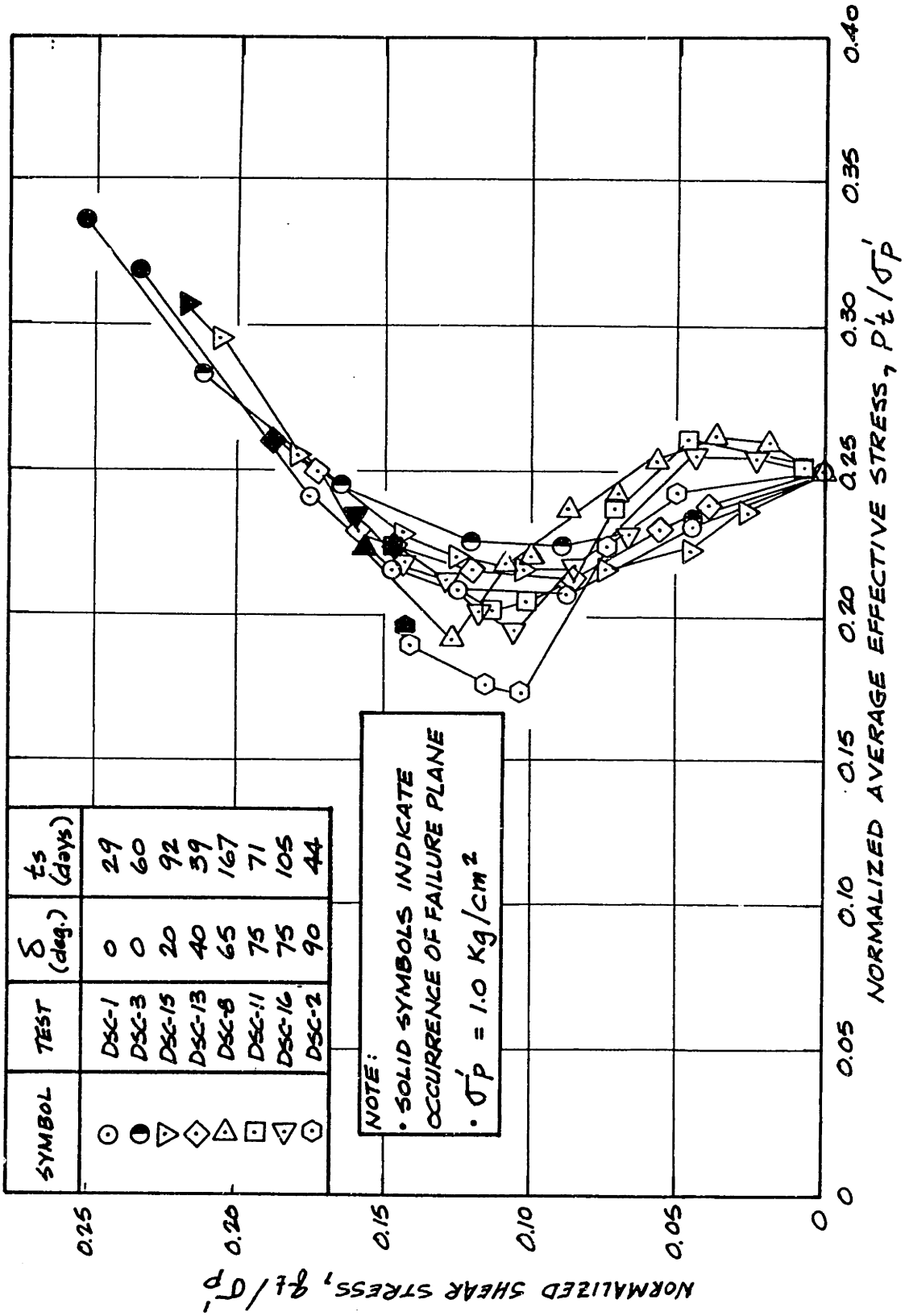

Figure 5.8: Normalized Effective Stress Paths from Anisotropic DSC Tests on Resedimented BBC (OCR=4); (Corrected for Thixotropic Effects).

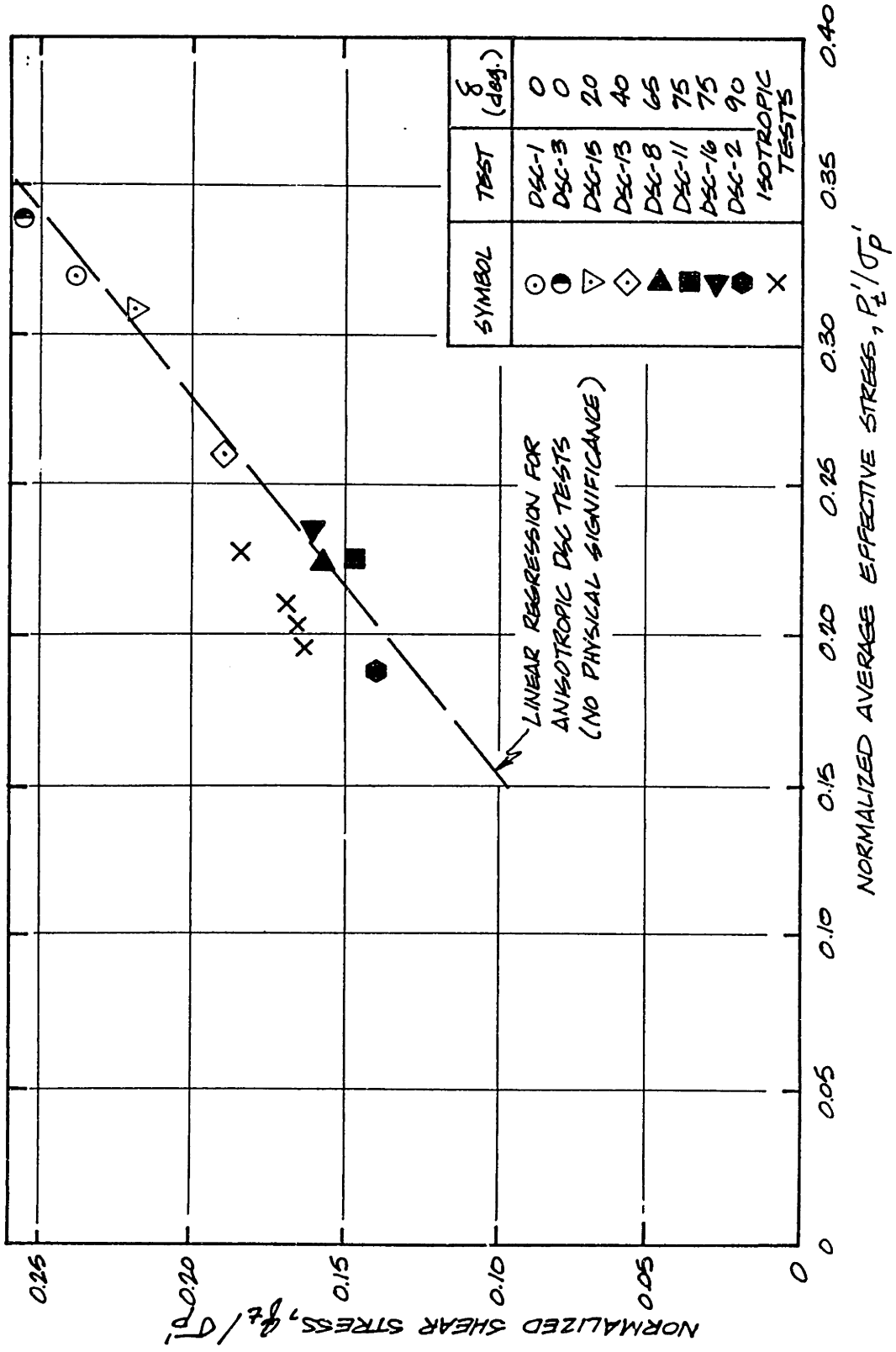

Figure 5.9: Effect of Anisotropy on Effective Stress Envelope.

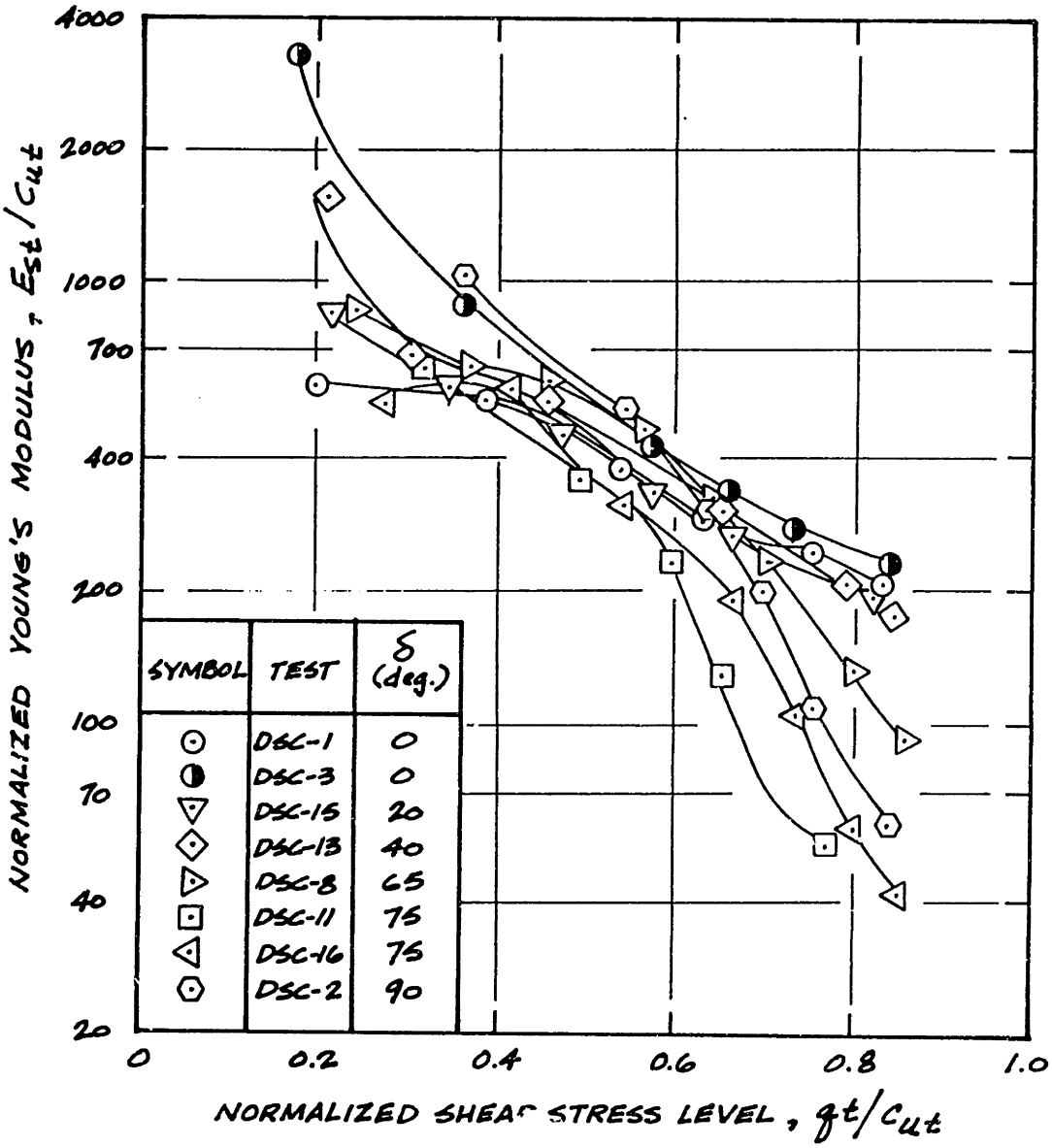

Figure 5.10:Variation of Normalized Young's Modulus with Shear Stress Level from Anisotropic DSC Tests on Resedimented BBC (OCR=4).

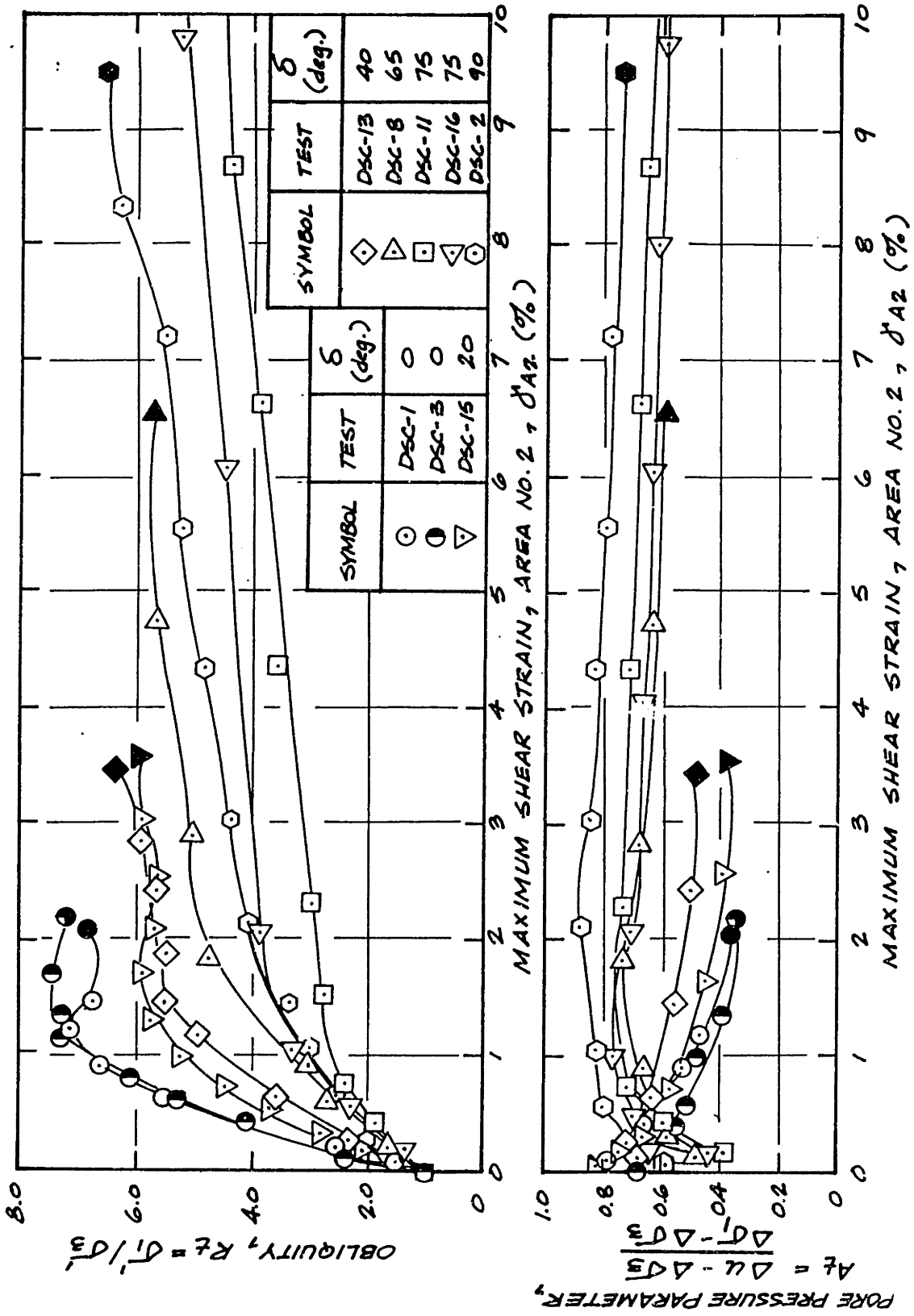

Figure 5.11: Obliquity and Pore Pressure Parameter vs. Maximum Shear Strain from Anisotropic DSC Tests on Resedimented BBC (OCR=4).

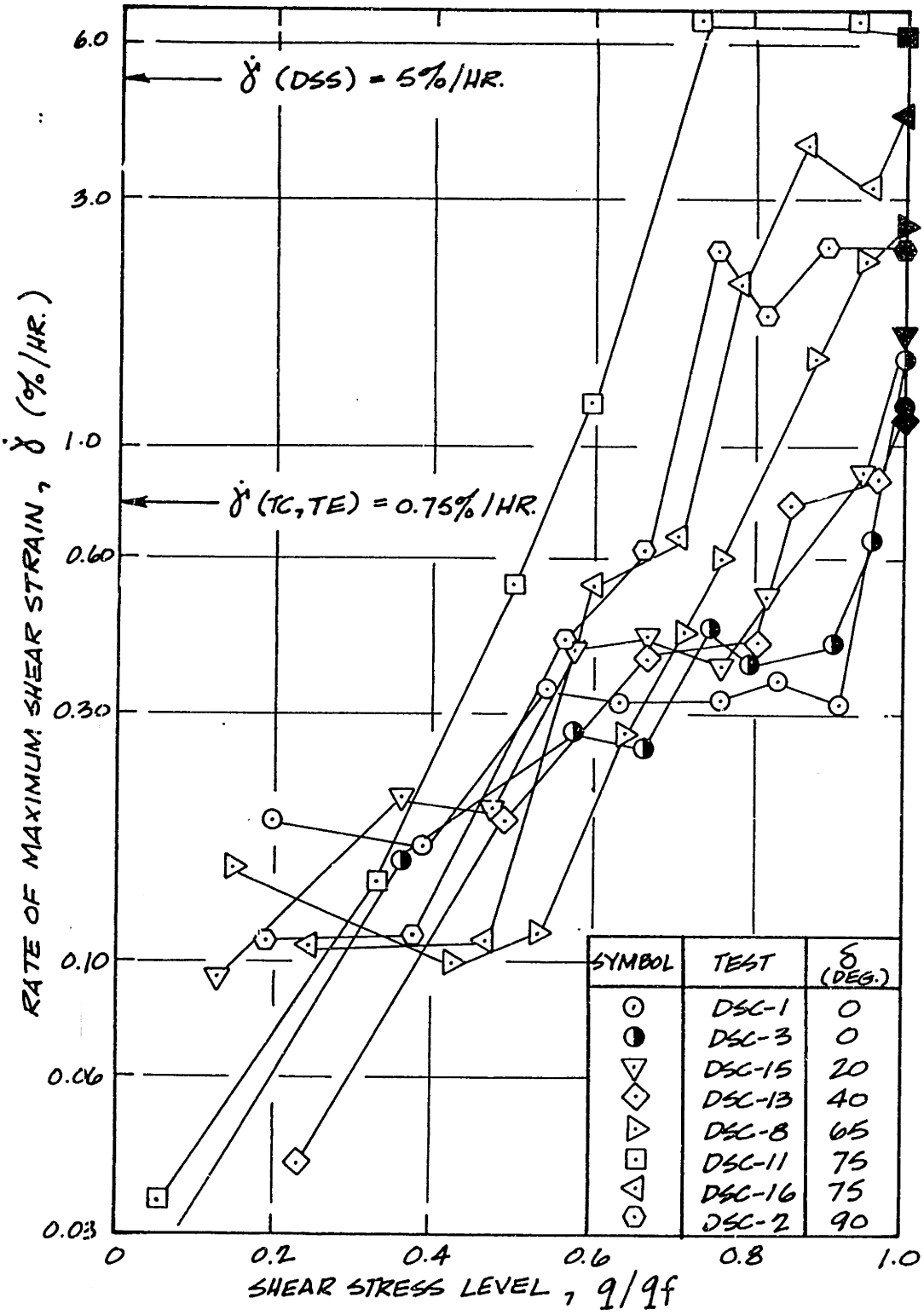

Figure 5.12: Rate of Maximum Shear Strain vs. Shear Stress Level for Anisotropic DSC Tests on Resedimented BBC (OCR=4).

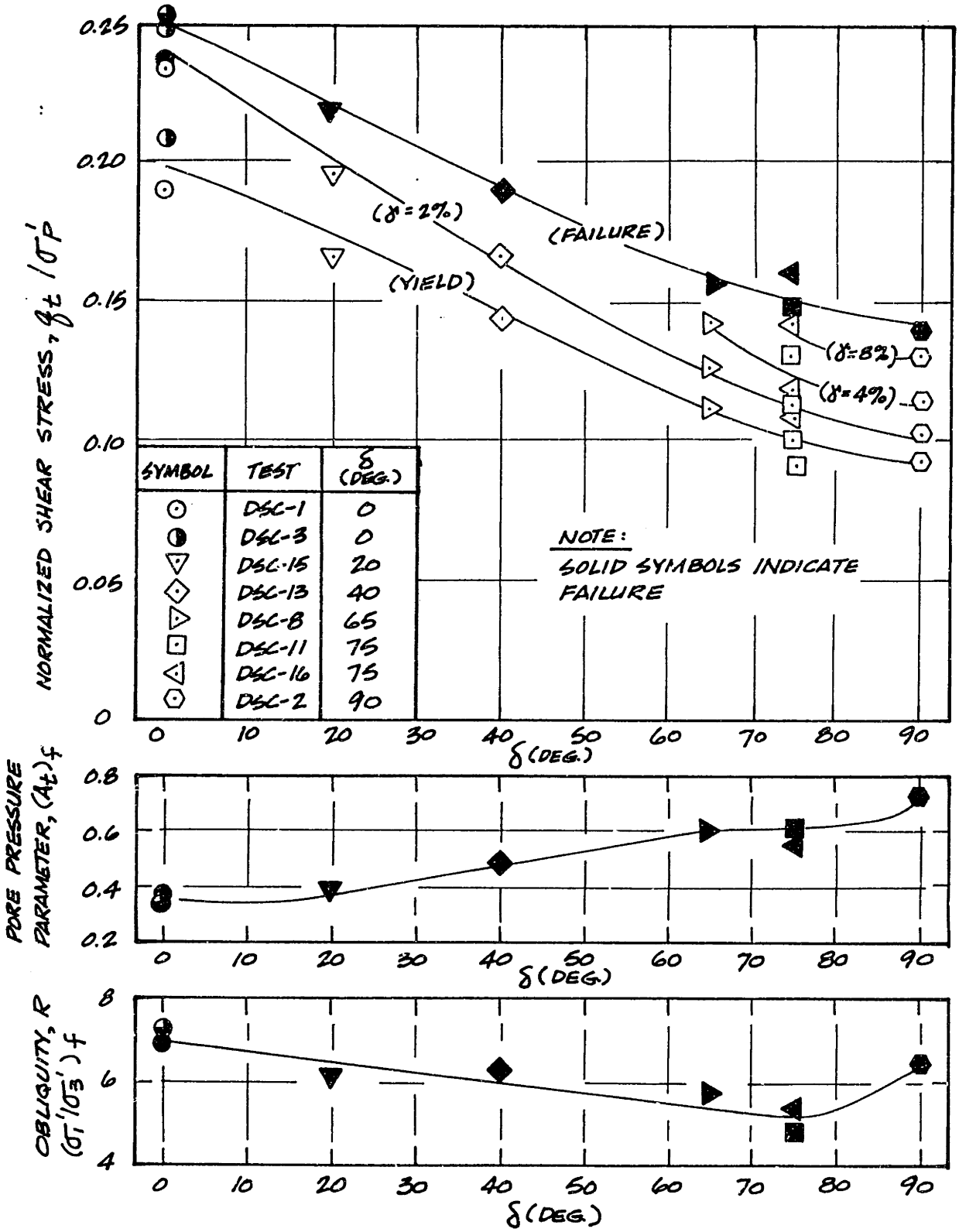

Figure 5.13: Variation in Undrained Shear Strength Parameters with δ from DSC Tests on Resedimented BBC (OCR=4).

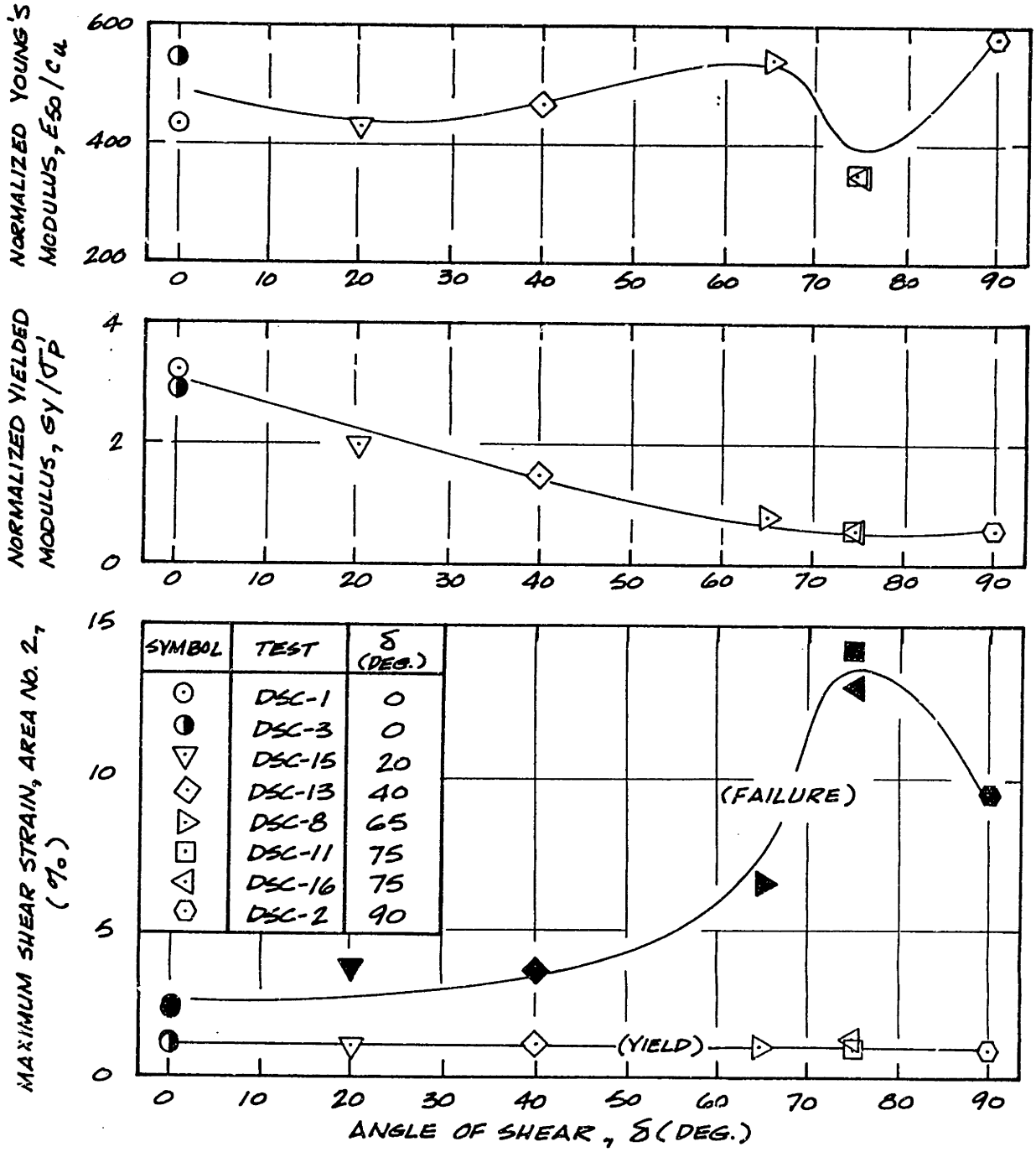

Figure 5.14: Variation in Normalized Moduli and Shear Strain at Yield and Failure with δ from DSC Tests on Resedimented BBC (OCR=4).

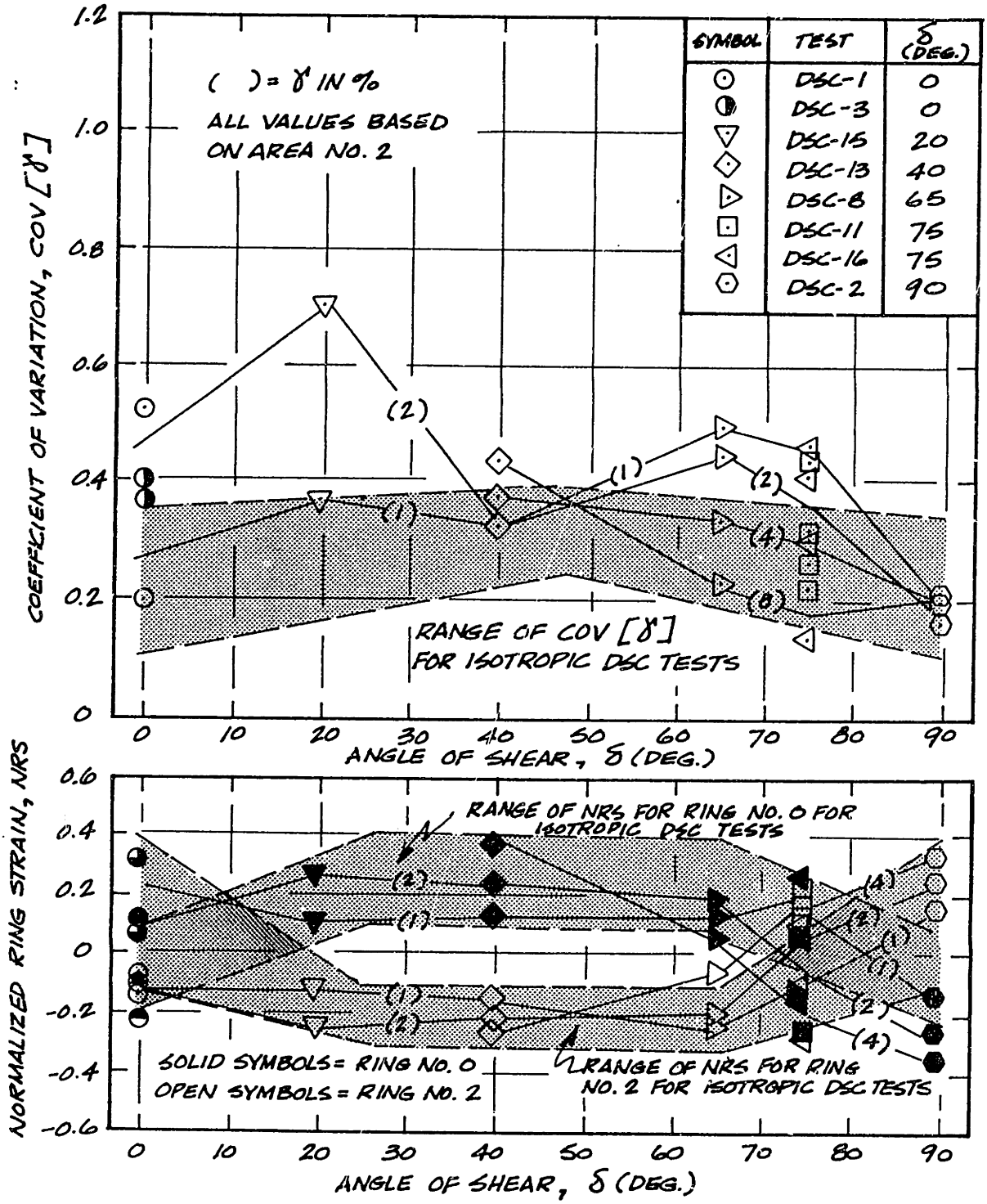

Figure 5.15: Effect of Angle of Shear on Coefficient of Variation of γ and Normalized Ring Strain from Anisotropic DSC Tests on Resedimented BBC (OCR=4).

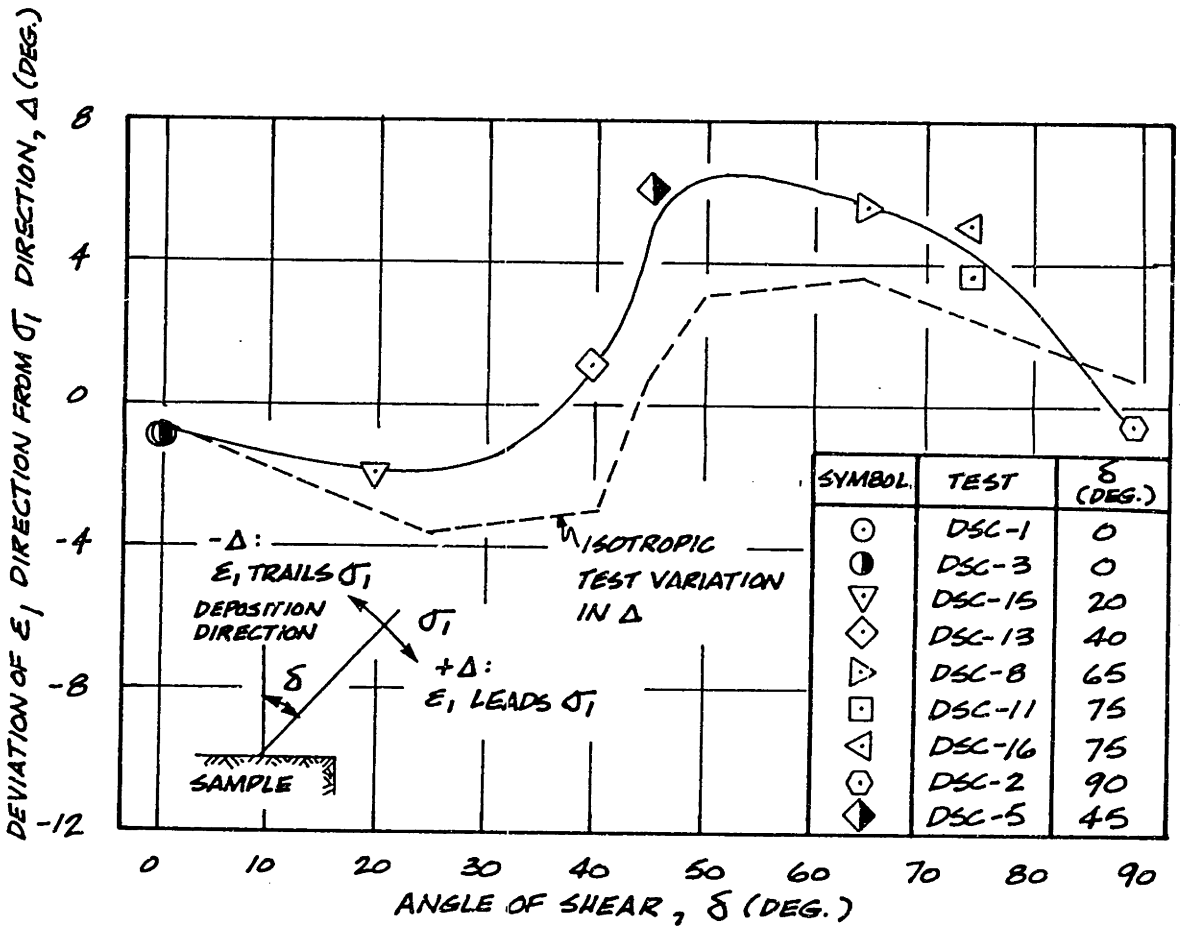

Figure 5.16: Deviation of the Direction of Principal Strain from that of Principal Stress vs. Angle of Shear from DSC Tests on Resedimented BBC (OCR=4).

CHAPTER 6

COMPARISON OF DSC DATA WITH RESULTS FROM OTHER TEST DEVICES

6.1 INTRODUCTION

It is of interest to compare results using a new device with behavior measured in more conventional apparatuses. Resedimented BBC has been studied at length under a variety of test conditions over the years (e.g., Ladd and Varallyay, 1965; Ladd et al., 1971; Ladd and Edgers, 1972; Germaine, 1982; Bensari, 1984). This research has contributed additional consolidation data plus triaxial and Direct Simple Shear tests on resedimented BBC, especially at OCR's of 4 and 1.

A number of factors must be borne in mind as comparisons at various angles of shear in various devices are made. In addition to the direction of major principal stress during shear, undrained shear behavior is affected by the relative intermediate stress ratio, b ($= \frac{(\sigma_2 - \sigma_3)}{(\sigma_1 - \sigma_3)}$), the rate of strain, the boundary conditions during shear (i.e., stress vs. strain control and flexible vs rigid load application elements) and the preshear consolidation history. The purpose of Chapter 6 is to compare the plane strain stress-controlled DSC results at appropriate angles of shear with triaxial, Direct Simple Shear and MIT plane strain results in order to help identify behavioral aspects due to factors other than the direction of σ_1 during shear. The DSC as a testing device has already been

proved reliable in Chapter 4. (Additional evidence with regard to the accuracy of DSC produced anisotropic data can only come from data produced under similar conditions in the torsional shear Hollow Cylinder Apparatus as discussed in Chapter 2). Therefore, it is emphasized that this chapter neither proves nor disproves the validity of the DSC results but rather further edifies the reader on the differences in behavior one might expect due to the effects of σ_2, boundary conditions, consolidation histories, etc. common to the devices in question.

Because the initial phases of DSC testing on saturated clay necessitated Recompression as the consolidation technique, a section of this chapter is devoted to clarifying differences in behavior due to varying the approach used to attain the preshear stress state. The effect of a consolidation method commonly adopted to reduce sampling disturbance, the SHANSEP method, is compared to that of the Recompression technique on several clay materials.

6.2 CONSOLIDATION STRESS HISTORY: RECOMPRESSION VS. SHANSEP

Since the method by which the DSC samples are prepared and placed in the test device (as described in Germaine, 1982) simulates "perfect sampling" (Ladd and Lambe, 1963) without any effects due to the removal of shear stress ($K_o \cong 1.0$), recompression to the desired stresses is the best method of consolidation. However, the "perfect sampling" achieved by the techniques utilized for this research is <u>not</u> generally

achievable when sampling from in situ conditions. Not only is release of shear stresses involved (Ladd et al., 1977) but the material usually experiences significant disturbance due to sampling even by fixed piston thin walled samplers. Baligh (1985) has shown analytically (via the Strain Path Method) that the material, even in the center of a thin-walled (B/t=48) sampling tube, may undergo a significant amount of strain ($\varepsilon_a \approx$ 0.5%), first in compression then in extension, in relation to the amount of strain necessary to cause failure in the respective modes. The lower the OCR, the more serious is the effect due to the lower strains at peak shear stress.

Because of the excessive disturbance commonly associated with sampling, Ladd and Foott (1974) suggest the SHANSEP (an acronym for Stress History And Normalized Soil Engineering Properties) method of testing. In order to use this method several qualifications must be met:

1) the soil must be proven to exhibit normalizable behavior in the stress range of interest;
2) one must be able to establish a well-defined stress history; and
3) The in situ overconsolidated behavior should be similar to that produced via mechanical overconsolidation used by SHANSEP to obtain normalized properties versus OCR.

Removal of the effects of sample disturbance as well as establishment of a known stress history are among the advantages of the SHANSEP method of consolidation. However,

laboratory investigations involving comparison of behavior from SHANSEP testing with that following Recompression demonstrates that there are consistent differences (Ladd and Edgers, 1972; Sambhandharaksa, 1977; and Gens, 1982).

The subject of the probable causes of these differences is broached following a detailed discussion of the effect of the method of consolidation on shear behavior. First it should be noted that Recompression can be accomplished in one of two ways:

1) The desired stress state is achieved directly from the sampled state using the standard approach recommended by Bjerrum (1973) wherein the sample is consolidated in increments to the estimated in situ state of stress.

2) The stress state of interest is assessed with regard to the desired overconsolidation ratio. First, the sample is consolidated sufficiently beyond its preconsolidation stress, σ'_p, to attain virgin consolidation. The sample is then unloaded in the device to an OCR approximately equal to that existing in the sample after sampling (i.e., OCR $\simeq \sigma'_p/\sigma'_s$ where σ'_s is equal to the absolute value of the initial pore pressure). Following unloading, the sample is reloaded to a vertical stress compatible with the OCR desired ($\sigma'_{vc} = \frac{\sigma'_{vm}}{OCR}$).

Data pertaining to the first type of Recompression is discussed first. Sambhandharaksa (1977) presents data from

SHANSEP and Recompression type triaxial compression and extension tests from block samples of varved clays. Varved clay was sampled from East Windsor, Connecticut where it existed at an in situ OCR equal to about 4. Assuming a $K_o \simeq 1$, recompression to σ'_{vo} was accomplished by isotropic consolidation. Stress-strain and effective stress behavior from Samdhandharaksa's laboratory investigation are presented in normalized fashion in Figure 6.1.

The type of Recompression used by Sambhandharaksa (i.e., consolidation to σ'_{vo} directly from the sampled state) is that utilized by this research in the performance of all Directional Shear Cell and Recompression type triaxial and DSS tests on resedimented BBC. Although the material is significantly different (varved clay vs. homogeneous silty clay) general trends regarding the effect of the method of consolidation are likely to be applicable.

From Fig. 6.1, the following general trends reveal themselves:

- The normalized shear stress at failure, q/σ'_p (from Recompression tests) is approximately 6% less than its analogue, q/σ'_{vm}, from the SHANSEP compression test and about 17% less than q/σ'_{vm} for the test in the extension mode. A portion of the very large reduction in strength under $\delta=90°$ conditions might be attributed to separation between the varves due to slight disturbance effects in the Recompression test. There is a possibility, however, that the ratio between SHANSEP and

Recompression peak stresses is larger for TE conditions than for TC conditions partially because of the difference in the directions of the final consolidation stresses for the two methods.

- The axial strain at failure for Recompression type tests is about half that for the SHANSEP type tests, both in compression and extension.
- The Recompression type tests have lower effective stresses than the SHANSEP tests. Similarly, Recompression values for the A parameter remain significantly greater than those from SHANSEP type tests as the sample continues to strain.
- Because of greater pore pressures for the Recompression tests, greater values of obliquity are achieved during shear than is the case for the SHANSEP tests. However, Recompression and SHANSEP type tests approach similar stress ratios, q/p', at large strains as can be seen in the stress path presented in Fig. 6.1.

Sambhandharaksa ran a similar series of tests at OCR = 2. In this series, Recompression type triaxial compression tests on varved clay were approximately 9% stronger at peak shear stress than the SHANSEP $\overline{CK_oU}$(C) tests. In the extension mode at OCR = 2, the Recompression test was 5% weaker than the SHANSEP test. As with the OCR = 4 tests, the Recompression tests have lower average effective stresses during shear than the SHANSEP tests, except in the compression case where the SHANSEP test experienced a rapid increase in A following peak stress,

causing the SHANSEP stress path to cross that of the Recompression test.

Gens (1982) performed a limited investigation into the effect of Recompression vs. SHANSEP on the undrained shear behavior of reconstituted samples of Lower Cromer Till, LCT, (I_p=12%, w_L=25%, ϕ'=30°) which is classified as a sandy clay. The type of Recompression is similar to that used by Sambhandharaksa (1977) and this research, i.e., that involving direct reconsolidation to the desired stress state without exceeding σ'_p. Since Gens ran tests on laboratory prepared batches of LCT, sampling disturbances were effectively minimized. In an effort to completely characterize the LCT material for the development of a rational framework to model behavior, a portion of the testing program involved the study of isotropically reconstituted material. As it was this isotropic material on which the Recompression vs. SHANSEP study was performed, there was no removal of shear stresses to further disturb the sample. The batches were sampled at OCR=4 with a final batch consolidation stress of 0.4 ksc.

The results of Gens' work at OCR=4 are presented in Fig. 6.2. The Recompression $\overline{CIU}$(C) stress-strain curve follows that from SHANSEP test at very low strains but yields at a lower stress level. At larger axial strains the Recompression stress-strain curve is parallel to that for the SHANSEP test. Although the Recompression stress at failure is about 3% less than the SHANSEP $\overline{CIU}$(C) strength (similar to the case with the East Windsor Varved Clay in Fig. 6.1 (Sambhandharaksa , 1977)),

the isotropic LCT Recompression test never behaves stiffer than the SHANSEP test as is the case with the varved clay.

In addition, the strains at failure (i.e., peak shear stress) for both LCT $\overline{CIU}$(C) tests are approximately equal whereas the varved clays consolidated in the Recompression mode failed at substantially lower strains than the SHANSEP tests. Since the varved clays were block samples of geologically sedimented material, the higher initial stiffness of the Recompression samples may be due to aging, thixotropy and/or cementation.

The isotropic LCT results demonstrate that Recompression as a method of consolidation leads to much lower effective stresses during shear than its SHANSEP counterpart - as is the case with the varved clays. Again, however, a difference exists between the varved clays and LCT in that the latter material exhibits values of the pore pressure parameter, A, and obliquity, R, at failure which seem relatively unaffected by the consolidation technique (see stress path in Fig. 6.2). These features are due to both the smaller difference in peak shear stresses as well as the very large strain required to reach the peak strength.

Gens (1982) also investigated the effect of Recompression as a consolidation technique on isotropically reconstituted LCT at OCR=2. Sambhandharaksa's (1977) results on varved clay at OCR=2 showed the Recompression test to be slightly stronger than the SHANSEP test. Gens' results showed the Recompression test to be slightly weaker than the SHANSEP test. Again, the

effective stresses of the Recompression samples were much lower during shear than the SHANSEP samples.

A limited amount of data regarding the effect of the method of consolidation on undrained shear behavior in the DSS are available on resedimented Boston Blue Clay at OCR=4. These data, one set from Ladd and Edgers (1972) and one set from this research, briefly presented in Chapter 3 to aid in assessment of Direct Simple Shear tests using pins (Section 3.2.2), are presented in Figs. 3.25 and 3.28. One of the Recompression type tests (from Ladd and Edgers, 1972, without pins) involved the second type of Recompression, i.e., that entailing K_o-consolidation in the device beyond σ'_p, unloading to an OCR=8 and subsequent reloading to a lower OCR (OCR=4 in this case). Use of this type of recompression essentially precludes any disturbance prior to shear. The other two Recompression DSS tests (DSS-14 and 15, from this research) involved direct recompression to 0.25 ksc.

As can be seen in Fig. 3.28 and as mentioned by Germaine (1982), the SHANSEP type OCR=4 DSS tests performed in this research were, on the average, about 8% stronger than those presented by Ladd and Edgers (1972), even though the material in both cases was resedimented BBC. (Normally consolidated tests, however, from both test programs yielded essentially identical results as can be seen in Figs. 3.29 and 3.30). In view of this discrepancy, the first set of comparisons are restricted to the tests from Ladd and Edgers.

The salient features of these data pertaining to the

comparison of Recompression vs. SHANSEP as a consolidation technique at OCR=4 are as follows:

- Although the SHANSEP test stress-strain curves of Fig. 3.28 demonstrate significant scatter, they consistently indicate greater strength than the Recompression test. On the average, this increase in the normalized maximum horizontal shear stress is approximately 14%.
- The shear strain at the maximum horizontal shear stress, τ_{hmax}, appears to be unaffected by the method of consolidation. The Recompression stress-strain curve follows the SHANSEP curve at very low strains and after yielding earlier than the SHANSEP curves, imitates the general shape of those curves (Fig. 3.28).
- Again, the effective stresses maintained by the Recompression test are much lower than those of the SHANSEP tests. Given the scatter of the SHANSEP tests, it can only be hypothesized that the Recompression test approaches the SHANSEP DSS normalized τ_h/σ'_{vm} vs. σ'_v/σ'_{vm} envelope at high strains.

Ladd and Edgers (1972) also performed a DSS test using the second type of recompression for consolidation to OCR=2. Comparison of these data with the results from SHANSEP DSS tests at OCR=2 show the same SHANSEP vs. Recompression ratio of strength, $(\frac{s_u(\text{SHANSEP})}{s_u(\text{Recomp.})} = 1.14)$, unlike the varved clay and the LCT data which showed a decrease in this ratio with decreasing OCR.

The DSS SHANSEP vs. Recompression data from this research involve use of the pins discussed in Chapter 3 to help prevent

slippage. Since there was substantial displacement of soil when inserting the pins and since the Recompression tests showed remarkable similarity with the SHANSEP τ_h vs γ curves (Fig. 3.25), it was concluded that the pins removed the strengthening effects of thixotropy (note that the Recompression tests in Fig. 3.25 were normalized to σ'_p=1.0 ksc, and not the $\sigma'_p(t)$ corresponding to the age of the sample). The comparisons are as follows:

- The Recompression stress-strain curve compared well with the SHANSEP curve.
- The Recompression tests had much lower effective stresses than the SHANSEP tests -even lower than those exhibited by the Ladd & Edgers (1972) series of tests.

Table 6.1 summarizes general trends with regard to the effect of the method of consolidation on the undrained shear behavior of a variety of materials under three different shearing conditions. Although the data are scant, the consistent appearance of a number of features gives one cause to expect such differences when comparing results from tests consolidated using the Recompression method with data from tests following SHANSEP precepts. The most prominent features (at OCR=4) are:

1) that the SHANSEP tests are from 3-21% stronger in undrained shear than the Recompression tests; the percentage seems to increase with increasing angle of shear, δ (although the data base includes varved clay which could be demonstrating anisotropic disturbance

effects);

2) that the SHANSEP tests have much higher effective stresses during shear than the Recompression tests, regardless of the angle of shear; and
3) that the failure envelope approached is relatively unaffected by the consolidation technique, i.e., at a given shear stress level, R from the Recompression tests is greater than that of SHANSEP tests but when q_f is reached the difference decreases and continues to decrease as larger strains are reached.

An important phenomenon to note is that the only Recompression data indicating stiffer response at low strains than SHANSEP samples are those associated with the block samples of varved clay from Sambhandharaksa (1977) in both triaxial compression and extension. The other two test series (Gens, 1982 and Ladd and Edgers, 1972) investigated laboratory reconsolidated samples.

In view of the above discussion on the effects to be expected when comparing SHANSEP tests with Recompression tests, the triaxial compression data on resedimented BBC generated by this research can be studied. However, due, to the thixotropic strengthening effect described in Chapter 3, all the Recompression tests presented in Figs. 6.3 to 6.5 have been subjected to the corrections developed in Chapter 3 (Sections 3.2.3 and 3.2.4). Since these corrections are related to the SHANSEP type triaxial compression test (Test No. TCSHAN), this series of triaxial tests cannot technically be used to

demonstrate the effects of consolidation technique. Ideally, the corrections of Chapter 3 should have utilized a Recompression test on a very young sample (i.e., $t_s \approx 1$ day), but such a specimen was unavailable.

Bearing the history of these Recompression data in mind, perusal is made of the data as compared to TCSHAN (corrected data are tabulated in Appendix H). Normalized stress-strain curves are presented in Fig. 6.3. Summary data are presented in Table 6.2. It is immediately evident that, contrary to data from tests on varved clay, the SHANSEP triaxial compression test is not only initially stiffer than the Recompression tests, but also fails at a lower shear stress. Given the high quality of the BBC samples, (supported by the σ'_p, c_v and C_α data from the consolidation tests in Chapter 3), as well as the reproduceability of the corrected stress-strain curves, it is unlikely that the Recompression samples were disturbed. Fig. 3.11, in which the uncorrected TC data are presented, reveals that the reduced stiffness of the Recompression tests relative to the SHANSEP test is not due solely to the correction for thixotropy.

The stiffness of the SHANSEP TC test at OCR=4 is considered suspect. Comparison with Young's moduli normalized with respect to $\sigma'_{oct,o} = \frac{(\sigma'_1 + \sigma'_2 + \sigma'_3)_o}{3}$ and plotted versus the log of axial strain for a number of soils tested at OCR=4 (Lower Cromer Till, (I_p=12%), North Sea Clay ($I_p \approx 20\%$), and London Clay ($I_p \approx 47\%$)), shows that the TCSHAN moduli data are relatively high. These data were provided by Hight (1985,

pers. comm.).

The preceding data on Lower Cromer Till (Fig. 6.2) and BBC in direct simple shear indicated stiffer SHANSEP tests which were, ultimately, also stronger than the Recompression tests. Unlike these data, the SHANSEP TC test on BBC (at OCR=4) is weaker than similar tests on samples recompressed to the "overburden" stress. (Sambhandharaksa, 1977, shows a Recompression TC test on a varved clay block sample at OCR=2 which is stronger than SHANSEP, although the Recompression test is initially stiffer).

Additionally, in all the cases cited in Table 6.1, either the strain at failure for the Recompression tests is less than or equal to that for the SHANSEP tests. For the BBC TC test series, ε_f for the Recompression tests is approximately double that for TCSHAN.

As far as effective stress behavior is concerned, BBC triaxial Recompression tests exhibit the same trend of decreased effective stresses during shear as compared to the SHANSEP test (Fig. 6.4). The increase in effective stresses for the SHANSEP test, however, is not as significant as that indicated by previous comparisons. For example, inspection of the variation of the obliquity, R, and the pore pressure parameter, A, with axial strain for Sambhandharaksa's varved clay in Fig. 6.1 reveals substantial deviation of the Recompression values vs. those from SHANSEP tests, particularly at low strains. Fig. 6.5 presents the paramet ; R and A for the BBC triaxial compression test series. Al h the scatter

associated with obliquity for the Recompression tests is considerable, the average trend (dashed line) is very similar to that for Test No. ERIC-1 in Fig. 6.1.

Considering that no filter strips were used to expedite pore pressure equilibration during the performance of the Recompression tests, yet strips were utilized for TCSHAN, the possibility exists that the rate of strain (0.5%/ hour) may have been too rapid to allow equalization of pore pressure in the Recompression samples, thus leading to the lower effective stresses. Pore pressures are measured at the base of the sample. Using the method suggested by Bishop and Henkel (1957) for vertical drainage only and a coefficient of consolidation, c_v, of the resedimented BBC at OCR=4 from Fig. 3.9 equal to 11×10^{-3} cm^2/sec, the strain rate used during shear allowed sufficient time for accurate pore pressure measurements.

In summary, the BBC results of this research just cited with respect to Recompression vs. SHANSEP as a method of consolidation seem reasonable, except that the much larger stiffness of TCSHAN may be suspect. The effective stresses appear to be a function of the direction (loading vs unloading) of the final consolidation increment. That the strength of the Recompression tests is greater than that of the SHANSEP test may be a real effect of the consolidation technique, or may be due partly to the inaccuracy of the thixotropic correction.

The possible causes of the different shear behavior between samples consolidated via SHANSEP and those consolidated according to the method of Recompression are as follows:

1) The two methods of consolidation lead to different preshear water contents when the maximum past pressure (SHANSEP) is equal to the preconsolidation pressure (Recompression); assuming that the sample for the SHANSEP test had an in situ preconsolidation pressure small enough that consolidation in the lab to at least a 50% greater stress would establish σ'_{vm} equal to σ'_p for the Recompression test. When consolidating a sample to the overburden stress directly from the sampled state the preshear water content will be less than in situ due to disturbance effects. On the other hand, when using the second Recompression technique (described earlier in this section) the Recompression water content is likely to be greater than its SHANSEP counterpart. (The reload portion of an unload-reload cycle in a device exists at slightly higher water contents at OCR's $\gtrsim$ 1.5 than the unload portion).
2) SHANSEP type consolidation effectively destroys any clay structure developed in the material at its in situ environment by causing large strains as the sample is consolidated into virgin territory. Effects such as those due to aging, thixotropy and/or cementation should be preserved by the first Recompression method of consolidation if not already altered by sample disturbance.
3) The direction of the final consolidation increment is negative (unloading) for the SHANSEP method of

consolidation and positive (loading) for Recompression. That this difference can affect shear behavior is proven by the Ladd and Edgers (1972) DSS tests that were unloaded to OCR=4 (SHANSEP) versus reloaded to OCR=4 from OCR=8 (the second Recompression technique).

Given the scarcity of data regarding the effect of the method of consolidation, only a very tentative hypothesis can be attempted. Both the triaxial compression and extension Recompression tests performed on varved clay had lower water contents than that which would be associated with a SHANSEP test at a similar OCR with a maximum past pressure equal to σ'_p for the Recompression tests. However, the Recompression extension test was substantially weaker than the SHANSEP extension test. Thus, the water content discrepancy is not considered the major cause for the effect of the method of consolidation.

Also, the Recompression vs. SHANSEP DSS test series (Ladd and Edgers, 1972) involved the second type of Recompression, yet resulted in effective stress differences between the Recompression and SHANSEP shear data similar in character to those exhibited by the direct Recompression TC and TE tests with SHANSEP triaxial tests of Sambhandharaksa (1977). D.W. Hight (1985, pers. comm.) indicated that data from direct Recompression tests compared well with tests on the same material at the same overconsolidation ratio following the second type of Recompression, which involved reloading beyond

$\sigma'p$. Therefore, the structural changes associated with extended time in situ or in storage are not always completely responsible for the effect of the method of consolidation. Of course, for highly sensitive clays or for cemented materials, direct Recompression will yield very different results when compared with either the second type of Recompression or with SHANSEP (e.g., SHANSEP tests on James Bay clay results in much lower $c_u/\sigma'p$ than direct Recompression tests (Jamiolkowski et al., 1985).

It is hypothesized, then, that the major cause of the variation in shear behavior due to the method of consolidation for laboratory-prepared specimens, i.e., uncemented, generally nonstructured clays, is the direction of the final consolidation stress (i.e., whether it is loading or unloading).

The effect of the method of consolidation is deemed deserving of focused attention to ascertain the true effect. General trends and tendencies have been identified but a precise, in-depth study on a variety of natural and artificial clays has yet to be produced. Jamiolkowski et al. (1985) call for a similar investigation.

6.3 COMPARISON OF DATA AT $\delta=0°$

The undrained shear strength of saturated low permeability cohesive soils with the major principal stress during shear coincident with the deposition direction can be measured in a variety of devices: the triaxial cell, conventional plane

strain apparatuses, the Directional Shear Cell, true triaxial apparatuses and the torsional shear Hollow Cylinder Apparatus. All of these devices are equally capable of performing extension tests wherein σ_1 is maintained perpendicular to the direction of deposition, the details of which are discussed in Section 6.4. As indicated in Table 2.2, only two of them are able to dictate the direction of σ_1 at orientations intermediate to either the active or the passive extreme. They are the Directional Shear Cell and the Hollow Cylinder Apparatus.

BBC at OCR=4 has been successfully tested under both triaxial and plane strain conditions. The latter environment is imposed by both the Directional Shear Cell and the MIT Plane Strain Device (PSD) (Ladd et al., 1971). Data from these devices for the case of active shear (δ=0°) are compared in this section.

The only data produced outside this research are those presented by Ladd et al. (1971) from PSA tests. The MIT PSD had problems with piston friction as well as difficulties measuring the intermediate principal stress, σ_2. Side friction was not measured and is also believed to be significant. In light of these difficulties, the apparatus was not used for subsequent research efforts at MIT. Careful backpressuring of the sample and correction for piston friction, as performed by Ladd et al. (1971), enable use of data from the two δ=0° (plane strain active) tests on BBC at OCR=4; PSA-5 and PSA-7. Measurements of σ_2 are essentially disregarded. These shear

tests were performed following SHANSEP type consolidation and hence no corrections for the effects of extended storage times are necessary.

First, comparison is made between results from the DSC (δ=0°) and those from triaxial compression tests. Although the devices to be compared involve different values of the relative intermediate principal stress parameter, b, they will first be compared with one another in the conventional format for stress vs strain, i.e., the maximum shear stress, q (= $(\sigma_1-\sigma_3)/2$) vs axial strain. Also, the two dimensional normalized stress path, i.e. q/σ'_p vs p'/σ'_p which disregards the magnitude of σ_2, is employed. Later, the results are presented in terms of octahedral stresses, τ_{oct} and σ_{oct}, which incorporate the magnitude of σ'_2.

Only one of the triaxial compression tests performed by this research involved loading beyond the thixotropic preconsolidation pressure, $\sigma'_p(t)$ and unloading to OCR=4. This test, TCSHAN, was compared to the recompression TC tests corrected for thixotropy on BBC in the previous section. As the individual tests have already been presented in Figs. 6.3 to 6.5, they are represented by bands in Figs. 6.6 to Fig. 6.10. As was noted in Section 6.2., TCSHAN is considered too stiff and without additional data from similar tests, is suspect.

Stress-strain curves from the δ=0° tests are presented in Fig. 6.6. The method of consolidation for each test is indicated in the key. Considering, first, the plane strain

tests, it can be seen that below an axial strain of about 0.4%, the SHANSEP-type PSA-5 and PSA-7 are just slightly stiffer than DSC's 1 and 3. The moduli at 50% of the maximum shear stress, listed in Table 6.3, indicate that, on average, the PSA and the DSC tests are essentially of equal stiffness, $(E_{50}/c_u)_{ave}$=516 and 494, respectively). Following yield, the plane strain tests of Ladd et al. (1971) reach a maximum shear stress at an axial strain approximately equal to 2%, compared with ε_f for the Recompression DSC tests equal to about 1%. The undrained strength for the SHANSEP PSA tests ($(q_f/\sigma'_{vm})_{ave}$ = 0.236) is, on the average slightly lower than that for DSC's 1 and 3 ($(q_{ft}/\sigma'_p)_{ave}$ = 0.246). The PSA tests exhibit slight strain softening, a feature not measurable by the stress controlled DSC tests.

To consider the effect of the consolidation technique, the general trends of the previous section are used. Since δ=0°, the trends associated with the triaxial compression tests in Table 6.1, in particular those pertaining to BBC, are applied. Thus, the low strain stiffness and slightly greater strength of the DSC tests in comparison with the PSA tests might be explained by the different methods of consolidation employed. However, the strain at failure for the Recompression DSC δ=0° tests is about half that of the SHANSEP PSA tests, opposite to the trend indicated by the triaxial Recompression vs. SHANSEP tests. Given the problems associated with the PSA device and the differences to be expected from using different methods of consolidation, the DSC and PSA δ=0° tests show remarkable

agreement.

The Recompression triaxial compression test data are also presented in Fig. 6.6. Here it can be seen that the Recompression TC tests are initially softer ($E_{t50}/c_{ut} \cong 254$ vs. 494 for TC and DSC tests, respectively, as averaged from Table 6.3) yet, ultimately, stronger ($q_{tf}/\sigma'_p \cong 0.279$ and 0.246 for the respective TC and DSC tests). It will be seen when the more generalized state of stress is discussed that these phenomena cannot be explained by the effect of b. Although already suspect because of its stiffness, TCSHAN is also slightly stronger than the SHANSEP plane strain active tests of Ladd et al. (1971), similar to the Recompression TC tests being slightly stronger than the DSC tests.

The stress paths followed by the $\delta=0°$ tests are presented in Fig. 6.7. PSA-5 and 7 develop much higher effective stresses than the plane strain DSC tests. Based on data from Section 6.2, this phenomena is most likely due to the effect of SHANSEP vs. Recompression. The Recompression triaxial compression tests also develop higher effective stresses than the DSC tests. Higher effective stresses - when neglecting the magnitude of σ_2 - are to be expected under triaxial compression conditions since incorporation of σ_2 (= σ_3) reduces the octahedral confining stress.

The variation of the effective stress parameters with axial strain are presented in Fig. 6.8. The DSC $\delta=0°$ tests achieve much higher obliquities than the PSA test series and the TC test series due, respectively, to the method of

consolidation and the effect of b.

According to Vaid and Campanella (1974), the results for all devices should be coincident in a generalized stress space. However, in checking this hypothesis, which they found worked well for normally consolidated Haney Clay, they noted some disparity between different device results in extension. The generalized stress-strain parameters, τ_{oct} and γ_{oct}, incorporate all the principal stresses and strains as follows:

$$\tau_{oct} = \frac{1}{3}\left[(\sigma_1 - \sigma_2)^2 + (\sigma_2 - \sigma_3)^2 + (\sigma_3 - \sigma_1)^2\right]^{1/2}$$

$$\gamma_{oct} = \frac{1}{3}\left[(\varepsilon_1 - \varepsilon_2)^2 + (\varepsilon_2 - \varepsilon_3)^2 + (\varepsilon_3 - \varepsilon_1)^2\right]^{1/2}$$

For the DSC tests, wherein σ_2 was not measured, b was estimated at 0.35 for shear strains greater than 0.8%. For small strains, b was varied almost linearly from 0.5 to 0.35 for γ=0 to 0.8%. This estimate of the relative intermediate stress ratio is discussed in Section 3.2.4.

Octahedral stress-strain curves are presented for both δ = 0° and δ = 90° in Fig. 6.9. The former case is discussed herein while the δ = 90° case is attended to following the conventional presentation of the extension results.

From these data, there appear to be significant differences between the plane strain (both DSC and PSA series) and the triaxial results, despite Vaid and Campanella's (1974) contention for coincidence. A number of the technical performance differences which exist between the DSC and the triaxial tests also exist between the DSC and the MIT plane strain apparatus tests; such as stress control vs. strain

control and flexible loading elements vs. rigid. The PSA test series compares well with the DSC series, taking into account the method of consolidation. Hence, boundary conditions and stress vs. strain control cannot explain the high octahedral shear stress attained by the triaxial tests $((\tau_{oct,t}/\sigma'_p)_{max}(TC)$ is approximately 24% greater than $(\tau_{oct,t}/\sigma'_p)_{max}(DSC))$.

As noted above, the experimental study performed by Vaid and Campanella (1974) on undisturbed Haney clay (I_p=18%, w_L=44%) involved plane strain and triaxial tests on normally consolidated samples only. Data pertaining to the variation of stress-strain-strength behavior as measured in plane strain vs triaxial as the overconsolidation ratio is increased are scarce.

Gens (1982), however, presents some data on anisotropically consolidated LCT at different OCR's which indicate that with increasing OCR, TC undrained strength becomes greater than that measured under plane strain conditions. Although the magnitude of the increase in undrained strength of LCT from triaxial results over plane strain results at OCR's 4 and 7 is only about 4% and 11%, respectively, as compared with the 14% increase in q_t/σ'_p exhibited by the resedimented BBC, the trend is similar. The LCT data also indicate that as OCR increases, the difference between the octahedral shear strain at peak stress for the triaxial test and that for the plane strain test increases from zero for OCR=1 to approximately 0.5% for OCR = 4, with triaxial

tests having the larger strain. For resedimented BBC, at OCR=4, the differences are larger, namely γ_{oct}(TC) ≈ 3.5%, γ_{oct}(PS) ≈ 1%, resulting $\Delta\gamma_{oct}$ ≈ 2.5%. (Vaid and Campanella, 1974, report γ_{oct}(TC) > γ_{oct}(PS) for normally consolidated Haney Clay, while Lade and Musante (1978) indicate the opposite trend for OCR=1 tests).

Generalized stress paths are presented in Fig. 6.10, again for both active and passive cases. For the δ=0° condition, it is evident that both SHANSEP triaxial and plane strain tests lead to higher effective stresses. In the octahedral stress space, differences in the value of b during shear are taken into account and, hence, theoretically one might expect concurrence of triaxial and plane strain results. The variation in generalized stress paths between TCSHAN and PSA-7 is somewhat similar to the variation presented by Gens (1982) for triaxial compression vs. plane strain compression tests on anisotropic LCT at OCR=4.

From the generalized stress path it seems likely that there is some problem with PSA-5 as it has much higher effective stresses than PSA-7. That the other tests do not approach a similar octahedral stress ratio, τ_{oct}/σ'_{oct}, is probably related to the formation of failure planes precluding accurate large strain behavior for the triaxial tests.

6.4 COMPARISON OF DATA AT δ = 90°

There are less available data pertaining to the behavior of resedimented BBC at OCR=4 under passive shear conditions

than under active conditions. To orient the major principal stress such that it is perpendicular to the direction of deposition is possible in most devices capable of $\delta=0°$ tests. For triaxial test situations, extension tests are frequently performed by unloading, since this is easiest for strain control. (Vaid and Campanella, 1974, present data on Haney clay showing that the total stress path does not affect the effective stress path which should be the case for fully saturated materials). The six Recompression triaxial extension (unload) tests corrected for the storage effect are presented in Figs. 6.11-6.13.

Ladd et al. (1971) performed several passive plane strain tests in the device described in their report. However, due to friction problems, the only test at OCR=4 considered reasonably valid is Test No. PSP-12H. This test was sheared by increasing the stress on the face parallel to the depositional axis thus producing a loading total stress path. SHANSEP type consolidation was used and hence no correction for the effect of thixotropy is necessary. Data for PSP-12H are also presented in Figs. 6.11-6.13.

DSC-2 is the only DSC test performed with σ_1 and σ_2 oriented perpendicular to the direction of deposition. As with all the DSC tests, shearing followed Recompression type consolidation to $\sigma'_{vc}=0.25$ ksc.

Conventional deviatoric stress vs. axial strain curves for the $\delta=90°$ tests performed on resedimented BBC at OCR=4 are presented in Fig. 6.11. The plane strain tests, DSC-2 and

PSP-12H, are approximately 75% stronger than the triaxial Recompression tests at yield. Further, the SHANSEP plane strain PSP-12H is slightly stronger than the Recompression DSC-2.

The method of consolidation might be used to explain some of the latter strength difference between the two plane strain tests. Referring to Table 6.1, it is seen that the East Windsor varved clay is much stronger in extension following SHANSEP consolidation than when following Recompression. However, because the varved clay is particularly suited to low $\delta=90°$ strengths upon Recompression since separations between the varves may not be closed, it is not possible to fully rely on these data to establish conclusive trends for a homogeneous silty clay such as BBC. Yet, bearing the applicability of the varved clay data in mind, a general trend might be noted. Hence, although for the $\delta=0°$ tests the Recompression results (both in plane strain and triaxial environments) indicated slightly greater strength than SHANSEP results, under $\delta=90°$ conditions the trend could possibly be the opposite. Therefore, that PSP-12H is stronger than DSC-2 may be the result of the use of SHANSEP in the case of the former and Recompression in the case of the latter. On the other hand, the higher PSP-12H strength may have resulted from problems with the apparatus rather than the consolidation method.

That TE tests give lower shear stress vs. strain curves than DSC-2 is not completely explained by the effect of b; as will be seen when the more generalized states of stress are

studied. The stress paths followed by the extension tests are presented in Fig. 6.12. In keeping with SHANSEP vs. Recompression behavior, the plane strain passive test, PSP-12H, has much higher effective stresses than the δ=90° DSC test. And, considering the effect of differing values of b on the stress paths, the triaxial extension results occupy suitably lower effective stresses than the DSC test - both having been subjected to Recompression type consolidation. Again, inspection of these data in octahedral stress space will clarify this contention.

The variation of the effective stress behavior with axial strain is presented in Fig. 6.13. Here it can be seen that all the δ=90° tests exhibit approximately similar obliquities, R, at low axial strains, while at large strains, the TE tests climb rapidly to higher values of R. The large variation in R at high axial strains is probably attributable to the low precision of the data at these low stresses.

The triaxial tests exhibit much greater values of the pore pressure parameter, A, at low strains as compared with the plane strain tests. Also, the DSC δ=90° test demonstrates greater values of A than does PSP-12H. Whether or not the δ=90° tests approach the same failure envelope is a function of the magnitude of the cohesion intercept, which was not measured in this research. Also, behavior at various overconsolidation ratios is necessary to accurately estimate the failure envelope.

The generalized stress conditions for δ=90° tests are

presented in Figs. 6.9 and 6.10. The Recompression triaxial tests are represented as bands for the sake of simplicity. Although Vaid and Campanella (1974) had to resort to the use of the change in octahedral shear stress vs. γ_{oct} in order to achieve coincidence of triaxial and plane strain extension results, this was unnecessary for the resedimented BBC at OCR=4 since the preshear state of stress is isotropic.

It is evident from the lower portion of Fig. 6.9 that the TE test results consistently have lower octahedral shear stress levels than the DSC δ=90° test. As γ_{oct} increases the TE band approaches and passes that of DSC-2, resulting in a ratio of $\tau_{oct}(TE)/\tau_{oct}(PS)$ equal to 1.16 at peak. (At peak deviator stress, q_f, the ratio of undrained strength, $q_f(TE)/q_f(PS)$, (using the DSC test) is approximately equal to 1.04 from Table 6.4. This ratio is much larger than that reported by Ladd et al. (1977) for OCR=1 clays where $q_f(TE)/q_f(PS)$=0.82).

The generalized stress paths presented in Fig. 6.10 reveal the tendency of the triaxial tests at δ=90° to at first generate more negative shear-induced pore pressures, Δu_s, followed by greater positive values of Δu_s at given normalized octahedral shear stress levels than either of the plane strain tests. Ultimately, however, all the extension tests, regardless of testing device or method of consolidation, approach a similar stress ratio, τ_{oct}/σ'_{oct}, at large strains.

6.5 COMPARISON OF DATA AT INTERMEDIATE VALUES OF δ

The device commonly employed in the measurement of

undrained shear strengths indicative of orientations of the major principal stress intermediate between $\delta=0°$ and 90° is the Direct Simple Shear apparatus. Several studies have been undertaken to assess the stresses in a DSS sample (e.g., Soydemir, 1976; Ladd and Edgers, 1972; Lucks et al., 1972; Saada et al., 1981). One main difficulty in the assessment of the stresses arises due to the inability of the wire reinforced membrane to generate shear stresses complementary to those applied at the top and bottom of the sample.

The DSS was severely criticized as a soil testing device by Saada et al. (1981) on the basis of the nonuniformity of the stress state as indicated by photoelastic studies. However, the Saada et al. opinion has been refuted by several investigators, notably:

1) Lacasse and Vucetic (1981), who performed a series of DSS tests using three different height of sample to diameter of sample ratios (h/D = 0.14, 0.20 and 0.3). These data are presented in more comprehensiveness by Vucetic and Lacasse (1982). The results indicate that since there were no dissimilarities in behavior, the boundary effects due to stress application difficulties do <u>not</u> control behavior sufficiently to affect the measurements of the average stresses. Therefore, used with knowledge of the device inadequacies, the DSS should act as a valuable tool for special applications.
2) Christian (1981), who defended the results of the

finite element analyses presented by Lucks et al. (1972) by referring to the results of Shen et al. (1978). The latter analysts performed a more extensive parametric study of the cylindrical DSS sample using the same boundary conditions as Lucks et al. (1972) but also incorporating the effect of the membrane as well as the nonuniform stress distributions due to vertical consolidation stresses. Shen et al. conclude that by the time the sample has incurred large horizontal strains, initial nonuniformities in shear stress have been removed and that the stress and strain are relatively uniform over the middle portion of the sample. Christian (1981) further refutes the argument of Saada et al. (1981), regarding stress distribution based on photoelastic analysis, by pointing out that the photoelastic results are in error, possibly experimental in origin, since the variation in horizontal shear stress about the center indicates asymmetry. Such asymmetrical τ_h cannot be, according to Christian, for an isotropic elastic axially symmetric body loaded uniformly in one direction.

Consideration of the actual state of stress in a DSS sample is beyond the scope of this thesis. It is of interest, only, to compare results from DSS tests with those of DSC tests wherein the angle of shear is intermediate, i.e., δ=40°, 65° and 75°. By so doing, it is proposed that the angle (or

angles) of shear which the DSS best simulates will be determined.

Confronting the issue of the mechanics of comparison (i.e., the actual shear stress from the DSS to be compared with the maximum shear stress, q $(= (\sigma_1 - \sigma_3)/2)$ from the DSC tests), Ladd and Edgers (1972) was consulted. It was ultimately concluded in that study that the maximum horizontal stress, τ_h, probably lies somewhere between the undrained shear strength, q_f, and the shear stress on the failure plane, τ_{ff} $(= q_f \cos\phi')$. The effective friction angle, as estimated from the DSC for angles of shear between 40° and 75°, could range between 34° and 30° (assuming $c'/\sigma'_p \simeq 0.04$). Thus assuming $\tau_h = q_f$ may underestimate q by up to about 15%. However, for overconsolidated clays where $K_o \simeq 1.0$ (as is the case for the resedimented BBC) one of the possible analyses of DSS applied stress states (that of pure shear) produces results equivalent to the $\tau_h = q_f$ assumption. Also, other analyses summarized by Ladd and Edgers (1972) [such as Kenney (1966), Morgenstern and Tschalenko (1967) and Roscoe, Basset and Cole (1967)] suggest that $\tau_h = q_f$ may be a reasonable approximation of the undrained shear strength. In any case, the assumption that $\tau_h = q_f$ will be made for purposes of comparison although the actual q may be up to 15% higher.

The stress-strain curves in Fig. 6.14 represent horizontal shear stress vs. shear strain from the three SHANSEP type DSS tests in comparison with the shear stress, q, vs. shear strain from DSC's-13, 8, 11 and 15, performed following recompression

with δ = 40°, 65°, 75° and 75°, respectively. Since both the DSS and the DSC subject the sample to plane strain conditions during shear, it is considered unnecessary (and, indeed, impossible given the unknowns associated with the DSS imposed state of stress) to determine generalized states of stress and strain for comparison (i.e., τ_{oct}, σ'_{oct} and γ_{oct}). It is evident from the data in Fig. 6.14 that the DSS results definitely simulate behavior at intermediate angles of shear, with the angle of shear imitated increasing with increasing shear strain, if τ_h from the DSS test is a reasonable measure of q.

The effect of the method of consolidation in the DSS device might be best garnered from the Ladd and Edgers (1972) data (Fig. 3.28 and Table 6.1). It is seen that SHANSEP type tests indicate approximately 10% higher shear strength at yield and thereafter. These data are based on a Recompression test at OCR=4 (from OCR=8) which involved consolidation beyond σ'_p and hence that test (Test No. 1002A) should be free of both disturbance and time effects (i.e., t_s=0).

However, since the DSS data on BBC at OCR=4 presented by Ladd and Edgers was consistently lower than the DSS data in this research, as shown in Fig. 3.28, Recompression Test No. 1002A may not be comparable to the DSC data from this research. Even so, this test is presented in Figs. 6.14 and 6.15 with the DSS and DSC data of this research.

Figure 6.14 also presents the stress-strain curves from the DSS tests performed in this research - both SHANSEP tests

(DSS-7, 9 and 15A) and Recompression tests (DSS-14 and 15, (with pins)) are shown. The Recompression tests were not corrected for the effect of thixotropy (even though they were both over 100 days "old") since it was hypothesized in Section 3.2.2 that the pins destroyed at least some of the strengthening effect of storage time. Without the aid of additional Recompression DSS tests with pins - particularly prior to prolonged storage - it is not possible to estimate a different method of correction. In light of Ladd and Edgers (1972) data, the behavior of the Recompression tests of this research (DSS-14 and 15) is stronger than it should be, due either to the effects of remnants of the thixotropic strength gain or to the effects of the pins or both.

Taking the above factors affecting the various DSS tests shown in Figs. 6.14 and 6.15, it is evident that more data, such as a Recompression DSS test (the second type discussed in Section 6.1, so as to remove the need for pins) on the resedimented BBC used in this research, are needed. Without such information, it is hypothesized that actual Recompression DSS stress-strain behavior falls somewhere between Ladd and Edgers Test No. 1002A and the DSS tests of this research (DSS-7, 9, 14, 15 and 15A). Keeping this in mind, the angle of shear that the DSS simulates can be estimated by comparing the DSS stress-strain behavior with that from DSC tests performed at intermediate angles of shear (see Fig. 6.14).

It is concluded, from study of Fig. 6.14, that the DSS produces results simulating an angle of shear continuously

rotating from $\delta \simeq 50°$ at low shear strain to $\delta \simeq 70°$ at high shear strains. It is important to note that the behavior simulated by the DSS is for $\delta > 45°$; at these greater angles of shear, stress-strain behavior is generally much less brittle and more ductile than that for low values of δ. Failure, or maximum shear stresses are attained at large strains. Therefore, when a strength (defined as $(\tau_h)_{max}$) is quoted from a DSS test, it is important to incorporate the strain at failure when considering the angle of shear simulated by that strength. That the angle of shear increases with increasing shear strain was hypothesized by Ladd and Edgers (1972).

In the case of BBC at OCR = 4 where the strains at failure range from about 5% to 10% (from Table 3.5; stress-strain curve becomes very flat and hence the scatter associated with γ_f is considerable), the DSS strength at failure best simulates that for $\delta \simeq 70°$. (Note that the comment made by Germaine (1982) to the effect that DSS tests on overconsolidated BBC (OCR = 4) might be "...subject to significant progressive failure due to stress concentrations" was made prior to consideration for the strengthening effect of extended storage time on the $\delta = 45°$ and 65° DSC tests). If on the other hand the DSS maximum horizontal shear stress results were considered equal to τ_{ff} as opposed to q, the OCR=4 result of $\tau_h/\sigma'_p \simeq 0.149$ would lead to $q/\sigma'_p \simeq 0.173$ $\left(\frac{(\tau_h)_{max}/\sigma'_p}{\cos \phi'} = \frac{0.149}{\cos 30.5°}\right)$ which, in turn, would simulate an angle of shear approximately equal to 55° (from Fig. 5.13). At strains beyond the failure strength, δ probably continues to increase, leading to weaker and weaker behavior

and thus a very flat or even strain softening stress-strain curve. As strains continue, progressive yielding may occur as well.

The effective stress behavior of the DSS is difficult to assess due to the uncertainty with respect to both the magnitude of the applied stresses and their direction. Fig. 6.15 presents the normalized stress paths of the Recompression DSC tests (δ = 40°, 65° and 75°) as well as the normalized horizontal shear stress versus vertical normal stress from the SHANSEP and Recompression DSS tests. The SHANSEP DSS tests appear to dilate much more than the DSC tests. Even the general trend of the Ladd and Edgers Recompression test (dashed line) is more dilative. The "stress paths" of the Recompression tests with pins, DSS-14 and 15, however, coincide fairly well with those followed by the DSC tests at δ=40, 65 and 75°.

Because of the continuous rotation of δ and the uncertain stress state in the DSS, it is difficult to compare effective stress behavior. In addition, since the DSC results indicate that there is only slight variation in the stress path as δ is increased and the DSS effective stress behavior falls far to the right of the general DSC trend, nothing can be concluded in comparing the two devices with regard to effective stress behavior.

Because the DSS is capable of producing empirically useful stress-strain curves, the device has been used to generate data with respect to the undrained modulus. The convenience and

ease with which tests can be performed in the DSS has enabled the production of a large data base on the variation of the modulus with both overconsolidation ratio and soil type (e.g. Ladd and Edgers, 1972). Ladd (1981) states that these data are significant since both the strength and the modulus from the DSS correlate well with backfigured in situ results.

It is of interest, therefore, to inspect the normalized moduli generated by the DSS in comparison with those from the DSC. Fig. 6.16 presents these moduli as they vary with shear stress level. The results in Chapter 5 indicate little dependence of the DSC normalized secant moduli to the direction of shear, i.e. E_u and q_f both decrease at almost the same rate. Again disregarding Test No. DSS-15A because of pin interference, the SHANSEP DSS tests produce moduli essentially the same as Recompression DSC. Attempting to remove the effect of the type of consolidation, the dashed line indicates that the normalized secant moduli from the DSS may be equal to or slightly greater than that from the DSC.

It is concluded that DSS tests on BBC at OCR=4 lead to undrained Young's moduli, E_u, that seem appropriate to use as average values for predicting in situ deformations. Also, the undrained shear strength, c_u, obtained from DSS tests on BBC at OCR=4 seems appropriate to use for predicting stability in problems, such as potential slope failure, where the strengths at different locations along the predicted slip surface will be mobilized under stress conditions involving different angles of shear. However, it is difficult to obtain effective stress

parameters from the DSS, even though the "stress paths" of the Recompression DSS tests with pins were fairly similar to those of the DSC tests at intermediate angles. More data are necessary to further compare the DSS effective stress behavior with DSC tests which have intermediate angles of shear but known boundary conditions to interpret DSS effective stress behavior.

MATERIAL	SOURCE	TRIAXIAL COMPRESSION (δ=0°)		TRIAXIAL EXTENSION (δ=90°)		DIRECT SIMPLE SHEAR (0°<δ<90°)	
		RECOMPRESSION	SHANSEP	RECOMPRESSION (CK_oU=CIU)	SHANSEP	RECOMPRESSION	SHANSEP
East Windsor Varved Clay (block samples of in situ material;OCR=4)	Sambhandharaksa (1977)	(CK_oU=CIU) • higher $(\frac{\sigma_1'}{\sigma_3'})_{max}$ • higher A_f • approximately equal (q/p') at high strains	(CK_oU(C)) • 6% higher $(q/\sigma'_{vm})_f$ • 100% higher ϵ_f • much higher effective stresses during shear	• higher A_f • approximately equal $(q/p')_f$	(CK_oU(E)) • 21% higher $(q/\sigma'_{vm})_f$ • 100% higher ϵ_f • much higher effective stresses during shear		
Lower Cromer Till (isotropically resedimented to OCR=4)	Gens (1982)	• higher $(\frac{\sigma_1'}{\sigma_3'})_{max}$ • approximately equal ϵ_f • approximately equal $(q'/p')_f$ • approximately equal A_f	($\overline{CIU}$(C)) • 3% higher $(q/\sigma'_{vm})_f$ • much higher effective stresses during shear				
Boston Blue Clay (anisotropically resedimented to OCR=4)	Ladd and Edgers (1972)					• 14% higher $(\frac{\tau_h}{\sigma'_{vc}})_{max}$ • much higher effective stresses during shear • approximately equal γ_f • approach similar failure envelope	
	This Research (recompression tests, performed with pins, not corrected for thixotropy)					• much higher effective stresses during shear • slightly higher γ_f • approximately equal $(\tau_h/\sigma'_{vc})_{max}$ • approach similar failure envelope	
	This Research	• ~ 10% higher $(q_f/\sigma'_p)_f$ • higher ϵ_f • higher $(\frac{\sigma_1'}{\sigma_3'})_{max}$ • approximately equal A_f • approach similar q/p' at high strains	($\overline{CK_oU}$(C)) • higher effective stresses during shear				

Table 6.1 : Effect of Method of Consolidation on Undrained Shear Behavior

TEST TYPE	TEST NO.	METHOD OF CONSOLI-DATION*	t_s (days)	σ'_p(R) or σ'_{vm}(S) (ksc)	σ'_{vc} (ksc)	@ $(\sigma_1-\sigma_3)_{max}$					$\frac{E_{50t}}{C_{ut}}$
						$\frac{q_t}{\sigma'_p}$	ε_a (%)	$\frac{p'_t}{\sigma'_p}$	$\frac{\sigma'_{1t}}{\sigma'_{3t}}$	A_t	
	TC-1	R	29	1.0	0.25	0.275	5.9	0.444	4.25	0.147	300
	TC-2	R	78	1.0	0.25	0.273	5.2	--	--	--	220
Triaxial	TC-3	R	225	1.0	0.25	0.290	4.3	0.438	4.92	0.184	250
$\overline{CK_oU}$(C)	TC-4	R	112	1.0	0.25	0.259	6.0	0.428	4.07	0.154	300
	TC-6	R	65	1.0	0.25	0.291	4.3	0.432	5.13	0.187	209
	TC-7	R	150	1.0	0.25	0.286	4.3	0.436	4.81	0.177	246
	TCSHAN	S	0	2.46	0.62	0.252	2.5	0.449	3.56	0.057	793

* S=SHANSEP, R=Recompression (all recompression values corrected for thixotropic effect)

Table 6.2 : Summary of Triaxial Test Results on Resedimented BBC (OCR=4)

TEST TYPE (SOURCE)	TEST NO.	b	METHOD OF CONSOLI-DATION*	$\sigma'_p(R)$ or $\sigma'_{vm}(S)$ (ksc)	σ'_{vc} (ksc)	@ $(\sigma_1-\sigma_3)_{max}$					$\frac{E_{50t}}{C_{ut}}$
						$\frac{q_t}{\sigma'_p}$	ε_a (%)	$\frac{p'_t}{\sigma'_p}$	$\frac{\sigma'_{1t}}{\sigma'_{3t}}$	A_t	
Plane Strain Active (Ladd et al.,1971)	PSA-5	PS	S	2.89	0.73	0.229	1.8	0.416	3.45	0.081	470
	PSA-7	PS	S	5.99	1.46	0.243	1.9	0.372	4.77	0.184	563
Direc-tional Shear Cell (δ=0°) (this research)	DSC-1	PS	R	1.0	0.25	0.237	1.1	0.318	6.85	0.357	406
	DSC-3	PS	R	1.0	0.25	0.254	1.1	0.337	7.12	0.329	582
Triaxial $\overline{CK_oU}$(C) (this re-search)	TCSHAN	0.0	S	2.46	0.62	0.252	2.5	0.449	3.56	0.057	793
	Average from all recom-pression TC tests in Table 6.2	0.0	R	1.0	0.25	0.279	5.0	0.436	4.64	0.170	254

* S=SHANSEP, R=Recompression (all recompression values corrected for thixotropic effect)

Table 6.3: Summary of δ=0° Test Results on Resedimented BBC (OCR=4)

TEST TYPE (SOURCE)	TEST NO.	b	METHOD OF CONSOLI-DATION*	σ'_p(R) or σ'_{vm}(S) (ksc)	σ'_{vc} (ksc)	@ $(\sigma_1-\sigma_3)_{max}$					$\frac{E_{50t}}{q_{ft}}$
						ε_a (%)	$\frac{q_t}{\sigma'_p}$	$\frac{p'_t}{\sigma'_p}$	$\frac{\sigma'_{1t}}{\sigma'_{3t}}$	A_t	
Plane Strain Passive (Ladd et al.,1971)	PSP-12H	PS	S	4.0	1.01	-5.3	0.161	0.227	5.9	0.506	385
Directional Shear Cell (δ=90°, this research)	DSC-2	PS	R	1.0	0.25	-4.7	0.138	0.188	6.5	0.725	632
Triaxial $\overline{CK_oU}$(E) (this research)	TE-1	1.0	R	1.0	0.25	-10.0	0.147	0.137	28	0.895	141
	TE-2				0.26	-10.0	0.159	--	--	--	62
	TE-5				0.25	-10.3	0.132	0.140	34	0.928	80
	TE-7				0.25	-11.8	0.147	0.169	14.4	0.776	74
	TE-10				0.25	-12.4	0.132	0.154	13	0.831	41
	average from all TE tests	1.0	R	1.0	0.25	-10.9	0.143	0.150	22	0.858	80

* S=SHANSEP, R=Recompression (all recompression values corrected for thixotropic effect)

Table 6.4: Summary of δ=90° Test Results on Resedimented BBC (OCR=4)

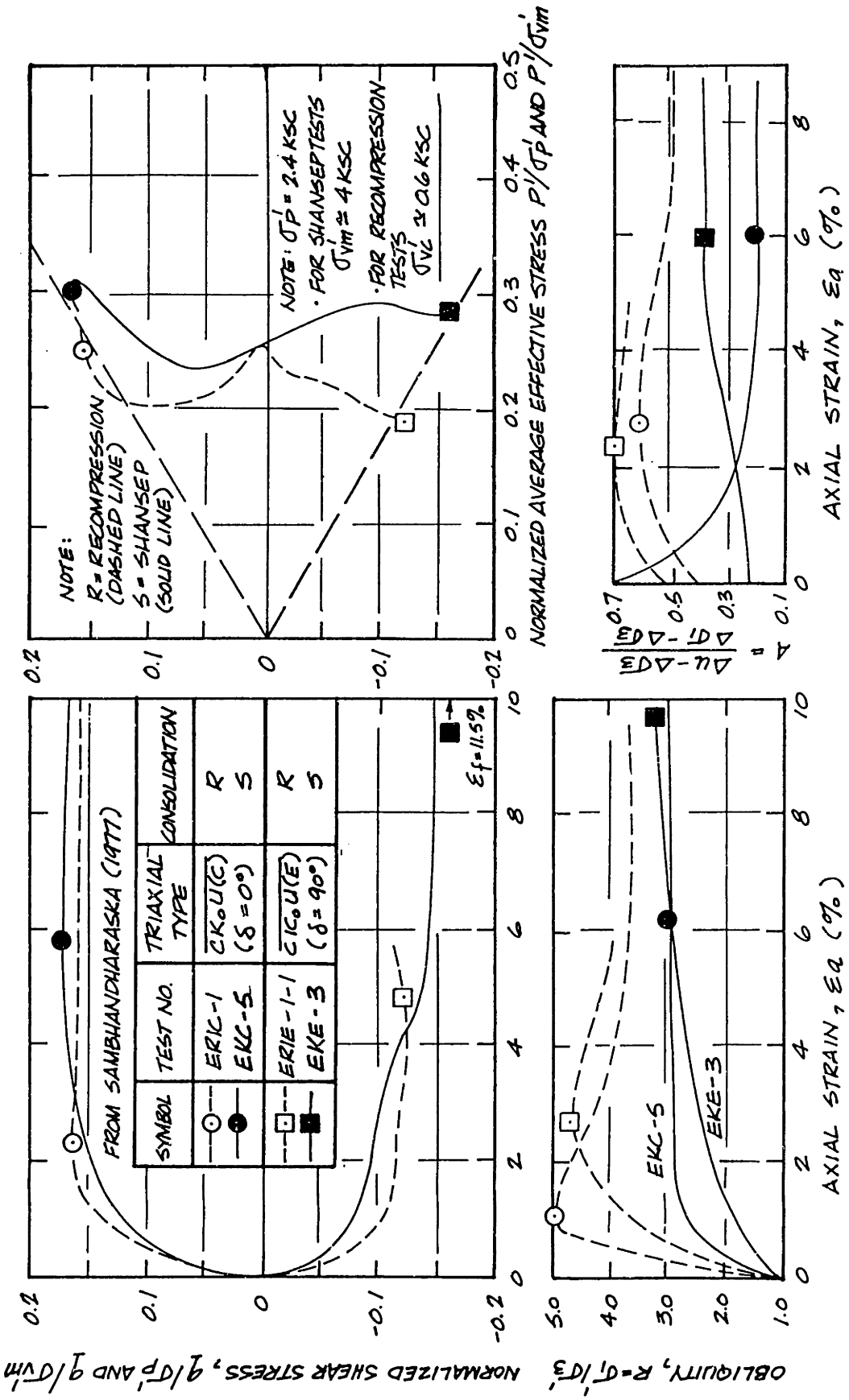

Figure 6.1 : Normalized Stress-Strain Curves and Effective Stress Data from $\overline{CK_oU}$(C) and $\overline{CK_oU}$(E) Triaxial Tests on East Windsor Varved Clay (OCR=4) (after Sambhandharaksa, 1977).

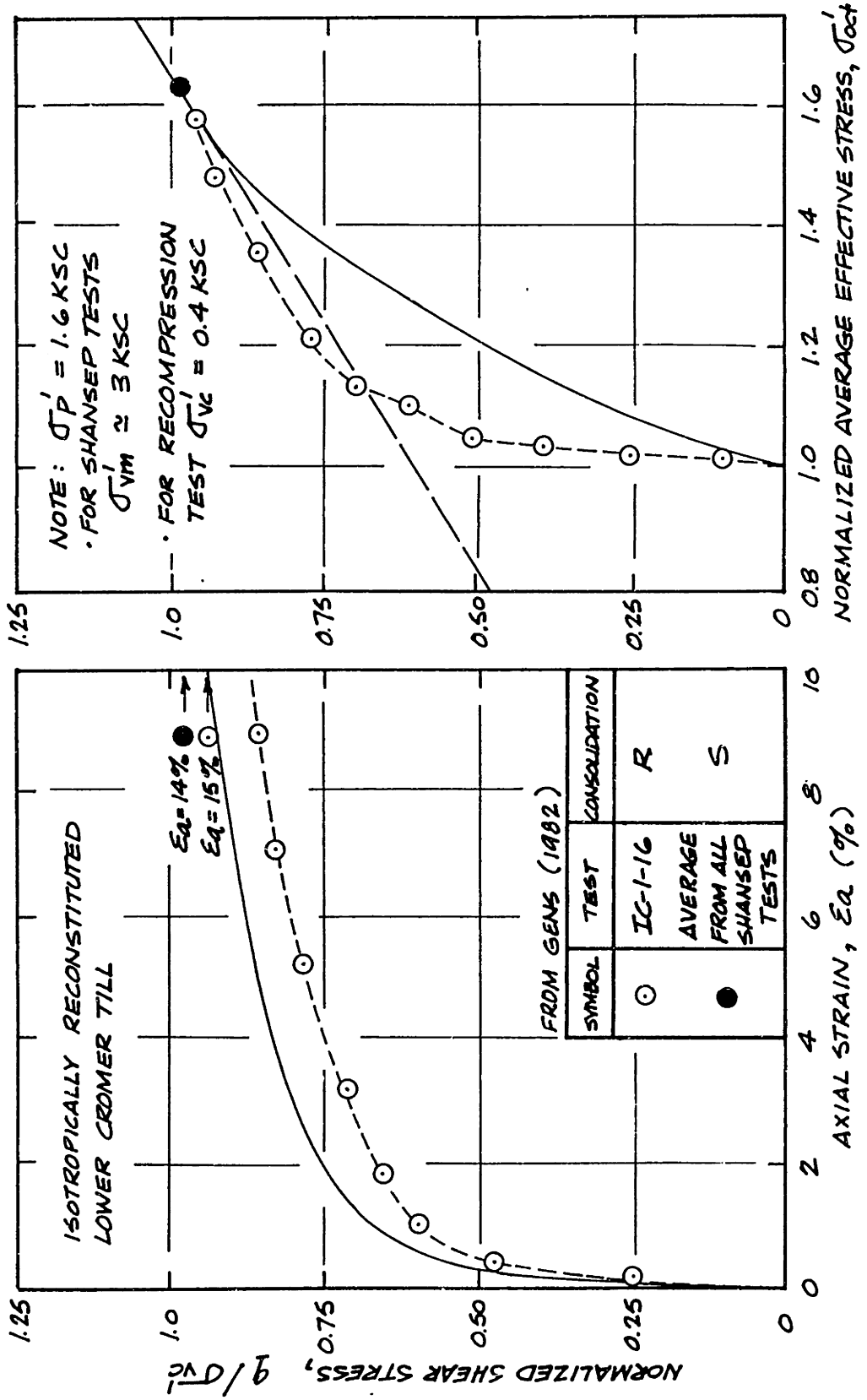

Figure 6.2: Normalized Stress Strain Curves and Effective Stress Paths from $\overline{CIU}$(C) Triaxial Tests on Lower Cromer Till (OCR=4) (after Gens, 1982).

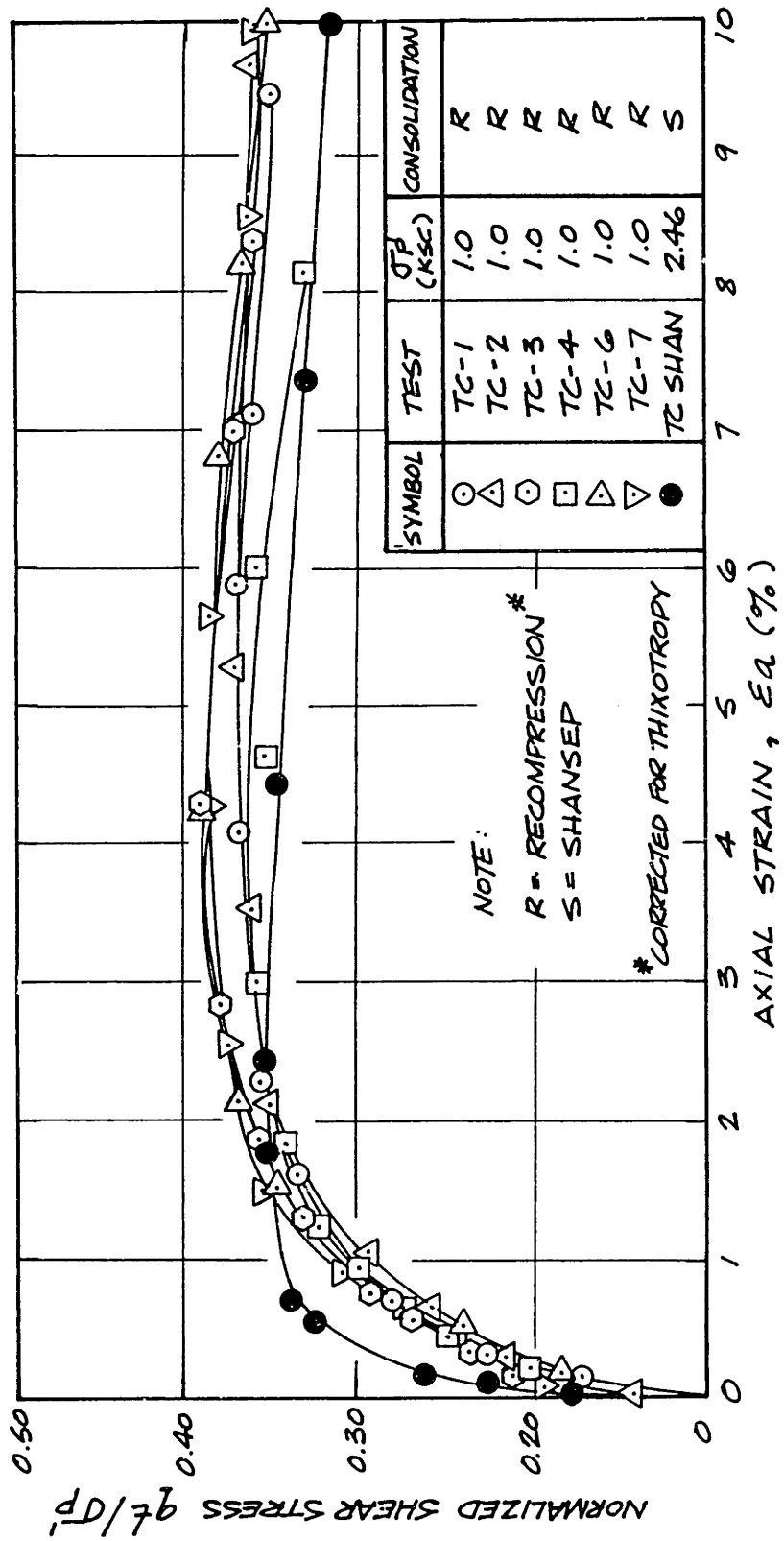

Figure 6.3: Normalized Stress-Strain Curves from Recompression and SHANSEP Triaxial Compression Tests on Resedimented BBC (OCR=4).

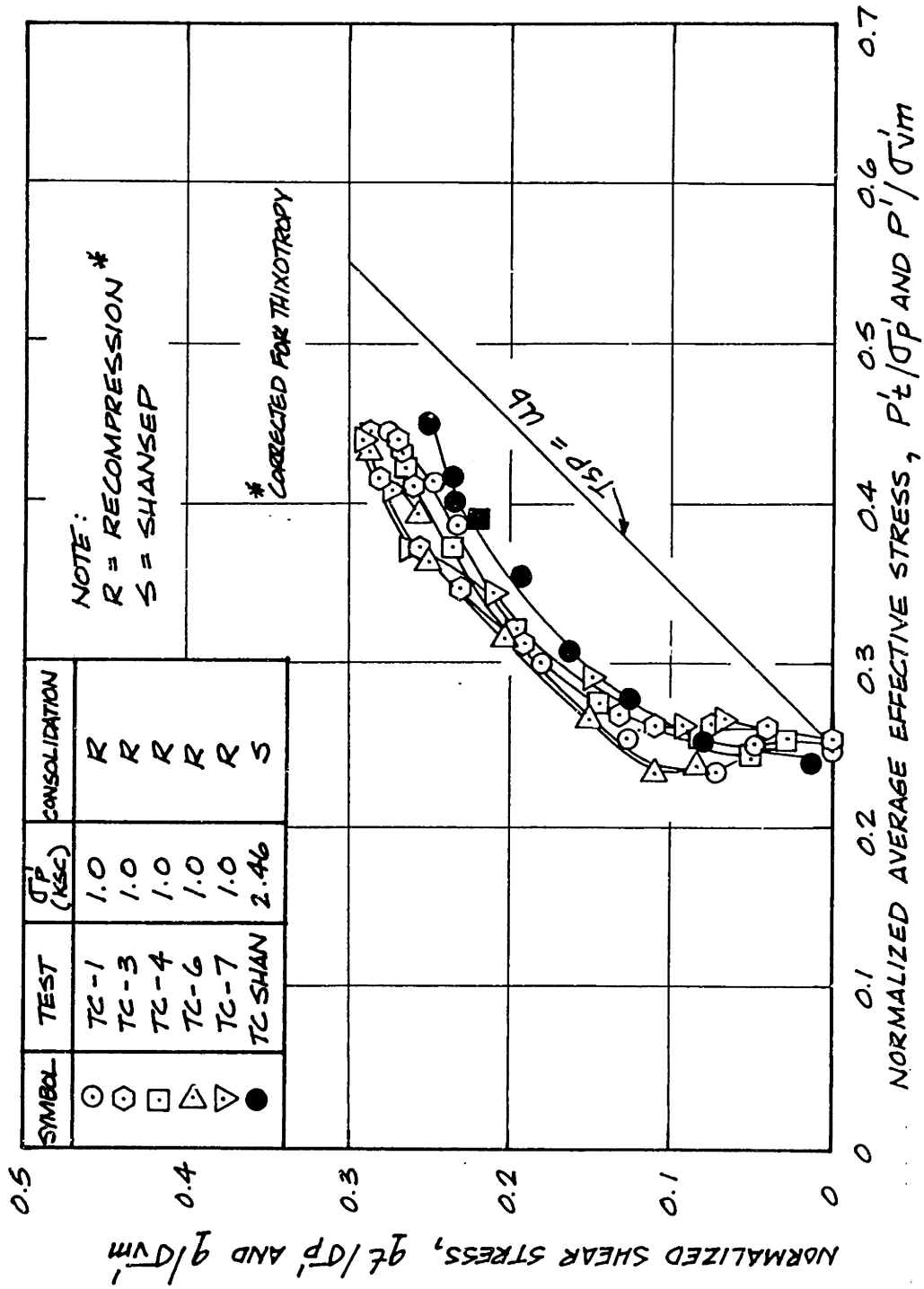

Figure 6.4: Normalized Effective Stress Paths from Recompression and SHANSEP Triaxial Compression Tests on Resedimented BBC (OCR=4).

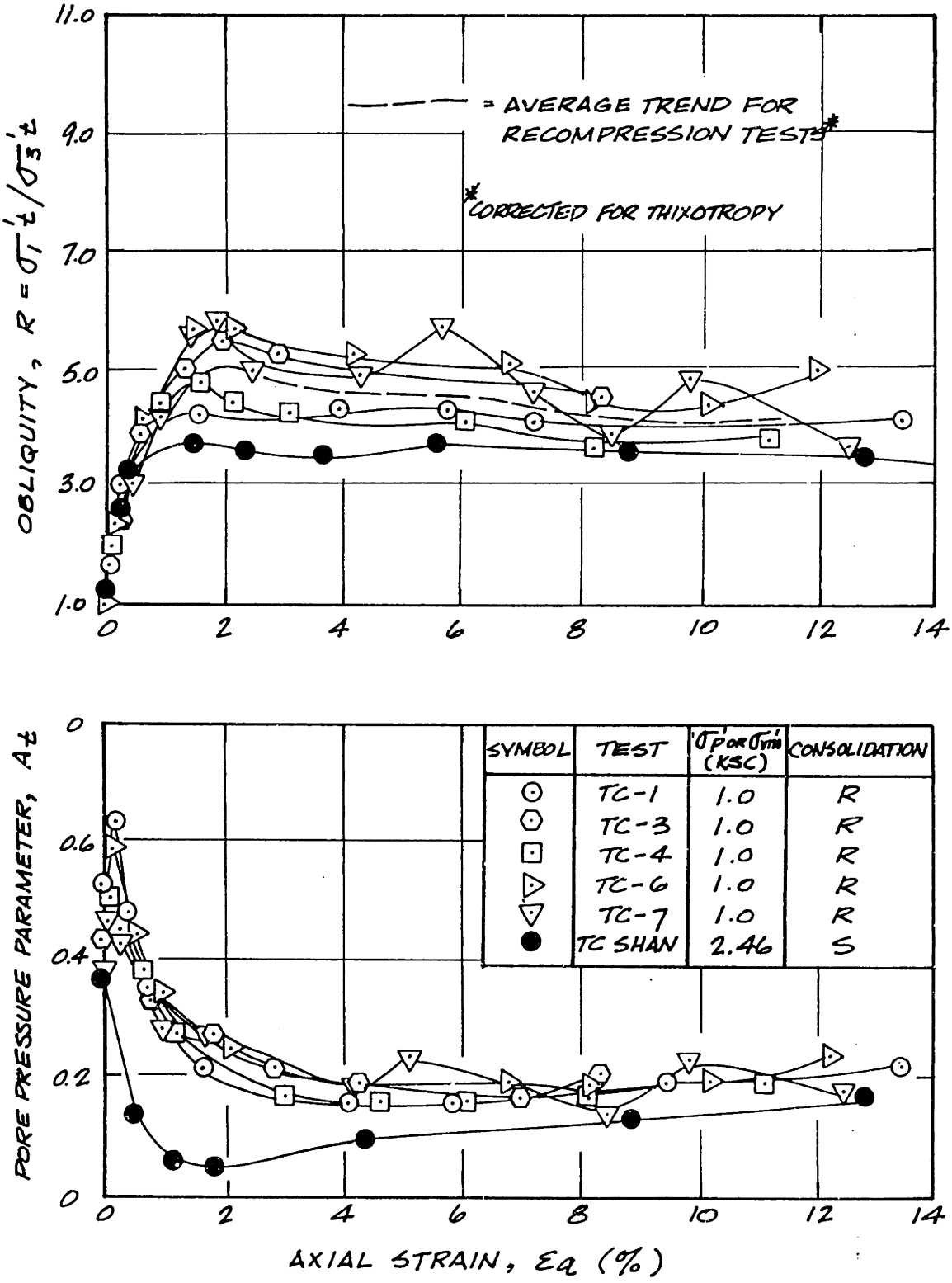

Figure 6.5: Obliquity and Skempton's Pore Pressure Parameter, A, vs. Axial Strain from Recompression and SHANSEP Triaxial Compression Tests on Resedimented BBC (OCR=4).

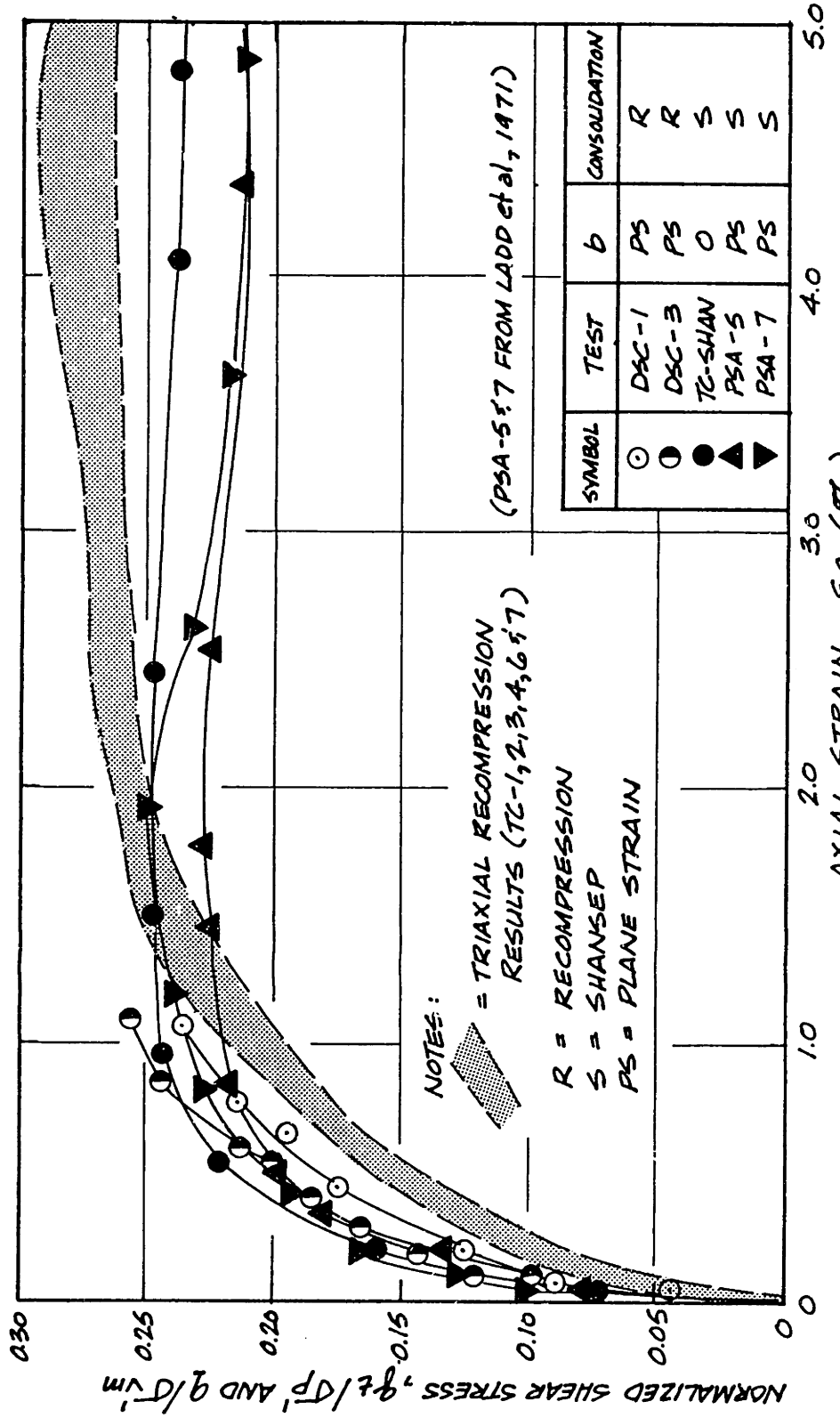

Figure 6.6: Normalized Stress-Strain Curves from δ=0° Tests on Resedimented BBC (OCR=4).

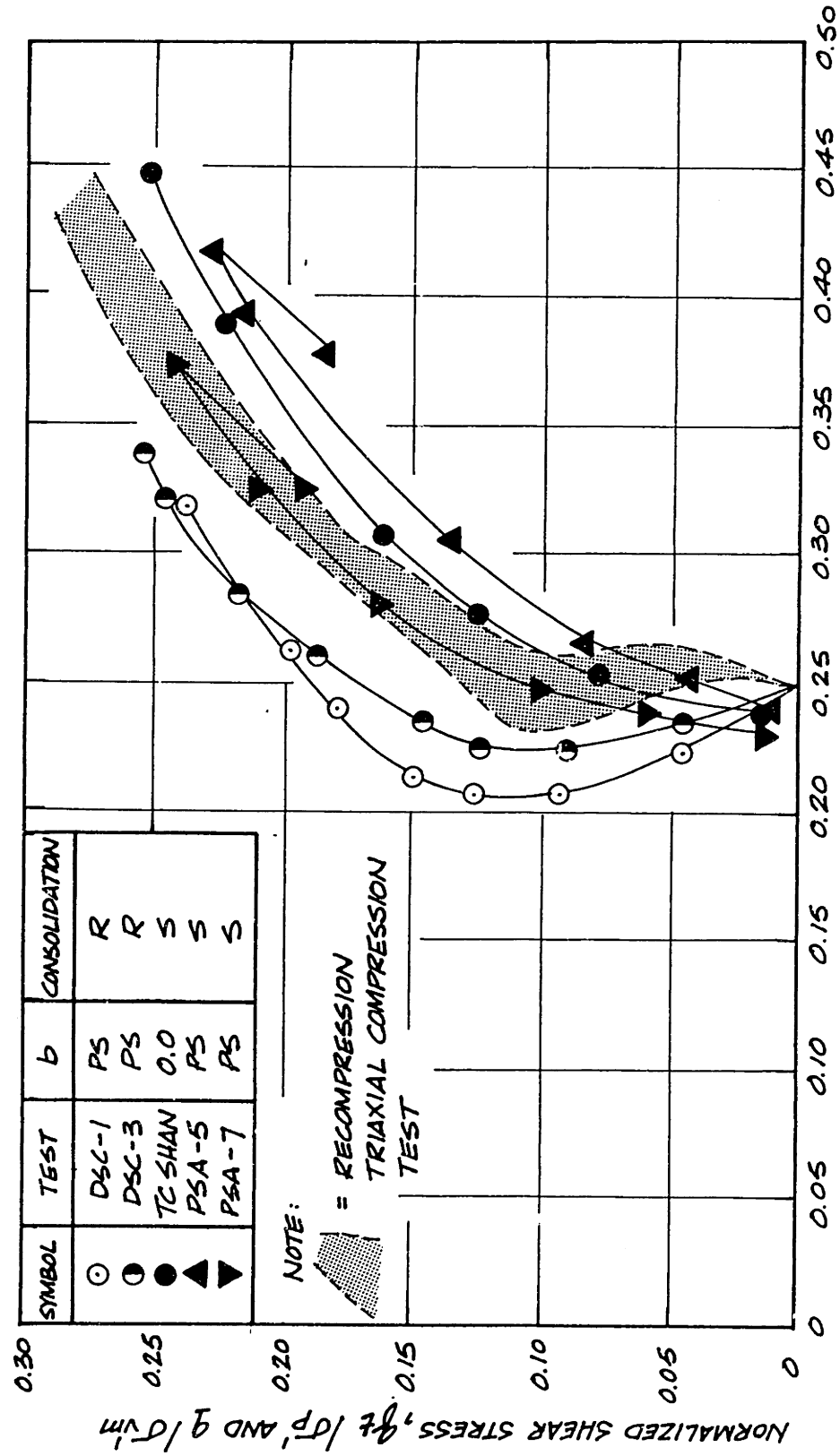

Figure 6.7: Normalized Effective Stress Paths from δ=0° Tests on Resedimented BBC (OCR=4).

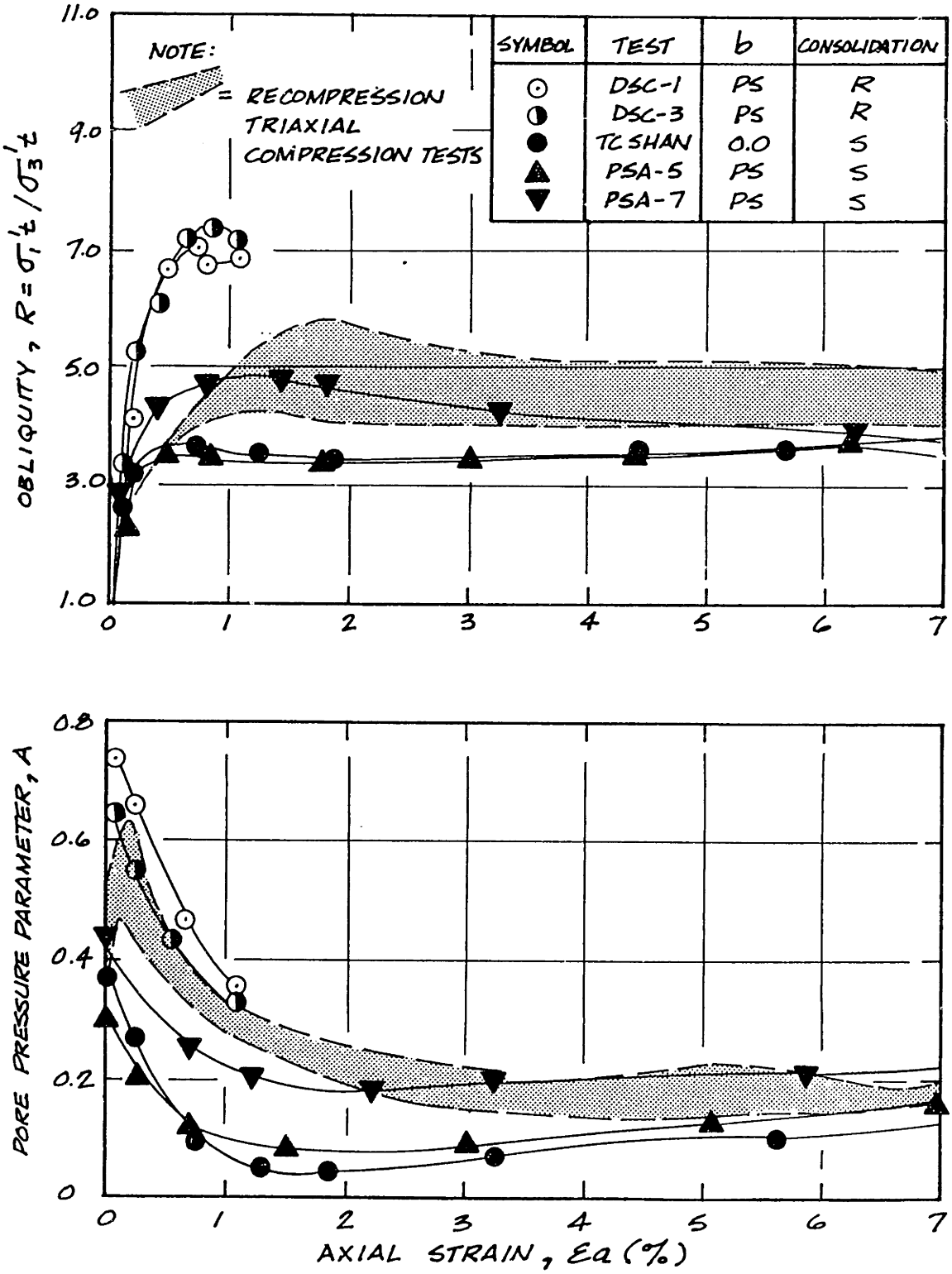

Figure 6.8: Obliquity and Skempton's Pore Pressure Parameter, A, vs. Axial Strain from $\delta=0°$ Tests on Resedimented BBC (OCR=4).

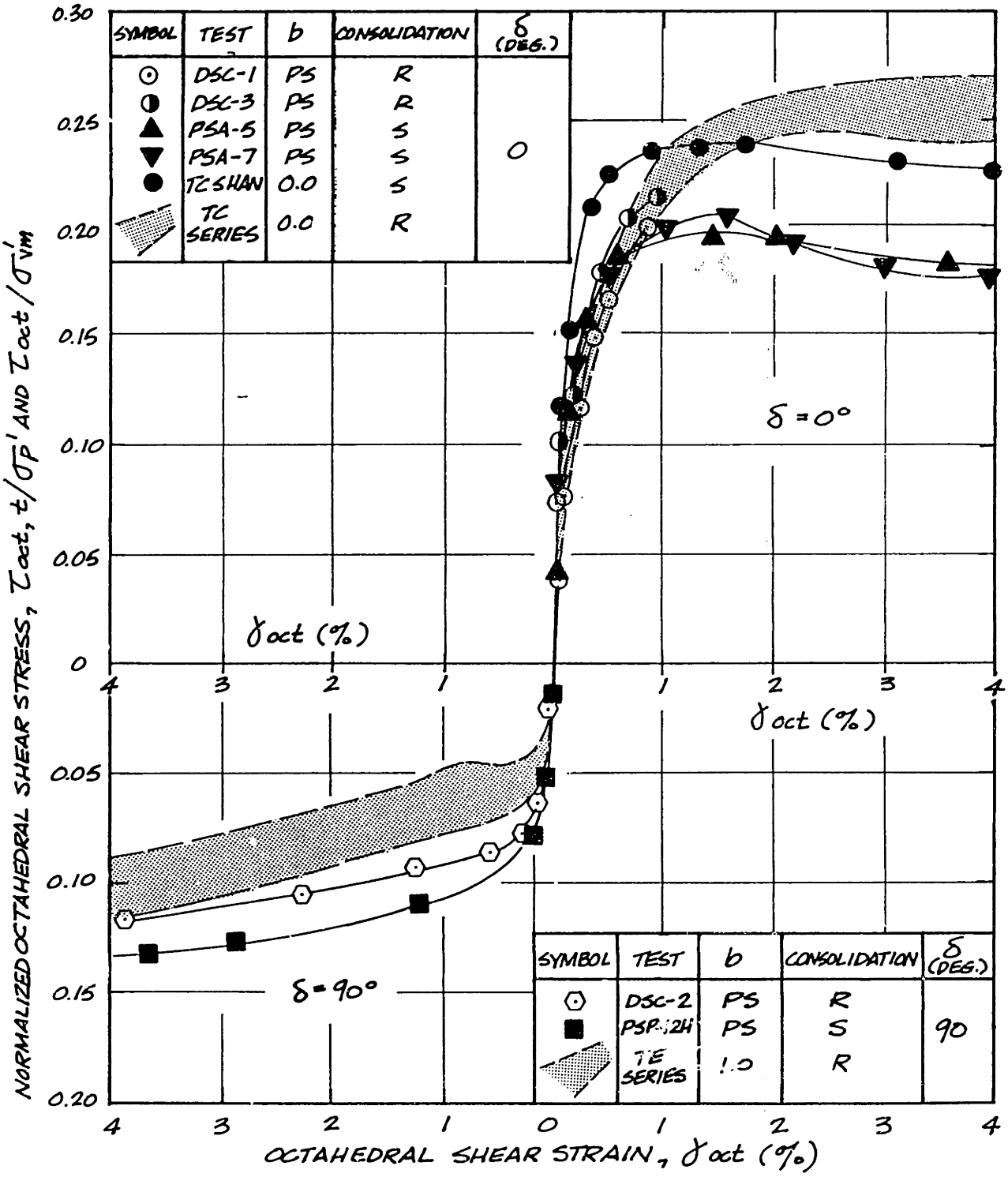

Figure 6.9: Normalized Octahedral Stress-Strain Curves from δ=0° and δ=90° Tests on Resedimented BBC (OCR=4).

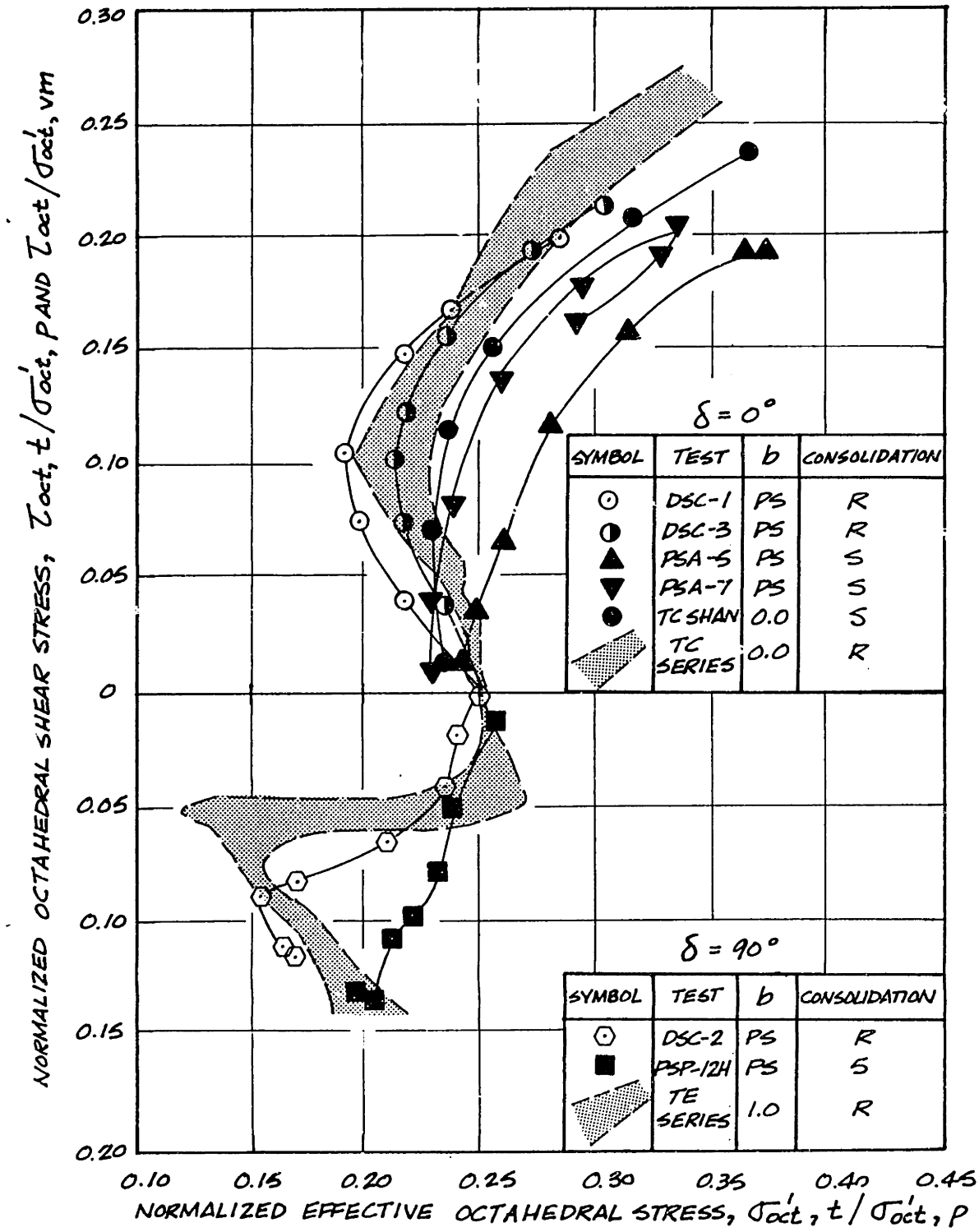

Figure 6.10: Normalized Octahedral Effective Stress Paths from $\delta=0°$ and $\delta=90°$ Tests on Resedimented BBC (OCR=4).

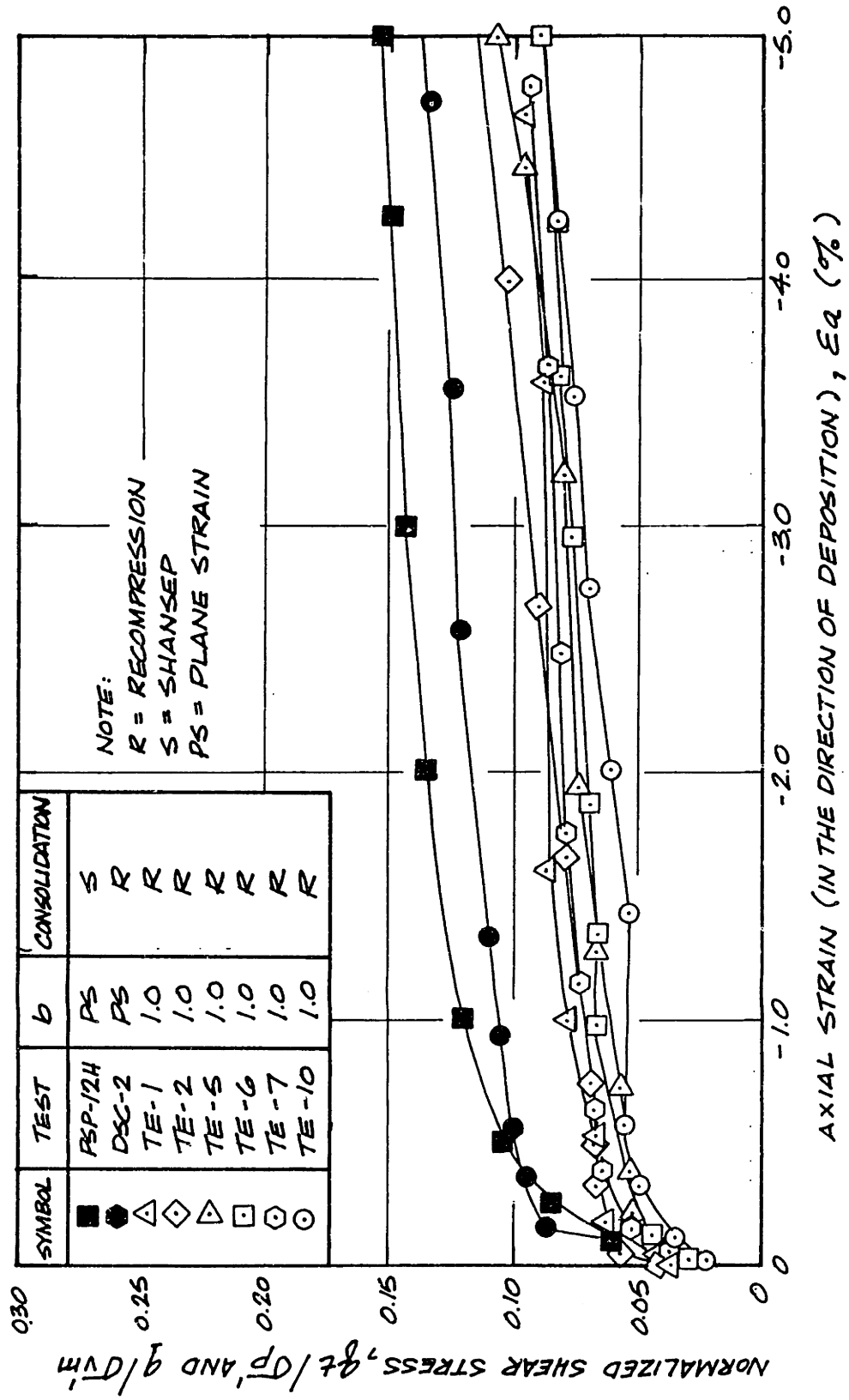

Figure 6.11: Normalized Stress-Strain Curves from δ=90° Tests on Resedimented BBC (OCR=4).

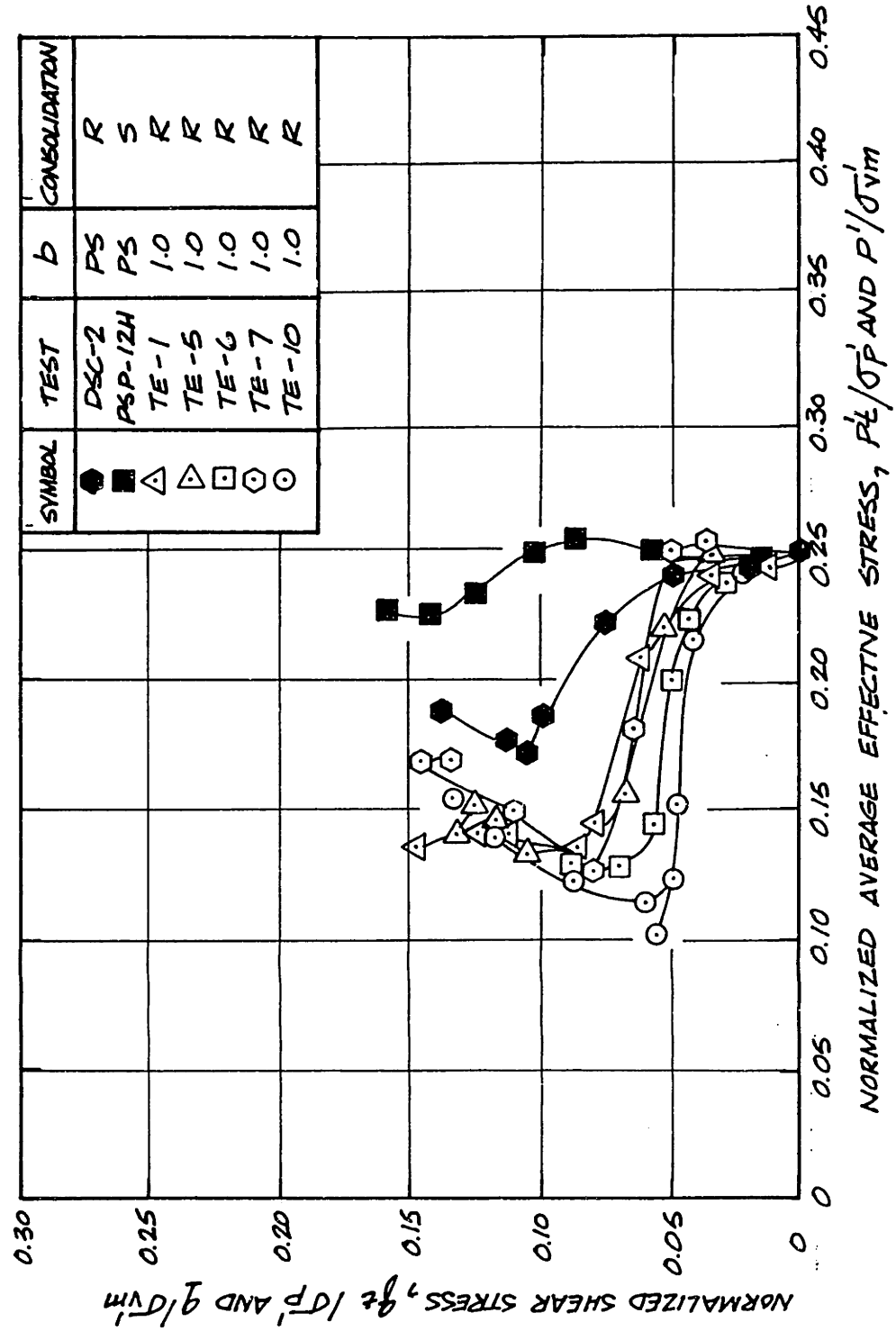

Figure 6.12: Normalized Effective Stress Paths from δ=90° Tests on Resedimented BBC (OCR=4).

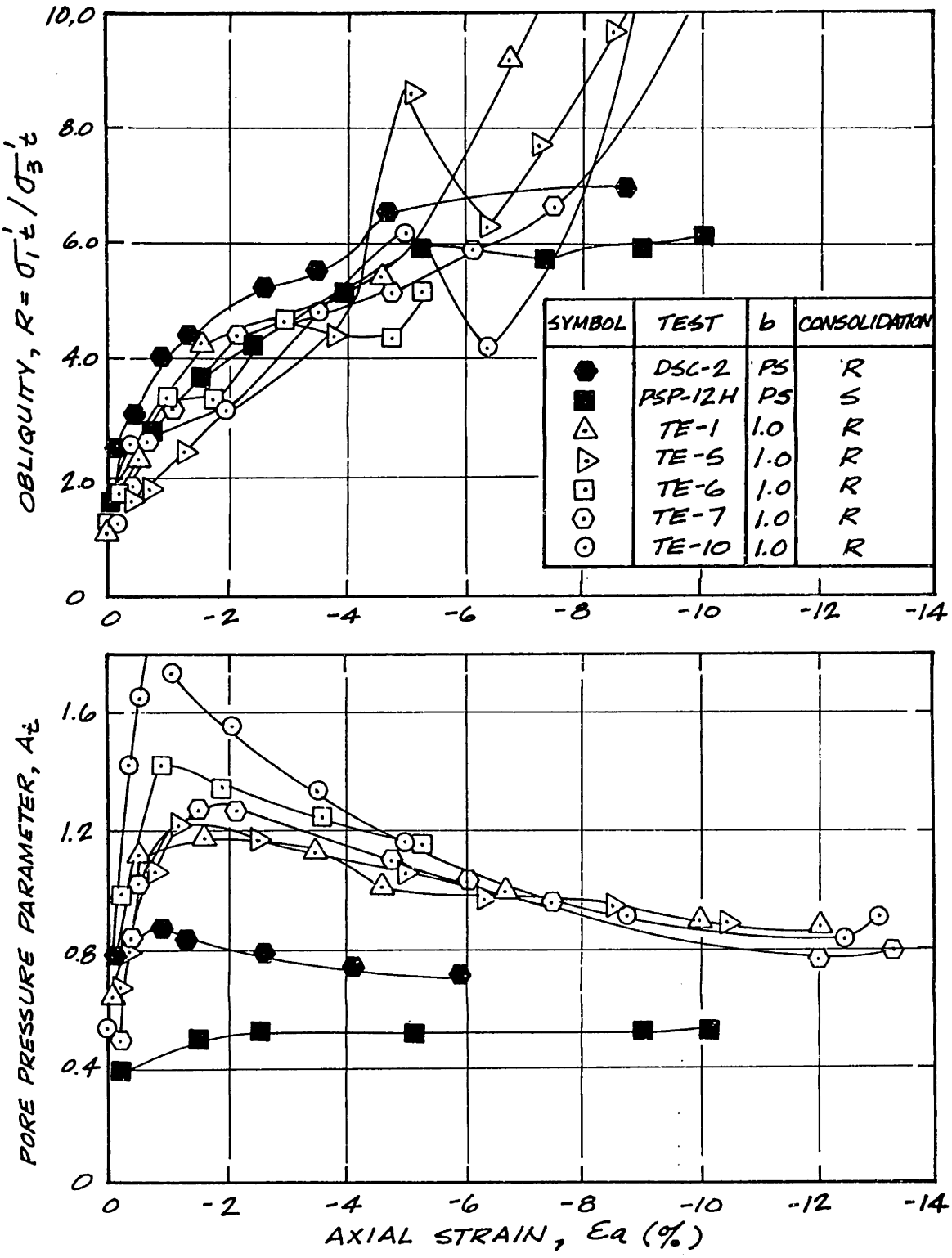

Figure 6.13: Obliquity and Skempton's Pore Pressure Parameter, A, vs. Axial Strain from $\delta=90°$ Tests on Resedimented BBC (OCR=4).

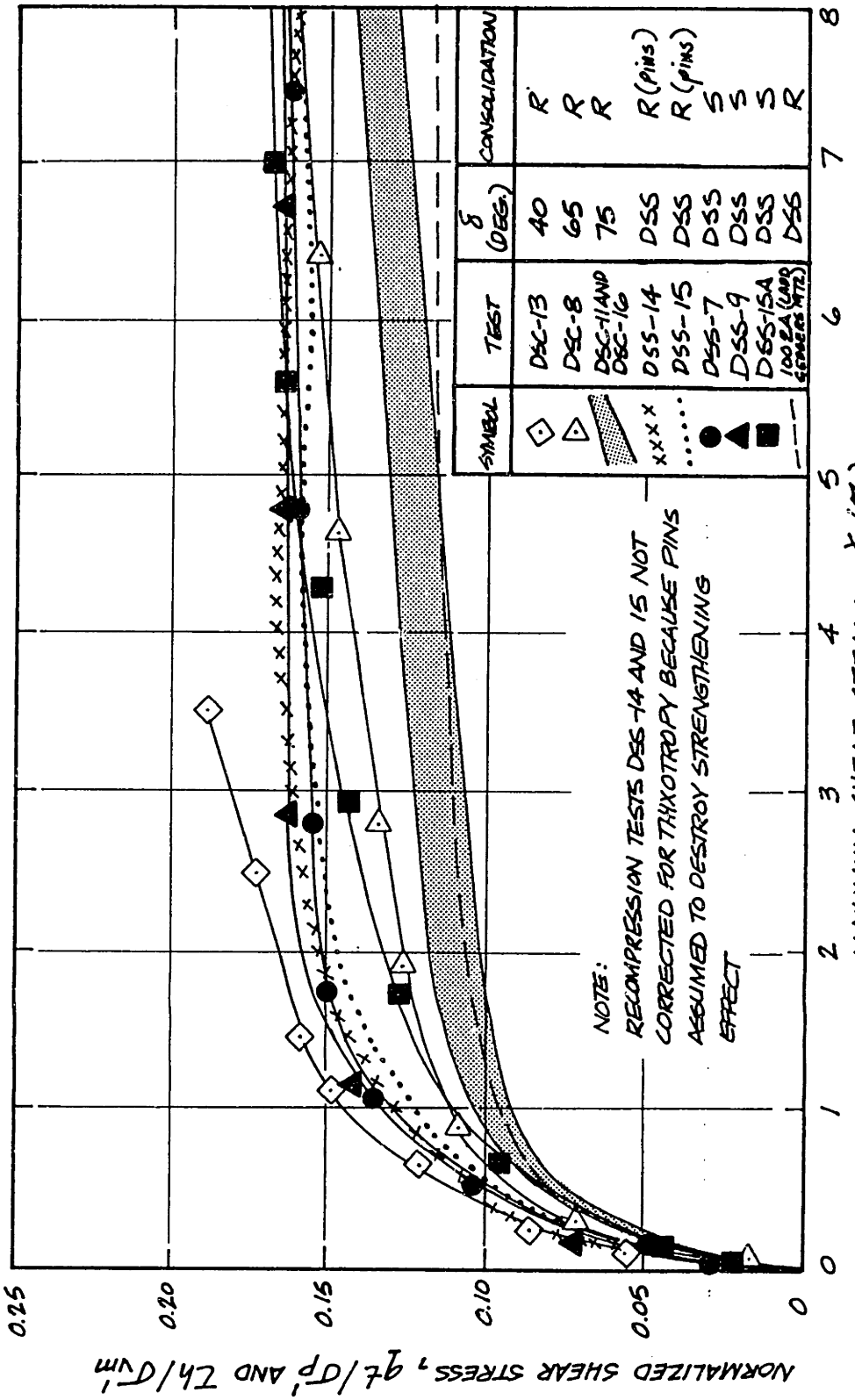

Figure 6.14: Normalized Stress-Strain Curves from DSC Tests at Intermediate δ Angles (δ=40°, 65° and 75°) and from DSS Tests on Resedimented BBC (OCR=4).

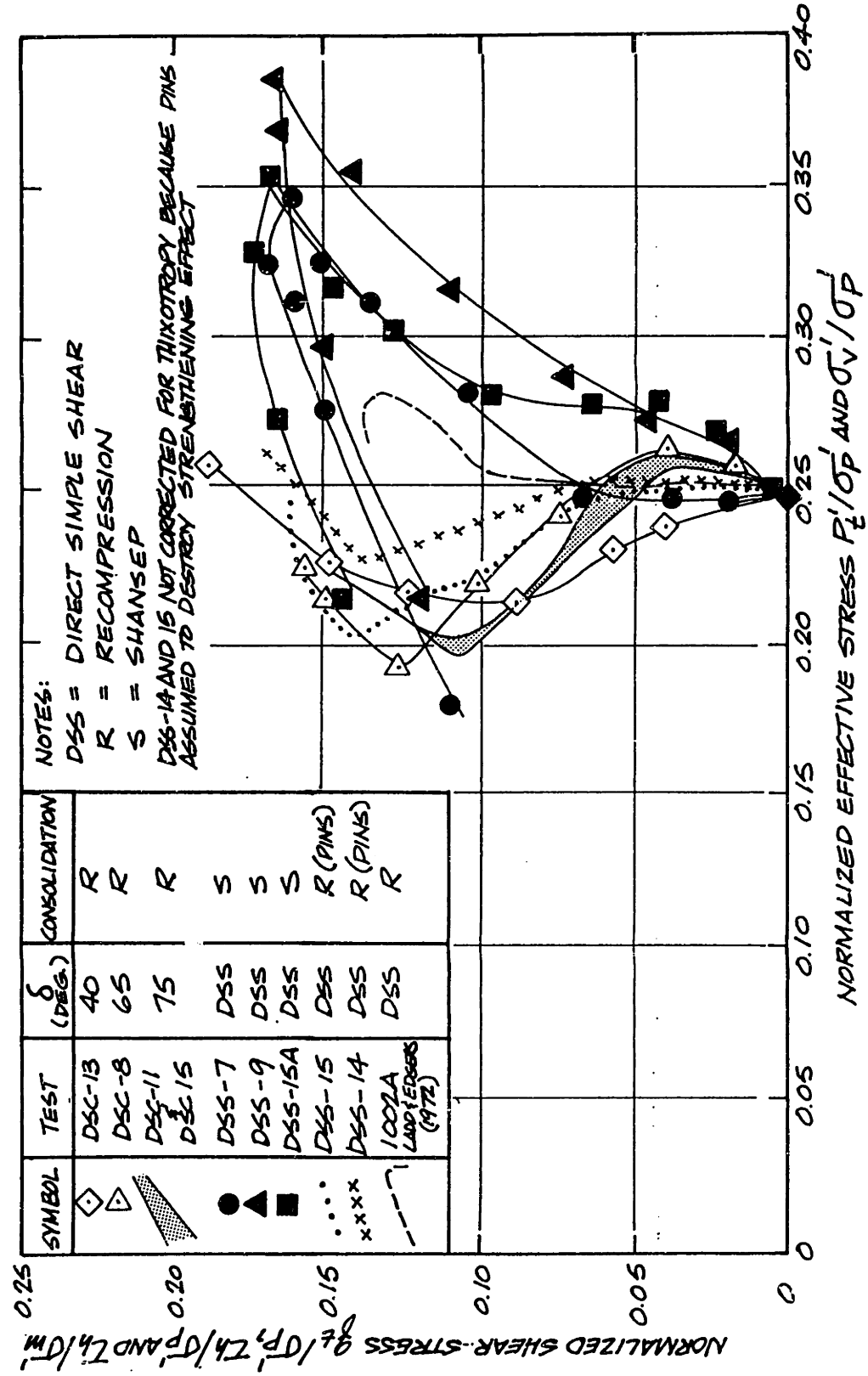

Figure 6.15: Normalized Effective Stress Paths from DSC Tests at Intermediate δ Angles (δ=40°, 65° and 75°) and Normalized Horizontal Shear Stress vs. Vertical Normal Stress from DSS Tests on Resedimented BBC (OCR=4).

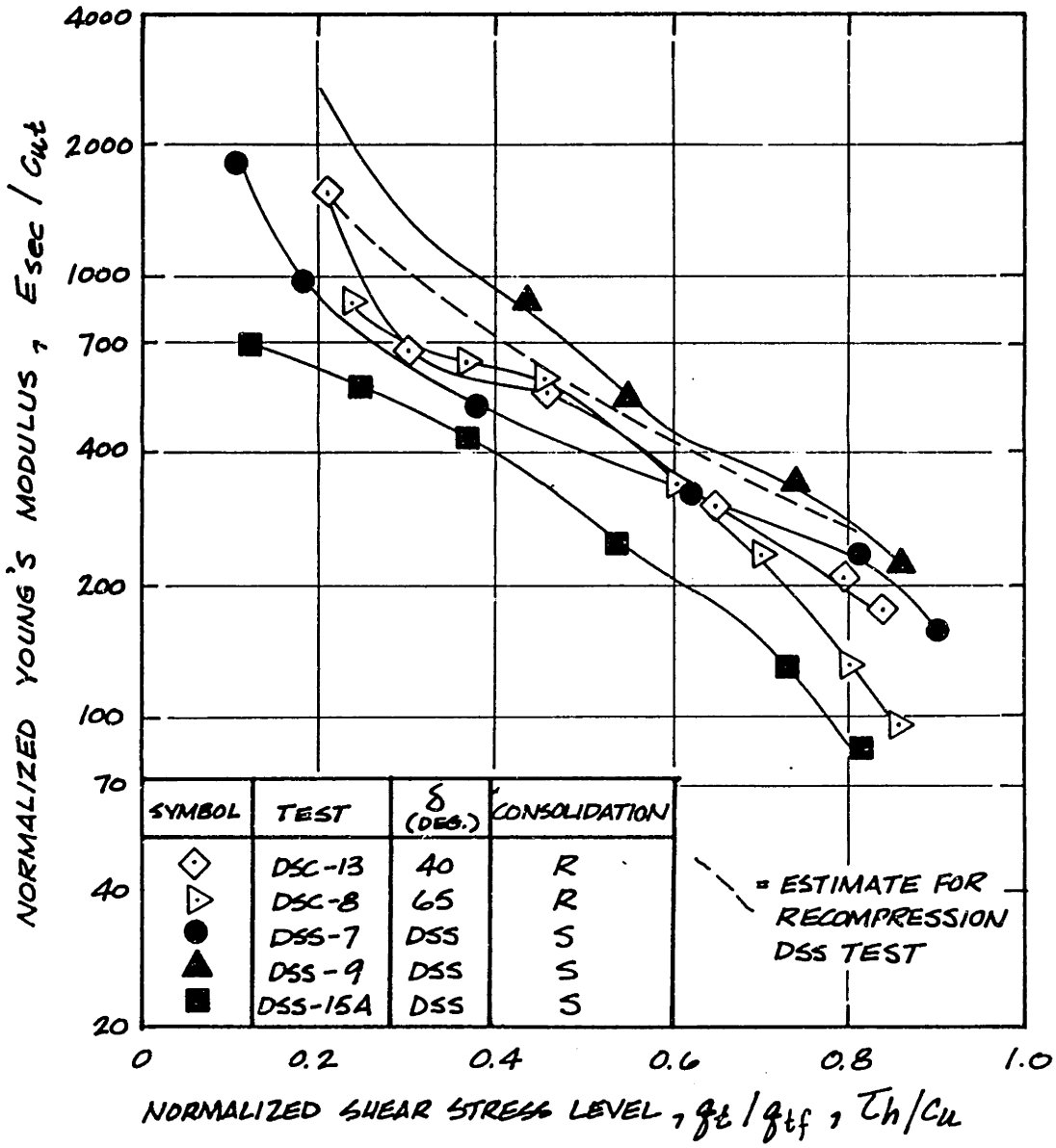

Figure 6.16: Normalized Young's Modulus vs. Shear Stress Level from DSC Tests at Intermediate δ Angles (δ=40° and 65°) and from DSS Tests on Resedimented BBC (OCR=4).

CHAPTER 7

SUMMARY, CONCLUSIONS AND RECOMMENDATIONS

7.1 INTRODUCTION

This research utilizes the Directional Shear Cell (DSC), a plane strain, stress controlled apparatus capable of rotating the major principal stress direction, to investigate the undrained anisotropy of laboratory resedimented Boston Blue Clay (BBC), a low plasticity (I_p=20%, w_L=41%) silty clay. The DSC controls the σ_1 direction during plane strain shear by varying the normal stress (via pressure bags) and the shear stress (via unique shear sheets) acting on the four faces of a cubical sample constrained between two rigid end platens (Section 2.2 and Figs. 2.3 to 2.5). The K_o-consolidated stress history of the OCR=4 BBC has a preconsolidation pressure equal to 1.0 ksc and a final vertical stress equal to 0.25 ksc.

The attraction associated with the use of the DSC is that the rotation of σ_1 occurs without either an accompanying variation in the intermediate principal stress ratio, b [= $(\sigma_2-\sigma_3)/(\sigma_1-\sigma_3)$], or extraneous development of moments due to rigid loading elements. Conventional apparatuses, such as the triaxial cell, the plane strain device (PSD), the Direct Simple Shear (DSS) device, are incapable of measuring solely anisotropic behavior because of various combinations of factors, such as varying b values, development of moments, and difficulties in accomplishing K_o-consolidation prior to shear.

The only other device capable of measuring anisotropic stress-strain-strength behavior is the torsional shear Hollow Cylinder Apparatus (HCA). The HCA sample geometry is of importance in order to minimize both the stress gradient across the thickness of the wall and the end effects. At present, Imperial College has a well-designed HCA which has been used to test the anisotropy of sand. Ultimately, it would be of value to compare results from the DSC with those from the HCA.

Originally, the purpose of this research was to supplement the data regarding the undrained anisotropy of overconsolidated, resedimented BBC presented by Germaine (1982). As experimentation progressed, it became increasingly evident that the elapsed time between sample preparation and shear testing significantly affected the stress-strain-strength results. Much of the effort for this thesis, therefore, was focused on researching the effect of this time-dependent phenomenon (i.e., thixotropy).

The contents of this thesis include:

1) a detailed study of the effect of thixotropy on one-dimensional consolidation characteristics and on Recompression triaxial stress-strain and pore pressure behavior. This latter set of data, from both compression and extension tests, was necessary for the development of a method by which to correct Recompression DSC tests for comparison with one another. (Due to the testing conditions imposed by the present capabilities of the DSC, strains upon

consolidation in the device had to be minimized, therefore, all DSC tests involved Recompression as the method of consolidation.);

2) a complete set of "proof" tests enabling a detailed evaluation of the DSC device including improved testing techniques;

3) a complete set of anisotropic DSC tests, characterizing resedimented BBC at OCR=4 as δ varies from 0° to 90° (δ is the angle between σ_1 and the vertical depositional direction); and 4) comparisons between Recompression and SHANSEP test data, DSC and triaxial data, DSC and data from the MIT plane strain device; and DSC and DSS data.

7.2 SUMMARY AND CONCLUSIONS

7.2.1 Effect of Thixotropy on Overconsolidated Resedimented BBC

Batches of BBC were K_o-consolidated in a large oedometer from a slurry at a water content equal to 100% to σ'_p=1.0 ksc and unloaded to σ'_{vc}=0.25 ksc. After careful extrusion, samples were cut and then stored at constant water content (w≈40%). All DSC test specimens were isotropically reconsolidated (assuming $K_o \simeq$ 1.0) to 0.25 ksc prior to undrained shear. Since thixotropy caused a significant stiffening of BBC during storage (e.g., the measured σ'_p increased by 30% after three months and by 90% after two years), it also had an important effect on the undrained shear

behavior measured in the Recompression DSC test program.

It is hypothesized that the low stress levels, the liquidity index, and the relative youth of the resedimented material (in comparison with in situ materials), in addition to use of the Recompression method of consolidation in the DSC, all contributed to the ultimate importance of the thixotropic effect on undrained shear behavior. The effect of storage time is quantified in Chapter 3; Figs. 3.5, 3.15 and 3.23 present the effect of thixotropy on the measured preconsolidation pressure, triaxial compression and extension yield stress (q_y) and shear-induced pore pressure (Δu_s) respectively. A method by which tests sheared following consolidation using the Recompression technique can be corrected is also presented in Sections 3.2.3 and 3.2.4. The thixotropic phenomenon affects both the resistance of undisturbed resedimented BBC to deviatoric stresses as well as the effective stress behavior. Employing the corrections, tests performed on samples experiencing different storage times can be compared with one another.

Corrections for q ($=0.5(\sigma_1-\sigma_3)$) and p' ($=0.5(\sigma'_1+\sigma'_3)$) pertain only to resedimented BBC at OCR=4 since they were experimentally derived. It is not known if thixotropy causes an absolute change in the 1-D consolidation yield stress and triaxial strength or if the magnitude of the effect is proportional to σ'_p (i.e. normalizeable) since all data are from batches consolidated to the same stress conditions.

The importance of the corrections is demonstrated by the

following data which show the change in the undrained shear strength (q_f) and effective stress at failure (p'_f) when the length of storage (t_s) is taken into account. The basis for these corrections are presented in Table 3.6 and Fig. 3.24. Note that, since corrected values (q_{tf} and p'_{tf}) from the three triaxial compression and three extension tests are not identical, the correction is not perfect. However, the scatter is very small, i.e., a coefficient of variation of only 2% for p'_{tf} in TC and about 6% for q_{tf} in TC, and p'_{tf} and q_{tf} in TE.

Test	δ (deg)	t_s (days)	q_{tf} ($=q_f-\Delta q_y$) (ksc)	p'_{tf} ($=p'_f-\Delta p'$) (ksc)	$\frac{\Delta q_y}{q_f}$ (%)	$\frac{\Delta p'}{p'_f}$ (%)
TC-1	0	29	0.275	0.444	5.8	7.5
TC-4	0	112	0.259	0.428	9.8	9.1
TC-3	0	225	0.290	0.438	17.1	20.1
TE-1	90	36	0.147	0.137	11.4	15.4
TE-5	90	62	0.132	0.140	13.7	17.6
TE-10	90	359	0.132	0.154	36.2	39.1
DSC-1	0	29	0.237	0.318	7.1	9.4
DSC-3	0	60	0.254	0.337	7.6	10.1
DSC-15	20	92	0.219	0.307	9.5	12.0
DSC-13	40	39	0.189	0.260	9.1	11.6
DSC-8	65	167	0.156	0.223	22.8	25.2
DSC-11	75	71	0.147	0.224	13.0	14.8
DSC-16	75	105	0.160	0.234	14.4	15.5
DSC-2	90	44	0.138	0.188	12.7	15.7

Recompression triaxial compression tests have a correction from about 6% to 17% on q_f and from 8% to 20% for p'_f. (Only a very "young" TC test (t_s=29 days), a very "old" test (t_s=225 days) and a test of approximately the average age for the TC test series are shown). Data from Chapter 3, specifically

presented in Fig. 3.13 and 3.23, indicate the isotropic nature of the thixotropic effect. Due to the much lower strength in triaxial extension, the impact of correction is much greater: an 11% to 36% decrease in undrained shear strength and a 15% to 39% decrease in p'_f. (Again only a young, an old and an intermediate test are shown). It is interesting to note that the percentage decrease in q is approximately equal to (although usually slightly less than) that for the average effective stress, p'.

For the DSC tests, correction for storage amounts to between 7% and 23% of the undrained shear strength and between 9% and 25% of the average effective stress at failure. Clearly, failure to consider the effect of hardening on undrained shear behavior would lead to incorrect assessments as to variation in stress-strain-strength parameters with either angle of shear or the applied stress system.

7.2.2 Proof Testing the DSC

The stress application capabilities of the DSC as well as its ability to handle the sample strain response are evaluated in Chapter 4. Much of the evaluation is based upon results of five DSC tests performed in the isotropic plane of BBC. (K_o-consolidation of the batch produces a cross anisotropic material in which the plane perpendicular to the direction of deposition [i.e., the horizontal X-Y plane in Fig. 2.5] is isotropic).

Potential corrections to applied stresses due to the

effects of the membrane, the shear sheets and the silicon-teflon grease are assessed. The membrane correction is judged negligible, the shear sheets are determined to not appreciably affect behavior if their orientation with respect to the side of the sample is closely monitored during shear and the measured adhesion of the silicon-teflon grease is only 0.007 ksc. Correction for the effect of the grease is applied only as a reduction of the shear sheet traction, although grease is present on the glass platens as well. The latter case affects applied shear stresses and normal stresses but is very complicated to assess and is probably small.

Isotropic DSC test stress-strain curves and effective stress paths are plotted in Figs. 4.21 and 4.22, respectively. Pertinent data from the series of tests performed in the isotropic plane are listed below (all corrected for thixotropic hardening):

Test	ψ (deg)	$\frac{q_{vf}}{\sigma'_p}$	$\frac{G_{v,f}}{\sigma'_p}$	@ $(\sigma_1-\sigma_3)_f$					Θ (deg)	Δ (deg)
				γ (%)	$\frac{q_f}{\sigma'_p}$	$\frac{p'_f}{\sigma'_p}$	$\frac{\sigma_{1f}'}{\sigma_{3}'_f}$	A_f		
DSC-6	0	0.144	0.67	6.9	0.183	0.227	9.32	0.56	--	-0.6
DSC-12	0 (w/SS)	0.132	0.67	7.0	0.169	0.210	9.24	0.62	25±1	-0.6
DSC-9	25	0.122	1.0	4.4	0.163	0.193	11.9	0.68	31±3	-3.5
DSC-14	40	0.132	0.87	4.3	0.166	0.202	10.2	0.65	25±1	-2.9

where ψ = angle of shear as defined in Fig. 2.5

σ_y = yield stress

G_y = shear modulus after yielding

A = Skempton's A parameter subscript t indicates that the value has been corrected for thixotropy

θ = angle between failure plane and major principal stress direction

Δ = deviation between the direction of major principal strain and major principal stress.

subscript t indicates that the value has been corrected for thixotropy.

DSC-7 (ψ=45°) is not included since this test failed to pass the stress application standard (described in Section 4.3.2.2). DSC tests performed in the isotropic plane simulate a stress system essentially equivalent to that in which both pressuremeter tests and cavity expansion analyses are interpreted.

The average normalized undrained shear strength of resedimented BBC as measured at various ψ angles in the DSC is equal to 0.170 ± 0.009 SD. The average maximum shear strain at failure (as indicated by onset of failure plane formation) is about equal to 6%. Stress-strain behavior is such that the isotropic plane is more ductile than the anisotropic test at δ=40° but is stronger than the anisotropic test at δ=65°; that is the isotropic curves fall between these two anisotropic tests. The mean normalized average effective stress, p'_t/σ'_p, at failure is 0.208, with an average obliquity equal to 10.2 and an average pore pressure parameter at failure, A_f, of 0.63.

The data tabulated above and Figs. 4.21 and 4.22 show that tests sheared (undrained) via the pressure bags (i.e., DSC's-6 and 12) failed at slightly greater shear stress levels, greater shear strain levels and greater average effective stresses compared to those tests using shear sheets (ψ=25° and 40°). All of these tendencies are believed to be associated with inhibition of strain caused by stressed shear sheets. Failure values of q_t and p'_t for all the isotropic tests suggest a unique failure envelope (Figs. 4.22 and 5.9). Hence, when the sample is constrained by the shear sheets, it reaches this envelope at lower values of q because positive dilation (decreasing shear-induced pore pressures) is inhibited. Careful maintenance of the orientation of the shear sheets and the pressure bags parallel to the faces of the sample minimizes this effect.

The strain distribution pattern of the isotropic DSC tests presented in Fig. 4.27 provides further evidence that there is some device-induced strain behavior. The Normalized Ring Strain (NRS) variation with the angle of shear, ψ, shows that samples sheared using shear sheets tend to strain more near the faces of the sample, while samples sheared using only differential normal stresses strained slightly more in the central portion. In addition, the DSC appears to cause a slight deviation between the direction of the major principal strain and that of the major principal stress at angles of shear which involve use of both pressure bags and shear sheets. The measure of this deviation, Δ, presented in the lower plot

of Fig. 4.27, should have been equal to zero, regardless of the value of ψ if the device was capable of applying uniform stresses in an ideal manner. The pattern of Δ vs. ψ developed from isotropic DSC tests is taken into account in assessing Δ associated with anisotropic DSC tests.

In summary, the isotropic DSC tests probably constitute the only test series on clay which provide "proof" tests for a complex shear device. These data show that there are device related problems associated with the shear sheets. Use of these flexible, shear traction application elements leads to lower shear strengths and strains at failure, larger values of Δ and more scatter in the strain distribution.

To put this information into perspective, the measured $COV[q_f]=5\%$ from the isotropic DSC tests which involve very different means of applying shear stress (i.e., pressure bags vs. shear sheets) is compared with COV values from other test programs. The following COV values were computed from data reported in the literature for tests having identical modes of shearing.

a) Lade and Musante (1978) report data from True Triaxial (TTA) tests on Grundite Clay at b=0.2 and 0.4: $COV[c_u/\sigma'_{vc}]$ = 8% and 11%, respectively.

b) Saada and Bianchini (1975) report data from CIU Hollow Cylinder Apparatus tests on Edgar Plastic Kaolin at δ=15°, 32°, 58° and 75°:

Material	σ'_c(psi)	COV[$\frac{c_u}{\sigma'_{vc}}$]
Edgar Plastic Kaolin	40	11 ± 8
	60	6 ± 1
	80	7 ± 5
Atchafalaya Clay	40	2.5 ± 2
	60	6 ± 2
	80	5 ± 2

Note that the HCA technique used by Saada involved use of equal inner and outer cell pressures leading to a unique variation in b with δ (Fig. 2.1).

Therefore, the isotropic DSC data appear as or more reproduceable than either TTA or HCA (from Saada and Bianchini, 1975) tests. In addition, the errors on an absolute basis for the isotropic DSC tests are considered very small, except for the Δ angles wherein the measured values are used to correct the anisotropic Δ values. In addition, there is some error involved in the surface measurement of strain as opposed to internal measurement (Wong and Arthur, 1985). Hence, the DSC is judged reliable as a device for measuring the anisotropy of clays.

7.2.3 Effect of Principal Stress Direction on the Undrained Shear Behavior of Overconsolidated Resedimented BBC

Anisotropic stress-strain-strength behavior of BBC was measured in the DSC using samples consolidated via Recompression to an overconsolidation ratio of four. Several

of the DSC tests performed in the cross anisotropic plane were discarded because they failed to pass either the strain distribution standard explained in Section 4.1.1 and applied in Section 5.2.1.1 (e.g., DSC-4 (δ=45°) and DSC-10 (δ=20°) or the stress application standard discussed in Section 4.1.2 and applied in Section 5.2.1.2 (e.g., DSC-5 [δ=45°]).

Anisotropic DSC stress-strain effective stress path and obliquity and A-parameter data are presented in Figs. 5.7, 5.8 and 5.11, respectively. Some of the important parameters from the anisotropic DSC tests passing the standards are tabulated below:

TEST	δ (deg)	$\frac{q_{yt}}{\sigma'_p}$	$\frac{G_{yt}}{\sigma'_p}$	@ $(\sigma_1-\sigma_3)_f$					θ (deg)	Δ^* (deg)
				γ (%)	$\frac{q_t}{\sigma'_p}$	$\frac{p't}{\sigma'_p}$	$\frac{\sigma_1't}{\sigma_3't}$	A_t		
DSC-1 DSC-3	0	0.199	3.00	2.2	0.246	0.328	6.99	0.343	22±1	-0.4
DSC-15	20	0.166	1.95	3.6	0.219	0.307	5.98	0.370	27±3	+1.0
DSC-13	40	0.144	1.48	3.5	0.189	0.260	6.32	0.474	34±2	+4.0
DSC-8	65	0.112	0.79	6.5	0.156	0.223	5.66	0.587	31±2	+1.9
DSC-11 DSC-16	75	0.100	0.55	13.5	0.154	0.229	5.07	0.569	27±3	+2.1
DSC-2	90	0.093	0.55	9.5	0.138	0.188	6.52	0.725		-1.1

* Value of Δ takes isotropic DSC Δ values as zero.

Further data are presented in Chapter 5 with Figs. 5.13 to 5.15 graphically illustrating the variation of the yield and failure strengths, the strain at failure, γ, the pore pressure

parameter, A and the obliquity, R with increasing angle of shear, δ.

It is evident from these data that resedimented BBC at OCR=4 exhibits an inherent anisotropy of sufficient degree to decrease the yield stress, q_{yt}/σ'_p by 53% and to decrease the shear stress at failure, q_{ft}/σ'_p, by 44% as the angle of shear increases from $\delta=0°$ to $\delta=90°$. Following yield, the shear modulus decreases linearly as δ is increased until the passive region of shear (i.e., $\delta>45°$) is reached. The decrease in G_y/σ'_p with increasing δ in the passive region is much smaller than in the active region. This pattern of more rapid change in engineering properties in the active region ($0°<\delta<45°$) as compared to change in the passive region applies to the pore pressure parameter, A, and the obliquity, R, as well.

Although less conclusive, the data indicate positive values of the Δ angle (meaning that ε_1 leads the σ_1 direction) that reach a peak of about 4° at $\delta\approx45°$ and decrease to about zero at $\delta=0°$ and 90°.

7.2.4 Comparison of DSC Test Results with Data from Other Devices

7.2.4.1 Introduction

DSC test data on the cross anisotropic plane of resedimented BBC were compared with results from several, more conventional, devices. For tests having the same (or similar) δ angles, the variables were:

1) the magnitude of σ_2 as measured by the relative

intermediate principal stress ratio, b (= $(\sigma_2-\sigma_3)/(\sigma_1-\sigma_3)$); and

2) the method of consolidation: Recompression vs. SHANSEP.

Specifically, the following types of data are compared for OCR=4 BBC:

δ (deg)	RECOMPRESSION	SHANSEP
0	DSC TC	PSA (Plane Strain Active) TC
90	DSC TE	PSP (Plane Strain Passive)
Intermediate	DSC DSS	DSS

7.2.4.2 Effect of the Method of Consolidation

From the scant data available concerning the effect of Recompression vs. SHANSEP as the method of consolidation, discussed at length in Section 6.2 and summarized in Table 6.1, the following trends are noted:

- In triaxial compression tests (i.e., $\delta=0°$) on resedimented BBC at OCR=4, the Recompression tests gave slightly (~10%) greater peak strengths than the SHANSEP test although the SHANSEP test was much stiffer than the Recompression tests (Fig. 6.3). Strain at peak stress was much lower in the SHANSEP test. The average effective stresses of the SHANSEP test were slightly greater, during shear, than p' from the Recompression tests, except at peak strength

where p' was approximately the same for data from both methods (Fig. 6.4). Therefore, the obliquity at peak stress was greater for the Recompression tests than for the SHANSEP test.

- For $\delta=90°$, there are no triaxial data for comparison of consolidation methods. The only data available are the PSA test of Ladd et al. (1971), PSP-12H, which is a SHANSEP type test, for comparison to DSC-2 ($\delta=90°$) which is a Recompression type test. Bearing in mind the difficulties associated with the PSP test, it can only be tentatively concluded that the SHANSEP test leads to a greater peak strength and to higher average effective stresses than the Recompression DSC test (see Figs. 6.11 and 6.12).
- At intermediate angles of shear, as measured in the DSS, SHANSEP tests on resedimented BBC showed very similar stress-strain characteristics when compared with Recompression tests (performed with pins to prevent slippage and not corrected for thixotropy, Fig. 3.25). As with tests at $\delta=0°$ and $\delta=90°$, the Recompression tests have lower effective stresses at given shear stress levels (Fig. 3.26).
- For SHANSEP vs. Recompression data on other soils, such as Connecticut Valley Varved Clay and Lower Cromer Till, refer to Section 6.2 and Figs. 6.1 and 6.2.
- It is hypothesized that the cause of the effect of the method of consolidation on undrained shear for

overconsolidated soils lies not in the difference in water content nor in the degree of disturbance but rather in the direction of the consolidation increment immediately prior to shear (i.e., unloading vs. reloading).

7.2.4.3 Comparison of Results at $\delta=0°$

At $\delta=0°$, the plane strain DSC tests, DSC-1 and 3, are compared to triaxial compression and conventional plane strain tests. Detailed comparisons are presented in Section 6.3.

Tests performed at $\delta=0°$ on resedimented BBC at OCR=4 are presented in the following table which also identifies the method of consolidation employed and the value of b during shear. (For plane strain tests where σ_2 was not measured but usually attains a value of approximately 0.4, the letters "PS" are used to indicate that strain was zero in the σ_2 direction).

Test	Source	Method of Consolidation	b $(= \frac{(\sigma_2-\sigma_3)}{(\sigma_1-\sigma_3)})$	$\frac{q_{tf}}{\sigma'_p}; \frac{q_f}{\sigma'_p}$
DSC-1 DSC-3	This research	Recompression	PS PS	0.246
PSA-5 PSA-7	Ladd et al. (1971)	SHANSEP	PS PS	0.236
TC series	This research	Recompression	0	0.279 ± 0.012
TC-SHAN		SHANSEP	0	0.252

Table 6.3 summarizes the results at peak shear stress for these $\delta=0°$ tests. The following points regarding undrained shear behavior are noteworthy:

- As shown in Fig. 6.6, the DSC and PSA tests compare well with one another. The Recompression triaxial compression (TC) series, on the other hand, resulted in higher peak shear stresses at higher levels of axial strain (i.e., strain parallel to the axis of deposition) than did the plane strain (DSC and PSA) tests. When considered in a generalized stress state, the plane strain DSC test results coincide with the Recompression triaxial tests (Fig. 6.9), until a failure plane develops in the DSC tests. The triaxial tests then continue to strain, reaching peak shear stress at greater values of both γ_{oct} and τ_{oct}/σ'_{oct} (Fig. 6.10) than do the DSC tests.
- The Recompression TC tests are initially softer than the plane strain tests (for axial strains less than 1%) when considering normalized maximum shear stress vs. maximum shear strain. However, in octahedral stress-strain space, the Recompression TC, DSC and SHANSEP PSA tests exhibit similar stiffnesses. The SHANSEP TC test is much stiffer than the SHANSEP PSA tests in the octahedral τ vs. γ space in Fig. 6.9. As discussed in Section 6.2, it is possible that the TC-SHAN data are suspect.
- The DSC $\delta=0°$ effective stress paths have lower average effective stresses than the triaxial tests, a feature essentially attributable to the effect of the relative magnitude of σ_2. (The PSA tests have higher normalized average effective stress in both q vs. p' and τ_{oct} vs. σ'_{oct} space due to the SHANSEP method of consolidation

used in these tests).

- The DSC $\delta=0°$ tests attain much higher (29%) obliquities than either the triaxial or PSA tests.
- The Recompression type tests (DSC and triaxial) exhibit essentially similar variation in Skempton's pore pressure parameter, A, with axial strain (Fig. 6.8) although the DSC values are slightly greater. The SHANSEP tests exhibit consistently lower values of A.

7.2.4.4 Comparison of Results at $\delta=90°$

Data from tests performed in the extension mode on resedimented BBC at OCR=4 are available from three devices: the DSC, the MIT plane strain apparatus and the conventional triaxial device. The following table identifies the tests performed and the method of consolidation employed.

Test	Source	Method of Consolidation	$b\ (=\frac{(\sigma_2-\sigma_3)}{(\sigma_1-\sigma_3)})$	$\frac{q_{tf}}{\sigma'_p}$
DSC-2	This research	Recompression	PS	0.138
PSP-12H	Ladd et al. (1971)	SHANSEP	PS	0.161
TE series	This research	Recompression	0	0.143 ± 0.012

The most noteworthy results of comparisons of undrained shear behavior from the various devices are as follows:

- The plane strain test performed in the old MIT device,

PSP-12H, is stronger than DSC-2 (Fig. 6.11), a phenomenon attributed to the SHANSEP type consolidation used in the former test.

- The plane strain tests (DSC (δ=90°) and PSP) are about 75% stronger than Recompression TE when comparing shear stresses at equal axial strain of less than 5% (Fig. 6.11).
- There is less difference, however, in τ_{oct} vs. γ_{oct} space (Fig. 6.9). τ_{oct}/σ'_p [DSC-2 (δ=90°)] is only about 15% greater than τ_{oct}/σ'_p[TE].
- In normalized q vs p' space (Fig. 6.12), the triaxial extension tests exist at much lower effective stresses than either DSC-2 or PSP-12H. (The latter plane strain test has higher effective stresses than the DSC test due to SHANSEP consolidation).
- As seen in Fig. 6.13, all the δ=90° tests attain similar obliquities at axial strain levels less than about 6%. At higher strain levels TE tests approach significantly higher values of R than the plane strain tests.
- The triaxial extension tests exhibit a higher pore pressure parameter at low axial strain but the difference between A from TE tests and that from the DSC test decreases with increasing strain.
- In normalized octahedral stress space (Fig. 6.10) the triaxial extension tests exhibit higher effective stresses (lower shear-induced pore pressures, Δu_s) at low values of τ_{oct}, greater values of Δu_s at intermediate stress levels

and end up at higher σ'_{oct} as compared with the DSC test.

7.2.4.5 Comparison of Results at Intermediate Values of δ

Section 6.5 discusses undrained shear behavior of BBC (OCR=4) as measured in the DSC at values of δ ranging from 40° to 75°, compared with results from the Direct Simple Shear (DSS) device on the same material. Since the DSS imposes a condition of continuous rotation of the major principal stress in an indeterminate stress state, the purpose of comparing the DSC results to the DSS data was to investigate the value of δ that DSS results best simulate, and to evaluate whether or not the DSS produces reasonable stress-strain data.

Taking the consolidation history of the samples into account (some of the DSS data are from SHANSEP type tests), the following trends are identified (note that all comparisons are based on the assumption that $\tau_h=q$ for the DSS):

- As shown in Fig. 6.14, the DSS stress-strain curves fall between those of δ=40° and δ=75° DSC tests. Bearing in mind consolidation history, use of pins and the lower strength behavior of Test No. 1002A, it is hypothesized that ideal Recompression behavior in the DSS is weaker than the SHANSEP and Recompression series of this research and stronger than Test No. 1002A. Taking this into account, at maximum shear strain levels less than 2%, the DSS results mirror the stress-strain behavior of the isotropic DSC test series presented in Fig. 4.21.
- The large strain (γ>2 to 3%) behavior of BBC tested under

DSS conditions is almost perfectly plastic (Fig. 6.14) while DSC results at intermediate values of δ indicate strain hardening (i.e., yielded shear moduli greater than 0.5). It is the strain-hardening nature of both anisotropic and isotropic DSC tests which causes deviation of those curves from the DSS data.

- It is concluded, based on the stress-strain behavior discussed above, that the DSS best simulates values of δ between 50° at low shear strains to about 70° at higher strains. The strength (i.e., the maximum horizontal shear stress at failure) measured by the DSS probably simulates the strength of the material at a particular value of δ which depends on the strain at failure. The greater γ_f, the greater the simulated δ. For resedimented BBC with γ_f=5 to 10%, the simulated value of δ is approximately 70°.
- The normalized DSC stress paths at intermediate values of δ compare well with the normalized τ_h vs. σ'_v paths followed by the Recompression DSS tests, (Fig. 6.15). The SHANSEP DSS tests, however, indicate significantly less shear-induced pore pressures, a feature common to all comparisons of SHANSEP to Recompression results.
- The normalized Young's modulus from the DSS tests is very similar to that resulting from DSC tests at δ=40° and 65° (Fig. 6.16).

It is concluded that SHANSEP consolidated DSS tests at OCR=4 will result in stress-strain curves which simulate lower

values of δ (i.e., stronger behavior) as compared with Recompression behavior. However, more DSS data are necessary to evaluate Recompression behavior in this device. The effect of the pins and top cap slippage require that Recompression behavior be studied by using the second type of Recompression (Section 6.2) which involves loading, unloading and reloading. The effect of storage time was not measurable with the Recompression data using pins, presumably due to the disturbance associated with them.

7.3 RECOMMENDATIONS FOR FUTURE RESEARCH

The recommendations which follow have three different sources of inspiration:

1) difficulties encountered during this research;
2) suggestions for experimental research on anisotropy of normally consolidated resedimented BBC; and
3) suggestions for the focus of future experimental attention.

The problems met during the research on overconsolidated BBC are discussed first. They are as follows:

- Reduction in the absolute value of the initial pore pressure, u_i, of the resedimented BBC samples is at least partially due to the extended amount of time the cake spends on the saturated bottom porous stone as the sides are excavated. In addition to decreasing $|u_i|$, it is believed that this procedure increases the water content of the batch by as much as 2%. A polyvinyl

chloride (PVC) base should be machined to the exact dimensions of the stainless steel base. After the batch is unloaded and the piston has been removed, the steel cylinder should be tipped gently on its side, the base unbolted, removed and replaced by the PVC base.

- Efforts should be made to measure σ_2, the stress in the no strain (ε_2) direction in the DSC.
- Additional pore pressure probes should be installed in the DSC sample to monitor the spatial variation in the plane of shear as well as at varying depths. Such additional data will help further evaluate the quality of the stress application and the effect of boundary conditions.
- Surface strain measurement should be checked for the degree to which it represents strain throughout the sample (as per work by Wong and Arthur, 1985). Small (1/32-inch diameter) tungsten carbide balls could be placed in a grid midheight in the sample by slicing the sample in half, gently tamping each sphere in and replacing the top half of the sample. The grid of tungsten carbide spheres would be perpendicular to the no strain (ε_2) direction. The membrane should be prepared with the Letroset dot grid for comparative purposes. A radiograph would be taken to monitor the interior grid and a photograph taken to monitor the surface. In preparing the sample for the balls, there is likely to be a loss of the 100% saturation state.

The second set of recommendations refer to adaptation of the DSC testing technique for measuring anisotropy of resedimented BBC in the normally consolidated state.

- In order to obtain normally consolidated behavior, $\sigma'_{vc}/\sigma'_{p}(t)$ must be greater than or equal to approximately 1.3 (see Figs. 3.5 and 3.32), leading to vertical strains of approximately 4 to 5% for BBC. The major problem associated with the performance of DSC tests at OCR=1 lies in accommodating these strains. During consolidation, frictionless sides must be maintained adjacent to the sample normal to the σ_3 direction. Immediately following consolidation, however, an adhesive contact must be established between the shear sheet inner surface and the sample membrane on the same, once frictionless, sides. Germaine (1983, personal communication) suggested the use of folded tetrafluorocarbon (Teflon) strips between the sample membrane and the shear sheets. These strips would have tails extending over the shear sheets and the pressure bags for easy access by the operator. When consolidation to the desired stress is complete, the strips (each approximately one inch wide) can be removed one at a time by the operator.
- An additional problem associated with normally consolidated BBC tests involves using the DSC at stress levels in excess of 1.0 ksc. At such stress levels, the integrity of the dacron-reinforced pressure bags is

questionable. Even at low stress levels (less than 0.5 ksc), water leaking from corners of the bags was a common problem. Considerable effort will have to be invested in preparing higher capacity (better reinforced) pressure bags while maintaining their flexibility. Arthur (pers. comm., 1985) has developed higher capacity pressure bags at UCL, the design of which can be utilized.

The third and final set of recommendations springs from both difficulties met while evaluating the data, as well as the seeming incompleteness of the final conclusions of this thesis with respect to overall clay behavior. It is suggested that the following items be attended to:

- The method of consolidation, Recompression vs. SHANSEP, has been shown to have a distinct effect on the undrained shear behavior. However, the effect has yet to be accurately quantified, either with respect to its variation with angle of shear in a given material or as it varies with different materials. Efforts should be directed at clarifying the effect of the direction of the final consolidation increment.
- Much effort has been spent in proving the DSC as a device for measuring anisotropy of resedimented BBC at OCR=4. However, these data would be far more useful if they were accompanied by similar anisotropic data at OCR=1 as well as at additional OCR's such as 1.5, 2, and 8.
- A series of drained DSC tests at various OCR's would

help to provide definition of the yield and failure envelopes (as per Ladd, 1985, personal communication).

- Similar anisotropic data banks are much needed on materials of different plasticity, mineralogy and environment of deposition.
- Material identical to that studied using the DSC should be tested in the only other currently available device capable of measuring anisotropic parameters, the Hollow Cylinder Apparatus, to further assess the impact of the errors associated with each device.

Some specific tests which should be performed to further clarify the data contained here are as follows:

1) another SHANSEP TC test at OCR=4

2) a SHANSEP TE test at OCR=4

3) a Recompression TC test at OCR=4 on a very "young" (t_s<5 days) sample

4) Recompression (second type) TC and TE tests at OCR=4

5) a Recompression (second type) DSS test at OCR=4

REFERENCES

Note:
- ASCE = American Society of Civil Engineers
- ASTM = American Society for Testing and Materials
- FHWA = Federal Highway Administration
- ICSMFE = International Conference on Soil Mechanics and Foundation Engineering
- JGED = Journal of the Geotechnical Engineering Division
- JSMFD = Journal of the Soil Mechanics and Foundations Division
- MIT = Massachusetts Institute of Technology
- STP = Special Technical Publication
- UCL = University College London

Allison, L.E. (1965), "Walkley-Black Method," Methods of Soil Analysis, C.A. Black, ed., sponsored by ASTM, Part 2, pp. 1372-1376.

Arthur, J.R.F. (1984), University College London, personal communication.

Arthur, J.R.F., S. Bekenstein, J.T. Germaine and C.C. Ladd (1981), "Stress Path Tests with Controlled Rotation of Principal Stress Directions," ASTM Symposium on Laboratory Shear Strength of Soil, Chicago, STP NO. 740, pp. 516-540.

Arthur, J.R.F., K.S. Chua and T. Dunstan (1977), "Induced Anisotropy in a Sand," Geotechnique, Vol. 27, No. 1, pp. 13-36.

Arthur, J.R.F., K.S. Chua, T. Dunstan and J.I. Rodriquez del C. (1980), "Principal Stress Rotation, A Missing Parameter," JGED, ASCE, Vol. 106, No. GT4, pp. 419-433.

Arthur, J.R.F. and B.K. Menzies (1972), "Inherent Anisotropy in a Sand," Geotechnique, Vol. 22, No. 1, pp. 115-128.

Baligh, M.M. (1985), "The Strain Path Method," JGED, ASCE (Accepted for Publication).

Bekenstein, S. (1980), "Directional Shear Tests on Leighton Buzzard Sand," S.M. Thesis, Department of Civil Engineering, MIT, 307 p.

Bensari, J. (1984), "Stress-Strain Characteristics from Undrained and Drained Triaxial Tests on Resedimented Boston Blue Clay," M.S. Thesis, Dept. of Civil Engineering, MIT, Cambridge, MA., 193 p.

Bishop, A.W. (1966), "The Strength of Soils as Engineering Materials," 6th Rankine Lecture, Geotechnique, Vol. 16, pp. 89-130.

Bishop, A.W. and D.J. Henkel (1957), The Measurement of Soil Properties in the Triaxial Test, (Edward Arnold Ltd., London), 228 p.

Bjerrum, L. (1973), "Problems of Soil Mechanics and Construction on Soft Clays," State-of-the-Art Report, Session 4, Proc. 8th ICSMFE, Moscow, Vol. 3, pp. 109-159.

Bjerrum, L. and K.Y. Lo (1963), "Effect of Aging on the Shear-Strength Properties of a Normally Consolidated Clay," Geotechnique, Vol. 13, pp. 147-157.

Broms, B.B. and A.O. Casbarian (1965), "Effects of Rotation of the Principal Stress Axes and the Intermediate Principal Stress on the Shear Strength," Proc. 6th ICSMFE, Montreal, Vol. I, pp. 179-183.

Butterfield, R. (1979), "A Natural Compression Law for Soils (An Advance on e-log p')," Geotechnique, Vol. 29, No. 4, pp. 469-480.

Casagrande, A. and N. Carillo (1944), "Shear Failure of Anisotropic Materials," Proc. Boston Soc. of Civil Engr., Vol. 31, pp. 74-87.

Christian, J.T. (1981), "Discussion of State of the Art: Laboratory Strength Testing of Soils," Laboratory Shear Strength of Soil, ASTM STP 740, R.N. Yong and F.C. Townsend, eds., pp. 638-640.

Clough, G.W. and M.L. Silver (1983), "A Report of the Workshop on Research Needs in Experimental Soil Engineering," supported by the National Science Foundation, Virginia Polytechnic Institute and State Univ., Blacksburg, VA.

Duncan, J.M. and H.B. Seed (1966a), "Anisotropy and Stress Reorientation in Clay," JSMFD, ASCE, Vol. 92, No. SM5, pp. 21-50.

Duncan, J.M. and H.B. Seed (1966b), "Strength Variation Along Failure Surfaces in Clay," JSMFD, ASCE, Vol. 92, No. SM6, pp. 81-104.

Gens, A. (1982), "Stress-Strain and Strength Characteristics of a Low Plasticity Clay," Ph.D. Thesis, Imperial College of Science & Technology, London, 856 p.

Germaine, J.T. (1982), "Development of the Directional Shear Cell for Measuring Cross Anisotropic Clay Properties," Sc.D. Thesis, Dept. of Civil Eng., MIT, Cambridge, 530 p.

Graham, J. and G.T. Houlsby (1983), "Anisotropic Elasticity of a Natural Clay," Geotechnique, Vol. 33, No. 2, pp. 165-180.

Hansen, J.B. and R.E. Gibson (1949), "Undrained Shear Strengths of Anisotropically Consolidated Clays," Geotechnique, Vol. 1, No. 3, pp. 189-204.

Hansen, L.A. and G.W. Clough (1980), "Application of Plasticity and Generalized Stress-Strain in Geotechnical Engineering," Proc. Symposium on Limit Equilibrium, Plasticity and Generalized Stress Strain Applications in Geotechnical Engineering, Hollywood, FL.

Hight, D.W. (1985), Geotechnical Consulting Group, London, England, personal communcation.

Hight, D.W., A. Gens and M.J. Symes (1983), "The Development of a New Hollow Cylinder Apparatus for Investigating the Effects of Principal Stress Rotation in Soils," Geotechnique, Vol. 33, No. 4, pp. 355-384.

Houlsby, G.T. (1982), "Theoretical Analyses of the Fall Cone Test," Geotechnique, Vol. 32, No. 2, pp. 111-118.

Jamiolkowski, M., C.C. Ladd, J.T. Germaine and R. Lancellotta, (1985), "New Developments in Field and Laboratory Testing of Soils," 11th ICSMFE, San Francisco, 97 p.

Jordan, W.S. (1979), "Determination of Negative Pore Pressures for Embankment Design," S.M. Thesis, Dept. of Civil Engr., MIT, Cambridge, 144 p.

Kavvadas, M. (1981), "Non-Linear Consolidation Around Driven Piles in Clays," Sc.D. Thesis, Dept. of Civil Eng., MIT, Cambridge, 666 p.

Kenney, T.C. (1964), "Sea-Level Movement and the Geologic Histories of the Postglacial Marine Soils at Boston, Nicolet, Ottawa and Oslo," Geotechnique, Vol. 14, No. 3, pp. 203-230.

Kinner, E.B. and C.C. Ladd (1970), "Load Deformation Behavior of Saturated Clays during Undrained Shear," Res. Report R70-27, No. 259, Dept. of Civil Engr., MIT, Cambridge, 302 p.

Ko, H.Y. and R.F. Scott (1967), "A New Soil Testing Apparatus," Geotechnique, Vol. 17, No. 1, pp. 40-57.

Lacasse, S.M. and M. Vucetic (1981), "Discussion of Saada et al. (1981)," Laboratory Shear Strength of Soil, ASTM STP 740, R.N. Yong and F.C. Townsend, eds., pp. 633-637.

Ladd, C.C. (1981), "Discussion on Laboratory Shear Devices," Laboratory Shear Strength of Soil, ASTM, STP 740, R.N. Yong and F.C. Townsend, eds., pp. 643-652.

Ladd, C.C., R.B. Bovee, L. Edgers and J.J. Rixner (1971), "Consolidated-Undrained Plane Strain Shear Tests on Boston Blue Clay," Res. Report R71-13, No. 273, Dept. of Civil Engr., MIT, Cambridge, 243 p.

Ladd, C.C. and L. Edgers (1972), "Consolidated-Undrained Direct-Simple Shear Tests on Saturated Clays," Res. Report R72-82, No. 284, Dept. of Civil Engr., MIT, Cambridge, 354 p.

Ladd, C.C. and R. Foott (1974), "New Design Procedure for Stability of Soft Clays," JGED, ASCE, No. GT7, pp. 763-786.

Ladd, C.C. and R. Foott (1977), "Foundation Design of Embankments Constructed on Varved Clays," U.S. Dept. of Transportation, FHWA Report TS-77-214, 234 p.

Ladd, C.C. and R. Foott (1980), "The Behavior of Embankments on Clay Foundations: Discussion," Canadian Geotechnical Journal, Vol. 17, No. 3, pp. 454-460.

Ladd, C.C., R. Foott, K. Ishihara, F. Schlosser and H.G. Poulos (1977), "Stress-Deformation and Strength Characteristics," State-of-the-Art Report for Session 1, Proc. 9th ICSMFE, Tokyo, Vol. 2, pp. 421-494.

Ladd, C.C. and E.B. Kinner (1967), "The Strength of Clays at Low Effective Stress," U.S. Army Engineer Waterways Experiment Station Report No. 3-101; Phase Report No. 8, Dept. of Civil Engineering Publication R67-4, MIT, January.

Ladd, C.C. and T.W. Lambe (1963), "The Strength of 'Undisturbed' Clay Determined from Undrained Tests," ASTM, STP 361, pp. 342-371.

Ladd, C.C. and J. Varallyay (1965), "The Influence of Stress System on the Behavior of Saturated Clays during Undrained Shear, Res. Report R65-11, No. 177, Dept. of Civil Engr., MIT, Cambridge, 263 p.

Lade, P.V. and H.M. Musante (1978), "Three Dimensional Behavior of Remolded Clay," JGED, ASCE, Vol. 104, GT2, pp. 193-209.

Lefebvre, G., C.C. Ladd, G. Mesri and F. Tavenas (1983), "Report of the Committee of Specialists on Sensitive Clays on the NBR Complex," SEBJ, Montreal, Annexe II.

Levadoux, J.N. (1980), "Pore Pressures in Clays due to Cone Penetration," Ph.D. Thesis, Dept. of Civil Engr., MIT, Cambridge, 753 p.

Lucks, A.S., J.T. Christian, G.E. Brandow and K. Höeg (1972), "Stress Conditions in NGI Simple Shear Test," JSMFD, ASCE,

Vol. 98, SM1, pp. 155-160.

Martin, R.T. (1970), "Suggested Method of Test for Determination for Soluble Salts in Soil," ASTM, STP 479, PP. 288-290.

Martin, R.T. and C.C. Ladd (1970), "Fabric of Consolidated Kaolinite," Res. Report R70-15, Soils Publication No. 254.

Menzies, B.K. (1970), "Stress-Strain Anisotropy in Sands," Ph.D. Thesis, University of London.

Menzies and Phillips (1972), "On the Making of Rubber Membranes," Geotechnique, Technical Note, Vol. 1, pp. 153-155.

Mesri, G., A. Rokhsar and B.F. Bohor (1975), "Composition and Compressibility of Typical Samples of Mexico City Clay," Geotechnique, Vol. 25, No. 3, pp. 527-554.

Mitchell, J.K. (1960), "Fundamental Aspects of Thixotropy in Soils," JSMFD, ASCE, Vol. 86, No. SM3, pp. 19-52.

Mitchell, J.K. (1976), Fundamentals of Soil Behavior, John Wiley and Sons, New York, 422 p.

Mitchell, R.J. (1972), "Some Deviations from Isotropy in a Lightly Overconsolidated Clay," Geotechnique, Vol. 22, No. 3, pp. 459-467.

Phillips, A.B. (1972), "Strength and Deformation of Layered Sand," Ph.D. Thesis, UCL, 339 p.

Prevost, J.-H. and K. Hoeg (1977), "Plasticity Model for Undrained Stress-Strain Behavior," Proc. 9th ICSMFE, Tokyo, Vol. 1, pp. 255-261.

Rodriguez del C., J.I. (1977), "Induced Anisotropy in a Loose Sand," Ph.D. Thesis, Engineering Dept., UCL, 327 p.

Roscoe, K.H. and J.B. Burland (1968), "On the Generalized Stress-Strain Behavior of 'Wet' Clay," in Engineering Plasticity, Cambridge Univ. Press, pp. 535-609, (ed. by J. Heyman).

Saada, A.S. (1970), "Testing of Anisotropic Clay Soils," JSMFD, ASCE, Vol. 96, SM5, pp. 1847-1852.

Saada, A.S. and G.F. Bianchini (1975), "Strength of One-Dimensionally Consolidated Clays," JGED, ASCE, Vol. 101, GT11, pp. 1151-1164.

Saada, A.S. and G.F. Bianchini (1977), "Strength of One Dimensional Consolidated Clays," Discussion Closure, JGED, ASCE, Vol. 103, No. GT6, pp. 655-660.

Saada, A.S. and C.D. Ou (1973), "Stress-Strain Relations and Failure of Anisotropic Clays," JSMFD, ASCE, Vol. 99, SM12, pp. 1091-1111.

Saada, A.S. and F.H. Townsend, (1981), "State of the Art: Strength Testing of Soils," Laboratory Shear Strength of Soil, ASTM, STP 740, R.N. Yong and F.C. Townsend, eds., pp. 7-77.

Saada, A.S. and K.K. Zamani (1969), "The Mechanical Behavior of Cross Anisotropic Clays," Proc. 7th ICSMFE, Mexico, Vol. 1, pp. 351-359.

Sambhandharaksa, S. (1977), "Stress-Strain-Strength Anisotropy of Varved Clays," Sc.D. Thesis, Dept. of Civil Engr., MIT, Cambridge, 506 p.

Scott, R.F. (1981), Foundation Analysis, Prentice-Hall, Inc., Englewood Cliffs, N.J., 545 p.

Seed, H.B. and C.K. Chan (1957), "Thixotropic Characteristics of Compacted Clays," JSMFD, ASCE, Vol. 83, SM4, pp. 1427-1 to 1427-35.

Shen, C.K., K. Sadigh and L.R. Herrmann (1978), "An Analysis of NGI Simple Shear Apparatus for Cyclic Soil Testing," ASTM, STP 654, pp. 148-162.

Skempton, A.W. (1954), "The Pore-Pressure Coefficients A and B," Geotechnique, Vol 4, No. 4, pp. 143-152.

Skempton, A.W. and R.D. Northey (1952), "The Sensitivity of Clays," Geotechnique, Vol. 3, No. 1, pp. 30-53.

Soydemir, C. (1976), "Strength Anisotropy Observed Through Simple Shear Tests," Laurits Bjerrum Memorial Volume, Norwegian Geotechnical Institute, pp. 99-113.

Symes, M.J.P.R. (1983), "Rotation of Principal Stresses in Sand," Ph.D. Thesis, Dept. of Civil Engineering, Imperial College of Science and Technology, London.

Symes, M.J.P.R., A. Gens and D.W. Hight (1984), "Undrained Anisotropy and Principal Stress Rotation in Saturated Sand," Geotechnique, Vol. 34, No. 1, pp. 11-27.

Tavenas, F., J.P. des Rosiers, S. Leroueil, P. LaRochelle and M. Roy (1979), "The Use of Strain Energy as a Yield and Creep Criterion for Lightly Overconsolidated Clays," Geotechnique, Vol. 29, No. 3, pp. 285-303.

Tavenas, F. and S. Leroueil (1977), "Effects of Stresses and Time on Yielding of Clays," Proc. 9th ICSMFE, Tokyo, Vol. 1, pp. 319-326.

Vaid, Y.P. and R.G. Campanella (1974), "Triaxial and Plane Strain Behavior of Natural Clay," JGED, ASCE, Vol. 100, No. GT3, pp. 207-224.

Vucetic, M. and S. Lacasse (1982), "Specimen Size Effect in Simple Shear Test," JGED, ASCE, Vol. 108, GT12, pp. 1567-1585.

Wong, R.K.S. and J.R.F. Arthur (1985), "Determinations and uses of Strain Distributions in Sand Samples," accepted for publication in ASTM Geotechnical Testing Journal.

Wroth, C.P. and D.M. Wood (1978), "The Correlation of Index Properties with Some Basic Engineering Properties of Soils," Canadian Geotechnical Journal, Vol. 15, No. 2, pp. 137-145.

Yong, R.N. and H.Y. Ko (1980), "Soil Constitutive Relationships and Modelling of Soil Behavior," NSF/NSERC North America Workshop on Plasticity Theories and Generalized Stress-Strain Modeling of Soils, McGill University, Montreal, 9 p.